

Connectivity of Geohydrological Processes and the Interaction with the Surface Hydrology of the Letaba River

Reinardt Raubenheimer

Submitted in fulfilment of the requirements for the degree
Magister Scientiae Geohydrology
in the
Faculty of Natural and Agricultural Sciences
(Institute for Groundwater Studies)
at the
University of the Free State

Study leader: Amy Allwright
Co-Study leader: Dr Eddie Ridell

BLOEMFONTEIN
January 2018

Declaration

I, Reinardt Raubenheimer, declare that the dissertation hereby submitted by me for the Magister Scientiae in Geohydrology degree at the University of the Free State, is my own independent work and has not previously been submitted by me at another university/faculty.

I further declare that all sources cited or quoted are indicated and acknowledged by means of a list of references.

Reinardt Raubenheimer furthermore cede copyright of the dissertation in favour of the University of the Free State.



Reinardt Raubenheimer

Student number: 2007014232

26/01/2018

Acknowledgements

I would like to express my sincere gratitude to each of the following people, as this dissertation could not have been possible without their assistance.

- First and foremost, I would like to thank my Heavenly Father for providing me with the strength, knowledge and opportunity to undertake this dissertation.
- My supervisor, Ms. Amy Allwright from the Institute for Groundwater Studies (IGS) at the University of the Free State for her continual assistance, guidance and eye for detail.
- My co-supervisor, Dr Eddie Riddell from SANParks scientific services for his patience and positive attitude while mentoring and guiding me throughout this dissertation.
- Dr. Jacobus M. Nel from Groundwater Consulting Services (GCS) for his guidance, mentorship and providing the opportunity to work on this project.
- Dr. Tony Swemmer from the South African Earth Observation Network (SAEON) for his kind assistance in providing equipment, vehicles and funding for this dissertation.
- Ms, Tercia Strydom from SANParks scientific services for her assistance in fieldwork and providing her Hydrocensus dataset.
- Mr. Raymond Minaar and Ms. Tercia Strydom for providing their geophysical dataset.
- Shaeden Gokool for his assistance in fieldwork and providing his isotope dataset.
- Environmental monitor Ms. Queen Malatji for her field assistance in the 43°C heat.
- Mr. Mike Butler at iThemba Labs for analyses of the isotope samples.
- The Water Research Commission for funding this project.
- My family and friends for their support and encouragement.
- My partner Chantel Weidenmann for her fieldwork assistance (pumping tests, fluid logs, sampling and continual water level measuring), encouragement and support throughout the dissertation.

Table of Contents

Chapter 1 - INTRODUCTION	1
1.1 BACKGROUND	1
1.2 AIMS AND OBJECTIVES OF THE PROJECT	3
1.2.1 Main aim	4
1.2.2 Key objectives	5
1.2.3 The key questions to achieve the objectives are:	5
Chapter 2 - LITERATURE REVIEW	6
2.1 BASIC PRINCIPLES OF GROUNDWATER – SURFACE WATER INTERACTION.....	6
2.2 DIFFERENT TYPES OF GROUNDWATER INTERACTIONS WITH STREAMS	9
2.3 RIVERINE LANDSCAPES	13
2.4 METHODS USED FOR GROUNDWATER – SURFACE WATER INTERACTION.....	14
2.4.1 Direct measurements of water flux	14
2.4.2 Heat tracer methods.....	15
2.4.3 Methods based on Darcy’s Law	16
2.4.4 Mass balance approaches	20
2.4.9 Discussion	22
2.5 LITERATURE REVIEW ON METHODOLOGY USED	23
2.5.1 Magnetic survey method	23
2.5.2 Electrical resistivity method.....	24
2.5.3 Borehole drilling	26
2.5.4 Fluid logging	26
2.5.5 Slug tests	26
2.5.6 Pumping tests	27

2.5.7 Analysis of aquifer test.....	28
2.5.8 Monitoring of groundwater and surface water.....	28
2.5.9 Water sampling of groundwater and surface water.....	29
2.5.10 Down hole camera investigation.....	29
2.6 GENERAL ASSUMPTIONS.....	30
2.7 RECENT RESEARCH ON GROUNDWATER SURFACE WATER INTERACTION WITHIN SOUTH AFRICA.....	31
Chapter 3 - SITE CHARACTERISATION: GENRAL OVERVIEW.....	32
3.1 STUDY SITE LOCATION.....	32
3.2 HYDROLOGY.....	35
3.3 CLIMATE.....	35
3.4 GEOLOGY AND TOPOGRAPHY.....	36
3.5 GEOHYDROLOGY.....	37
Chapter 4 - SITE CHARACTERISATION: DATA COLLECTION.....	41
4.1 HYDROCENSUS.....	41
4.2 GEOLOGICAL SUBSTRATE INVESTIGATION.....	41
4.2.1 Geophysical survey technique.....	41
(A) Farming Area.....	42
(B) Protected Areas.....	43
4.2.1 Magnetic Survey technique.....	44
4.3 DRILLING OF SITED BOREHOLES.....	44
4.4 LITHOLOGY LOGS OF BOREHOLES.....	47
4.5 MONITORING.....	48
4.5.1 Ground water levels.....	48
4.5.2 Fluid logging.....	50
4.5.3 Down hole camera.....	51
4.6 AQUIFER TESTING.....	54

4.6.1 Slug test	54
4.6.2 Pumping tests	55
4.7 SAMPLING	57
4.7.1 Sampling for hydrochemistry	57
4.7.2 Sampling for Isotopes.....	57
4.8 WEATHER STATIONS.....	58
Chapter 5 - SITE CHARACTERISATION: DATA ANALYSIS	59
5.1 HYDROCENSUS	59
5.1.1 Mbaula.....	59
5.1.2 Mthimkhulu.....	60
5.1.3 River abstraction	60
5.2 PRECIPITATION ON STUDY SITE	61
5.3 GEOLOGICAL CHARACTERISATION	63
5.3.1 Farming Area.....	63
5.3.2 Protected Area	75
5.4 AQUIFER CHARACTERISATION	85
5.4.1 Slug tests	86
5.4.2 Step tests.....	87
5.4.3 Constant rate tests.....	90
5.4.4 Transmissivity	92
5.4.5 Hydraulic gradient distribution	93
5.4.6 Fluid logging	99
5.4.7 Down hole Camera.....	122
5.4.8 Assessing peak flow transmission losses	125
5.4.9 Groundwater flow direction from hydraulic heads	129
5.4.10 Groundwater stream flow process across dolerite dyke.....	132
5.4.11 Isotope analysis	133

5.4.12 Groundwater – surface water mass balance	138
Chapter 6 - CONCEPTUAL MODEL: DISCUSSION AND ASSUMPTIONS	141
6.1. TRAVERSE 1	141
6.2 TRAVERSE 2.....	142
6.3 TRAVERSE 3.....	143
6.4 TRAVERSE 4.....	144
6.5 DOLERITE DYKE INFLUENCE.....	144
Chapter 7 - CONCLUSIONS AND RECOMMENDATIONS.....	148
7.1 CONCLUSION AND DISCUSSION	148
7.2 RECOMMENDATIONS FOR FUTURE RESEARCH.....	151
7.3 RECOMMENDATIONS FOR MANAGEMENT	152
REFERENCES	153
APPENDIX A	161
APPENDIX B.....	165
APPENDIX C.....	192
APPENDIX D	201
ABSTRACT	202
OPSOMMING.....	203

List of Figures

Figure 2.1 Of the four main pools of water located on Earth, groundwater is the second smallest with river flow to the oceans as one of the smallest fluxes. Nevertheless groundwater and surface water are the components of the hydrologic cycle that we utilise the most (Winter et al., 1998).	7
Figure 2.2 Groundwater – surface water interaction within landscapes from mountainous areas to an ocean, within a theoretical landscape. M, mountainous; K, karst; G, glacial; R, riverine (small); V, riverine (large); C, coastal (Winter et al., 1998).	8
Figure 2.3 Gaining stream (A). Water table contours used for gaining or losing stream determination (B) (Winter et al., 1998).	9
Figure 2.4 Losing stream (A). Water table contours used for gaining or losing stream determination (B) (Winter et al., 1998).	10
Figure 2.5 Disconnected stream separated from the groundwater system (Winter et al., 1998).	11
Figure 2.6 Bank storage from the increase in stream level (Winter et al., 1998).	11
Figure 2.7 Floodwaters will recharge the groundwater if the stream levels rise higher than their banks (Winter et al., 1998).	12
Figure 2.8 In wide river valleys, local groundwater systems overlie larger regional groundwater systems. Seasonal flood events further increase the already complex river hydrology(Winter et al., 1998).	14
Figure 2.9 Spatial measuring scales of the different methods to measure interactions between groundwater and surface water. The spatial scale is given as radius or distance of influence. Dots represent point measurements (pm), (Kalbus, 2006).	23
Figure 2.10 Representative of a magnetic body beneath the earth (Roux et al., 1980)..	24
Figure 2.11 Types of arrays, a: Common resistivity electrode arrays that consists of two current electrodes namely A and B, as well as two potential electrodes namely M and N, b: Schlumberger array, and c: Wenner array (van Zijl, 1985).	25

Figure 3.1 Location of study site in perspective to South Africa (www.sothafricatoursandtravel.com, 2017).	32
Figure 3.2 Regional locality map of study area (1:50 000 Topo-sheet 2331CA).	33
Figure 3.3 Aerial imagery locality map of the study area (Google Earth, 2016).	34
Figure 3.4 Location of the Letaba River Catchment within South Africa (DWAF, 2006), (Blue areas is indicative of protected area, e.g. Nature reserve, National park).	36
Figure 3.5 Generalised topography of the study area.	38
Figure 3.6 Generalised groundwater level of the study area.	39
Figure 3.7 Geological map of study area (1:250 000 Geological Map Series 2831 Phalaborwa).	40
Figure 4.1 Locality map of the geophysics transects over two different land-uses (Ridell, 2016).	42
Figure 4.2 Locality map of the geophysics transects the Farms area (Ridell, 2016).	43
Figure 4.3 Locality map of the geophysics transects over the Protected areas (Ridell, 2016).	43
Figure 4.4 Geotron Proton Magnetometer, model G5 used for the magnetic survey (www.geotron.co.za, 2017).	44
Figure 4.5 Final location of all boreholes on study site, as well as their specific transects (Google Earth, 2016).	46
Figure 4.6 Piezometric design of boreholes at each specific site (Gokool et. al, 2015).	47
Figure 4.7 Typical example of a borehole Lithology log.	48
Figure 4.8 Movement of groundwater from a point of high elevation to a point of low elevation (DWS, 2006b).	49
Figure 4.9 Hand measurements of groundwater levels taken on a weekly basis.	50
Figure 4.10 YSI (Yellow Spring Incorporated) 600XLM Sonde multi-parameter in-situ monitoring apparatus.	51

Figure 4.11 Equipment used for down hole camera investigation.	52
Figure 4.12 Pumping rig and equipment used during pumping tests.	56
Figure 4.13 Custom made rain sampler for isotope samples.....	58
Figure 4.14 Locations of the Three Davis Vantage Pro weather stations in the broader study area (Google Earth, 2017).....	58
Figure 5.1 Abstraction rates of farms located on study site (Riddell, 2016).....	61
Figure 5.2 Measured precipitation from the three weather stations compared against the groundwater level of three boreholes on site.....	62
Figure 5.3 Locality map of the geophysics transects over the Farms section (Ridell, 2016).....	63
Figure 5.4 Geophysical traverse LF001 with incorporated magnetic and resistivity profiles (modified after Gokool et al., 2015).....	68
Figure 5.5 Geophysical traverse LF002 with incorporated magnetic and resistivity profiles (modified after Gokool et al., 2015).....	69
Figure 5.6 Geophysical traverse LF003 with incorporated magnetic and resistivity profiles (modified after Gokool et al., 2015).....	70
Figure 5.7 Geophysical traverse LF004 with incorporated magnetic and resistivity profiles (modified after Gokool et al., 2015).....	71
Figure 5.8 Geophysical traverse LF005 with incorporated magnetic and resistivity profiles (modified after Gokool et al., 2015).....	72
Figure 5.9 Geophysical traverse LF006.1 with incorporated magnetic and resistivity profiles (modified after Gokool et al., 2015).....	73
Figure 5.10 Geophysical traverse LF006.2 with incorporated magnetic and resistivity profiles (modified after Gokool et al., 2015).....	74
Figure 5.11 Locality map of the geophysics transects over the Protected area (Ridell, 2016).....	75

Figure 5.12 Geophysical traverse LM001 with incorporated magnetic and resistivity profiles (modified after Gokool et al., 2015).....	79
Figure 5.13 Geophysical traverse LM002 with incorporated magnetic and resistivity profiles (modified after Gokool et al., 2015).....	80
Figure 5.14 Geophysical traverse LM003 with incorporated magnetic and resistivity profiles (modified after Gokool et al., 2015).....	81
Figure 5.15 Geophysical traverse LM004 with incorporated magnetic and resistivity profiles (modified after Gokool et al., 2015).....	82
Figure 5.16 Geophysical traverse LM005 with incorporated magnetic and resistivity profiles (modified after Gokool et al., 2015).....	83
Figure 5.17 Geophysical traverse LM006 with incorporated magnetic and resistivity profiles (modified after Gokool et al., 2015).....	84
Figure 5.18 Overview of study site with borehole locations.....	85
Figure 5.19 Step test performed on LR005B.....	88
Figure 5.20 Results through using the FC – Non Linear Method.	89
Figure 5.21 An example of the constant rate test data entered into AQT SOLV.....	91
Figure 5.22 Comparison of all boreholes Transmissivity.....	93
Figure 5.23 Hydraulic gradient cross-section plot of transect 1.....	94
Figure 5.24 Hydraulic gradient cross-section plot of transect 2.....	95
Figure 5.25 Hydraulic gradient cross-section plot of transect 3.....	96
Figure 5.26 Hydraulic gradient cross-section plot of transect 4.....	97
Figure 5.27 Hydraulic gradient cross-section plot of transect 4-B.....	98
Figure 5.28 Fluid log of LF002 (A – above, B – below).....	101
Figure 5.29 Fluid log of LF0021.	102
Figure 5.30 Fluid log of LF004 (A – above, B – below).....	103

Figure 5.31 Fluid log of LF0031.	105
Figure 5.32 Fluid log of LF003.	107
Figure 5.33 Fluid log of LF005 (A – above, B – mid, C – below).....	109
Figure 5.34 Fluid log of LF0051 (A- above, B – below).	111
Figure 5.35 Fluid log of LR002A.	112
Figure 5.36 Fluid log of LR004 (A – above, B – below).	114
Figure 5.37 Fluid log of LR0011A.	115
Figure 5.38 Fluid log of LR001A.	116
Figure 5.39 Fluid log of LR005 (A – above, B – below).	118
Figure 5.40 Fluid log of LR003.....	118
Figure 5.41 Fluid log of LRW001 (above) and LRW002 (below).....	120
Figure 5.42 Dolerite dyke intersecting the Letaba River at LRW001/2.....	121
Figure 5.43 Groundwater enter the borehole at the bottom of the casing (LR004A)...	123
Figure 5.44 Fracture with iron staining at 34 m (LR004A).....	123
Figure 5.45 Fracture at 43 m (LR004A).	124
Figure 5.46 Casing break and fracture of borehole LF0051B.	124
Figure 5.47 Reaction of boreholes to the flood event of March 2016 on transect 1 (Ridell, 2016).....	126
Figure 5.48 Reaction of boreholes to the flood event of March 2016 on transect 2 (Ridell, 2016).....	127
Figure 5.49 Reaction of boreholes to the flood event of March 2016 on transect 3. ...	128
Figure 5.50 Reaction of boreholes to the flood event of March 2016 on transect 4. ...	129
Figure 5.51 Borehole LR005A’s conductivity reaction to rainfall and the March 2016 flood.....	129

Figure 5.52 Groundwater flow direction before (Top) and after (Bottom) the flood event.	131
Figure 5.53 Groundwater-Streamflow processes across dolerite dyke	132
Figure 5.54 Overview of borehole locations and transects.	134
Figure 5.55 A graph indicating the relationship between $\delta^2\text{H}$ and $\delta^{18}\text{O}$ values of samples taken on the study site in terms of each transect.	137
Figure 5.56 A graph indicating the relationship between $\delta^2\text{H}$ and $\delta^{18}\text{O}$ values of samples taken on the study site in terms of each borehole.....	137
Figure 5.57 Graph comparing streamflow, baseflow and quickflow.	139
Figure 6.1 Conceptual model of study site.	146
Figure 6.2 Conceptual model of the protected area and farms area.	147
Appendix A-1: ABEM Terrameter that was used for the geophysical survey (Strydom, 2014).	161
Appendix A-2: The drilling rig is a modified old 10 ton 6x6 SAMIL truck with a super rock 5000 air percussion rig and a 900CFM compressor.	161
Appendix A-3: An example of a water strike at LF004A.	162
Appendix A-4: An example of the shallow and deep boreholes drilled at LF004A. ...	162
Appendix A-5: Analysis of core log samples.	163
Appendix A-6: Solinst TM TLC dipmeter.	163
Appendix A-7: Slug used for slug tests.	164

List of Tables

Table 2.6 General Assumptions.	30
Table 4.1 Borehole names and metadata.	53
Table 5.1 Hydrocensus information from Mthimkhulu (Strydom, 2014).....	60
Table 5.2 Hydrocensus data from July 2015 (Riddell, 2016).....	61
Table 5.3 Initial K and T values from slug tests.....	89
Table 5.4 Final K and T values obtained from the constant rate tests.....	91

List of Equations

Equation (2.1): Darcy's equation	16
Equation (2.2): Groundwater velocity	17
Equation (2.3): Apparent resistivity	25
Equation (4.1): Length of displacement	54
Equation (5.1): Correction on Cooper - Jacob equation.....	88
Equation (5.2): Step drawdown test	90
Equation (5.3): Quickflow	138
Equation (5.4): Streamflow	138
Equation (5.5): Baseflow	138

List of Acronyms and Abbreviations

2D	Two dimensions
°C	Degrees Celsius
L/s	Litres per second
mS/cm	Millisiemens per centimetre
m ² /d	Metres squared per day
m	Meters
mm	Millimetres
DWA	Department of Water Affairs
EC	Electrical conductivity
ERT	Electrical Resistivity Tomography
FL	Fluid logging
GPS	Global positioning system
KNP	Kruger National Park
mamsl	meters above mean sea level
mbgl	meters below ground level
SANParks	South African National Parks
S	Storativity
SAEON	South African Environmental Observation Network
TDS	Total dissolved solids
T	Transmissivity
WRC	Water Research Commission

Definitions

Conceptual Model: A conceptual model consists of the designing and assembling of an equal, although simplified circumstances for the actual problem within reality (DWA, 2006).

Consolidated rock or hard rock: This type of rock consists of solid material where the individual minerals are cemented together, while their separation does not occur easily (Nonner, 2003).

Deuterium: Is a stable isotope of hydrogen and consists of one proton and one neutron in its nucleus (www.idc-online.com, 2017).

Dolerite: Is a fine to medium crystalline rock that consists of the minerals pyroxene and plagioclase (DWA, 2006).

Electrical conductivity: Is the measurement of to what a degree a material allows the transport of an electric charge. With an increase in EC there is an increase in total dissolved salts (DWA, 2006).

Environmental flows: Is the water regime found within a coastal zone, river or wetland that maintains ecosystems and their benefits where water uses are competitive and regulated (Dyson and Scanlon, 2003).

Hydrocensus: Basically, it means a water census. This involves the gathering of information on aspects such as sources of water supply, water features and potential water pollution sources within a particular area (DWA, 2004).

Piezometer: Is used for the measuring of the elevation of a water table or the collection of water samples. The borehole is generally not in use, with a small diameter (DWA, 2006).

Riparian zone: The area located directly next to a river or stream that is influenced by river induced or associated processes (DWA, 2006).

Stable isotopes: Is a non spontaneous radioactive isotope of a chemical element. Chemical elements can exist in unstable (radioactive), as well as stable forms.

The Reserve: The quality, quantity and assurance of water, which are required for the protection of basic human needs, as well as the function and structure of ecosystems to ultimately ensure ecological sustainable development and utilisation (DWAF, 1999).

Transmissivity (T): Is the tempo that water is transmitted throughout a unit width of an aquifer subjected to a unit hydraulic gradient. It is generally expressed as the result of the thickness of a saturated portion and the average hydraulic conductivity of an aquifer (DWA, 2006).

Unconsolidated rock: Consists of loose material, normally separated minerals (Nonner, 2003).

Chapter 1 - INTRODUCTION

1.1 BACKGROUND

Continued population and economic growth within South Africa have led to increased water use by industry, agriculture, mining, domestic users and other uses over the past few decades. This increased usage has come close or even surpassed the threshold of renewable water resources within river basins. Water that flows out of basins is normally committed to other downstream uses, while outflow to the sea normally has many overlooked functions. Such as: washing out of sediments, dilution of polluted water, sustaining coastal ecosystems and the controlling of salinity intrusion. When a river discharge does not meet these commitments throughout the year, the basin is said to be closing or closed. Low flows and degradation of water quality has led to severe environmental degradation and rendered water unusable to downstream users. Water demand now effectively exceeds supply, such that a large number of catchments within South Africa are either closing or already closed, where there is little to no options for further allocation (Molle et al., 2010).

With the closure of a basin the interconnectedness of the water users, water cycle and the aquatic ecosystems increases significantly. Total runoff percentage is increased by diversions; the amount of precipitation that evapotranspires are modified by alteration of land use, thus decreasing the residual water that is potentially available; return flows from users are normally utilised again, resulting in downstream users being more sensitive to upstream alterations in efficiency; and groundwater surface water interactions are also more noticeable (e.g. Molle et al., 2010).

After 1994 South Africa commenced an ambitious restructuring process, emerging from a new democratic dispensation. This process gave emphasis to the establishment of principles such as equity and sustainability that form the basis for water resource management (WRM) of catchments. The framework for this restructuring process is the Integrated Water Resources Management (IWRM) whose principles are encapsulated in the National Water Act (DWAF 1998).

The accurate quantification of groundwater – surface water interaction remains a difficult task, because of the spatial heterogeneity and scale of aquifers (Becker et al., 2004; Kalbus et al., 2008). This is especially true for South Africa where groundwater quantification and its interaction with surface water, prove to be challenging. This is because most of South Africa's aquifers are fractured rock aquifers found within a heterogeneous and anisotropic setting. However, in South Africa this is still essential for the successful implementation of the NWA, as water use licenses are approved only after the Reserve is determine (Levy, 2011).

It was recognised that South Africa faces significant challenges in terms of water reform, involving major administrative and policy shifts, thus the attention has shifted to implementation. A three-year study termed the Shared Rivers Initiative (SRI) focused on six river basins flowing through the South African Lowveld, a term used to describe the area located between Mozambique and the Drakensberg escarpment. The SRI displayed that regardless of the implication of legislative frameworks for water resource management restructuring and environmental flows (see definitions section) since 1998, the rivers in the Lowveld of South Africa have been decreasing in quality and quantity, in spite of political efforts and dedication (Pollard and du Toit, 2011a).

Thus, water resource management has become of utmost importance to ensure that water users still receive an adequate supply, while at the same time the environmental flows are managed. Surface and groundwater processes have typically been studied as separate disciplines, regardless of their obvious association. More recently there has been a considerable development in the literature combining these into the science of groundwater-surface water interactions, resulting in an integrated water resources system (Ransley et al., 2007).

Groundwater and surface water are both components of the hydrologic system however, they are not isolated components and interact in a range of climatic and physiographic landscapes. Thus, the contamination, over usage or development of one affects the other. Consequently, a better understanding of the primary principles of the connectivity between the groundwater and surface water is essential for the successful management of water resources (Sophocleous, 2002).

Recent research in the Kruger National Park (Riddell et al, 2015) focused on the so-called *Supersites* (un-manipulated sites) that were established to monitor the ecological processes and connectivity of these processes within a savanna landscape. Knowledge obtained from these sites would then be used by management in order to improve supervision of savanna systems and allow extrapolation of knowledge to the rest of the Kruger National Park.

They developed a conceptual framework specifically for savanna landscape classification. This was based on the principle that the temporal and spatial distribution of water at different scales is the primary driver for ecological and geomorphological processes within these landscapes, additionally these will provide recurring effects on hydrological processes. There is a close connectivity of hydrological, geological, and ecological processes within the Lowveld savannas of Limpopo province, which resulted in the formation of distinct landscape patterns over millions of years. The different hydro-geo-ecological processes provided a distinct hierarchy of ecological patches, resulting in the management of the ecological variability within a system. The project ended with numerous recommendations for the conservation management of the Kruger National Park. One of these recommendations was that the management of the catchment area was the most essential, seeing as the ecological processes are interconnected on a complex level in such a pristine area (Cullum and Rogers, 2011).

Similar to the Supersite project the aim of this project will be to develop a conceptual model of the study site and determine the groundwater – surface water interaction with the intention to provide information for successful management of water resources within South Africa.

This is important, as South African and international water resource managers have gained a lot of knowledge from ecological principles for instance SAM (Strategic Adaptive Management) in their IWRM (Integrated Water Resource Management) frameworks. SAM indicated the importance of river flow variability especially when meeting environmental water necessities (Ridell et al., 2014).

1.2 AIMS AND OBJECTIVES OF THE PROJECT

The main aim for the South African Environmental Observation Network (SAEON), is to provide dependable information and data concerning environmental change within

the long term. It accomplishes this by establishing and maintaining long term environmental observation systems within South Africa.

Thus, this specific study site will be used for long term monitoring of the hydrological, geological, and ecological processes and attract an array of non-manipulative ecological research. Environmental change is best monitored through long term observations, because of the ever-present entropy, as well as the variability found within natural systems.

Because the study site overlaps agricultural areas, as well as protected areas it provides an ideal environment for further research on comparing these two areas. On this basis the project attempted to conceptualise the short-term connectivity of geohydrological processes and the interaction with the surface hydrology (perennial Letaba River). Meanwhile this also provides a basis for long term monitoring.

Because of our limited understanding of groundwater – surface water interaction within catchments, especially within the Kruger National Park, it is of utmost importance to obtain further knowledge on this subject. As, this will provide the necessary information needed by the water resource management within the KNP, as well as within South Africa to ultimately provide better management of this sparse resource in terms of environmental flows and protecting/determining the Reserve.

Thus, this study will be aimed to provide a better understanding of the groundwater – surface water interaction within the catchment, providing information for water resource management, helping them to make knowledgeable recommendations in the future.

Ultimately a conceptual model will be developed to indicate the connectivity between the surface hydrology of the Letaba River and the surrounding geohydrological processes.

1.2.1 Main aim

The main aim of this dissertation is:

- Conceptualisation of the connectivity of groundwater – surface water interaction within the Letaba River.

1.2.2 Key objectives

The key objectives of this dissertation are:

- To characterise spatial temporal interaction between the aquifer and the Letaba River.
- To determine groundwater flow paths and their interaction with the Letaba River.
- To determine changes in groundwater flow paths and their interaction with seasonal variability.
- To determine the aquifers reaction during rainfall events, as well as during high flow events.
- To develop a conceptual model of the study site that illustrates the function and behavior of the groundwater – surface water interaction.

1.2.3 The key questions to achieve the objectives are:

What is the reaction of the groundwater's hydraulic head gradients during the hydrological season?

What are the geological and geohydrological characteristics of the study site?

How do the isotopic analyses, pumping tests, fluid logs and groundwater fluxes interpret the groundwater – surface water interaction?

What is the groundwater flow paths associated with?

What is the reaction of groundwater flow paths with seasonal variability and during high flow periods?

How does the chemical base flow separation technique interpret the groundwater – surface water interaction?

What do the findings state to groundwater management?

Chapter 2 - LITERATURE REVIEW

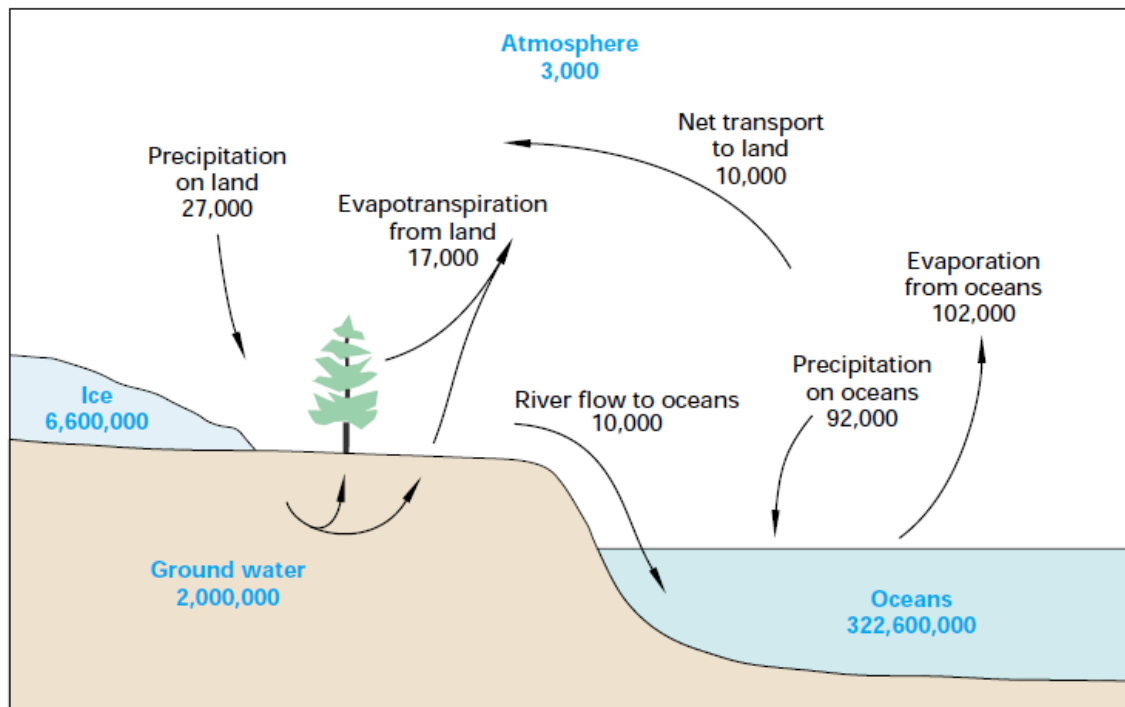
The purpose of this chapter is to provide the theoretical foundation for groundwater – surface water interaction on which this study will be based and provide information on similar research done on this subject. A section explaining the methods used for groundwater-surface water interaction quantification is discussed within this chapter. A section on the literature review of the data collection methodology used will also be included within this chapter.

2.1 BASIC PRINCIPLES OF GROUNDWATER – SURFACE WATER INTERACTION

The hydrologic cycle is used to describe the continuous movement of water on the Earth's surface (surface water), as well as the movement of water below the Earth's surface (ground water). Surface water normally occurs in the form of streams, wetlands, pools, lakes, ice and snow. Whereas groundwater is found within fractures, pores and cavities within rock and soil located below the water table (Winter et al., 1998).

Since the movement of water below and on the surface of the earth is part of a cycle, each component will be linked to each other (to a certain degree) and dependent upon one another, in order to be sustained. This is definitely the situation with surface water and groundwater interaction, as they share the same interface. Even though the groundwater – surface water connection is scientifically recognised, the acknowledgement of it is limited (Mace et al., 2007).

The hydrologic cycle is normally displayed as a highly simplified diagram that portrays only major transfers of water between oceans and land masses (Figure 2.1). It is of utmost importance to view the hydrologic cycle at a wide range of scales while assuming a great deal of variability in time and space, in order to truly understand the hydrologic processes and to manage water resources. An example is precipitation, which occurs almost everywhere, although the distribution is highly variable. The relative scale of the individual components, for example transpiration, can differ significantly even at a small scale (Winter et al., 1998).



Pools are in cubic miles
Fluxes are in cubic miles per year

Figure 2.1 Of the four main pools of water located on Earth, groundwater is the second smallest with river flow to the oceans as one of the smallest fluxes. Nevertheless groundwater and surface water are the components of the hydrologic cycle that we utilise the most (Winter et al., 1998).

The theoretical landscape displays in a simplified manner the interaction of groundwater and different types of surface water sources, for instance lakes, streams, wetlands and numerous other terrains from the mountains to the oceans (Winter et al., 1998), see (Figure 2.2).

Normally the movement of water on the earth's surface and within the atmosphere can be visualised relatively easily, as you can physically see the movement, thus it is generally difficult to visualise the movement of groundwater where you cannot see the movement (Winter et al., 1998).

Groundwater – surface water interaction occurs where groundwater discharges to a surface water body, where surface water discharges into groundwater, or where groundwater emerges at the surface. Within arid and semi-arid regions, surface water systems in return represent important zones of recharge to groundwater. Water that moves from the groundwater to the surface water includes base-flow and spring flow to surface streams and lakes (Mace et al., 2007; Saayman et al., 2004).

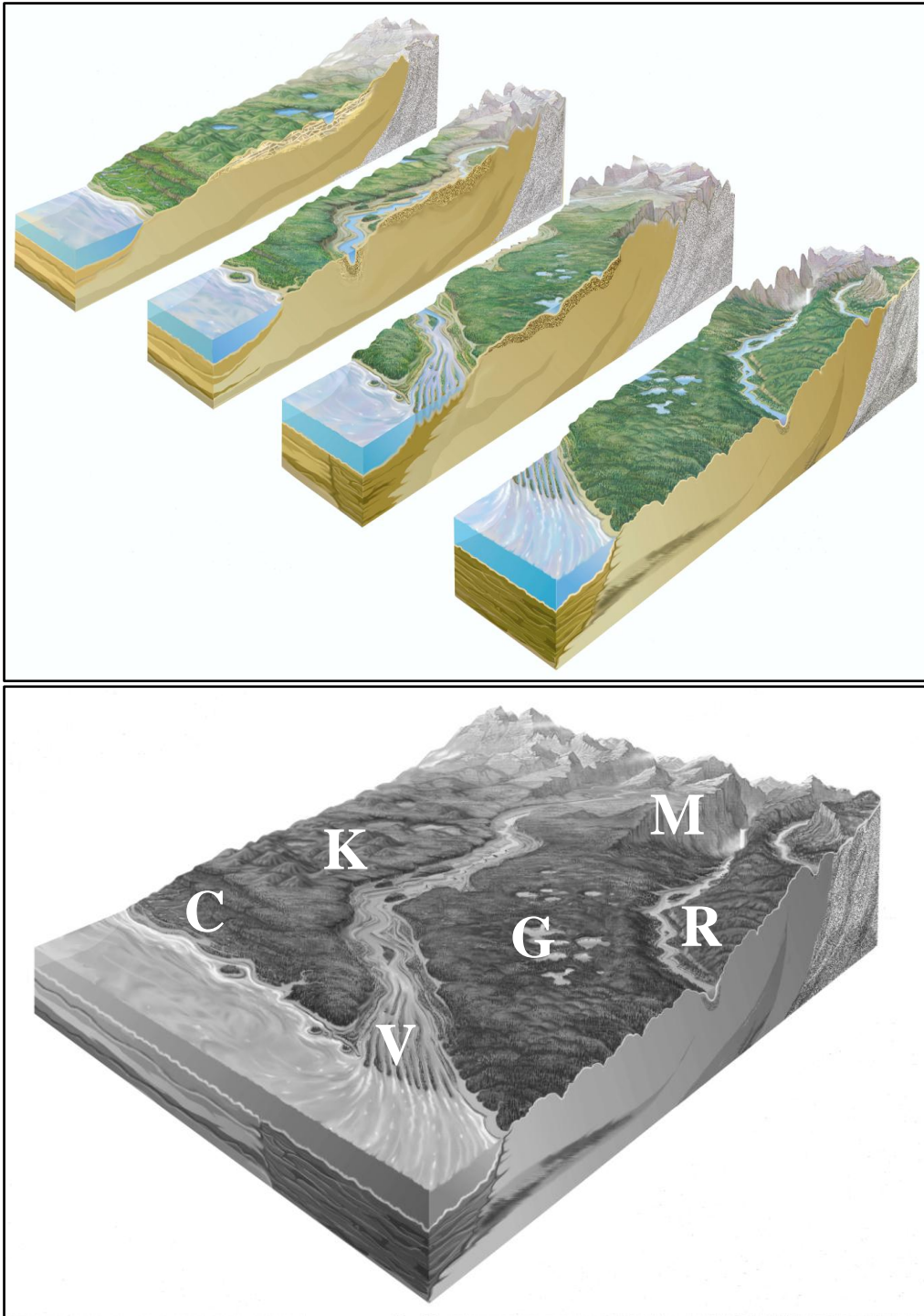


Figure 2.2 Groundwater – surface water interaction within landscapes from mountainous areas to an ocean, within a theoretical landscape. M, mountainous; K, karst; G, glacial; R, riverine (small); V, riverine (large); C, coastal (Winter et al., 1998).

2.2 DIFFERENT TYPES OF GROUNDWATER INTERACTIONS WITH STREAMS

Groundwater interacts with streams in many different ways depending on the type of landscape. The interactions can be divided into 3 basic types of interactions namely; gaining streams (influent), losing streams (effluent) or it can be gaining in some reaches and losing in other. A gaining stream receives water from the inflow of groundwater through the streambed (Figure 2.3A). Whereas, a losing stream loses water to the surrounding groundwater, by outflow through the streambed (Figure 2.4A). In order for groundwater to flow into a stream channel, the level of the groundwater table surrounding the stream must be higher than that of the stream, resulting in a hydraulic gradient towards the stream. Equally, for a stream to be a losing stream its level must be higher than the surrounding groundwater table's level, resulting in a hydraulic gradient away from the stream. The contours of the water tables can thus, be used to determine if the stream is losing or gaining. If the contours point in an upstream direction it is indicative of a gaining stream (Figure 2.3B), whilst contours that point in a downstream direction are indicative of a losing stream (Figure 2.4B) (Winter et al., 1998).

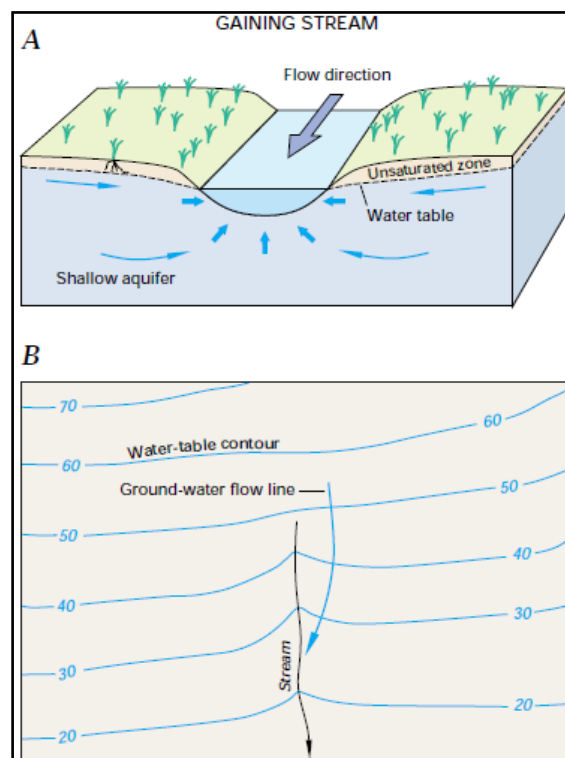


Figure 2.3 Gaining stream (A). Water table contours used for gaining or losing stream determination (B) (Winter et al., 1998).

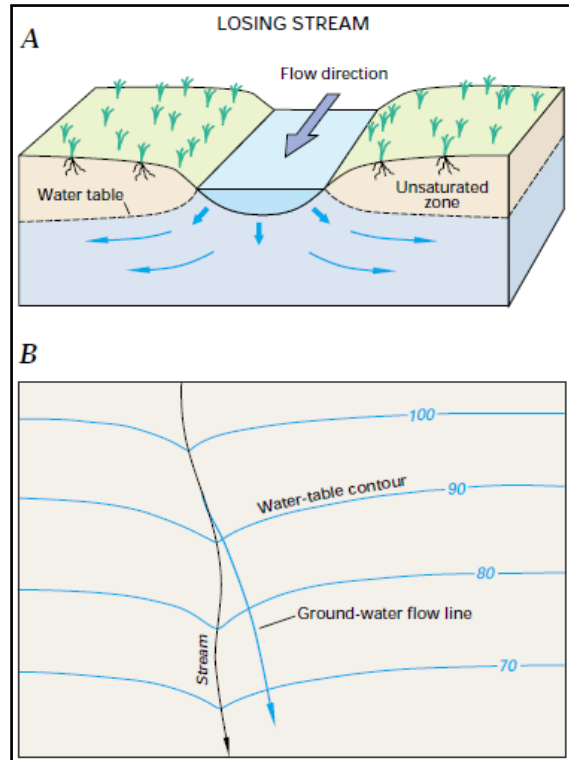


Figure 2.4 Losing stream (A). Water table contours used for gaining or losing stream determination (B) (Winter et al., 1998).

Additionally losing streams can be connected to the groundwater through an incessant saturated zone or it can be disconnected from the surrounding groundwater through an unsaturated zone (Figure 2.5). If the rate at which water moves through the streambed and unsaturated zone is faster than the rate at which lateral groundwater moves away from the water table, the water table can be at a noticeable depth below the stream (Winter et al., 1998).

In some environments a stream gain or loss can be continual. However, this is not always the case where a single stream may alternate between losing and gaining interactions over numerous sections of the stream. In addition, flow directions can also vary in extremely short time frames from the influence of a single, recharge at the stream bank, transpiration of groundwater from vegetation at the stream bank, or temporary flood peaks. At one stage or another rapid rise in stream level will occur, resulting in water moving from the stream into the stream banks. This process is called bank storage (Figure 2.6 and Figure 2.7B) and is normally caused by high rainfall events, swift snowmelts or a rapid release of water in an upstream reservoir. If the rise in water level within the stream does not flow over the stream banks, most of the water

that entered the stream banks will return within a few day or weeks. This tends to act as a buffer and reduces peak discharges in the river. If the rainfall is severe and the stream overflows its banks, widespread recharge of the groundwater will take place (Figure 2.7C). If this occurs the time it takes the newly recharged groundwater to reach the stream again can be weeks to even years, because of the much longer lengths of the groundwater flow paths compared to local bank storage (Winter et al., 1998).

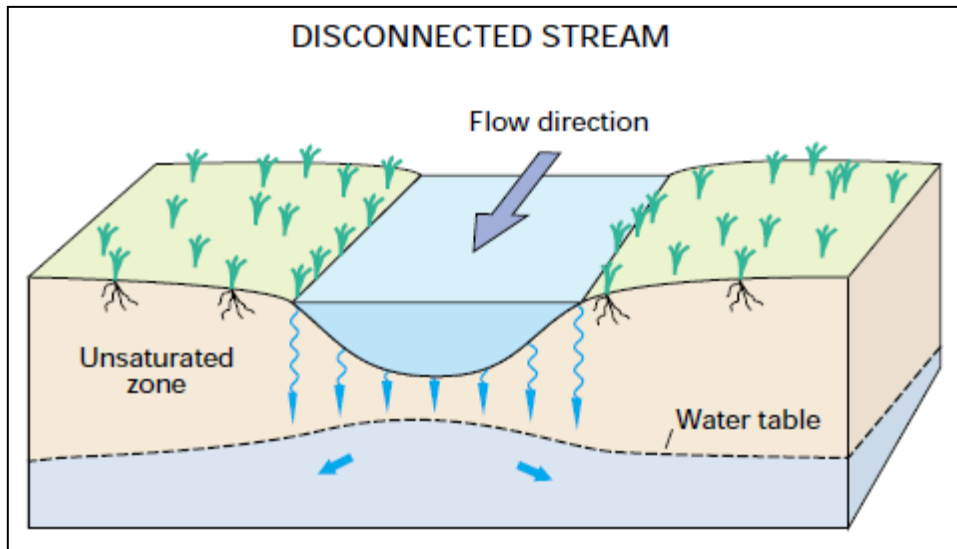


Figure 2.5 Disconnected stream separated from the groundwater system (Winter et al., 1998).

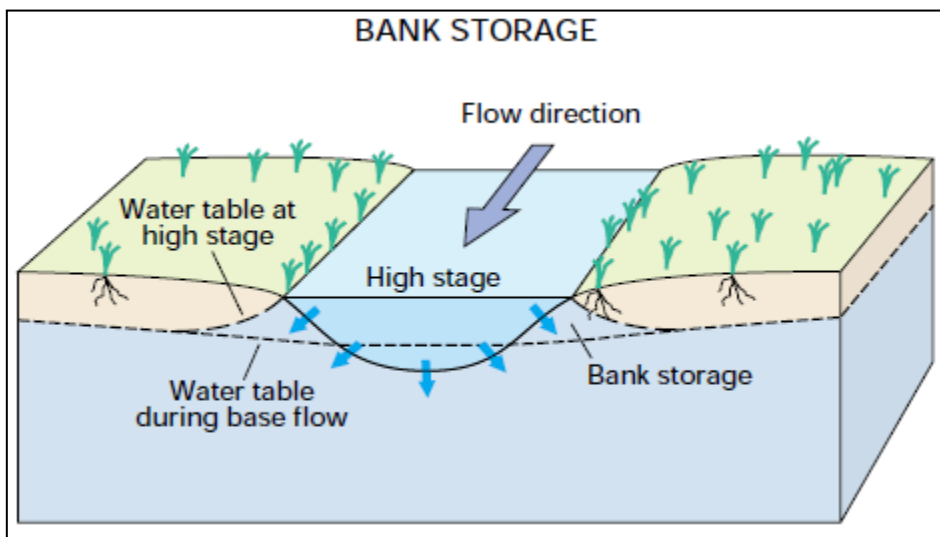
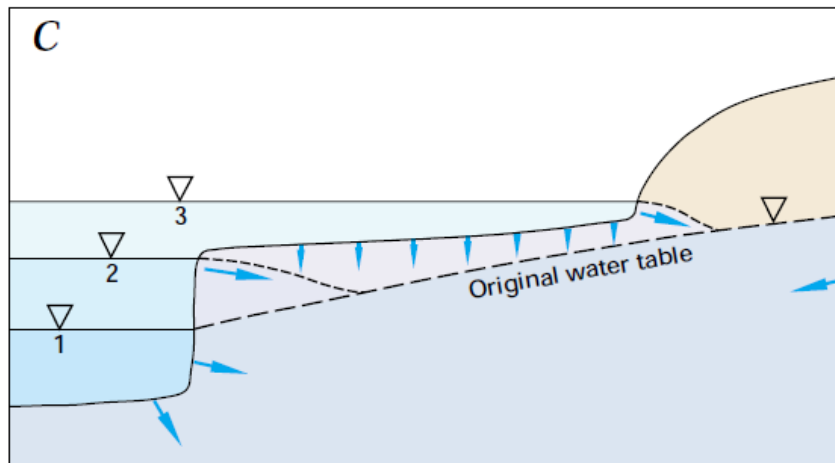
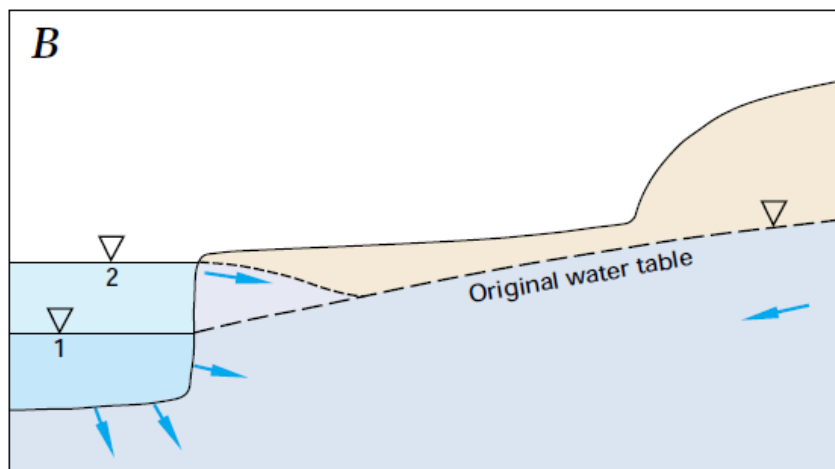
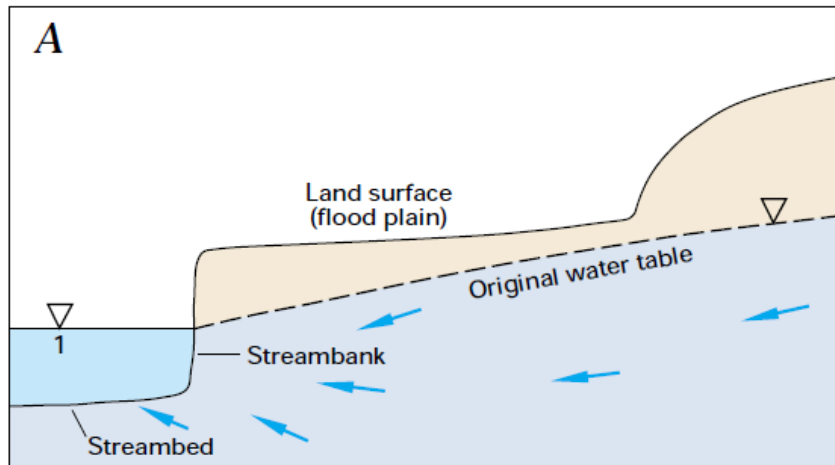


Figure 2.6 Bank storage from the increase in stream level (Winter et al., 1998).



EXPLANATION

- ▽ 1 ▽ 2 ▽ 3 Sequential stream stages
- ➔ Approximate direction of groundwater flow or recharge through the unsaturated zone

Figure 2.7 Floodwaters will recharge the groundwater if the stream levels rise higher than their banks (Winter et al., 1998).

2.3 RIVERINE LANDSCAPES

Groundwater – surface water interaction within river valleys is influenced by the interchange of regional and local groundwater systems and rivers. Other influential factors include flooding of the river and evapotranspiration through vegetation. Smaller streams usually receive their groundwater inflow mainly from the local groundwater system (Wenninger et al., 2008; Tetzlaff et al., 2010; Winter et al., 1998).

Thus, it is common for smaller streams to display a gaining or losing stream that varies depending on the season. Given the low rainfall in arid and semi-arid environments the consideration of localised hydrological flow processes found within a catchment would present insight as to how precipitation is dispersed, water storage as surface water, vadose zone and groundwater systems (Wenninger et al., 2008; Tetzlaff et al., 2010; Winter et al., 1998).

Larger rivers tend to show a groundwater – surface water interaction that is more spatially driven than those found within smaller streams. The regional groundwater system will discharge to the river as well as numerous locations along the flood plain (Figure 2.8) (Ochoa et al. 2013; Winter et al., 1998).

When terraces are located within the alluvial valley, each terrace can be associated with the local groundwater system. These shallow groundwater systems tend to be a key determinant of hydrological resilience facing climate variability (Ochoa et al. 2013; Winter et al., 1998).

In addition to the groundwater discharge distribution found within the valley, flooding also plays an effective role. During a flood water will move into the groundwater system as bank storage. This movement can occur through the river bank as lateral flow or as vertical flow through the flood plains (Winter et al., 1998).

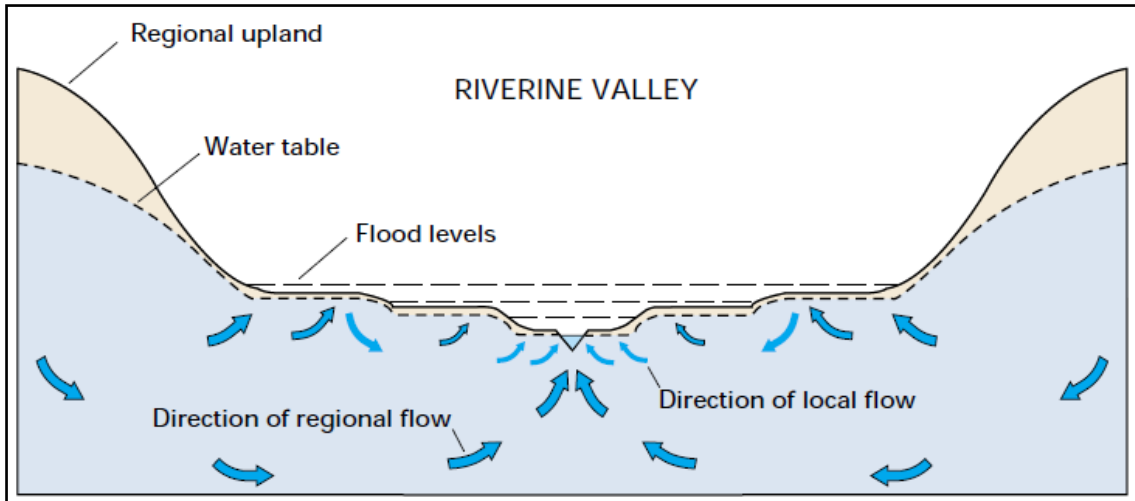


Figure 2.8 In wide river valleys, local groundwater systems overlie larger regional groundwater systems. Seasonal flood events further increase the already complex river hydrology (Winter et al., 1998).

2.4 METHODS USED FOR GROUNDWATER – SURFACE WATER INTERACTION

There are numerous methods that can be used to identify, quantify and monitor groundwater – surface water interaction. It is important to remember that the method used will greatly depend on the study purpose and methods chosen will have to be appropriate for the specific area and conditions. Some of the different methods are briefly discussed below.

2.4.1 Direct measurements of water flux

Lee (1977) proposed bag-type seepage meters that consists of a bottomless cylinder that is vented to a deflated plastic bag. The bottomless cylinder is twisted into the sediment, while the water flows from the groundwater to the surface water; it is collected in the plastic bag. After the volume is collected, the cylinders cross-sectional area can be calculated, as well as the collection period of the seepage flux. Where surface water is seeping into the sediment, a known volume of water is filled into the plastic bag before the installation. The infiltration rate is then calculated from the volume loss (Kalbus, 2006).

Despite the simplicity of the bag-type seepage meters, their performance is far from simple. The problem occurs where water flowing over the bag will affect the hydraulic

head within the bag, or the bag can become distorted and folded leading to decreased/increased flux measured by the seepage meter. Since then numerous types of automated seepage meters have been developed to overcome these problems (Murdoch et. Al, 2003)

The bag-type seepage meter is a method that has been used comprehensively within streams, reservoirs, lakes, dams and estuaries (Isiorho and Meyer, 1999 and Landon et al., 2001).

2.4.2 Heat tracer methods

The difference in temperature between surface water and groundwater can be applied to locate where groundwater discharges or recharges from the stream and calculate water fluxes that occur at the groundwater – surface water interface. The temperatures of groundwater are normally stable throughout the year, whereas stream temperatures can vary drastically on a daily and seasonal basis. Thus, if the river is a gaining stream the temperature of the sediment will be relatively stable, while at a losing stream the sediment temperatures will be highly variable. This allows the identification of the general character of a flow regime through the recording of the temperatures of sediments that surround a river or stream (Winter et al., 1998).

2.4.2.1 Thermal infrared remote sensing

Thermal infrared remote sensing is used to obtain water temperature measurements of released thermal infrared radiation. This provides a spatial distribution of the top layer of water. The thermal infrared data can be obtained through three conventional methods namely: satellite, airborne and ground. Each method has its own advantages and disadvantages, although as technology develops these seem to change. Since, thermal infrared imaging sensor systems have started to get smaller in size and price; their applications have increased drastically (Handcock, 2012).

Usually thermal imagery is obtained through manned aircrafts or satellites, although they have become expensive with limited flexibility and resolutions. With the development of UAV's or unmanned aerial vehicles, an alternative source for remote sensing has been found. UAV's can provide near-infrared, visual and thermal imagery

at a high temporal and spatial resolution, while providing it at a greatly lower cost than conventional sources (Jensen, 2012).

Even though great success have been obtained through using UAV;s (Jensen, 2012), there are still many challenges in terms of the lack of defined operating rules and licensing issues found in most countries (Handcock, 2012).

2.4.2.2 Stream bed temperatures

Conant (2004) and Schmidt et al. (2006) developed a different approach to calculate water fluxes within a streambed by using streambed temperatures. Within a short time period they measured the temperature differences in a stream bed at many locations. The underlying assumption was that the variations in temperature found in the sediments are because of spatial variations in water flux through the streambed and not to temporal variations during the measurement period (Conant, 2004; Schmidt et al., 2006; Kalbus, 2006).

Heat is an excellent tracer for determining groundwater surface-water interaction, although analysing enormous amounts of raw thermal data can provide many challenges. Fortunately, programs such as VFLUX have been developed for processing raw temperature time series and vertical water flux calculations (Gordon, 2013).

2.4.3 Methods based on Darcy's Law

The methods based on Darcy's Law are normally in correspondence to the methods that are implemented to study groundwater movement in terrestrial aquifers. These methods characteristically necessitate measurements of the components from Darcy's equation (Darcy, 1856):

$$q = -K \frac{dh}{dl} \quad (2.1)$$

where:

dh/dl = Hydraulic head gradient

K = Hydraulic conductivity (m/s)

q = Specific discharge (m³/s)

Darcy's velocity or Darcy's flux is when the specific discharge has the dimensions of a velocity or flux. Groundwater velocity is the flow velocity between two points within an aquifer, observed through for example tracer methods, and includes the porosity of the aquifer.

$$v = \frac{q}{n} \quad (2.2)$$

where:

v = Fluid velocity (m/s)

q = Darcy's flux (m³/s)

n = Porosity (percentage)

Therefore, to calculate water flux variations within the subsurface one would generally need information on the hydraulic conductivity, hydraulic gradient, groundwater velocity and porosity (Kalbus, 2006).

2.4.3.1 Hydraulic gradient

One method making use of Darcy's Law and the hydraulic gradient requires the installation of piezometers directly into the streambed. Piezometers such as pipes or tubes are easy and quick to install and often used for smaller scale applications (Winter et al., 1998).

They are placed into the subsurface in order to measure the hydraulic head differences at a specific point in the subsurface. The differences between the hydraulic heads can be used to determine the local groundwater flow direction between the individual piezometers that were installed in groups. Groundwater movement may be effected by temporal variations, therefore it is of importance that hydraulic head measurements should be taken more or less at the same time, which will represent its contour and flow field maps of that specific time (Winter et al., 1998).

With the assumption of vertical flow beneath the streambed the hydraulic gradient can be obtained from the variation in water level between the piezometer and stream, as well as the distance from the centre of the piezometer screen and the sediment surface (freeze and Cherry, 1979).

2.4.3.2 Hydraulic conductivity

Hydraulic conductivity is required for applications of Darcy's Law for the quantification of groundwater – surface water interaction. There are numerous methods to determine hydraulic conductivity, and selections of these additional methods are briefly discussed here for completeness sake.

2.4.3.2.1 Grain size analysis

By using empirical relations that involves hydraulic conductivity and statistical grain size parameters for example the effective diameter, median and geometric mean, approximations of the hydraulic conductivity can be made according to the distribution from the grain size of sediment samples (Shepherd, 1989).

The sediment structure and stratification of the grain size distribution during determination are destroyed and for this reason these associations yield a hydraulic conductivity value that will not represent the vertical or horizontal conductivity and will not represent the true hydraulic properties of the subsurface (Kalbus, 2006).

Grain size analysis therefore contains valuable information of subsurface materials from which the hydraulic conductivity values are used in order to obtain a first estimation for upcoming applications (Kalbus, 2006).

2.4.3.2.2 Permeameter tests

To perform a laboratory permeameter test a sediment sample can be placed between two permeable plates in a tube. Darcy's law is used to calculate hydraulic conductivity, while the discharge flow moves slowly through the system. For a falling head test the time it takes for the hydraulic head to drop between two points is recorded (Todd and Mays, 2005).

In situ permeameter tests provide helpful point measurements of hydraulic conductivities in the streambeds of sediments, which are quick and easy to perform and useful in the determination of streambeds heterogeneity (Kalbus, 2006).

2.4.3.2.3 Slug and bail tests

In a slug test, a small volume (or slug) of water is suddenly displaced in a well, after which the rate of rise of the water level in the well is measured. From these

measurements, the aquifer's hydraulic properties such as transmissivity or hydraulic conductivity can be determined. (Kruseman and Ridder, 1994).

2.4.3.2.4 Pumping tests

This test is performed to evaluate the productivity of the aquifer according to its response to the abstraction of water. The drawdown is then measured in either at observation wells, the pumped well or in both, with the dip meter as per prescribed time intervals. The drawdown is then measured in either at observation wells, the pumped well or in both, with the dip meter as per prescribed time intervals (Kalbus, 2006).

A step drawdown test is most of the time a single well test. It stresses the aquifer by increasing the rate of discharge at a specific time interval up to a maximum discharge rate. With the information collected the best possible yield for the long- and medium-term use of the borehole can be determined. The rate at which the water is abstracted can be determined by using the slug test recovery data (Kalbus, 2006).

Numerous numerical solutions are available and can be used to determine aquifers parameters from data acquired during a pump test. The analytical techniques that use numerical solutions are pump test definite as well as aquifer and flow specific with indication to certain assumptions and limitations. All of the numerical models are all primarily based on Darcy's law (Kalbus, 2006).

2.4.3.3 Groundwater velocity

Groundwater velocity can be measured by introducing a tracer such as dye, uranine or salt into a borehole. The travel time for the tracer to arrive at the downstream observation well is then recorded. The distance data and travel time can then be used to calculate the groundwater velocity of a specific area (Freeze and Cherry, 1979).

2.4.3.4 Porosity

By comparing the bulk mass density to the particle mass density of a sample, the porosity of a sediment sample can be determined. The water displacement test is used, which are the oven dried mass of the particle mass density, divided by the solid particles volume (Freeze and Cherry, 1979).

2.4.4 Mass balance approaches

The primary assumption of the mass balance approach, in terms of groundwater – surface water interactions, is that any variation in the properties of surface water or any gain/loss of surface water can be traced back to the water source, thus the groundwater constituent can be recognised and calculated. Selected mass balance approaches for groundwater – surface water interaction, include the incremental stream flow method, the hydrograph separation method, environmental tracer methods and solute tracer methods (Kalbus, 2006).

2.4.4.1 Incremental stream flow

Through the measuring of the streamflow discharge between successive rated cross sections, groundwater – surface water exchange can be determined by computing the variation in discharge across the cross sections. Various methods can be used to measure streamflow discharge; this includes the velocity gauging method that deploys any type of current meter (Carter and Davidian, 1968) or gauging flumes (Kilpatrick and Schneider, 1983).

An additional method would be the dilution gauging method, this method uses a solute tracer that is injected into the stream and the tracer breakthrough curves are then recorded at successive cross sections. From these measurements the volumetric discharge can be calculated (Kilpatrick and Cobb, 1985).

2.4.4.2 Hydrograph separation

Through the separation of a stream hydrograph into different runoff components, for example baseflow and quickflow, and then assuming that baseflow represents groundwater discharge into the stream an assessment of the groundwater contribution to streamflow can be observed (Davie, 2002).

In order to correctly execute the hydrograph separation method, the validity of the underlying assumptions is critical. These assumptions are that the hydraulic characteristics of the aquifer can be approximated from records of stream-discharge; that stages of solely groundwater discharge can be dependably identified; and that stream-discharge peaks estimate the extent and timing of recharge events. Additionally, in scenarios where drainage from bank storage, lakes, wetlands, soils, or snowpacks add

to stream discharge, the assumption that baseflow discharge correspond to groundwater discharge may not stand (Halford, 2000; Kalbus, 2006).

2.4.4.3 Environmental tracer methods

Tracer based hydrograph separation by implementing isotopic and geochemical tracers produce information on the spatial and temporal origin of streamflow components. Isotopic tracers which are stable are usually utilised (hydrogen isotopes, oxygen isotopes) to distinguish rainfall event flow from pre-event flow, this is due to the fact that rain water usually has a different isotope composition than that of water which is already in the catchment (Kendall and Caldwell, 1998).

To determine the fractions of water that flows along different subsurface flowpaths, geochemical tracers (e.g. major chemical parameters, such as sodium, nitrate, silica or conductivity) and trace elements are used. The key drawbacks of the tracer abased hydrograph separation method is the similarity in isotope composition of event and pre-event waters and the irregularity of the isotope composition in space and time (Cook and Herczeg, 2000).

The concentration differences of environmental tracers in terms of groundwater and surface water are used to identify and delineate zones of groundwater recharge or discharge. This is only sufficient if there is a significant difference between the signatures. The most generally used stable isotopes are oxygen (^{18}O) and hydrogen (^2H), this is due to the fact that groundwater is generally less enriched in deuterium (see definitions section) (^2H) and ^{18}O than surface water (Hinkle et al., 2001).

Several other geochemical and isotopic tracers have been implemented to study the surface water groundwater interaction, including alkalinity, electrical conductivity, isotopes of radon, chlorofluorocarbons, strontium and radium According to many researchers working with environmental tracers, the most reliable results are obtained by using a combination of various tracers (Cook and Herczeg, 2000),

2.4.4.4 Solute tracer methods

The solute tracer method is generally used to study the stream water interaction with interstitial water within the streambed sediments. The momentary detainment of stream

water in the voids found in sediment or in any other stagnant pockets of water is referred to as transient storage (Bencala and Walters, 1983).

Generally, it is studied by injecting a conservative tracer into the stream, then a model is fitted to the breakthrough curves that yield the determination of the storage zone size and exchange rate. The only problem with this method is that the surface storage and storage in the streambed sediments are lumped together and the identification of the actual subsurface components are often difficult (Runkel et al., 2003).

2.4.9 Discussion

There are many more techniques to measure groundwater – surface water interaction although; only those that are most applicable to the specific study have been discussed above. The methods vary in sampled volume, resolution and the represented time scales. With the investigation of a study site the spatial measurement scales of the various methods have to be considered, in terms of the integration of diverse measurements (Figure 2.9). Detailed information on the heterogeneity of the measured parameters is generally obtained from densely spaced point measurements, although the reaches connecting the measurement locations remains unidentified. Thus, the risk is present to miss extreme values of the parameter distribution, ultimately affecting computed results (Kalbus, 2006).

Frequently the choice of methods will result in a trade-off among resolution of spatial and temporal heterogeneities and sampled volume. Thus, to obtain the best results for groundwater – surface water interaction of the specific site the following methods and parameters were used.

- Hydraulic gradients
- Geological characterisation
- Aquifer characterisation
- Fluid logs
- Environmental tracer method
- Chemical base flow separation

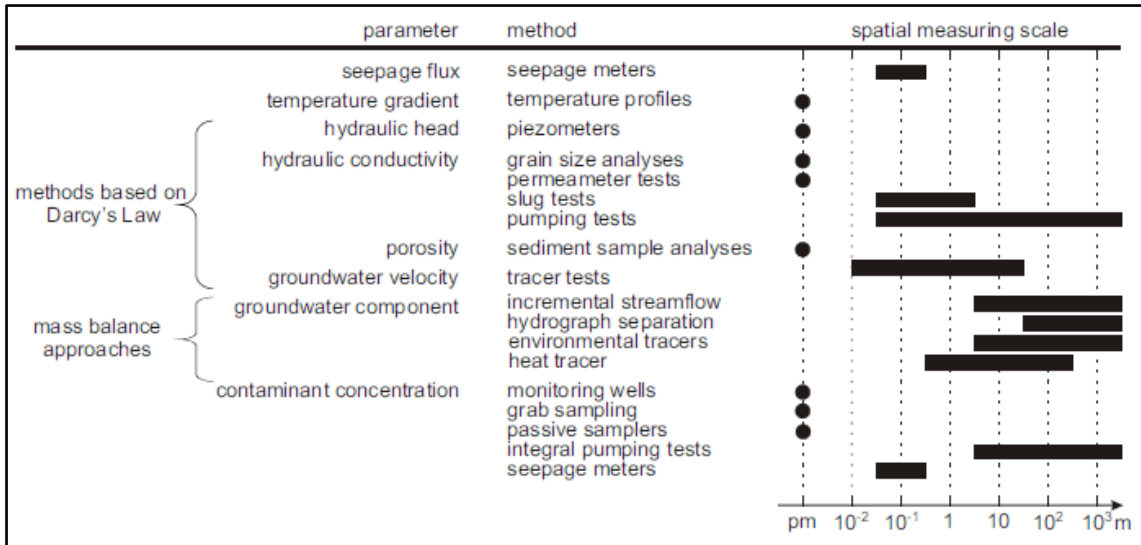


Figure 2.9 Spatial measuring scales of the different methods to measure interactions between groundwater and surface water. The spatial scale is given as radius or distance of influence. Dots represent point measurements (pm), (Kalbus, 2006).

2.5 LITERATURE REVIEW ON METHODOLOGY USED

This section sets out to explain the literature review on the specific methodologies that were implemented during this study. Each method is explained in detail to provide a better understanding of the method, ultimately resulting in a better interpretation of the data obtained.

2.5.1 Magnetic survey method

The main purpose of this method will be to determine the depth and orientation of magnetic structure on the study site to ultimately obtain a better understanding of the subsurface geology and the best location of proposed boreholes.

The instrument that is used for the measuring of magnetic fields is called a magnetometer. These instruments are exceptionally sensitive and are able to measure small differences in the magnetic field of two adjacent rock types. Thus, prominent anomalies can be detected from small dolerite dykes to large magnetic ore bodies (Figure 2.10) (Roux et al., 1980).

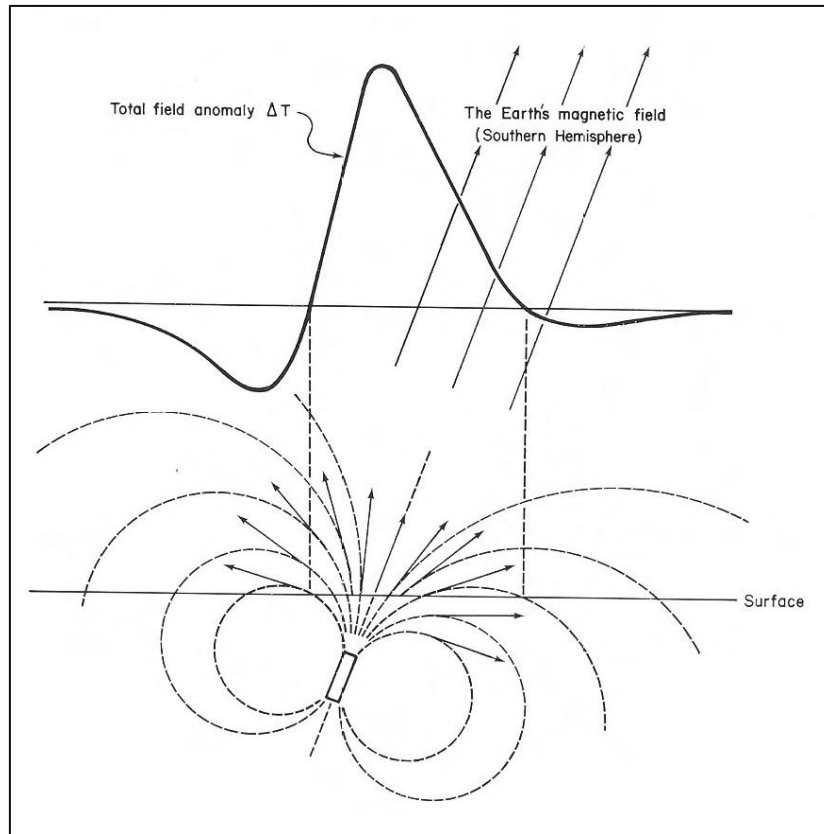


Figure 2.10 Representative of a magnetic body beneath the earth (Roux et al., 1980).

2.5.2 Electrical resistivity method

Similar to the magnetic method the resistivity method will provide information of the subsurface in order to obtain geological knowledge of the subsurface, as well as to provide a best possible location for the boreholes location.

The resistivity method measures the activities of electrical current within the subsurface. The depth of investigation is infinite, as the energy source is artificial. The resolution quality can be interpreted as medium resolution that places it between the gravimetric (low resolution) and seismic refraction method (high resolution) (van Zijl, 1985).

Electrical resistivity data is obtained by sending an electrical current into the subsurface through a pair of current electrodes, measuring the potential drop transversely between a pair of potential electrodes. The depth of penetration is managed by the spacing of electrodes. At each system arrangement the apparent resistivity is formulated on the grounds of the calculated potential drop, electrode spacing and the applied current (Kearey et al., 2002).

To carry out resistivity measurements no less than four electrodes are required (Figure 2.11), electrodes are used as current electrodes (A and B) through which a known current is sent into the subsurface and two potential electrodes (M and N) where the potential difference is measured (van Zijl, 1985).

To calculate the apparent resistivity (p_a) the following formula is given:

$$p_a = \frac{2\pi}{\left(\frac{I}{AM} - \frac{I}{AN}\right) - \left(\frac{I}{BM} - \frac{I}{BN}\right)} \frac{\Delta V}{I} \quad (2.3)$$

where:

p_a = apparent resistivity (ohm-meters).

ΔV = potential difference between M and N (volts).

I = current flowing into the ground (ampere).

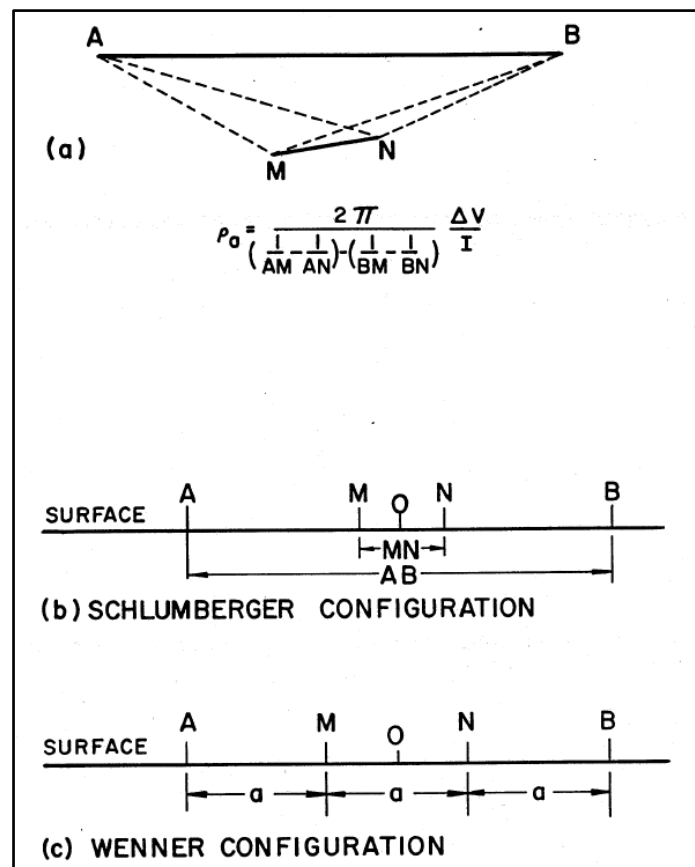


Figure 2.11 Types of arrays, a: Common resistivity electrode arrays that consists of two current electrodes namely A and B, as well as two potential electrodes namely M and N, b: Schlumberger array, and c: Wenner array (van Zijl, 1985).

2.5.3 Borehole drilling

The boreholes not only provide a detailed depiction of the geology at the study site as they are being drilled (borehole logs), but also provide access to the underlying aquifer for further analyses.

According to Moss, 1989 there are two basic drilling systems that are used: the hydraulic rotary method and the percussion drilling method (generally referred to as the cable tool method). In South Africa a combination of the two systems are used, referred to as an air rotary percussion drilling system:

- It is a low costing method that suits the geology of South Africa.
- It can produce good quality samples within unconsolidated formations that are essential for borehole characterisation.
- A greater number of lithologies can be drilled when compared to other drilling techniques.
- Most repairs can be done in the field with relatively low costs compared to other techniques.

2.5.4 Fluid logging

Down hole parameter probes are widely available and reasonably priced, making them a valuable tool for geohydrology. Eh, pH, temperature and electrical conductivity are the main parameters measured for groundwater quality, while rapid measurements of electrical conductivity and temperature can also be taken in monitoring wells (Michalski, 1989).

The resulted logs from the boreholes can provide valuable information that will contribute to an improved understanding of site's geohydrology and assurance check of the monitoring boreholes (Michal ski, 1989).

2.5.5 Slug tests

According to Bouwer and Rice 1976, a slug test can be used to obtain the hydraulic conductivity (K) or the transmissibility (T) of an aquifer in the vicinity of the borehole. However, in South Africa slug tests are implemented only to acquire a preliminary

hydraulic conductivity, as well as a first estimate of a boreholes yield (Q) (van Tonder et al. 2005).

With the slug test the K and T values can be acquired from the rate at which the water level in a borehole will rise after a certain volume of water is rapidly added or removed from the borehole. Slug tests are used because of their simplicity and efficiency, as well as the fact that observation boreholes and pumping of the boreholes are not needed as in the Theis pumping test (Bouwer and Rice, 1976).

The hydraulic conductivity will provide an indication on how easy water moves through the subsurface and the rate at which groundwater in the subsurface will move (Bouwer and Rice, 1976), providing further information on the geohydrology of the area.

For this project the slug test will mostly be used for a first estimate of a borehole yields, however preliminary hydraulic conductivities will also be estimated.

2.5.6 Pumping tests

One of the most fundamental tests that can be done during the investigation of an aquifer is pumping tests. These tests are the only tests that can provide simultaneous information on the hydraulic performance of a borehole, the reservoir and the aquifer boundaries. This is indispensable when determining the aquifer efficiency and for well field management (Kawecki, 1995).

2.5.6.1 Step - drawdown tests

One of the most commonly used pumping tests is the step-drawdown test, especially in the occasion of single wells. They can be used to obtain a variety of information and depend on the aims of the survey. Step- drawdown tests can be used to (Kawecki, 1995):

- Determine the performance of the borehole.
- Evaluate the well losses.
- Calculate the efficiency of the borehole.
- Determine the aquifer parameters.

However, for this project step tests will only be used to determine the boreholes performance to conduct a better constant rate test.

2.5.6.2 Constant-rate pumping test

A constant-rate pumping test, otherwise referred to as constant-rate discharge test, is performed by extracting water from a borehole at a constant rate. This rate is usually determined by the step test. While the constant-rate test is performed the water-level response within the borehole is monitored during and after the test when the pumping is terminated, the latter is termed the recovery test. The data obtained from the monitoring of the drawdown and recovery of the stressed borehole, and any observation boreholes, can then be utilised to provide hydraulic properties of the aquifer and in addition help determine borehole and aquifer parameters such as borehole inefficiency, presence of boundaries, wellbore storage etc. The analytical methods mainly used for analysing constant-rate discharge tests are the straight-line method and type-curve matching (Spane and Vermeul, 1994).

The constant-rate test will provide the final parameters that will be used to describe the movement and characteristics of the aquifer.

2.5.7 Analysis of aquifer test

Step drawdown tests and constant rate tests are a valuable implement that can be used to approximate the long term yield of boreholes. However, the analytical methods that are used for the analysis of these tests are all based on the assumption of drawdown within a borehole are a linear function of the discharge rate (van Tonder, et. al., 2005).

The analytical methods used were derived by Thiem in 1906 and developed by Theis 1936 (Kresic, 2007). These solutions then provided the basis for other analytical solutions for instance Cooper and Jacob (1946), Hantush (1962) and Bouwer and Rice (1976) which formulate parameters for example hydraulic conductivity (K) and transmissivity (T) of an aquifer. These analytical solutions are all supported by the various assumptions, for instance the assumption that the saturated thickness remains constant through the area that is influenced by the aquifer test (Heath, 1983).

2.5.8 Monitoring of groundwater and surface water

In order to perform a water balance real time monitoring data of the groundwater, as well as the river is required to understand the connectivity between the groundwater and surface water (Seago et al., 2007).

The monitoring of groundwater and surface water will also aid in the hydraulic gradient method that estimates groundwater inflow, supported by local aquifer properties, as well as the observed hydraulic gradient among nearby observation boreholes and river gauging stations (AGWF, 2012).

For the monitoring of groundwater and surface water levels dataloggers will be installed within drilled boreholes, as well as in the river. Barologgers will also be installed on site for analytical purposes.

2.5.9 Water sampling of groundwater and surface water

Water samples will be taken to provide information on the hydrochemistry and determination of stable isotope signatures. These can be implemented to divide stream flow into different contributing water sources. The environmental tracers also have the ability to characterise groundwater and surface water interaction and have been described by Swarenski et al. (2001) and Sholkovitz et al. (2003).

2.5.10 Down hole camera investigation

As technology developed in recent years, thus have the use of borehole cameras in hydrologic investigations (Hawkins, 2004). Borehole cameras have been used to determine general borehole conditions, fractures, rock Lithology, possible faults and fracture density to great success (Mack, 1998), (Hawkins, 1996).

They also allow the investigation of drill hole features and conditions that would have been unknown to exist.

These conditions include:

- Pumping systems.
- Bacterial growth.
- Occurrence of foreign objects.
- Presence organisms.
- Historical water levels.
- Entry of gases.

The ability to graphically observe through a camera, can ultimately aid in verifying an observation, despite of the source of the problem (Hawkins, 2004).

2.6 GENERAL ASSUMPTIONS

It is of utmost importance to remember that most methods have assumptions, thus the methods assumptions first needs to be considered before it is interpreted or implemented. Below are the methods used and some general assumptions summarised in Table 2.6

Table 2.6 General Assumptions.

Method	Assumption
Electrical Resistivity Tomography	The materials electrical conductivity is constant within the spacing of current or potential electrodes.
Magnetometry	Magnetisation of certain rock types, as well as the uniformity of magnetisation.
Drilling of boreholes	Borehole construction were done properly, with no leakages and proper seals.
Hydraulic gradients	Water always move to the lowest point.
Groundwater movement	The geology is relatively homogeneous
Fluid logging	Groundwater entering the borehole will have a different temperature and electrical conductivity.
Slug tests	The geology and surrounding area is homogeneous and uniform in thickness.
	Water flows horizontally through the borehole screen.
	Drilling and borehole construction did not alter the hydraulic characteristic of the formation.
	The small area tested at the top of the borehole, represents the entire aquifer.
Pumping tests	The geology is homogeneous, uniform in thickness and isotropic.
	No recharge occurs during the test.
	Only one pump is currently pumping the aquifer.
	Before pumping starts, the groundwater table is horizontal.
Sampling	River samples were taken at the centre of the river to provide a true representative sample
	Sample bottles were washed three times to prevent contamination
	No air were trapped inside the bottle that could alter the sample in any way.
	Rain water samples were taken as soon as possible to prevent evaporation.
Weather stations	Weather stations were not tampered with.
Isotope analyses	The laboratory did proper analyses without any contamination.

2.7 RECENT RESEARCH ON GROUNDWATER SURFACE WATER INTERACTION WITHIN SOUTH AFRICA

The interaction between groundwater and surface water within South Africa has received increasing attention in the last few years, due to its importance to ecological systems and sustainability. Unfortunately many of South Africa's aquifers are within heterogeneous and anisotropic fractured rock aquifers, increasing the difficulty in obtaining accurate data and providing logical interpretations (Levy, 2011).

With the recent light shed on this subject, new and normally overlooked methods for determining this interaction have also been implemented. This includes recent research published by Johan van Tol (2016) that determines groundwater – surface water interaction through hydrogeological interpretation of soil distribution patterns. While research published by Jensen 2012, determined the connectivity through thermal infrared remote sensing with an autonomous unmanned aerial remote sensing platform (refer to section 2.4.2.1).

Van Tol (2016) indicated that soils are an essential part of the hydrological functioning landscape, while groundwater – surface water interaction studies normally do not consider soils as an important component.

However, Madlala (2015) indicated that using only a single method to determine groundwater – surface water interaction is ineffective. He indicated through his study that the use of several methods can provide the foundation for developing practical strategies that will lead to improved groundwater and surface water management (Madlala, 2015).

Madlala (2015) made use of three different methods: base flow separation, predominant hydrochemical facies and differential stream gauging. The study indicated that the upper Berg River catchment relies on subsurface water storage discharges to maintain flows through the dry season. It was also indicated that the particular chemical signature of the contributor is transmitted through surface water infiltration, as well as subsurface water discharge (Madlala, 2015).

Chapter 3 - SITE CHARACTERISATION: GENERAL OVERVIEW

Chapter 3 will describe the general overview of the study site, focussing on the location, hydrology, climate, geology and geohydrology. The study site is located within the Limpopo province, South Africa. It also falls within the Lowveld that stretches from the footslopes of the Drakensberg Great Escarpment in the west to the Lebombo Mountain and coastal plains of Mozambique in the east (Van Niekerk, 2014). The study site partially covers a part of the Letaba Ranch Game Reserve, that border the Kruger National Park without any fencing (Figure 3.1). This relatively pristine location was selected because of the little human interference that occurs, providing a great opportunity for uninfluenced research.



Figure 3.1 Location of study site in perspective to South Africa (www.sothafricatoursandtravel.com, 2017).

3.1 STUDY SITE LOCATION

The specific study site is located on the banks of the Letaba River approximately 45km north of the small mining town of Phalaborwa, Limpopo province, South Africa (Figure 3.2). It lies at an elevation of 340 mamsl at $-23.670925^{\circ}\text{S}$, 31.02864°E . The site covers an area of the Letaba Ranch Game Reserve, Mthimkulu Game Reserve (combined reserve area in the east of the study area). The rest of the site covers numerous small farms located next to the Letaba River (west study area), (Figure 3.3).

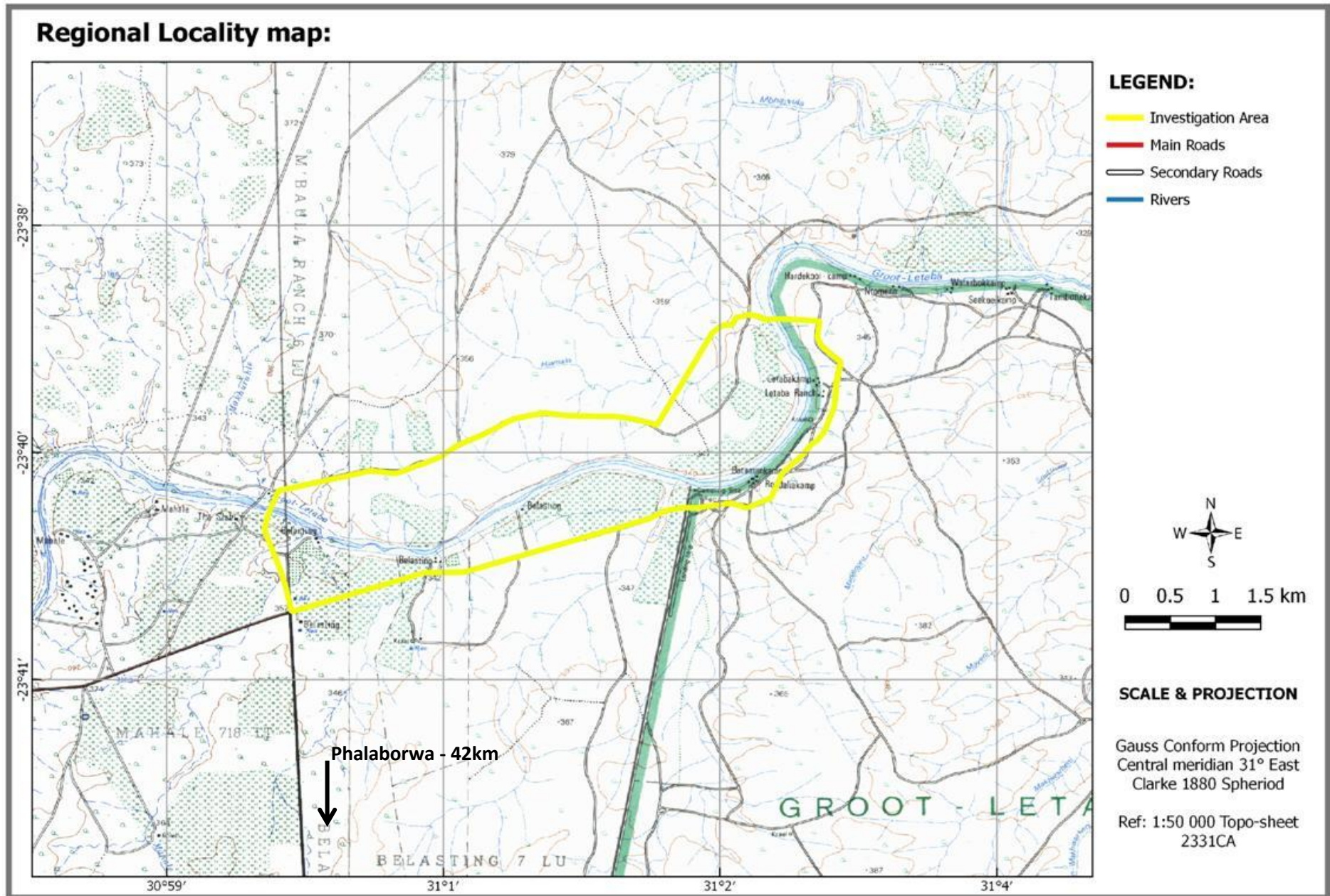


Figure 3.2 Regional locality map of study area (1:50 000 Topo-sheet 2331CA).

Aerial imagery locality map

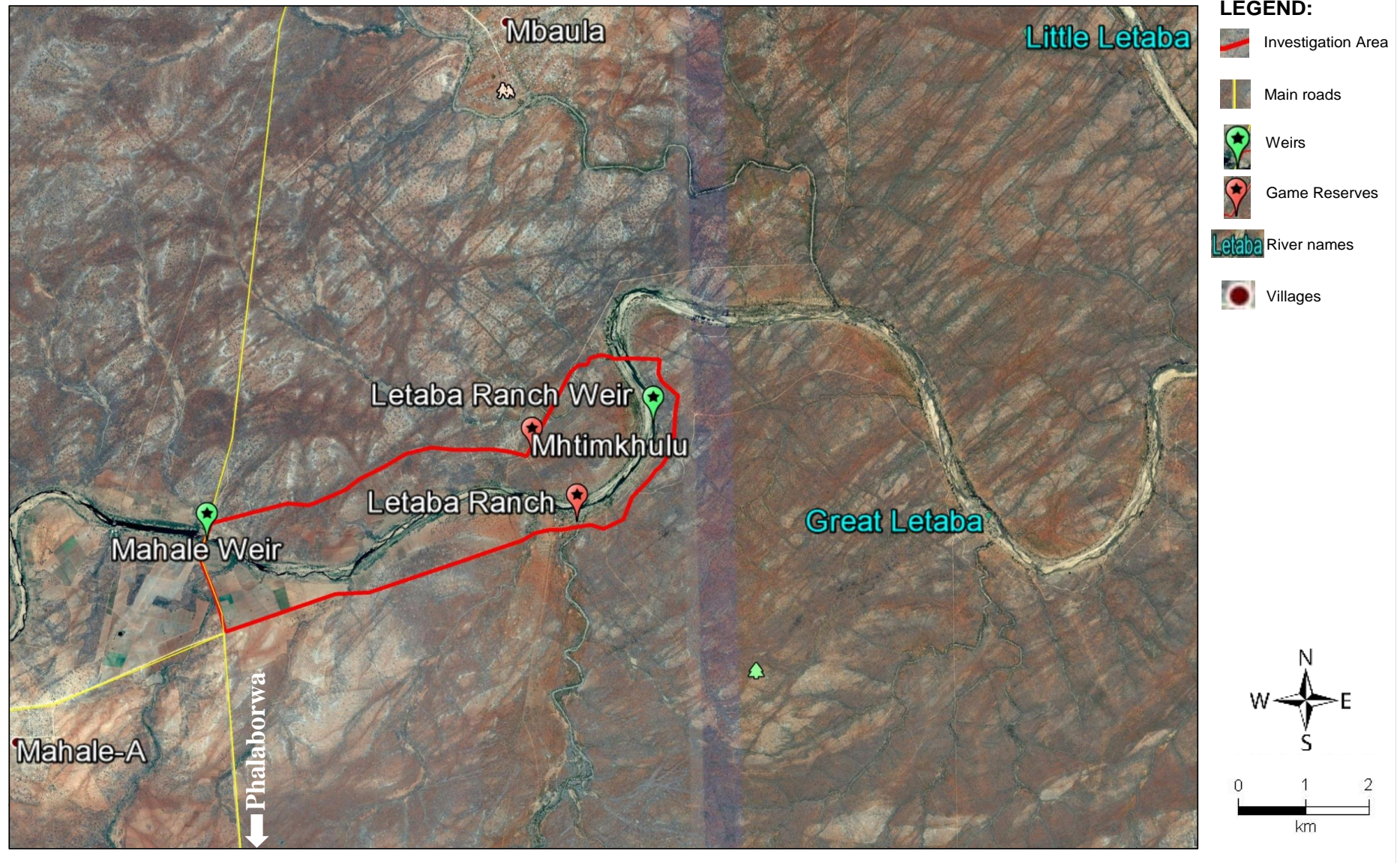


Figure 3.3 Aerial imagery locality map of the study area (Google Earth, 2016).

3.2 HYDROLOGY

The Letaba River falls within the Olifants River Water Management Area (Figure 3.4), and is a good example of a river system that has shown real difficulties for successful water management, because of the uncertainties in the gains and losses within the channel. Excessive water abstraction occurs along the Letaba River often exceeding the available water supply (DWAF, 2006; Pollard and du Toit, 2011).

The catchment can be sub-divided into tertiary catchments B81 (Groot Letaba – containing the study site), B82 (Middle/Klein Letaba) and B83 (Lower Letaba). Further downstream of the Middle Letaba dam, the Middle and Klein Letaba River meets and drains into the Groot Letaba River at the boundary of the Kruger National Park. The specific quaternary catchment that the study site is located in is the B81J catchment area (Figure 3.4) (DWAF, 2006).

The Letaba River catchment drains 13400 km² that stretches from the Drakensberg Escarpment in the west to the confluence with the Olifants River in the Kruger National Park close to the Mozambique border. The Groot Letaba sub-catchment is in itself drained via the Letsitele, Politsi, Molototsi, Thabina, Ga-Selati, Debengeni, Morotshwe perennial Rivers and Groot Letaba River (DWAF, 2006).

3.3 CLIMATE

The catchment falls in a semi-arid environment with summers that can be classified as wet and hot with the average temperatures ranging from 20°C to 33°C and highs of 43°C. Winter conditions are dry with some of the highest winter temperatures in South Africa. Mean annual precipitation (MAP) varies greatly from west to east. This is because mountainous areas are located to the west with a MAP of between 500 – 1200 mm, compared to the Lowveld area with a MAP of between 500 – 700 mm. The MAP of the entire Letaba river catchment is 623.58 mm with a Mean Annual Evaporation (MAE) of 1637 mm and a mean annual runoff (MAR) of 44.32 mm/a (DWAF, 2006). The specific MAP of the study site is 501.8 mm with an MAE of 1700 mm (GRDM, 2013).

The MAE is much higher than the MAP (as in most of South Africa), thus agriculture will require an additional water supply. When this is taken into consideration it becomes

apparent how stressed the catchment is with increasing demands for water security (Pollard et. al., 2011).

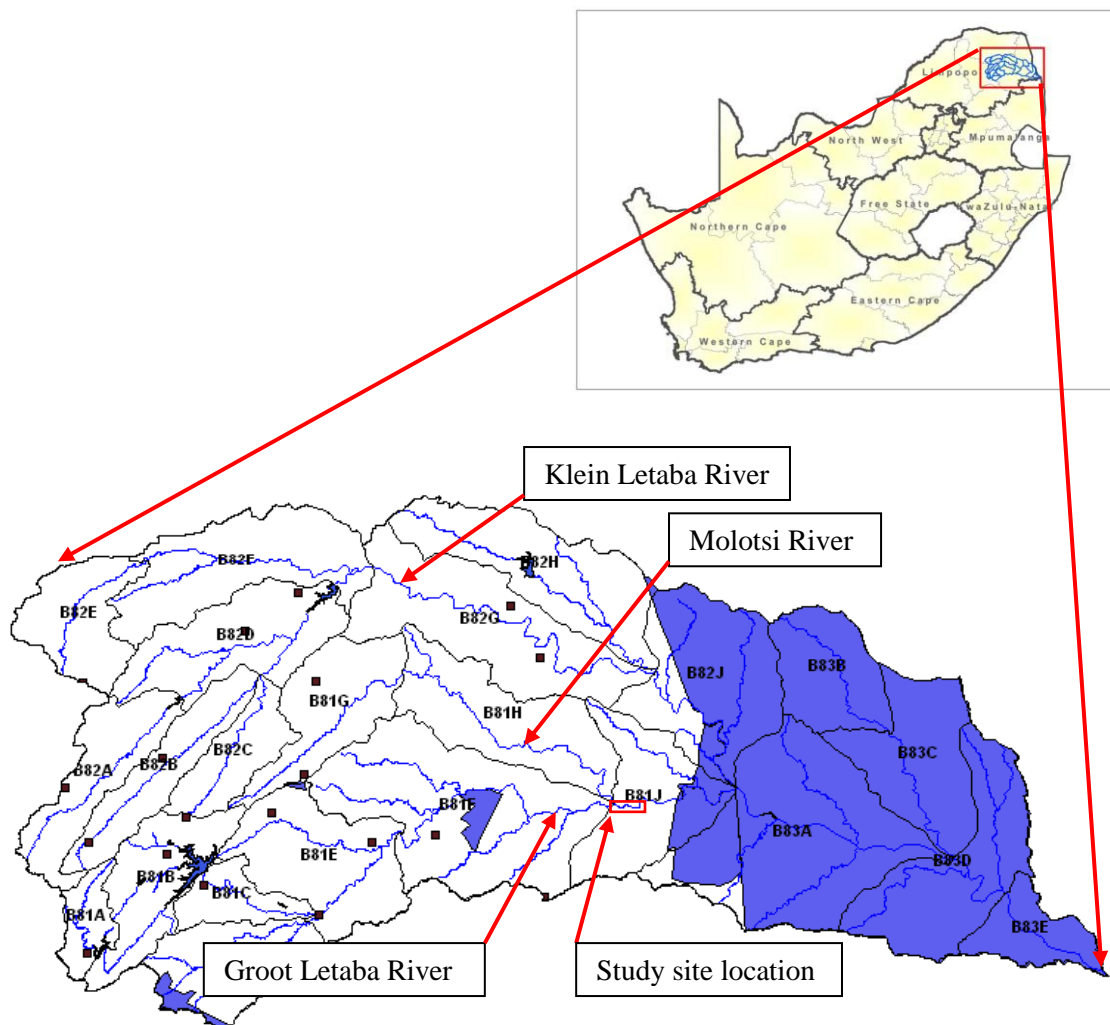


Figure 3.4 Location of the Letaba River Catchment within South Africa (DWAf, 2006), (Blue areas is indicative of protected area, e.g. Nature reserve, National park).

3.4 GEOLOGY AND TOPOGRAPHY

The study area is characterised by relatively flat plains with small gradual hills. The topography area ranges from around 326 mamsl to 354 mamsl. There is a general decrease in topography to the north-east (following the course of the Letaba River), where the river exists the study area. This is correspondingly the lowest part of the study area, while the highest point is located to the north-west (Figure 3.5).

The study site is located within the Granitoid gneisses between the Pietersburg – Giyani greenstone belts and the Murchison greenstone belt (Figure 3.7). These gneisses have

been grouped together and called the Groot-Letaba Gneiss and form part of the Mesoarchaeon intrusions (3200-2800 Ma). Formerly these gneisses were believed to be part of the Goudplaats Gneiss that occurs further north, they stretch from just Southeast of Polokwane towards the Lowveld in an easterly direction, where they overlay the Karoo sediments (Johnson et al., 2006). The Groot-Letaba Gneiss contains a variety of gneisses that include:

- Fine to medium grained tonalite
- Coarse grained trondhjemite
- Minor banded gneisses
- Linear gneisses

Unfortunately (According to Johnson, 2006) individual units have not been delineated. The rocks mainly consist of quartz, biotite, oligoclase and microcline. The accessory minerals are epidote, apatite, opaque and sphene. Foliation is weak, but strongly folded, some gneisses have been migmatized with the occurrence of leucosome bands that are associated with different magma intrusions (Johnson et al., 2006).

3.5 GEOHYDROLOGY

According to the 1:500 000 2330 Phalaborwa map series of the Republic of South Africa (Du Toit, 1998), the study site is specifically situated within an intergranular and fractured rock aquifer. The boreholes within the area typically display borehole yields that range from 0.5 to 2 l/s.

According to DWAF 2006, large groundwater abstraction occurs along the Groot Letaba River valley for irrigation use. This abstraction ranges from 1 to 2 million m³/a. Before the Molotsi River intersects the Groot Letaba River the borehole yields are >5 l/s, where after it decreases to 0.5 - 2 l/s. Numerous dolerite dykes and sills have intruded the granites and gneisses. These intrusive rocks are prone to weather faster than their hosting granites and gneisses. These features will thus ultimately create preferential flow paths for groundwater (DWAF, 2006). The general assumption is that the groundwater table follows the topography of the area, thus the general direction of the groundwater will be towards the river and to the north-east (Figure 3.6).

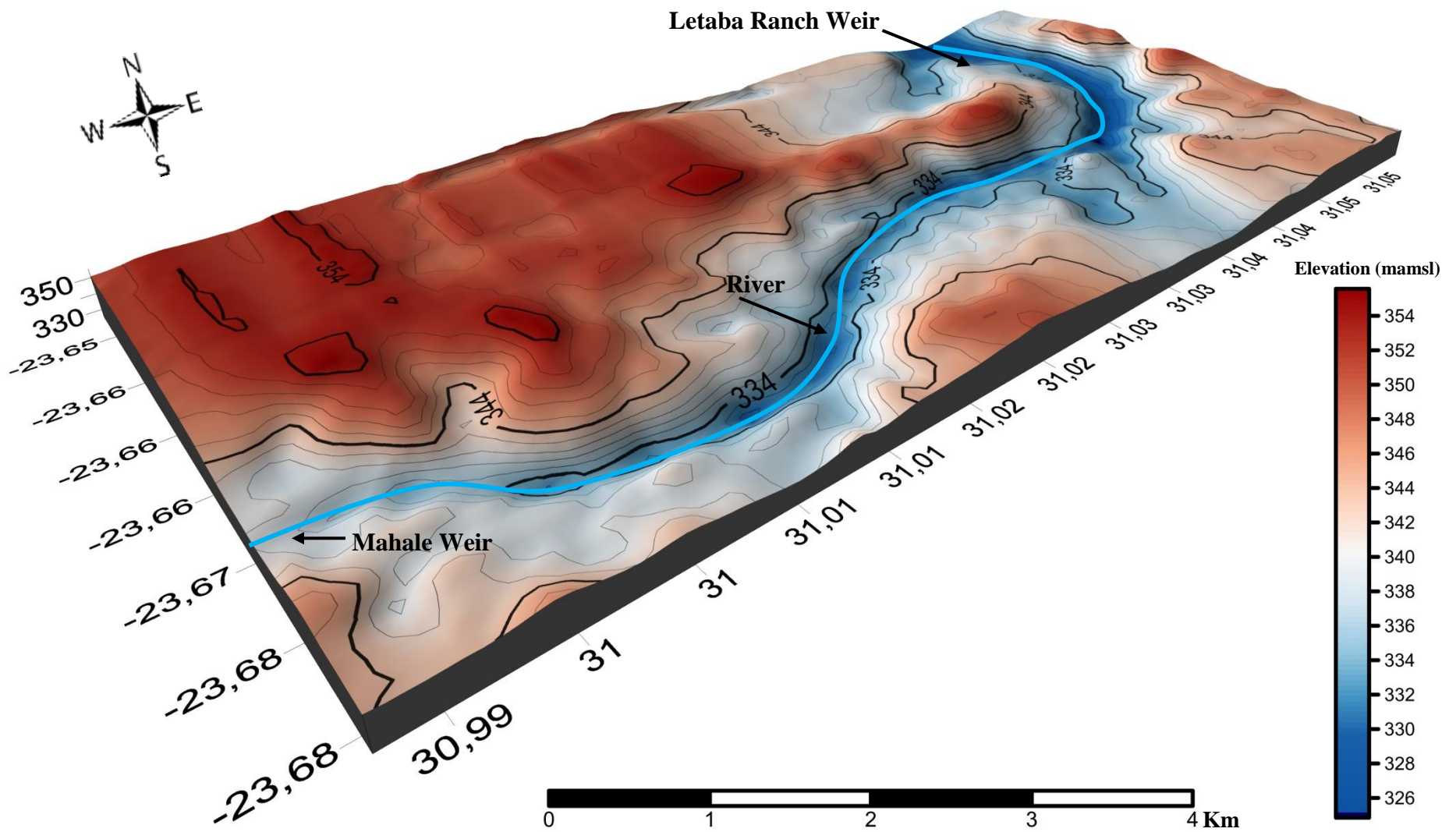


Figure 3.5 Generalised topography of the study area.

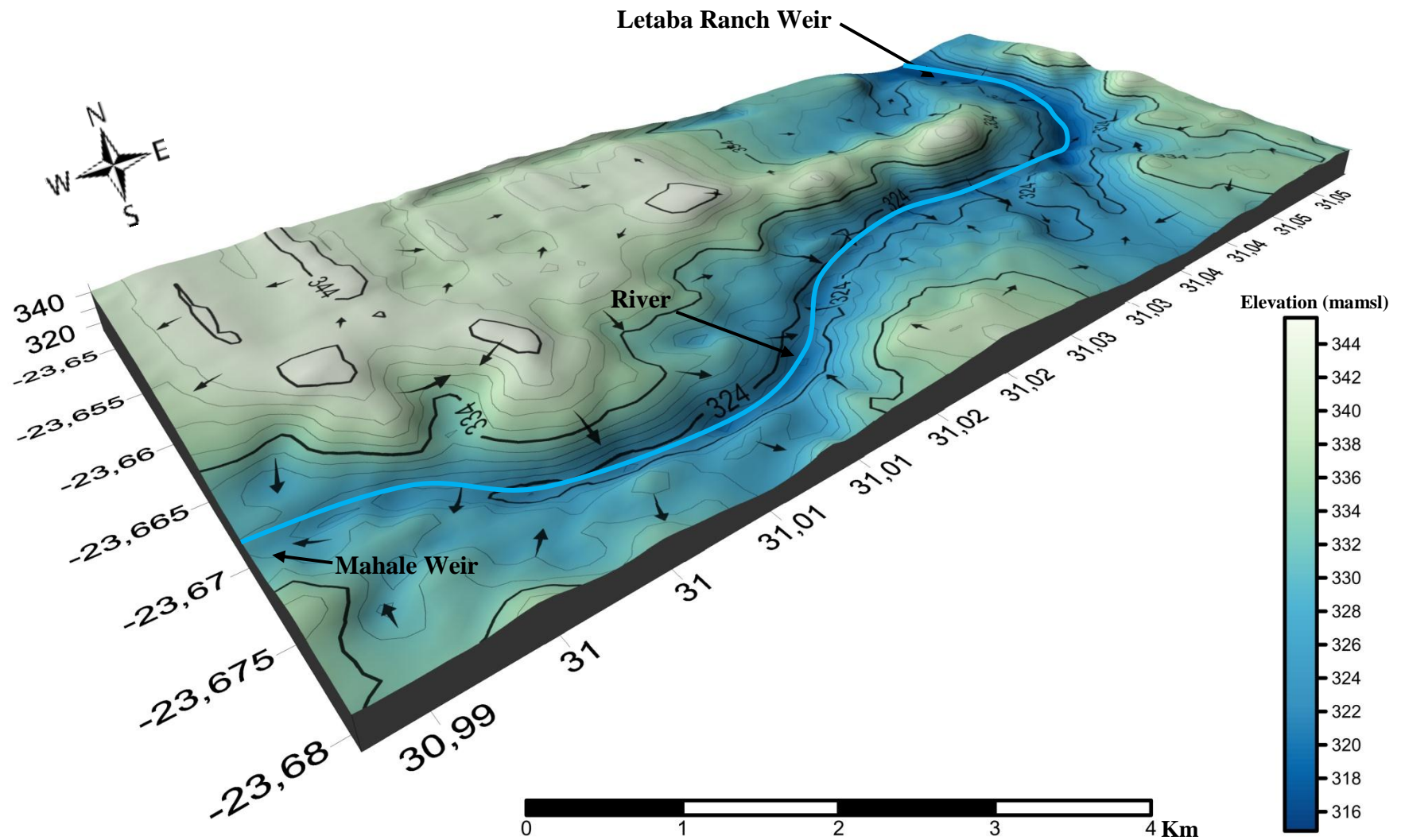


Figure 3.6 Generalised groundwater level of the study area.

Geological map of study site

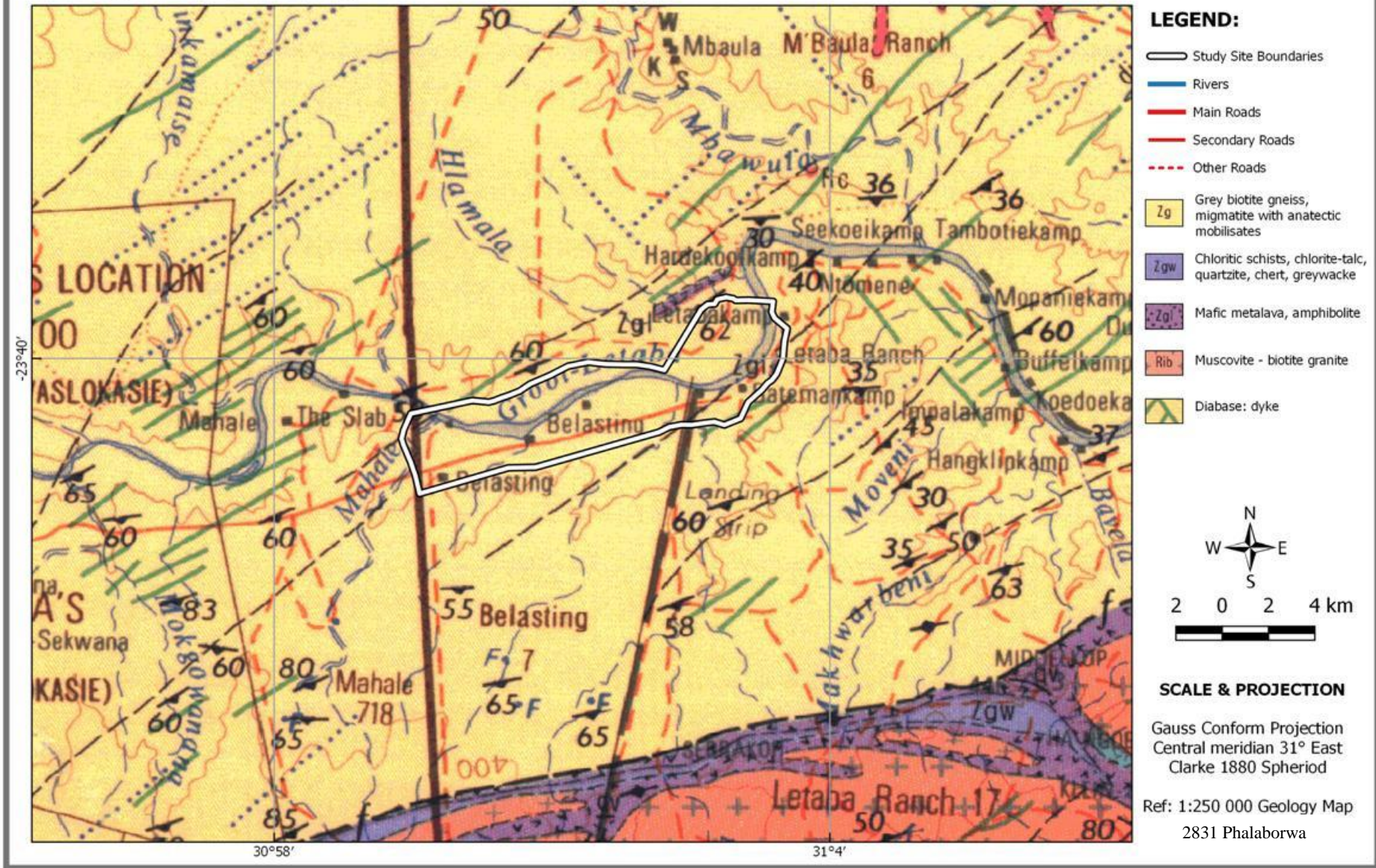


Figure 3.7 Geological map of study area (1:250 000 Geological Map Series 2831 Phalaborwa).

Chapter 4 - SITE CHARACTERISATION: DATA COLLECTION

A reconnaissance study was performed to establish a primary geohydrological conceptual model, because very little data could be obtained from the NGA (National Groundwater Archives). This model was then used to determine the most favourable borehole drilling targets. Different methodologies were implemented to determine the groundwater distribution within the study site, in order to ultimately achieve the study objectives. The position of all relevant transects can be seen in Figure 4.1 and a table displaying all borehole names and relevant information can be seen in Table 4.1.

4.1 HYDROCENSUS

An initial hydrocensus was conducted in Mbaula (a local community north of the study site), to obtain some information on the local groundwater and its abstraction data (refer to Figure 3.2 for Mbaula/Mthimkhulu's location). Data collected through the hydrocensus were borehole depth, static water level, usage, status, pH, Temp, Total Dissolved Solids and Electrical Conductivity. A total of 37 boreholes were identified in Mbaula and 6 within Mthimkhulu. This provided us with an initial indication of the local hydrochemistry within the area.

4.2 GEOLOGICAL SUBSTRATE INVESTIGATION

Two geophysical techniques were implemented to obtain more knowledge on the study site's geology and to determine the ideal location to site boreholes. The techniques were the Electrical Resistivity Tomography and Magnetometry.

4.2.1 Geophysical survey technique

The geophysical technique used was the Electrical Resistivity Tomography (ERT) survey technique and the specific equipment was the ABEM Terrameter (Appendix A-1). The study site was divided into two sections (different land-uses) on which the surveys were completed, the farming area and the protected area (Figure 4.1), and two transects were delineated perpendicular to river flow in each land-use. Furthermore, longitudinal surveys running parallel to the river were also conducted, these were

implemented to obtain knowledge on the subsurface running next to the river for example dykes crossing the area. On all transects the Schlumberger Protocol was applied, because only to current electrodes needs to be moved decreasing the time required for sounding and the electrodes remains in a fixed location, minimising the effects of near-surface lateral variations in resistivity.

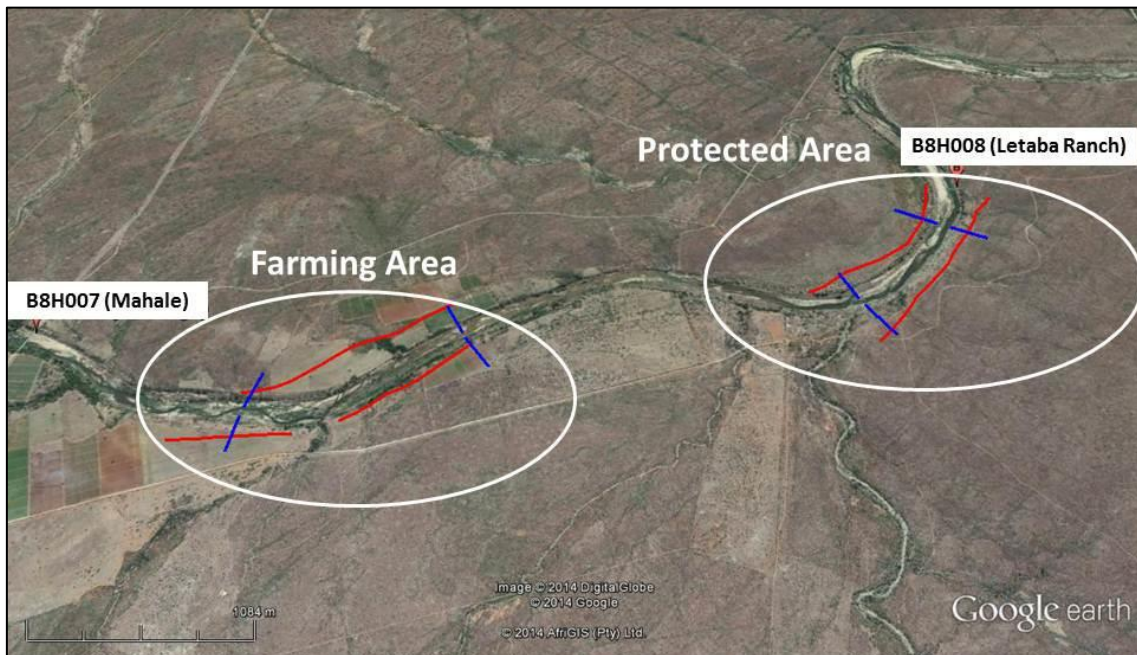


Figure 4.1 Locality map of the geophysics transects over two different land-uses (Ridell, 2016).

(A) Farming Area

On the farming area 4 transects were surveyed (Figure 4.2). Two transects ran parallel to the river (north/south) in an east west direction (red lines). On these transects a minimum electrode spacing of 5 m in the Schlumberger array were used in order to obtain deep resistivity profiles of approximately 70 m. The other two transects ran perpendicular across the river in a north – south direction. On these transects a minimum electrode spacing of 2.5 m in the Schlumberger array were used in order to obtain a shallower resistivity profile of 35 m. Unfortunately, these transects could not run over the river from one bank to another as initially suggested, because of accessibility constraints into the river channel itself. The transects were then split into two, starting at the river bed.

(B) Protected Areas

In the protected area (downstream of the farming area), the geophysical surveys were implemented in a similar fashion to the farming area (Figure 4.3). Two transects ran parallel to the river (red lines) with 5 m electrode spacing for a deep resistivity profile and two perpendicular to the river with 2.5 m electrode spacing for a shallow resistivity profile (blue lines).

Geophysics Transects: Farms

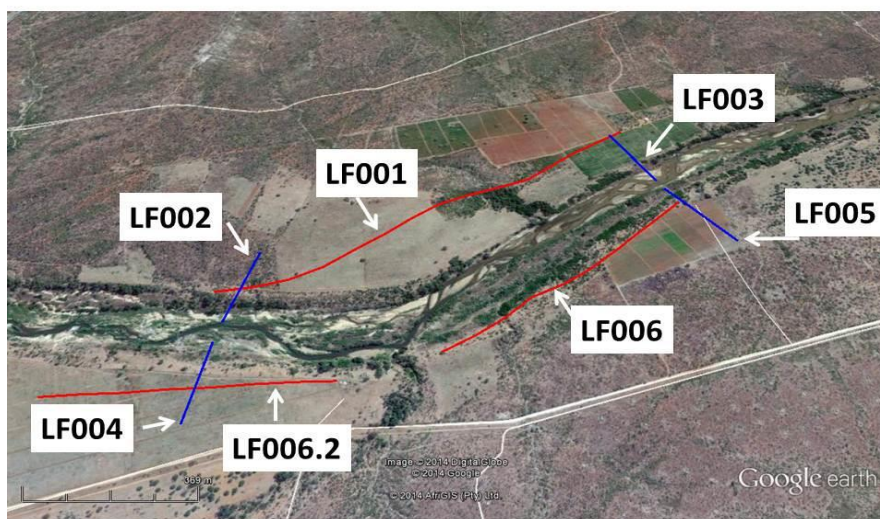


Figure 4.2 Locality map of the geophysics transects the Farms area (Ridell, 2016).

Geophysics Transects: Protected Areas

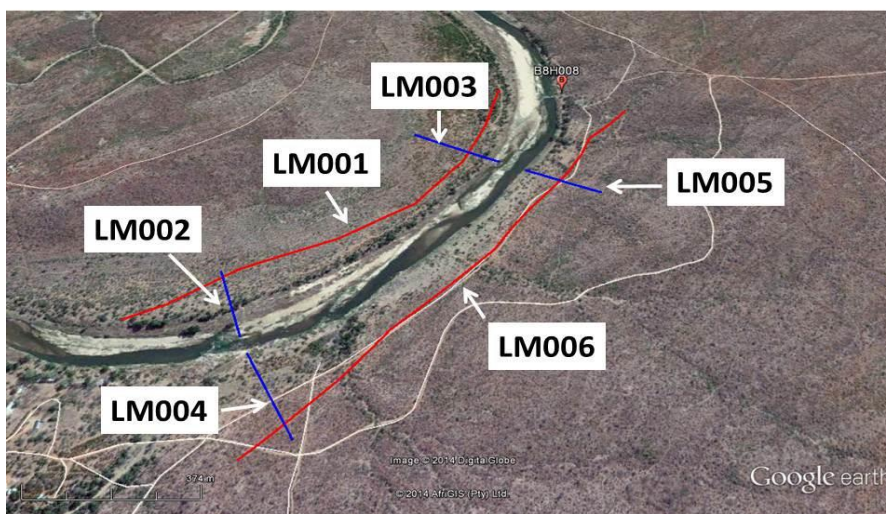


Figure 4.3 Locality map of the geophysics transects over the Protected areas (Ridell, 2016).

4.2.1 Magnetic Survey technique

After the geophysical survey was completed a magnetic survey were also conducted on the same transects. The data was then incorporated and overlaid with the geophysics survey data to confirm possible dyke intrusions, identified within the geophysics data. The specific instruments that were used for the magnetic survey was the Geotron Proton Magnetometer, model G5 (Figure 4.4).



Figure 4.4 Geotron Proton Magnetometer, model G5 used for the magnetic survey (www.geotron.co.za, 2017).

4.3 DRILLING OF SITED BOREHOLES

After the most appropriate positions for the boreholes were identified through the geophysical and magnetic survey, drilling commenced in 2015 by the Limpopo drilling office of the Department of Water and Sanitation, Polokwane. The method used for the drilling of the boreholes was Air Percussion drilling (Appendix A-2). This was favourable as it permitted the collection of detailed information of each geological subsurface material, as well as the water strikes (Appendix A-3), weathering depth and intersection with the consolidated zone.

In total 28 boreholes were sited and drilled in accordance to the piezometric design that is illustrated in Figure 4.6. The purpose of this design was to differentiate the groundwater hydrodynamics between the consolidated or hard rock, which consists of un-weathered rock and the unconsolidated zones or weathered material that consists of fragments of rock and loose material. Thus, almost all sited locations had an A – Deep borehole, ranging from 50 m to 70 m and a shallow borehole next to it in the range of 15 m to 35 m (Appendix A- 4) (Figure 4.6).

Within the deeper boreholes solid casings were installed through the unconsolidated material and into the hard rock (consolidated material). The bottom of the solid casing was sealed off with cement and a gravel pack installed. This was implemented to create a piezometer where the deeper aquifer is sealed off from the shallow aquifer, thus no interference will occur between each other. Shallow boreholes only received 6 m of solid casing, after which perforated casing were installed to the bottom of the borehole.

Only two boreholes differentiate from this design (LRW001/LRW002), as they were installed with only perforated casing. This was implemented, because they were drilled for four different reasons that would require the free movement of groundwater and surface water within the borehole.

- To obtain an accurate reading of the water level within the river macro – channel.
- To compare the water level within the streambed on both sides of a dolerite dyke cutting across the river.
- To obtain a hydrograph during large rain events.
- To observe each boreholes reaction during and after a high flow or flood event.

The position of these boreholes is ideal for the monitoring of the rivers water level and will obtain good data during high flow events that can ultimately be compared to the surrounding boreholes reactions.

Borehole locations map

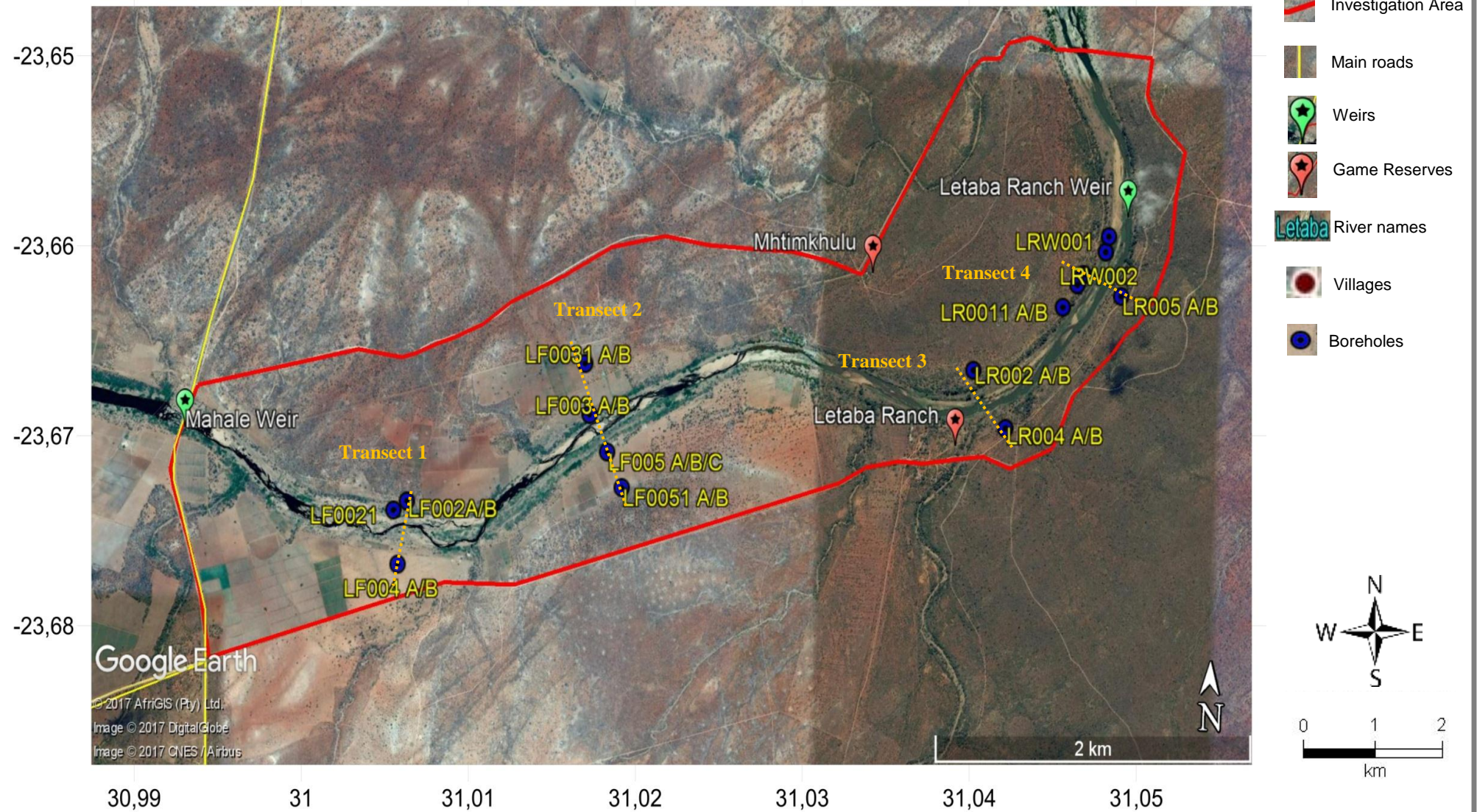


Figure 4.5 Final location of all boreholes on study site, as well as their specific transects (Google Earth, 2016).

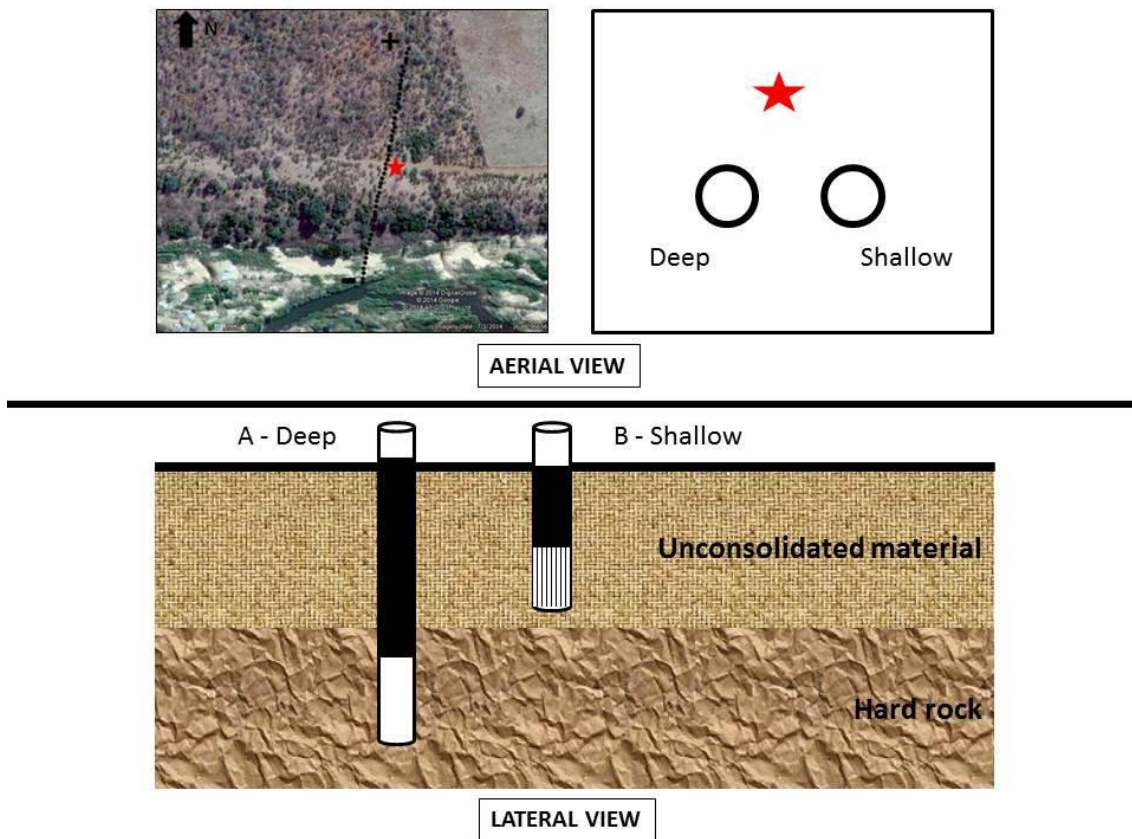


Figure 4.6 Piezometric design of boreholes at each specific site (Gokool et. al, 2015). The figure illustrates the borehole construction within the hard rock/consolidated zone (deep aquifer) and unconsolidated zone (shallow aquifer).

4.4 LITHOLOGY LOGS OF BOREHOLES

The lithological description is in a sense dependant on the type of drilling that was used to obtain the data, thus the process of obtaining samples from percussion drilling needs to be explained.

While the drill bit is turning and hammering at geological material small pieces of stone are chipped off. Compressed air is then forced through the 6 m extension rods by the 24 bar 900CFM compressor and out of the drill bit. The result is small stone chips are blown out of the borehole and distributed on the surface while the drilling is in process. At every successive meter of drill depth grab samples are then collected via a shovel and laid out onto the ground in rows of five or six (Figure 4.7).

Samples were then taken of each of these meter chips for later analyses. This analysis consisted of cleaning each sample to obtain a better view of the stone chips for a more

accurate identification (Appendix A-5). Properties of the rock such as, chip size, primary lithology, secondary lithology, trace elements, weathering, grain size, and colour were then captured into an excel spreadsheet. This allows a more precise delineation of weathered and hard rock material.

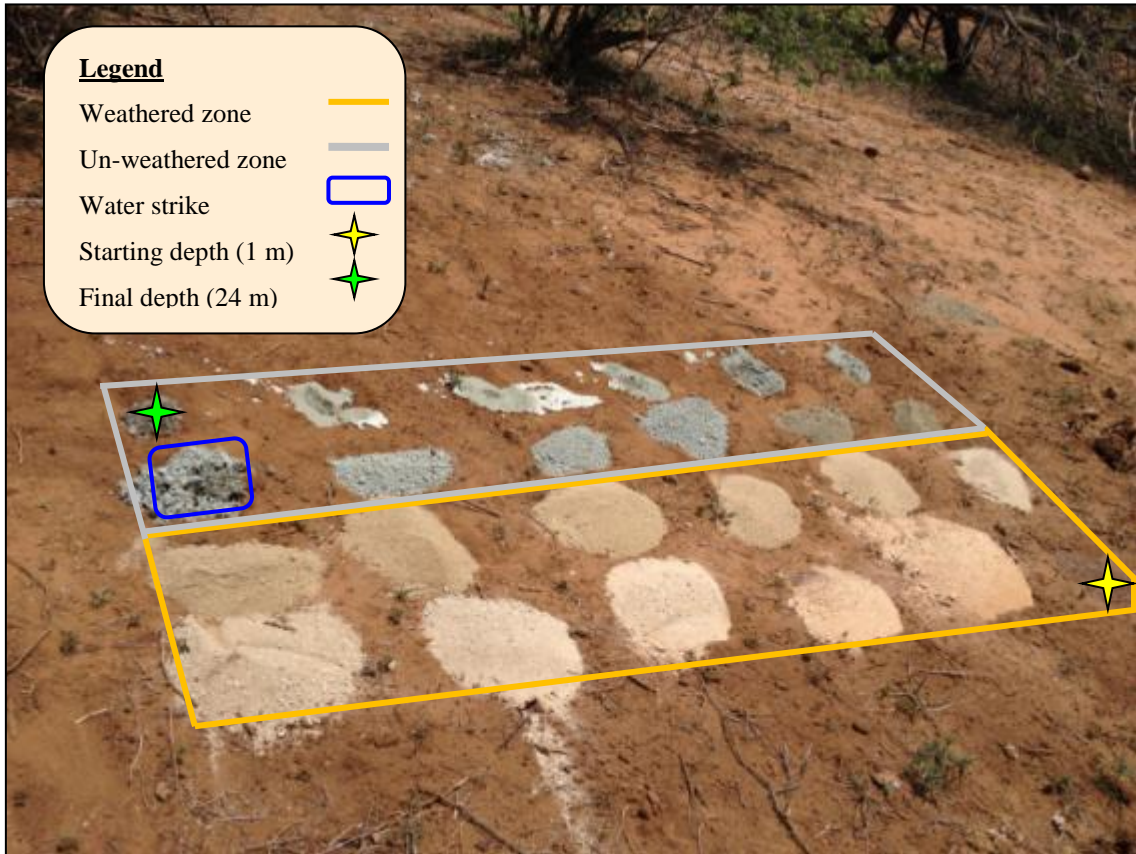


Figure 4.7 Typical example of a borehole Lithology log.

4.5 MONITORING

4.5.1 Ground water levels

According to The Groundwater Dictionary, the hydraulic gradient is the “difference in hydraulic head over a distance along the flow path between two points” (Figure 4.8) (DWA, 2006b). The general rule of thumb is that groundwater will move from the highest elevation to the lowest elevation, although this is the case most of the time. To determine hydraulic gradients the exact groundwater elevation needs to be taken or datum, also referred to as Metres above mean sea level (mamsl). This was accomplished through firstly installing Solinst™ water level loggers within the 21 boreholes (Table 4.1), and these were programmed to store pressure head every hour. Weekly hand

measured water levels were also taken (with a Solinst™ TLC dipmeter - Appendix A-6), by way of level logger reading calibration (Figure 4.9). Secondly, a Trimble Differential GPS to get the most accurate ground level elevations from each borehole. The water level measurements were subtracted from the casing height in order to obtain accurate mamsl elevations for each boreholes water level. The resultant data is then used to plot the groundwater phreatic surface in computer software (Surfer™ 11), which then provides hydraulic gradients that display the movement and direction of the groundwater flow.

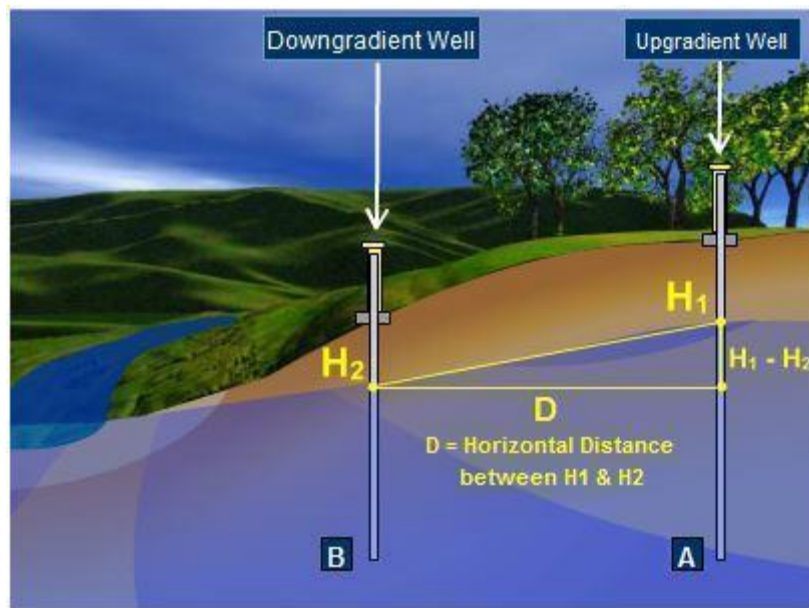


Figure 4.8 Movement of groundwater from a point of high elevation to a point of low elevation (DWS, 2006b).

Solinst™ level loggers were also installed within the river and corrected with the barometric pressure obtained from a Solinst™ Baro logger that was installed next to the river. These water levels could then be incorporated with the borehole water levels to confirm if the hydraulic gradient is dipping towards or away from the river. Thus, indicating a potentially losing or gaining reach of river.

The water levels measured within the deep and shallow boreholes also provided information on whether two aquifers are present (shallow/weathered and deep/fractured hard rock), and whether any interaction occurs between them. These measurements were specifically monitored during both rainfall and high flow (dramatically increase river level) events, to obtain information on the reaction time of each borehole and the interaction between the shallow and deep boreholes.



Figure 4.9 Hand measurements of groundwater levels taken on a weekly basis.

4.5.2 Fluid logging

The primary purpose of the fluid logging was to obtain in-situ borehole parameters for instance, temperature and specific conductance with depth. This would then be repeated in wet and dry seasons under ambient conditions to observe changes in parameters. These changes could then deduce direction of groundwater flow, zones of active groundwater flow and flow rate within fractures.

The equipment used was the YSI (Yellow Spring Incorporated) 600XLMD Sonde multi-parameter in-situ monitoring apparatus (further referred to as only Sonde) (Figure 4.10). After the Sonde was started it was slowly lowered down into the borehole until the Sonde sensors were submerged in the water. It was then kept there for 2 minutes until all the sensors have adjusted to the in-situ temperature and conductivity. The Sonde was then lifted slightly above the water level again to get in position for the start of the logging process. The Sonde takes a reading every 2 seconds, thus it was lowered 0.25 m after every 2 second pause resulting in 4 measurements within every 1 meter. The Sonde was then lowered in the 0.25 m intervals until it reached the bottom of the borehole. It was then removed from the borehole and the data downloaded to a laptop for further analyses of the data.



Figure 4.10 YSI (Yellow Spring Incorporated) 600XLM Sonde multi-parameter in-situ monitoring apparatus.

4.5.3 Down hole camera

The primary purposes for using this technique were only to obtain a better understanding of the influx of groundwater into the borehole, fracture characteristics and borehole construction.

Because a proper down hole camera could not be obtained for this project, a different technique had to be incorporated. This consisted of modifying a normal underwater camera (GoPro^{LTD} Hero 3). The only setback was that the camera could not be submerged below the water as deep as a proper down hole camera. Thus, this technique could only be implemented on boreholes that had a very low yield, as the groundwater level would rise too quickly. From the 5 low yielding boreholes that were tested, only 2 boreholes provided usable data. This was due to problems with the technique that consisted of various flaws, as well as boreholes that were recharging too quickly. The two boreholes that did provided data was LR004A and LF0051B.

First the submersible pump was lowered to the bottom of the borehole, after which the borehole was pumped until the water level reached the pump. The pump was then removed and the camera lowered into the borehole. Because of the low yield, the water level rose at a very slow rate. Thus, allowing enough time to lower the camera to the bottom of the borehole while monitoring the depth with the dipmeter (Figure 4.11).

Equipment used:

- GoPro^{LTD}, HERO 3 underwater camera.
- Dipmeter
- Flashlight
- Steel wire

A profile could thus be obtained of the geology, the borehole construction, as well as the fracture characteristics.

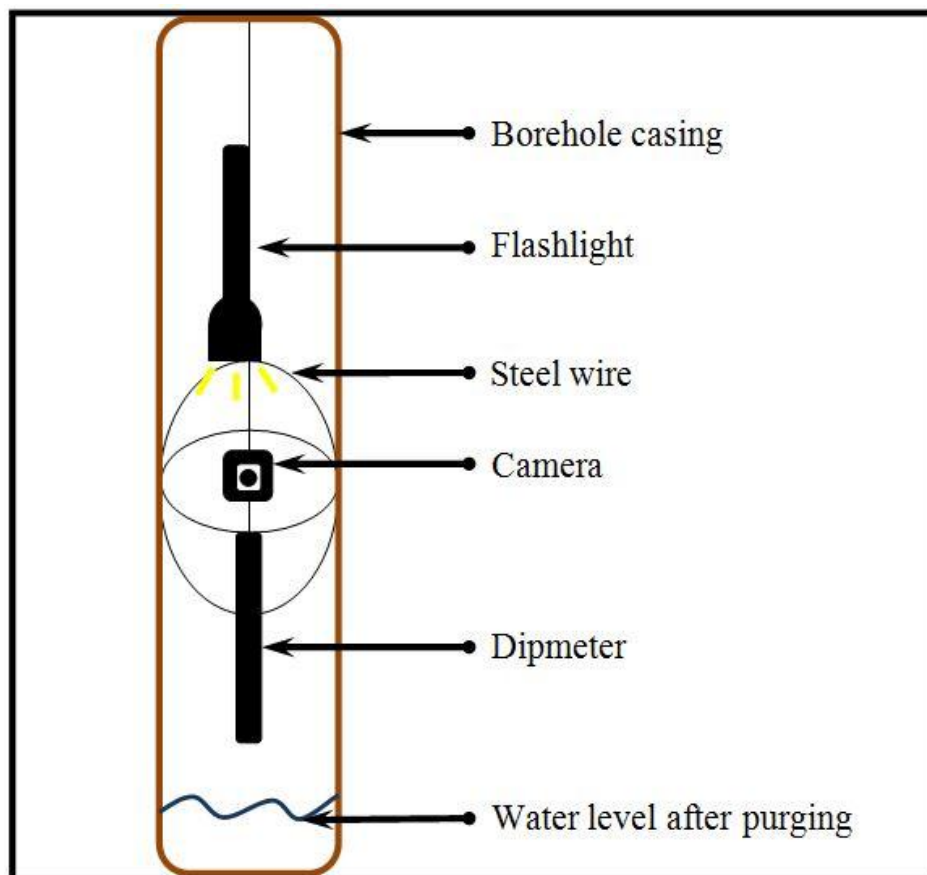


Figure 4.11 Equipment used for down hole camera investigation.

Table 4.1 Borehole names and metadata (see Figure 4.5 for borehole locations).

Site Name	Site Description	Latitude	Longitude	Altitude (m)	Depth (m)	Solid Casing Depth (m)	Casing/Collar height (m)	Initial Water level (m)	Hydraulic head (mamsl)
LF002A	Mabunda/Baloi	-23.674299°	31.005509°	332.816	60	6	0.51	11.51	321.630
LF002 B	Mabunda/Baloi	-23.674298°	31.005499°	332.966	15	6	0.58	11.78	321.700
LF0021	Mabunda/Baloi in river	-23.674765°	31.004663°	329.940	24	6	0.63	8.26	321.150
LF003 A	Maliesa's Farm	-23.669515°	31.016633°	332.840	72	36	0.7	10.97	317.840
LF003 B	Maliesa's Farm	-23.669520°	31.016568°	328.683	20	14	0.8	10.76	317.96
LF003C	Maliesa's Farm	-23.669495°	31.016673°	333.985	Dry				
LF0031 A	Maliesa's Farm	-23.667003°	31.016216°	333.183	60	24	0.22	12.95	319.72
LF0031 B	Maliesa's Farm	-23.667070°	31.016261°	335.904	20	6	0.255	12.68	320.07
LF004 A	Abram's Farm	-23.677412°	31.005063°	337.243	72	24	0.43	13.385	324.27
LF004 B	Abram's Farm	-23.677413°	31.005053°	338.883	15	10	0.46	13.39	324.39
LF005 A	Bongele,s Farm	-23.671245°	31.017842°	328.391	72	30	0.29	12.33	317.86
LF005 B	Bongele,s Farm	-23.671309°	31.017884°	330.151	42	6	0.305	12.15	317.96
LF005 C	Bongele,s Farm	-23.671223°	31.017831°	332.179	18	6	0.345	10.97	317.80
LF0051 A	Bongele,s Farm	-23.673003°	31.018832°	328.978	54	36	0.54	14.29	317.88
LF0051 B	Bongele,s Farm	-23.673047°	31.018857°	327.363	30	6	0.36	14.26	317.71
LR001 A	Mthimkhulu	-23.661769°	31.046823°	328.039	60	30	0.46	10.35	318.72
LR001 B	Mthimkhulu	-23.661764°	31.046806°	330.826	12	6	0.355	11.93	318.60
LR0011 A	Mthimkhulu	-23.662935°	31.045923°	324.700	72	24	0.3	10.3	321.42
LR0011 B	Mthimkhulu	-23.662914°	31.045962°	331.089	10	6	0.315	10.15	321.28
LR002 A	Mthimkhulu	-23.666323°	31.040506°	330.907	42	24	0.43	10.59	320.84
LR002 B	Mthimkhulu	-23.666330°	31.040511°	329.536	10	6	Dry		
LR003	Mthimkhulu. Tercias BH	-23.661233°	31.047127°	326.855	10	4	0.355	Initially dry	318.51
LR004 A	Letaba Ranch	-23.669463°	31.042412°	327.109	54	30	0.57	13.38	316.62
LR004 B	Letaba Ranch	-23.669448°	31.042414°	326.388	24	0	0.505	13.3	316.52
LR005 A	Letaba Ranch	-23.662268°	31.049552°	327.444	60	42	0.265	8.95	318.31
LR005 B	Letaba Ranch	-23.662270°	31.049503°	328.971	24	6	0.56	8.94	317.89
LRW001	Mthimkhulu in river downstream of dyke	-23.659273°	31.048663°	316.063	12	0	0.35	1.23	316.15
LRW002	Mthimkhulu in river upstream of dyke	-23.659964°	31.048604°	317.902	6	0	0.52	1	317.83

4.6 AQUIFER TESTING

4.6.1 Slug test

Slug tests were performed on all suitable boreholes to obtain preliminary hydraulic conductivity (K) and transmissivity (T) values (further referred to as K and T values), as well as information on whether a borehole possesses a yield strong enough to sustain a pumping test. It must be noted that these tests are preliminary and that data obtained is not as accurate as pumping tests (Kruseman and Ridder, 1994). This is due to the disadvantage that only a small volume of aquifer material immediately surrounding the well is tested, and which might have been altered during the drilling of the borehole.

Before the physical slug test was initiated calculations had to be completed. Initially, the following measurements and computation were done.

- Slug length: 1.55 m
- Slug radius: 0.055 m
- Slug volume: 0.015 m³
- Volume of 1.55 m casing: 0.033 m³
- Difference in volume: 0.018 m³

Equation used:

$$L = V/(\pi r^2) \quad (4.1)$$

Where: L is length (m), V is volume (m³) and r is the radius (m).

Thus, length of displacement = 0.861 m

Pullback = 95% recovery

Thus pullback = 4.31cm

The TLC (SolinstTM dipmeter) is thus lowered to the water level and “pulled back” 4.31cm. A SolinstTM level logger is also installed into the borehole at a depth of at least three meter below the static water level. Accurate measurements could thus be recorded

if the borehole had a high yield or if human error occurred. The “slug” or solid cylinder is then lowered into the borehole and suspended just above the water level (Appendix A-7). Then it is rapidly lowered into the borehole and the time the water level took to reach the TLC (95% recovery) was recorded. If it took longer than 3 minutes, further readings were taken at one-minute intervals. This data was then plotted in FC – EXCEL software developed by IGS (that uses the Bouwer and Rice 1976 method) to calculate the estimated yield of the borehole, as well as K and T values. For the slug tests the Bouwer and Rice method is suited for the study site, as it was developed for an unconfined or confined aquifer, with a fully or partially penetrating borehole.

The data logger data was also downloaded and plotted using AQTESOLV Pro V4.0 for more accurate K and T values and to confirm the values obtained through the FC – EXCEL method.

4.6.2 Pumping tests

The pumping test mainly consisted of two tests, a step draw down test and a constant rate test. These two tests were completed on only 19 boreholes, as the remaining 9 were either dry (LR002B, LR003, LF003C), too little water available within the borehole for a reliable test (LF005C, LF004B, LR0011B, LR001B), or drilled for other purposes (LRW001, LRW002).

4.6.2.1 Step drawdown tests

The step test is only a preliminary test to obtain information on what yield would be most suitable for the constant rate test (see section 2.5.6.1 step – drawdown tests). The step was done through lowering the pump to two m from the bottom of the borehole (Figure 4.12).

The SolinstTM level logger was then also lowered and placed one meter above the pump for data measuring. The borehole was then pumped at approximately 30% of the pumps maximum pumping capacity for 1 hour. While pumping took place the water level was also monitored by taking hand measurements with an in-situ dip meter. This decrease in water level induced by pumping is known as the drawdown. The discharges were also carefully monitored to keep it stable, as the discharge will decrease with time while the water level drop and the pump struggles to pump the water with the decrease in

pressure. After an hour the tap was opened to 60% of the pumps maximum pump rate for another hour. This was then also repeated for the last two steps at 90% and 100%. After these four steps the pump was switched of and the recovery of the boreholes hydraulic head was measured.

This data could then be plotted within the FC – EXCEL software to provide a sustainable yield that could be used for the constant rate test. AQTESOLV was then also implemented to obtain initial K and T values from the data.

4.6.2.2 Constant rate test

The constant rate test consisted of a similar process as the step drawdown test, although the aim was to get as much drawdown to the main fracture without dewatering the fracture. Thus, the data obtained will be from aquifer/fracture and not form wellbore storage. The borehole was then pumped as long as possible to obtain the most accurate data and observe if any boundaries (example a dolerite dyke) are present within the vicinity. After the test was completed the pump was shut down and the recovery was taken. This data was then imported into AQTESOLV to obtain the most accurate K and T values through the Cooper - Jacob equation as a single well test.



Figure 4.12 Pumping rig and equipment used during pumping tests.

4.7 SAMPLING

Samples were taken to acquire two objectives; the first objective was to gather information on the hydrochemistry of the boreholes and the second objective was to obtain isotopic data from the boreholes and the river itself.

4.7.1 Sampling for hydrochemistry

Samples were taken along the river section between the Mahale weir and Letaba Ranch weir to obtain longitudinal hydrochemical information on the river. This was repeated 3 times in 2014, 2015 and 2016. Testing of the samples was done by the LAR Mobile laboratory stationed in Phalaborwa for the Middle Olifants South Africa Project (MOSA). In 2015 9 boreholes were also tested for their hydrochemistry. The longitudinal hydrochemistry of the river reach was compared and characterised between years.

4.7.2 Sampling for Isotopes

On a weekly basis a sample was taken at Mahale weir for stable ^{18}O and ^2H isotope analyses. Rain samples, as well as some borehole samples were also collected on site and sent for isotope analyses to observe the difference in isotopic signature between the groundwater and the surface water. In order to collect the rain samples a specific rain sampler was custom made to prevent evaporation of samples, resulting in a change of the rains isotopic signature (Figure 4.14). To seal the inlet a table tennis ball was used, as it will float on the water falling in the funnel. When it stops raining the funnel will automatically close the lid, as no water is available the keep the ball floating. A 5-meter pipe (to minimise evaporation), were also attached to release the pressure as the bucket started to fill during a rain event. A final safety measure was to take the rain samples as soon as possible after the rainfall event. Living on-site for the period of the study, thus proved to be helpful.

Sample bottles were filled to the brim, thus allowing no air inside the bottle and stored inside a fridge to prevent any evaporation to occur.

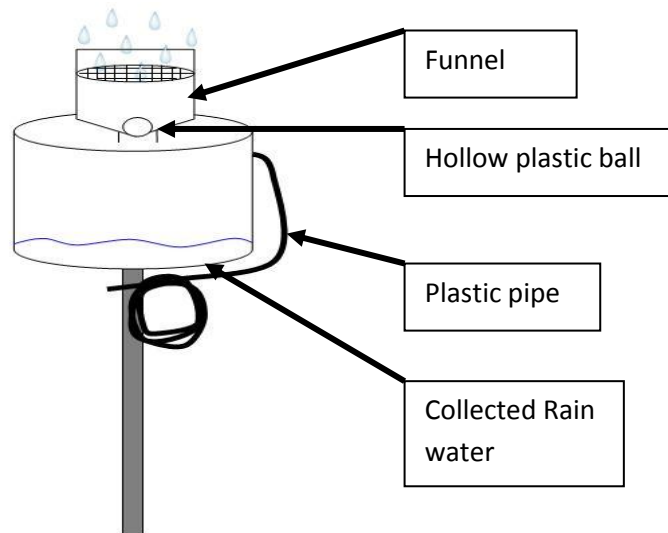


Figure 4.13 Custom made rain sampler for isotope samples.

4.8 WEATHER STATIONS

Meteorological data from three Davis Vantage Pro weather stations such as, wind speed, wind direction, mean air temperature, humidity, rain rate and amount of rain that fell every 30 minutes were collected during the study period. The specifications for the weather stations tipping bucket were 0.2 mm. These weather stations were downloaded on a monthly basis and are located at Mthimkhulu game reserve, Phalaubeni and Mahale farm (Figure 4.14).

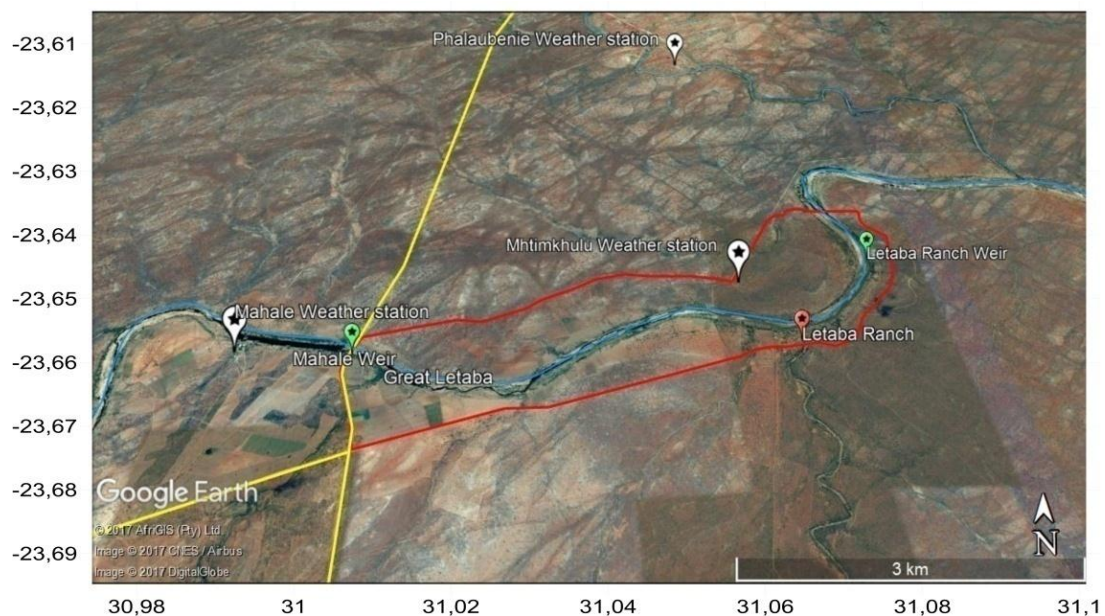


Figure 4.14 Locations of the Three Davis Vantage Pro weather stations in the broader study area (Google Earth, 2017).

Chapter 5 - SITE CHARACTERISATION: DATA ANALYSIS

Tanner (2013) stated, it is essential to obtain a good understanding of the interaction processes and how it relates to the actual hydrological processes to ultimately create a conceptual model, thus a spatial characterisation of the hydrogeological system is of utmost important and will be discussed within this chapter.

5.1 HYDROCENSUS

The initial hydrocensus was conducted in May 2014 in Mbaula and Mthimkhulu (4.1 HYDROCENSUS). The hydrocensus was conducted to ultimately provide an indication of the local hydrochemistry within the surrounding, as well as providing an indication of the amount of water that is being abstracted from the river.

This will ultimately aid in the interpretation of the fluid logs in terms of the conductivity and temperature of the boreholes within the surrounding area. It will also provide the amount of water abstracted from the river by the farmers and whether it has an effect on the river water level (monitored by a SolinstTM level logger). Thus, it will aid in the final interpretation of the conceptual model. The data displayed below stems from this initial hydrocensus and will be explained in more detail.

5.1.1 Mbaula

Of the 37 boreholes identified within Mbaula, only 32 could be measured due either to the operator or owner not being available to switch on the pump for the testing of a water sample. The average depth of the boreholes within Mbaula was 50 m with a pH averaging at 7.16 and temperatures at 24.44 °C. Of the 32 boreholes nine contained electrical conductivities (EC) that were extremely high and could not be measured because it was out of range.

Sixteen of the boreholes displayed an EC between 12000 and 19000uS/cm. The remaining seven boreholes displayed relatively fresher water with EC's ranging between 100 and 200uS/cm (Strydom, 2014).

5.1.2 Mthimkhulu

Of the six boreholes identified on the Mthimkhulu Game Reserve, only five could be accessed for data collection (**Table 5.1**). Most of the boreholes are not actively pumped. Boreholes with no pumps installed were sampled through the use of bailers.

When the groundwater of Mthimkhulu and Mbaula is compared the similarities are evident, thus providing a good indication of the hydrochemistry within the region. The average electrical conductivity (EC) is extremely high, indicating a possible high EC groundwater, although this will be confirmed during the analyses of the fluid logs.

If this is the case it will increase the difficulty in interpreting the fractures. The salts within the borehole will settle down to the bottom decreasing the EC within the borehole, thus fractures will be indicated by an increase rather than the normal decrease in electrical conductivity.

Table 5.1 Hydrocensus information from Mthimkhulu (Strydom, 2014).

Borehole ID	Status	Activity	Borehole Depth (m)	Water Level (m)	pH	EC (uS/cm)	Temp (°C)	TDS (ppt)
WP 019	Active	Domestic	?	Covered				
WP 020	Not always	Domestic, Watering Hole	50	10.21	6.9	14750	26.2	7.36
WP 021	Not active	Domestic	100	21.96	6.26	500	27.6	0.25
WP 022	Not active	Domestic, Watering Hole	30	2.32	6.9	13330	25.6	6.71
WP 023	Active	Domestic, Lodge	60	10.97	7	15500	20.2	7.64

5.1.3 River abstraction

Direct abstraction takes place throughout the study site, mostly for irrigation within the farming area. The farms on site primarily utilise drip irrigation and abstraction should be relatively low, although the total amount of abstraction still needs to be quantified to properly comprehend the differences in flow between the two weirs.

The survey displayed reasonably low abstraction rates from the river (Figure 5.1 and Table 5.2), with an approximate mean daily abstraction of 520 m³ (Riddell, 2016).

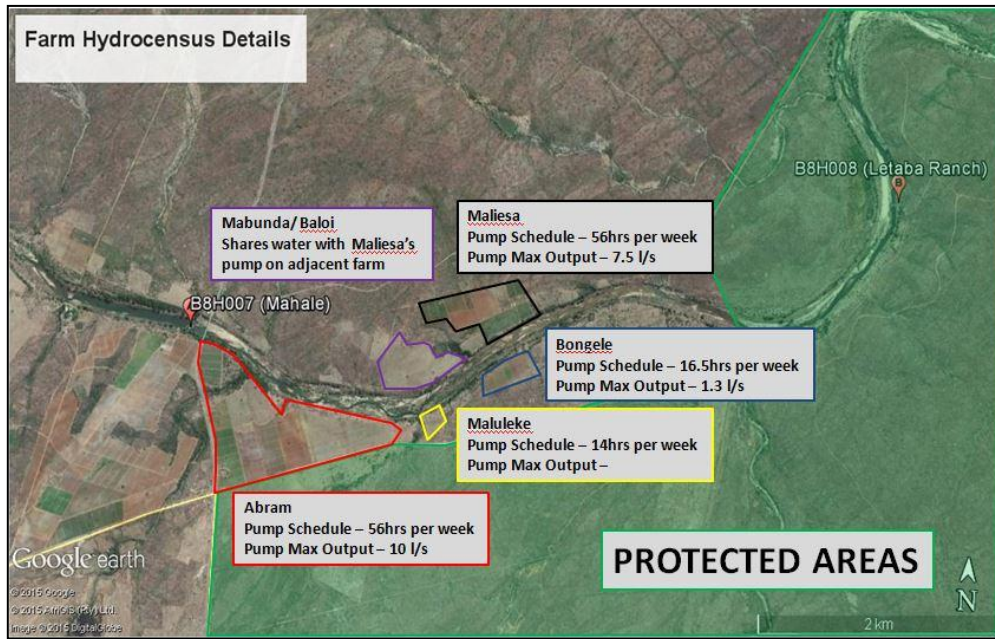


Figure 5.1 Abstraction rates of farms located on study site (Riddell, 2016).

Table 5.2 Hydrocensus data from July 2015 (Riddell, 2016).

Farm Name	Bank	No. of Boreholes	Farming Scale	Pump Max. Capacity (L/S)	Pumping schedule (hours/week)	Estimated volume per day (L)
Abram	Southern	0	Commercial	10	56	288000
Maliesa	Northern	4	Commercial	7.5	56	216000
Mabunda / Baloi	Northern	0	Commercial			
Bongeale	Southern	5	Commercial	1.3	16.5	11030
Maluleke	Southern	0	Commercial	1	14	7200
				Potential Abstractions per day (L)		522230
				m3/day		522

5.2 PRECIPITATION ON STUDY SITE

The three Davis Vantage Pro weather stations (Figure 4.14) provided the rainfall data for the study site (Mthimkhulu station and Mahale farm station) and surrounding area (Phalaubeni station) from October 2015 to August 2016. As can be seen in Figure 5.2, very little rainfall occurred within this period, because of the El-Niño induced drought that South Africa faced during this time. The study site received no more than 184 mm

over a period of 14 months, although it has an MAP of 501.8 mm indicating the severity of the drought. Most of the rainfall was obtained in a single event within March 2016.

Figure 5.2 displays the precipitation that occurred compared against the groundwater level of three boreholes on site. LRW002 is located within the river bed of the Letaba River on the protected side of the study site. Its reaction indicates the March flood event with the increase in the river level. LF002A is located within the riparian zone on the farms side of the study site. It reacts to the little precipitation occurring in March, but mostly to the flood event that took place. LF0051A is located on the farms side the study site. It displays and a small reaction to the rainfall event, but not to the flood event. This will be further elaborated on in section 5.4.8 Assessing peak flow transmission losses.

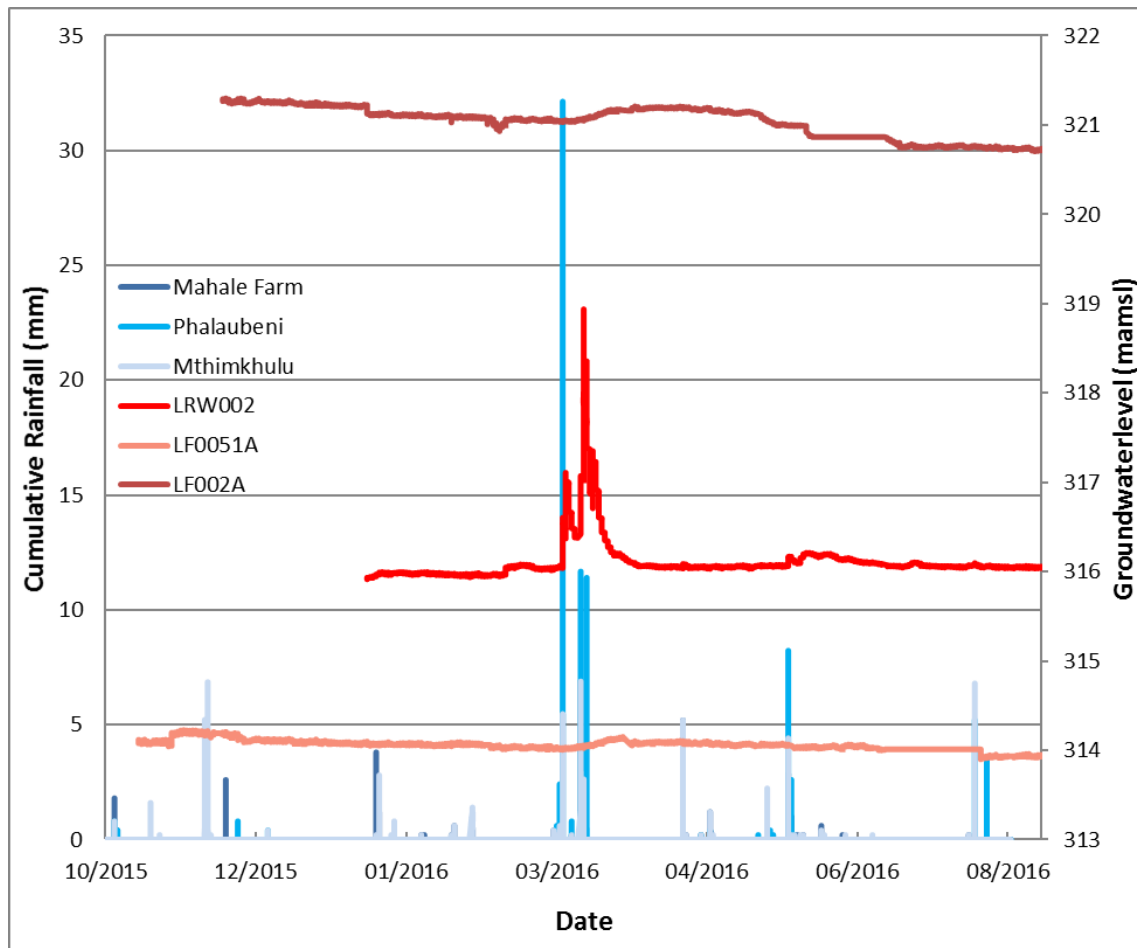


Figure 5.2 Measured precipitation from the three weather stations compared against the groundwater level of three boreholes on site.

5.3 GEOLOGICAL CHARACTERISATION

To characterise the geology geophysics (ERT and Magnetics) and borehole drilling was implemented to obtain the necessary data. The study site was divided into two selected areas according to their uses: the farming area and the reserve area (4.2 GEOLOGICAL SUBSTRATE INVESTIGATION). Six traverses were completed in each area, incorporating magnetic data and Electrical Resistivity Tomography (ERT) data. The principle was to extensively survey the subsurface geology with geophysical techniques not only for citing the ideal locations of boreholes for monitoring groundwater, but also for obtaining information of the subsurface geology.

5.3.1 Farming Area

Two geophysical transects were implemented on either side of the river, running parallel to the river or east to west (LF001, LF006, LF006.2), see Figure 5.3 below.

Geophysics Transects: Farms

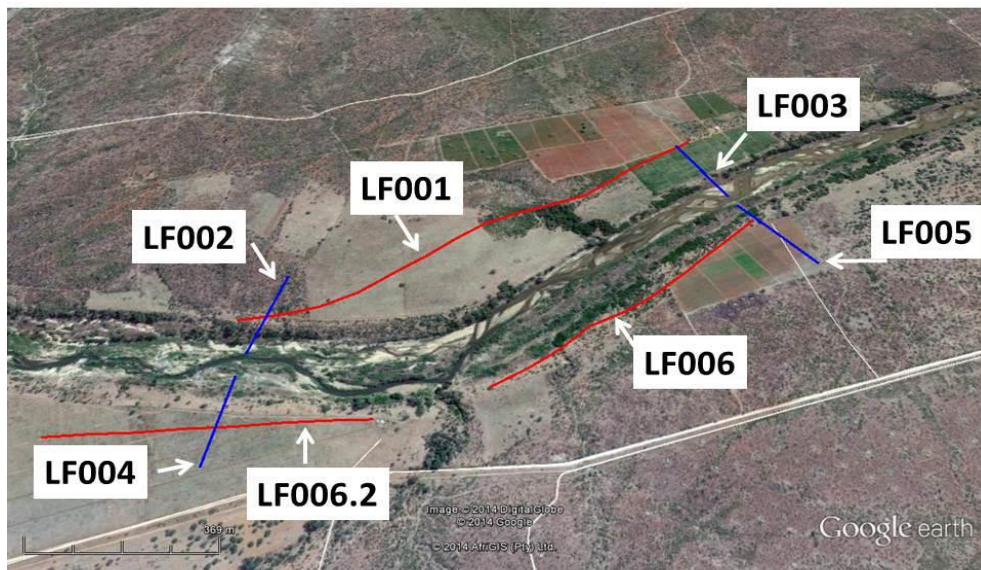


Figure 5.3 Locality map of the geophysics transects over the Farms section (Ridell, 2016).

These transects were applied to obtain deep resistivity measurements of approximately 70 m, thus an electrode spacing was used of 5 m in the Schlumberger array. The other four transects (LF002, LF003, LF005, and LF004) were intended to be only two long transects however, because of accessibility difficulties the river could not be crossed. These four transects ran perpendicular to the river with an electrode spacing of 2.5 m in

the Schlumberger array for shallower resistivity profiles of approximately 35 m. The intended monitoring boreholes were sited on these transects to monitor the groundwater flow towards or away from the river.

5.3.1.1 LF001

The incorporated resistivity and magnetic surveys of LF001 can be seen in Figure 5.4. The traverse runs in a Northeast to Southwest direction, parallel to the river. The unsaturated zone was interpreted at a depth ranging from 10 m (indicated by low resistivity values of between 10-114 Ωm), throughout most of the site and increases to a depth of 20 m to the west. The consolidated zone (hard rock), was interpreted by resistivity values ranging from approximately 577-4541 Ωm . Resistivity values falling between 114 – 577 Ωm could, thus be seen as an interface between the hard rock and the weathered (unconsolidated) zone. Type-curves identified a possible magnetic structure at 1400 m (indicated by the high magnetic value of 800 nT). This structure was located directly after the change in shallow depth resistivity. Shallow weathering was suggested by the low resistivity values (10 – 577 Ωm) between 500 m and 1100 m, as well as some evidence of tributary at 450 m with high resistivity values (577-1797 Ωm) occurring within one meter from the surface

5.3.1.2 LF002

The incorporated resistivity and magnetic surveys of LF002 can be seen in Figure 5.5. The traverse runs from South to North, perpendicular to the river. The low resistivity values (10-114 Ωm), indicated a relatively shallow weathering zone especially from 110-180 m, where hard rock is indicated with resistivity above 577 Ωm . The type-curves indicated no obvious structures. The Raw magnetic data did however display a moderately higher value than the background magnetic levels, thus indicating the probable presence of a structure over the complete traverse. The proposed borehole was sited at 100 m from the river (LF002A and LF002B) and borehole (LF0021) was sited at 55 m from the river within its floodplain, because these two areas indicated the lowest resistivity values (22.5-256 Ωm) throughout the traverse. Thus, the possible weathering zone and water table was indicated at approximately 10 m at LF002. LF0021 indicated high resistivity values (577-1300 Ωm), for the first 10 m, after which low resistivity values indicated a successive weathered zone. This inferred that the

water table might possibly lie at 10 m. The weathering zone would, thus reach approximately 20 m. After drilling LF002A/B (Appendix B-1) the groundwater level was confirmed at approximately 11.7 m, similar as the initial 10 m interpreted from the geophysical survey. The weathering was confirmed at a depth of approximately 10 m. As expected, because of the structure indicated by the geophysical survey from 110-108 m. The geological logs identified this structure as a dolerite dyke. After drilling LF0021 (Appendix B-2) within the flood plain of the river, a similar water level than initially interpreted from the resistivity data were again obtained. The water table were found at 8 m, with a surprisingly shallow weathering zone of 10 m.

5.3.1.3 LF003

The incorporated resistivity and magnetic surveys of LF003 can be seen in Figure 5.6. The traverse runs from South to North, perpendicular to the river. The type-curves indicated a possible magnetic structure around 100 - 150 m (250 nT). The structures location is in correlation with the relatively higher resistivity values (200 - 1297 Ω m), found at shallow and deep depths of up to 100 m. Deep weathering was indicated at more than 25 m by the resistivity values (10-100 Ω m) and a shallow water table at approximately 10 m. Two borehole locations were sited, one at 100 m (LF003A, LF003 and LF003C), because of the structure indicated by both the magnetic and resistivity data. Thus, indicating the presence of a possible dolerite dyke. These impermeable dykes were targeted as they block groundwater and create preferential flow paths for groundwater to move in. The second borehole location was at 388 m north of the river on the same transect (LF0031A, LF0031B). This was done to obtain a water level further away from the river and because of an indication of a dolerite intrusion.

After drilling LF003A/B (Appendix B-3) the groundwater level was confirmed at approximately 11.7 m, similar to the interpreted resistivity values. The weathering was confirmed at a depth of approximately 15 m by the geological logs. The structure indicated by the magnetic and resistivity survey was intersected at 13 m. This structure was identified by the geological logs as dolerite. After drilling LF0031 (Appendix B-4) just north of where transect LF003 ended, a deeper water level than initially interpreted were indicated at 13.5 m. Although the large drop in elevation moving towards the river might still result in groundwater moving towards the river.

5.3.1.4 LF004

The incorporated resistivity and magnetic surveys of LF004 can be seen in Figure 5.7. The traverse runs from North to South, perpendicular to the river. The type-curves indicated a possible magnetic structure at approximately 50 m (750 nT), as well as 200 m (600 nT). The resistivity data also indicated these structures with high resistivity values of 1297 to 5000 Ωm . Weathering were indicated up to 20 m (114-256 Ωm) and the water level at a shallow 10 m (10-114 Ωm). Closer to the river shallow weathering was observed around 10 m deep, with resistivity values of 10-114 Ωm . The proposed borehole was sited at approximately 100 m along the traverse, because of the sharp drop in nT (nanu tesla) in the magnetic data from -250 nT – 1100 nT and in the resistivity data from 5000 – 1300 Ωm , indicating that the structure (dyke) has ended. Thus, fracturing would be obtained at the interface of these two geological features, increasing the possibility of striking water. As, these fractures create preferential flow paths (LF004A and LF004B).

After drilling LF004A/B (Appendix B-5) the groundwater level was confirmed at approximately 13.5 m, similar to the initial 10 m interpreted from the resistivity survey. The weathering was confirmed to a depth of approximately 13 m, although slightly deeper but still in range as predicted by the resistivity survey. The geological logs indicated 6 m of red sand followed by 3 m of clay that supports the initial theory that this section is an old alluvial deposit from the Letaba River.

5.3.1.5 LF005

The incorporated resistivity and magnetic surveys of LF005 can be seen in Figure 5.8. The traverse runs from North to South, perpendicular to the river. The type-curves indicated a possible deep magnetic structure at approximately 50 m (60 nT), as well as at 250 m (50 nT).

The resistivity values also indicate the magnetic structures with high Ωm values of between 2000 and 5000 Ωm , thus suggesting that these structures a dolerite dykes. The resistivity data indicated deep weathering of around 20 m from the river up to around 200 m by low resistivity values (10 – 114 Ωm). The water level was predicted at around 8 m by the low resistivity values (10 – 50.6 Ωm) close to the surface. Red sand was located up to approximately 230 m from the river, this was initially thought to be river

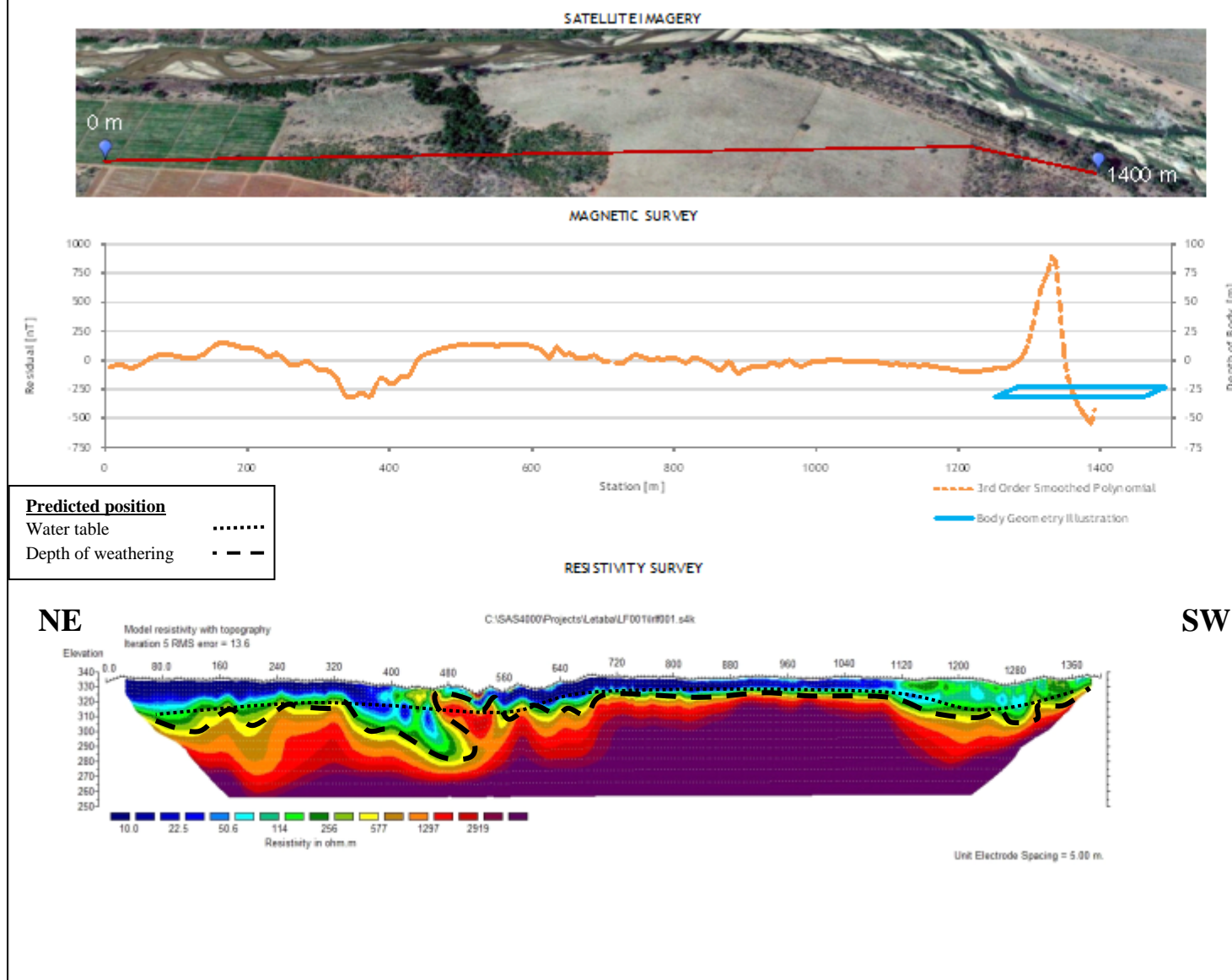
deposition on floodplains. The normal granitic soils were observed from 240 m onward. The proposed drilling locations were at 110 m, because of the geological feature indicated by the magnetic and resistivity data found at approximately 60 m. The borehole was not cited on the structure (dyke) itself, as the fracturing normally occurs on the side of the dykes. The second borehole was sited at 300 m along the traverse in order to provide a water level further away from the river and outside the possible old river deposits.

After drilling LF005A/B (Appendix B-6) the groundwater level was confirmed at a slightly deeper 12.8 m, although close to the initial interpretation from the resistivity survey. The weathering was confirmed at a depth of approximately 19 m, in close proximity to the predicted 20 m. Again, the theory of alluvial deposits is supported by old river pebble bed identified from 14 - 17 m within the geological logs. A deep sand layer was also identified of up to 13 m indicating that a possible alluvial aquifer might be present. After drilling LF0051A/B (Appendix B-7) the groundwater level was confirmed at approximately 14.8 m, much deeper than the initial 5 m interpreted from the limited resistivity data at that point. This large difference in water levels without a large variance in elevation already indicated the groundwater might be moving away from the river within this section.

5.3.1.6 LF006

The incorporated resistivity and magnetic surveys of LF006.1 and LF006.2 can be seen in Figure 5.9 and Figure 5.10 respectively. The traverse runs in a Northeast to Southwest direction, on the southern side parallel to the river. LF006.1 indicate deep weathering between 0 and 280 m with resistivity values ranging from 22.5 -114 Ω m. Slightly less, although still deep weathering is displayed between 470 and 750 m with resistivity values ranging from 22.5 – 256 Ω m. Type-curves identified a possible magnetic structure at 900 m with the sudden increase in nT to a high of 400 nT. This is supported by the resistivity data that indicates the same structure with high resistivity values of 2919nT and higher. The magnetic association of this structure indicates that it is possibly a dolerite dyke.LF006.2 displays a similar profile to LF005 with flood plain sediment ranging between 5 – 10 m of weathering with low resistivity values of 10 – 114 Ω m. Type-curves did however identify a possible magnetic structure at 300 m with the nT reaching a high of 2300 nT, this was also in correlation with high resistivity values of 2919 Ω m and more.

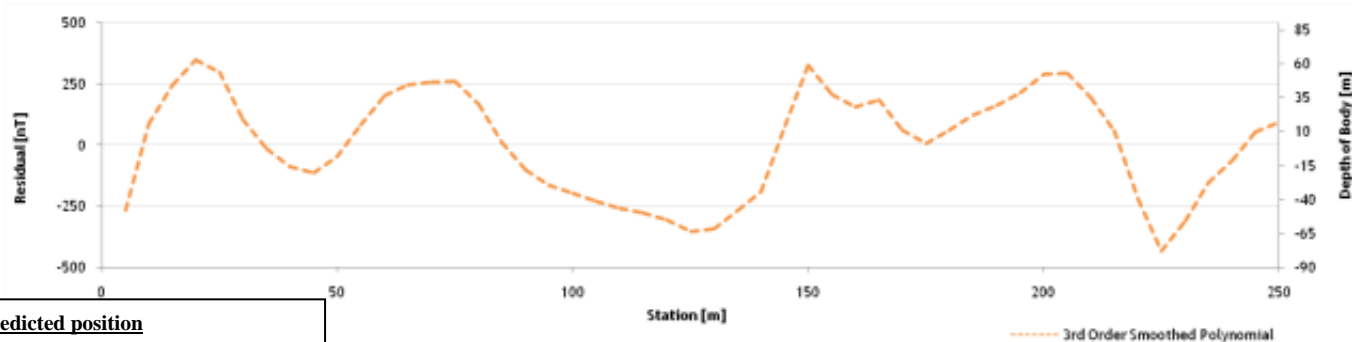
LETABA TRAVERSE LF001 - COMBINED GEOPHYSICAL INTERPRETATION



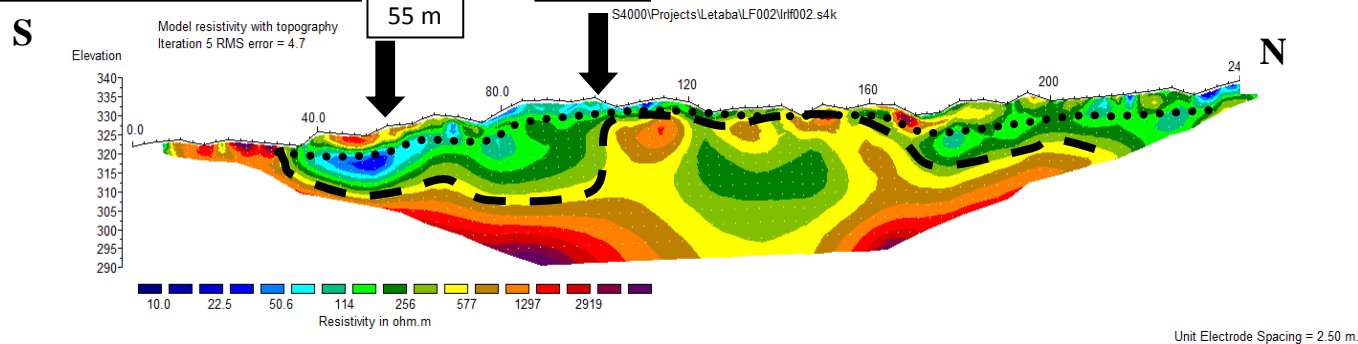
INTERPRETATION SUMMARY	
TRAVERSE INFORMATION	
INTERPRETED BODY GEOMETRY	
CENTER: 1386 m/station (E-Line (Warner, 1956))	DIP: 15 degrees (Roux, 1980)
WIDTH: 208 meter	DEPTH: 23 meter
FIGURE DETAILS	
Data Sources:	Google Earth TM mapping service: 2015 Imagery Date: 07/03/2014
FIGURE NO: -	MAP NUMBER: GCS001
PREPARED BY: R. Minnaar Hydrogeologist	REVIEWED BY: J. Nel Hydrogeologist
DATUM: Cape Traverse	DATE: 25/07/2015
PROJECTION: Mercator 1031	
PROJECT: Letaba River KS-2338	

Figure 5.4 Geophysical traverse LF001 with incorporated magnetic and resistivity profiles (modified after Gokool et al., 2015).

LETABA TRAVERSE LF002 - COMBINED GEOPHYSICAL INTERPRETATION

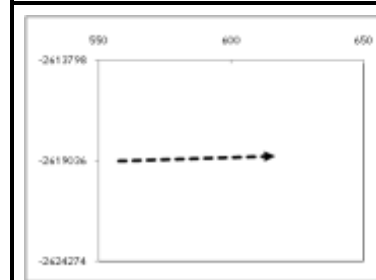


Predicted position
 Water table
 Depth of weathering - - - -
 Proposed drilling location →



INTERPRETATION SUMMARY

TRAVERSE INFORMATION



INTERPRETED BODY GEOMETRY

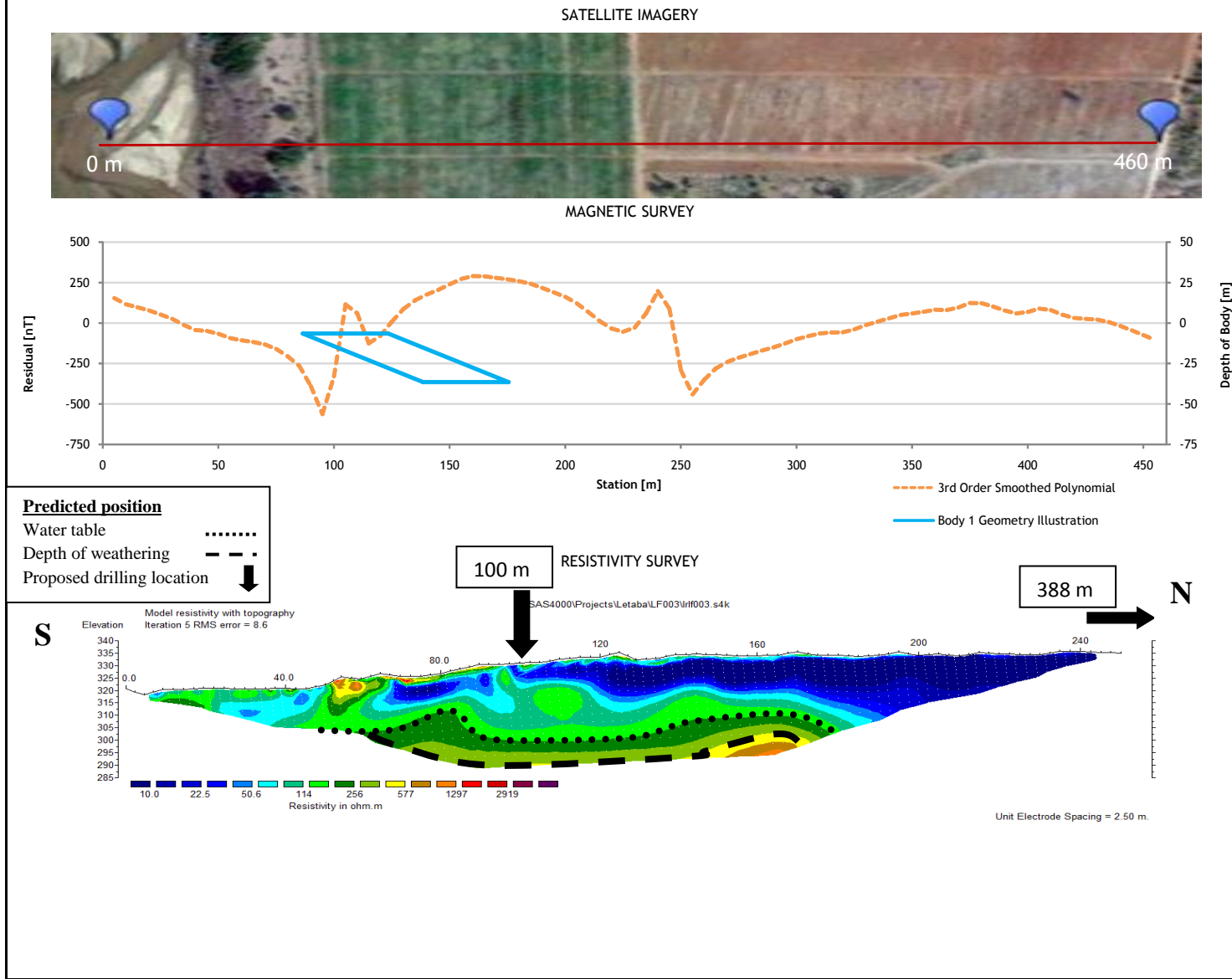
CENTER: - m/station (E-Line (Werner, 1956))	DIP: - degrees (Roux, 1980)
WIDTH: - meter	DEPTH: - meter

FIGURE DETAILS

Data	Google Eart TM mapping service: 2015		
Sources:	Imagery Date: 07/03/2014		
FIGURE NO	-	MAP NUMBER GCS002	
PREPARED BY:	R Minnaar Hydrogeologist	REVIEWED BY:	
DATUM:	Cape	DATE:	29/07/2015
PROJECTION:	Tranverse Mercator lo31		
PROJECT:	Letaba River K5-2338		

Figure 5.5 Geophysical traverse LF002 with incorporated magnetic and resistivity profiles (modified after Gokool et al., 2015).

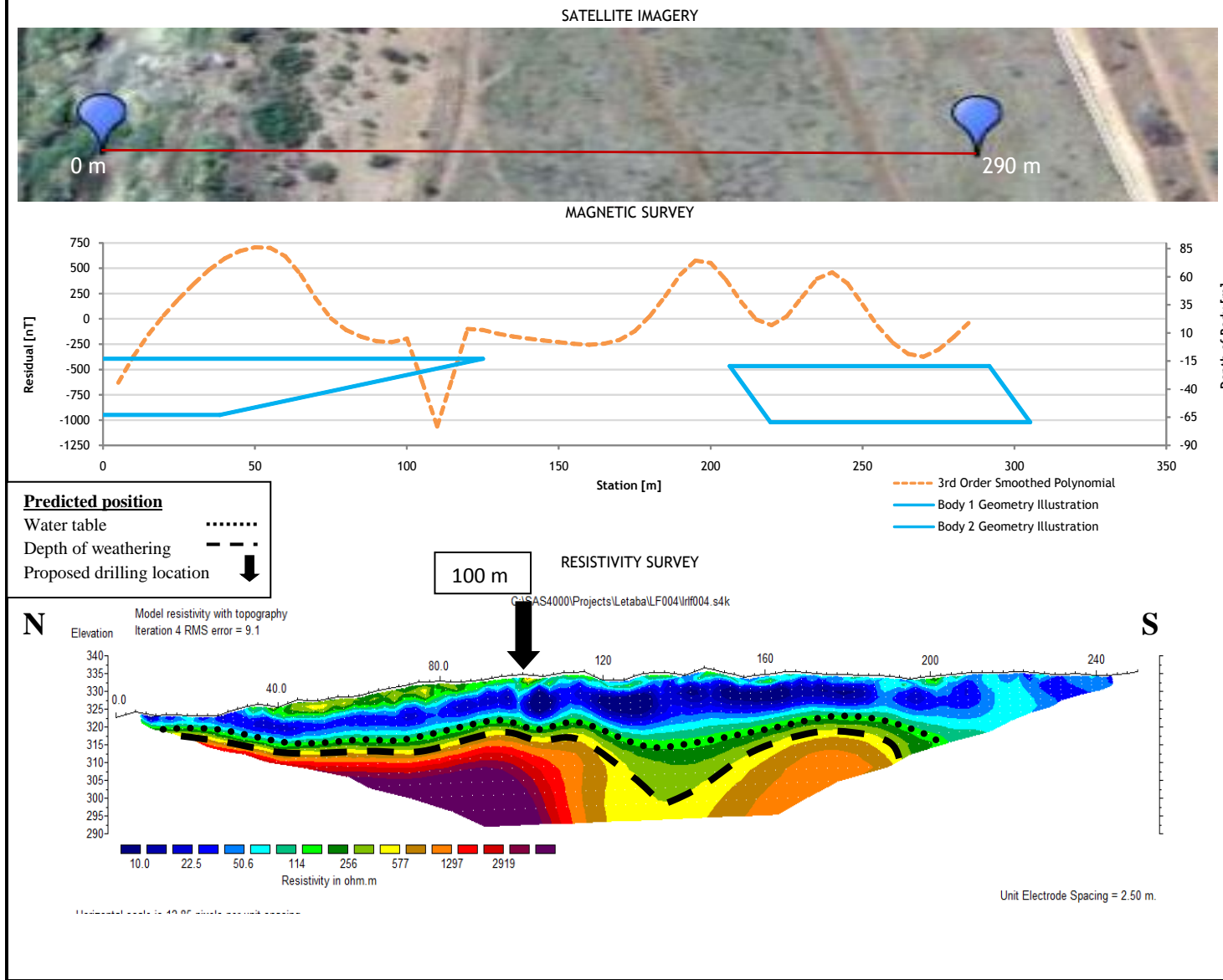
LETABA TRAVERSE LF003 - COMBINED GEOPHYSICAL INTERPRETATION



INTERPRETATION SUMMARY	
TRAVERSE INFORMATION	
INTERPRETED BODY GEOMETRY	
CENTER: 123 m/station (E-Line (Werner, 1956))	DIP: 30 degrees (Roux, 1980)
WIDTH: 35 meter	DEPTH: 7 meter
FIGURE DETAILS	
Data Sources:	Google Eart TM mapping service: 2015 Imagery Date: 07/03/2014
FIGURE NO	MAP NUMBER GCS003
PREPARED BY:	REVIEWED BY:
R Minnaar Hydrogeologist	J Nel Hydrogeologist
DATUM:	DATE:
Cape Traverse Mercator lo31	29/07/2015
PROJECT: Letaba River K5-2338	

Figure 5.6 Geophysical traverse LF003 with incorporated magnetic and resistivity profiles (modified after Gokool et al., 2015).

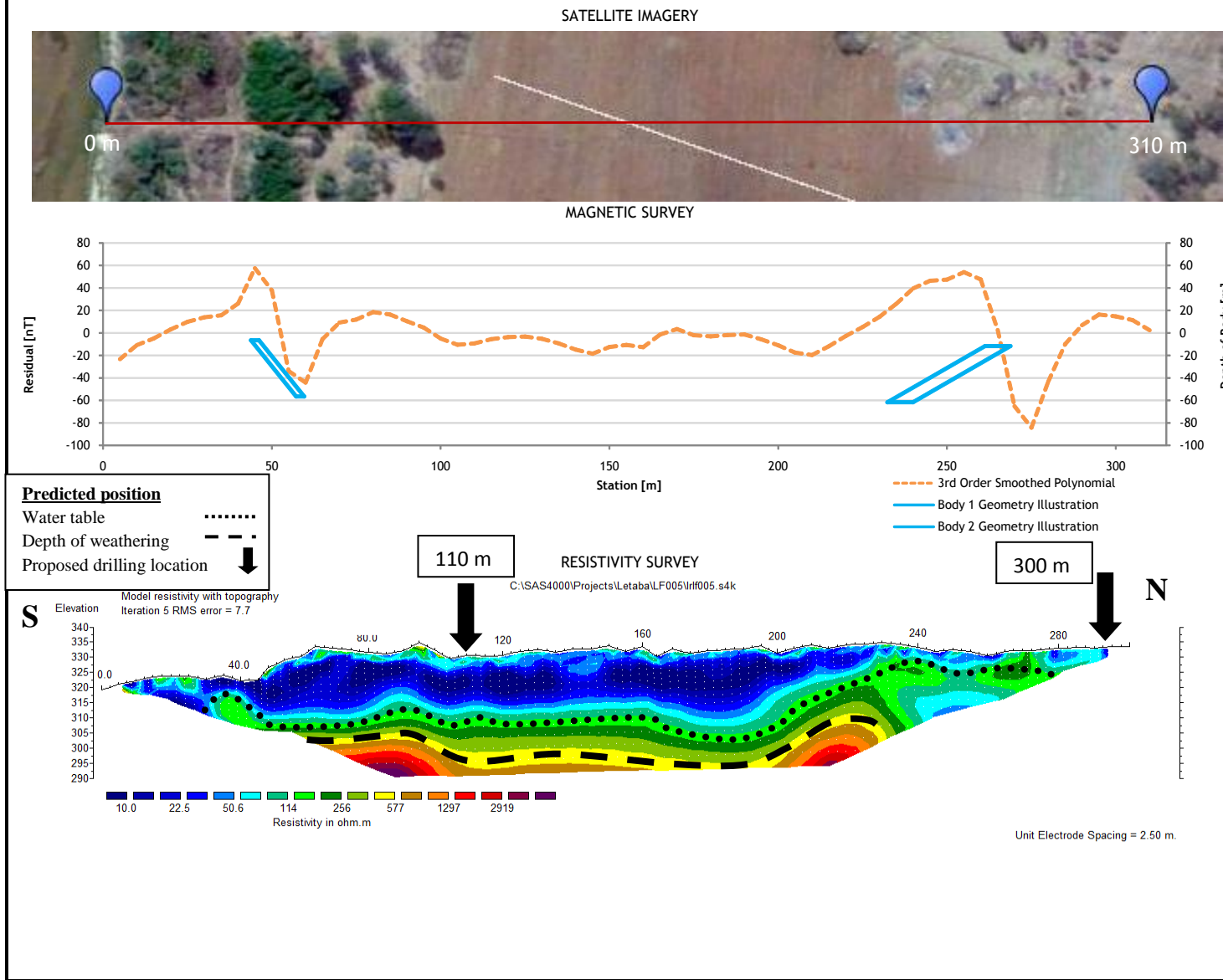
LETABA TRAVERSE LF004 - COMBINED GEOPHYSICAL INTERPRETATION



INTERPRETATION SUMMARY	
TRAVERSE INFORMATION	
INTERPRETED BODY GEOMETRY	
CENTER: 52/249 m/station <i>(E-Line (Werner, 1956))</i>	DIP: 35/75 degrees <i>(Roux, 1980)</i>
WIDTH: 146/85 meter	DEPTH: 13/20 meter
FIGURE DETAILS	
Data Sources:	Google Eart TM mapping service: 2015 Imagery Date: 07/03/2014
FIGURE NO	MAP NUMBER GCS004
PREPARED BY:	REVIEWED BY:
R Minnaar Hydrogeologist	J Nel Hydrogeologist
DATUM:	DATE:
Cape Tranverse Mercator lo31	25/07/2015
PROJECT: Letaba River K5-2338	

Figure 5.7 Geophysical traverse LF004 with incorporated magnetic and resistivity profiles (modified after Gokool et al., 2015).

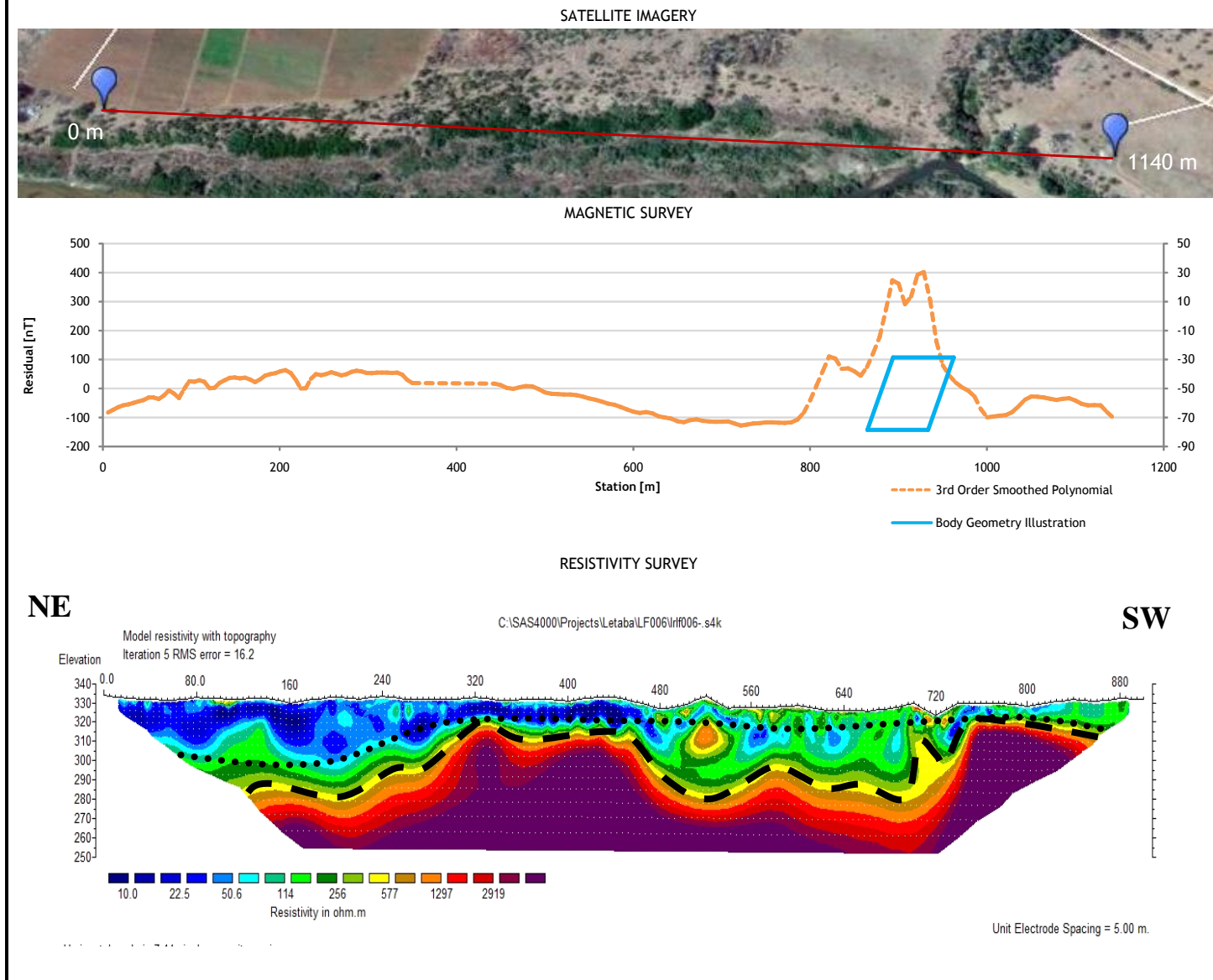
LETABA TRAVERSE LF005 - COMBINED GEOPHYSICAL INTERPRETATION



INTERPRETATION SUMMARY	
TRAVERSE INFORMATION	
INTERPRETED BODY GEOMETRY	
CENTER: 59/261 m/station <i>(E-Line (Werner, 1956))</i>	DIP: 75/45 degrees <i>(Roux, 1980)</i>
WIDTH: 3/7 meter	DEPTH: 7/12 meter
FIGURE DETAILS	
Data Sources:	Google Eart TM mapping service: 2015 Imagery Date: 07/03/2014
FIGURE NO	MAP NUMBER GCS005
PREPARED BY:	REVIEWED BY:
R Minnaar Hydrogeologist	
DATUM:	DATE:
Cape Traverse Mercator lo31	29/07/2015
PROJECT: Letaba River K5-2338	

Figure 5.8 Geophysical traverse LF005 with incorporated magnetic and resistivity profiles (modified after Gokool et al., 2015).

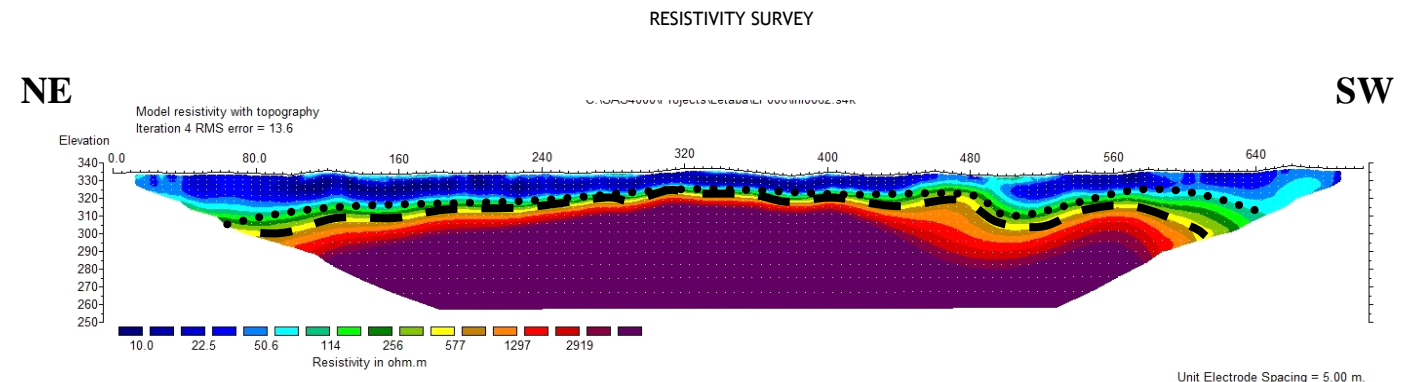
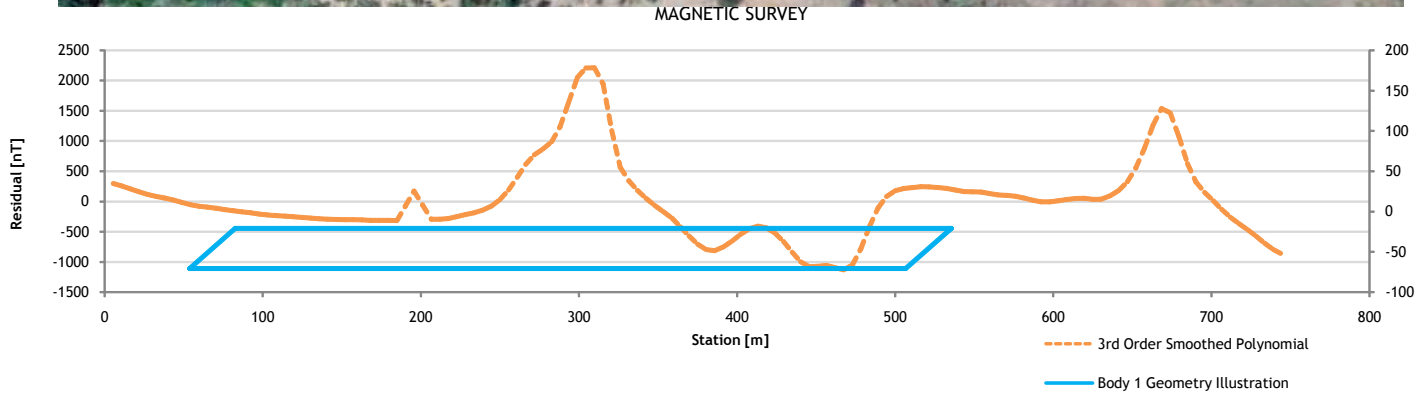
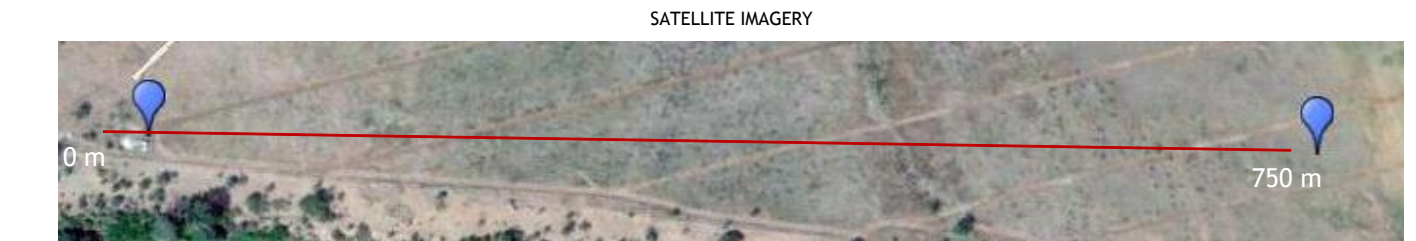
LETABA TRAVERSE LF006.1 - COMBINED GEOPHYSICAL INTERPRETATION



INTERPRETATION SUMMARY																							
<p>TRAVERSE INFORMATION</p>																							
<p>INTERPRETED BODY GEOMETRY</p> <table border="1"> <tr> <td>CENTER: 962 m/station (E-Line (Werner, 1956))</td> <td>DIP: 75 degrees (Roux, 1980)</td> </tr> <tr> <td>WIDTH: 69 meter</td> <td>DEPTH: 28 meter</td> </tr> </table>		CENTER: 962 m/station (E-Line (Werner, 1956))	DIP: 75 degrees (Roux, 1980)	WIDTH: 69 meter	DEPTH: 28 meter																		
CENTER: 962 m/station (E-Line (Werner, 1956))	DIP: 75 degrees (Roux, 1980)																						
WIDTH: 69 meter	DEPTH: 28 meter																						
<p>FIGURE DETAILS</p> <table border="1"> <tr> <td>Data Sources:</td> <td>Google Eart TM mapping service: 2015 Imagery Date: 07/03/2014</td> </tr> <tr> <td>FIGURE NO</td> <td>-</td> <td>MAP NUMBER</td> <td>GCS006</td> </tr> <tr> <td>PREPARED BY:</td> <td>R Minnaar Hydrogeologist</td> <td>REVIEWED BY:</td> <td></td> </tr> <tr> <td>DATUM:</td> <td>Cape</td> <td>DATE:</td> <td>29/07/2015</td> </tr> <tr> <td>PROJECTION:</td> <td>Tranverse Mercator lo31</td> <td></td> <td></td> </tr> <tr> <td>PROJECT:</td> <td colspan="3">Letaba River K5-2338</td> </tr> </table>		Data Sources:	Google Eart TM mapping service: 2015 Imagery Date: 07/03/2014	FIGURE NO	-	MAP NUMBER	GCS006	PREPARED BY:	R Minnaar Hydrogeologist	REVIEWED BY:		DATUM:	Cape	DATE:	29/07/2015	PROJECTION:	Tranverse Mercator lo31			PROJECT:	Letaba River K5-2338		
Data Sources:	Google Eart TM mapping service: 2015 Imagery Date: 07/03/2014																						
FIGURE NO	-	MAP NUMBER	GCS006																				
PREPARED BY:	R Minnaar Hydrogeologist	REVIEWED BY:																					
DATUM:	Cape	DATE:	29/07/2015																				
PROJECTION:	Tranverse Mercator lo31																						
PROJECT:	Letaba River K5-2338																						

Figure 5.9 Geophysical traverse LF006.1 with incorporated magnetic and resistivity profiles (modified after Gokool et al., 2015).

LETABA TRAVERSE LF006.2 - COMBINED GEOPHYSICAL INTERPRETATION



INTERPRETATION SUMMARY	
TRAVERSE INFORMATION	
INTERPRETED BODY GEOMETRY	
CENTER: 300 m/station (E-Line (Werner, 1956))	DIP: 75 degrees (Roux, 1980)
WIDTH: 441 meter	DEPTH: 20 meter
FIGURE DETAILS	
Data Sources:	Google Eart TM mapping service: 2015 Imagery Date: 07/03/2014
FIGURE NO: -	MAP NUMBER: GCS007
PREPARED BY: R Minnaar Hydrogeologist	REVIEWED BY:
DATUM: Cape Traverse	DATE: 29/07/2015
PROJECTION: Mercator lo31	
PROJECT: Letaba River K5-2338	

Figure 5.10 Geophysical traverse LF006.2 with incorporated magnetic and resistivity profiles (modified after Gokool et al., 2015).

5.3.2 Protected Area

Further downstream of the farm area a similar survey was done within the protected areas of Mthimkhulu and Letaba game reserves see Figure 5.11 below.

Geophysics Transects: Protected Areas

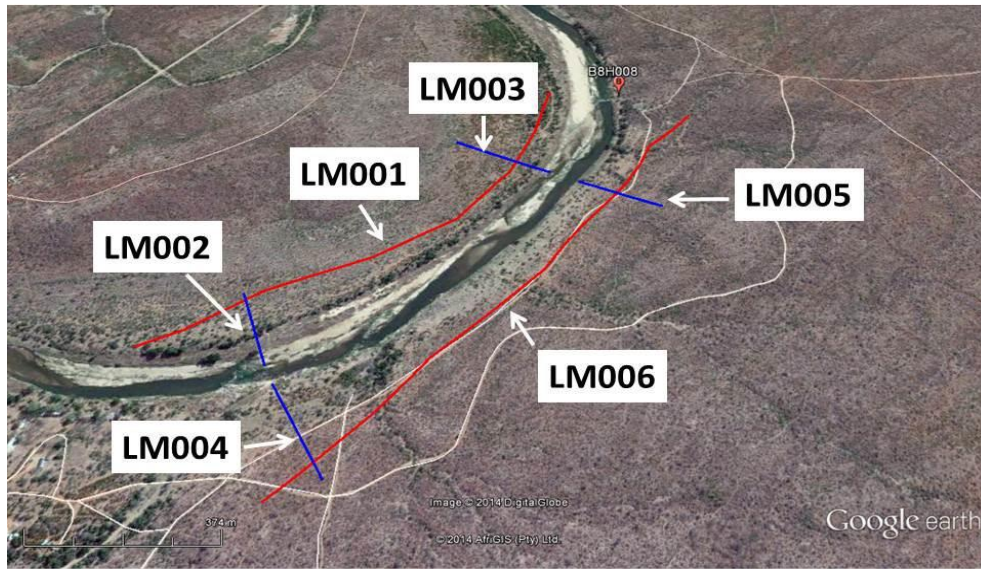


Figure 5.11 Locality map of the geophysics transects over the Protected area (Ridell, 2016).

Once again two transects were surveyed on both sides of the river, in an east – west direction. The northern transect (running parallel to the river) was spaced 2.5 m short and 5 m long while using the Schlumberger array (LM001, LM were later on replaced with LR for less confusion). The southern transect was spaced 5 m short and 10 m long, also implementing the Schlumberger array (LM006). The rest of the transects running perpendicular to the river were spaced 2.5 m short and 5 m long to obtain shallower resistivity profiles (35 m) (LM002 – LM005).

5.3.2.1 LM/LR001

The incorporated resistivity and magnetic surveys of LM001 can be seen in Figure 5.12. The traverse runs in a Northeast to Southwest direction, on the northern bank parallel to the river. Type curves indicated numerous possible magnetic structures at 380 m (indicated by 400 nT and 785 Ω m), 580 m (indicated by 800 nT and 785 Ω m), 750 m (indicated deeper with 600nT and 2000 Ω m) and 1080 m (a possible sill indicated by 1150 nT and 3122 Ω m). The proposed drilling locations were at 420 m and 670 m.

These boreholes were sited on the northern and southern side of a large dolerite dyke (cross cutting the river), that were identified by the geophysical survey on the northern bank. The purpose of this was to monitor the aquifers on both sections (north and south of the impermeable layer), responses to rainfall events and during high flow periods. Due to the little and shallow weathering indicated by the resistivity values ranging from 2.63 – 184 Ωm , the water level and weathering were interpreted at approximately 12 m. After drilling LR001A/B (Appendix B-7) at 420 m the groundwater level was confirmed at approximately 10.4 m, in line with the initial 12 m interpreted from the resistivity survey. The weathering was confirmed at a depth of approximately 17 m, relatively in range although a bit deeper than expected. Two structures were intersected one between 7 to 9 m and one at 43 m. This was expected as the magnetic and resistivity survey indicated numerous dykes within this area. After drilling LR0011A/B (Appendix B-8) at 670 m the groundwater level was confirmed at approximately 10.4 m, in line with the initial 12 m interpreted from the resistivity survey. The weathering was confirmed at a depth of approximately 8 m, in line with the predicted 12 m. Again, two structures were intersected, one large dyke stretching from 9 to 61 m followed by a 6 m section of granite with the rest of the log ending in dolerite.

5.3.2.2 LM/LR002

The incorporated resistivity and magnetic surveys of LM002 can be seen in Figure 5.13. The traverse runs in a Southeast to Northwest direction, perpendicular to the river. The type-curves indicated a possible magnetic structure at approximately 50 m (800 nT) and are in correlation with the higher resistivity values (256 – 1297 Ωm) when in comparison. The proposed borehole was sited at 210 m, because of the low resistivity values (10 – 50.6 Ωm) that indicates weathering increasing the chances of striking water. The water level was estimated at approximately 10 m, with the weathering indicated at around 15 m. After drilling LR002A/B (Appendix B-8) the groundwater level was confirmed at approximately 10.7 m, in the region of the initial 10 m interpreted from the resistivity survey. The weathering was confirmed at a depth of approximately 11 m, slightly shallower than the resistivity surveys prediction. The top seven meters were red sand, after which granite was intersected continuing to the bottom of the borehole log, this concurred with the resistivity survey, which indicated hard rock with high resistivity (1297 >) values from around 15 m.

5.3.2.3 LM/LR003

The incorporated resistivity and magnetic surveys of LM003 can be seen in Figure 5 14. The traverse runs in a Southeast to Northwest direction, perpendicular to the river. The type-curves indicated a possible magnetic structure at approximately 60 m (400 nT) and 250 m (780 nT). These findings are in correlation with the higher resistivity values (256 – 2919 Ωm) at depth, when in comparison. The structure seems to be running parallel to the river within this section (northwest - southeast), which is in correlation with the general direction of intruded dykes within the area. Deep weathering was displayed after 120 m to depths of up to 35 m, by low resistivity values of around 10 – 114 Ωm .

The proposed borehole was sited at 100 m. This was also implemented on purpose as to test the accuracy of the ERT and whether our interpretations have been exact. According to the ERT the structure that is made up of hard rock (>557nT) would be intersected at approximately 6 m during drilling and the water level would occur at around 8 m at the interface between the hard rock and unconsolidated zone. After drilling LR003 (Appendix B-9) the groundwater level was confirmed at approximately 11.4 m, slightly deeper than the initial 8 m interpreted from the resistivity survey. The weathering was confirmed at a depth of approximately 7 m, almost exactly as the initial predictions from the resistivity data. As seen from the geological logs the first 6 m was red sand with the structure (granite) being intersected at 7 m. Thus, confirming our interpretation was relatively accurate.

5.3.2.4 LM/LR004

The incorporated resistivity and magnetic surveys of LM004 can be seen in Figure 5.15. The traverse runs in a Northwest to Southeast direction, perpendicular to the river. The type-curves indicated a possible magnetic structure stretching from 100 -150 m (1400nT) and are in correlation with the higher resistivity values of 577 – 5000 Ωm when in comparison. The structure is possibly running parallel to the river with a plunge in the direction of the river. The proposed borehole location was at 150 m, with low magnetic and resistivity values indicating on fracturing/weathering for a greater possibility of obtaining a water strike. The groundwater level was interpreted at approximately 12 m, because of the slightly deeper weathering indicated at this region. Weathering was also predicted at around 10 m with resistivity values ranging from 50.6

to 557 Ωm . After drilling LR004 (Appendix B-10) the groundwater level was confirmed at approximately 11.4 m, close to the initial 12 m interpreted from the resistivity survey. The weathering was confirmed at a depth of approximately 10 m, slightly shallower than the initial predictions. The structure (granite) indicated by the resistivity survey were intersected at 11 m, almost the exact depth initially predicted by the high 577 < Ωm values.

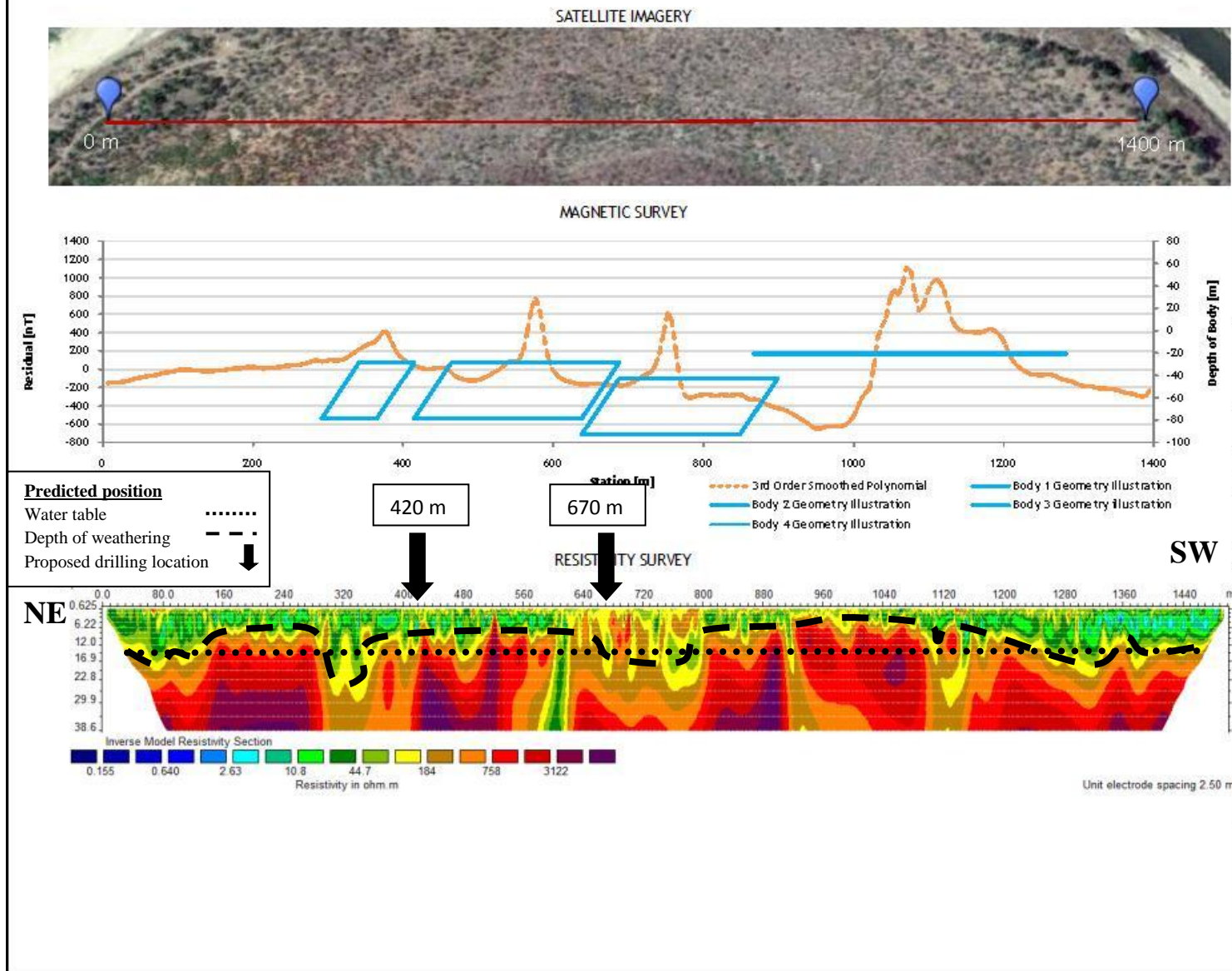
5.3.2.5 LM/LR005

The incorporated resistivity and magnetic surveys of LM005 can be seen in Figure 5.16. The traverse runs in a Northwest to Southeast direction, perpendicular to the river. The type-curves indicated a possible magnetic structure at approximately 60 m with high magnetic values of around 1400 nT and are in correlation with the higher resistivity values of around 2919 Ωm when in comparison. The structure is possibly striking parallel to the river. Deep weathering is indicated closer to the river with resistivity values ranging between 22.5 – 256 Ωm , that might possibly form part of an alluvial aquifer. The proposed location for drilling is at 100 m, in front of the detected structure, as it might be impermeable and be blocking the groundwater. The initial groundwater level was predicted at approximately 15 m from the deep weathering indicated by the low resistivity values (50.6 – 557 Ωm). The weathering was also predicted at around 15 m. After drilling LR005 (Appendix B-10) the groundwater level was confirmed at approximately 9.7 m, much shallower than the initial 15 m interpreted from the resistivity survey. Weathering also occurred much shallower at around 9 m as indicated by the geological logs. Oxidised iron precipitate was found on samples to a depth of 48 m, which might explain the deep weathering indicated by resistivity data. This indicates that water is moving through this section possibly in small fractures spread out through the granite.

5.3.2.6 LM/LR006

The incorporated resistivity and magnetic surveys of LM006 can be seen in Figure 5.17. The traverse runs in a Northeast to Southwest direction, on the southern bank parallel to the river. Type curves indicated numerous possible magnetic structures at 240 m (1800 nT), 390 m (2400 nT), 550 m (1800 nT) and at 800 m (500 nT). The structures are indicated in a northwest to southeast direction by the resistivity data (557 < Ωm). This is in correlation with the direction of dykes within this area.

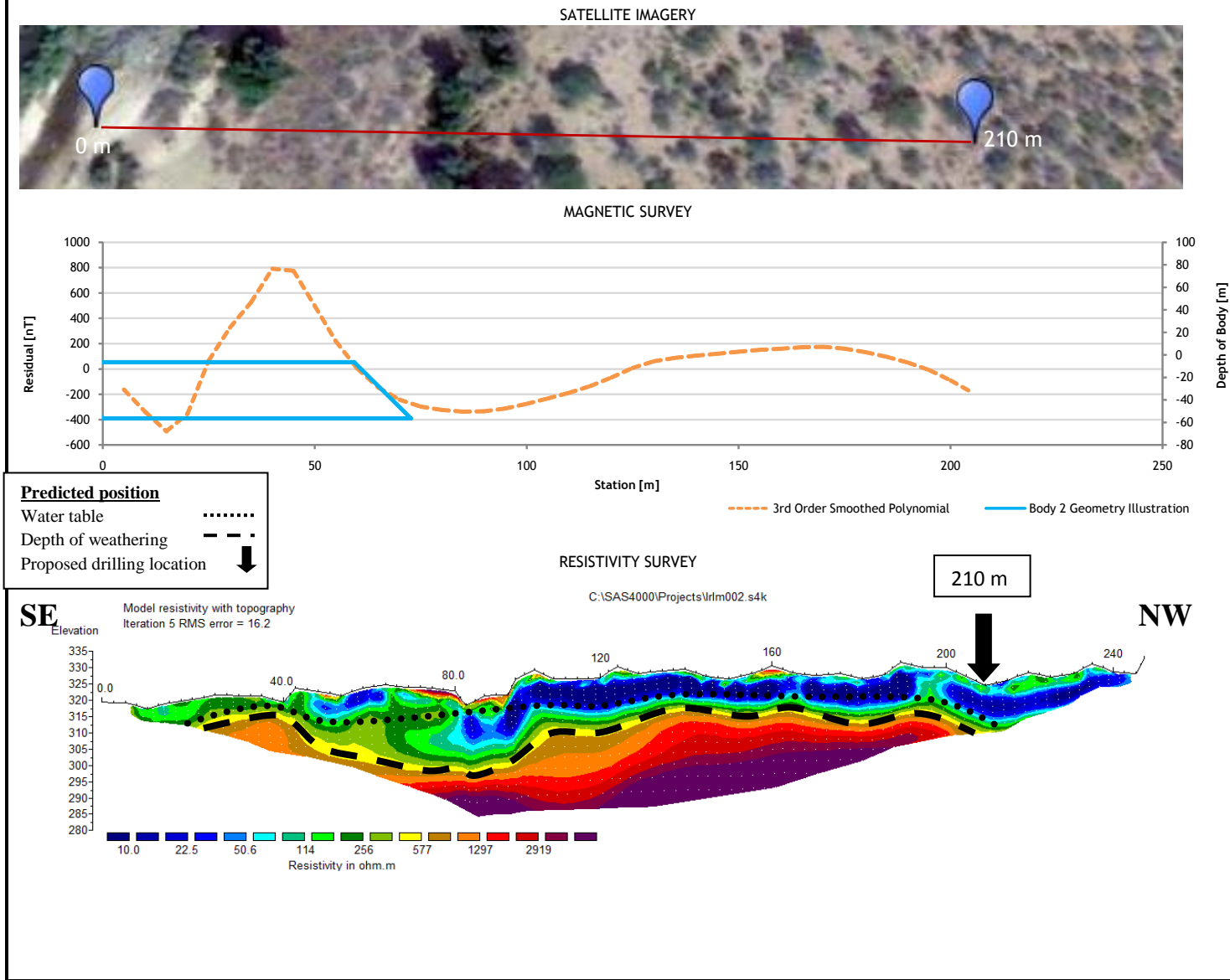
LETABA TRAVERSE LR001 - COMBINED GEOPHYSICAL INTERPRETATION



INTERPRETATION SUMMARY	
TRAVERSE INFORMATION 	
INTERPRETED BODY GEOMETRY	
CENTER: 378/576 m/station (E-Line (Werner, 1956))	DIP: 45 degrees (Roux, 1980)
WIDTH: 73/223 meter	DEPTH: 29 meter
FIGURE DETAILS	
Data	Google Earth TM mapping service: 2015
Sources:	Imagery Date: 07/03/2014
FIGURE NO	MAP NUMBER GCS008
PREPARED BY:	R Minnaar Hydrogeologist
REVIEWED BY:	
DATUM:	Cape
PROJECTION:	Transverse Mercator (o31)
DATE:	29/07/2015
PROJECT:	Letaba River K5-2338

Figure 5.12 Geophysical traverse LM001 with incorporated magnetic and resistivity profiles (modified after Gokool et al., 2015).

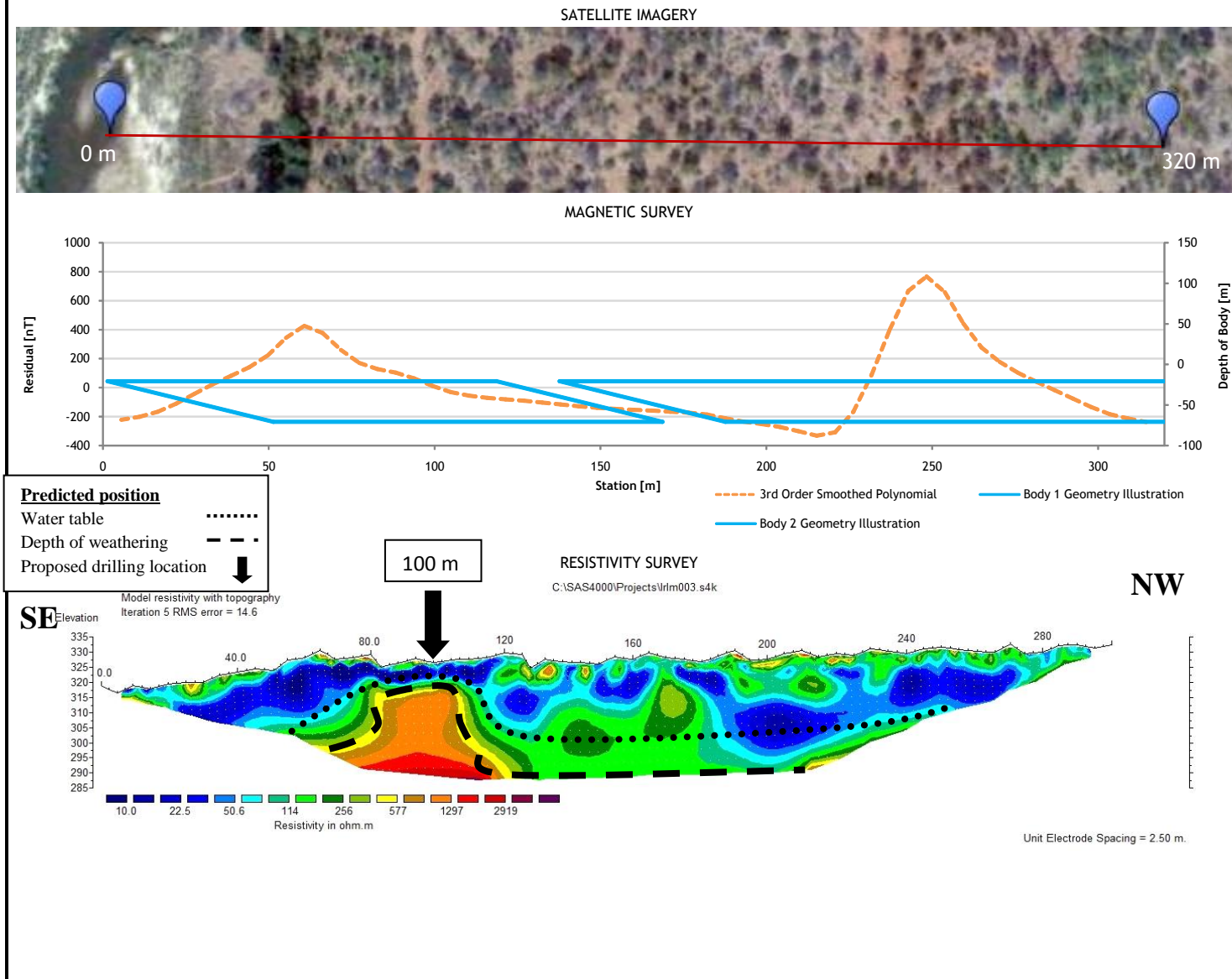
LETABA TRAVERSE LR002 - COMBINED GEOPHYSICAL INTERPRETATION



INTERPRETATION SUMMARY	
TRAVERSE INFORMATION	
INTERPRETED BODY GEOMETRY	
CENTER: 23 m/station (E-Line (Werner, 1956))	DIP: 75 degrees (Roux, 1980)
WIDTH: 85 meter	DEPTH: 7 meter
FIGURE DETAILS	
Data	Google Eart TM mapping service: 2015
Sources:	Imagery Date: 07/03/2014
FIGURE NO	-
MAP NUMBER	GCS009
PREPARED BY:	R Minnaar Hydrogeologist
REVIEWED BY:	
DATUM:	Cape
PROJECTION:	Tranverse Mercator lo31
DATE:	29/07/2015
PROJECT:	Letaba River K5-2338

Figure 5.13 Geophysical traverse LM002 with incorporated magnetic and resistivity profiles (modified after Gokool et al., 2015).

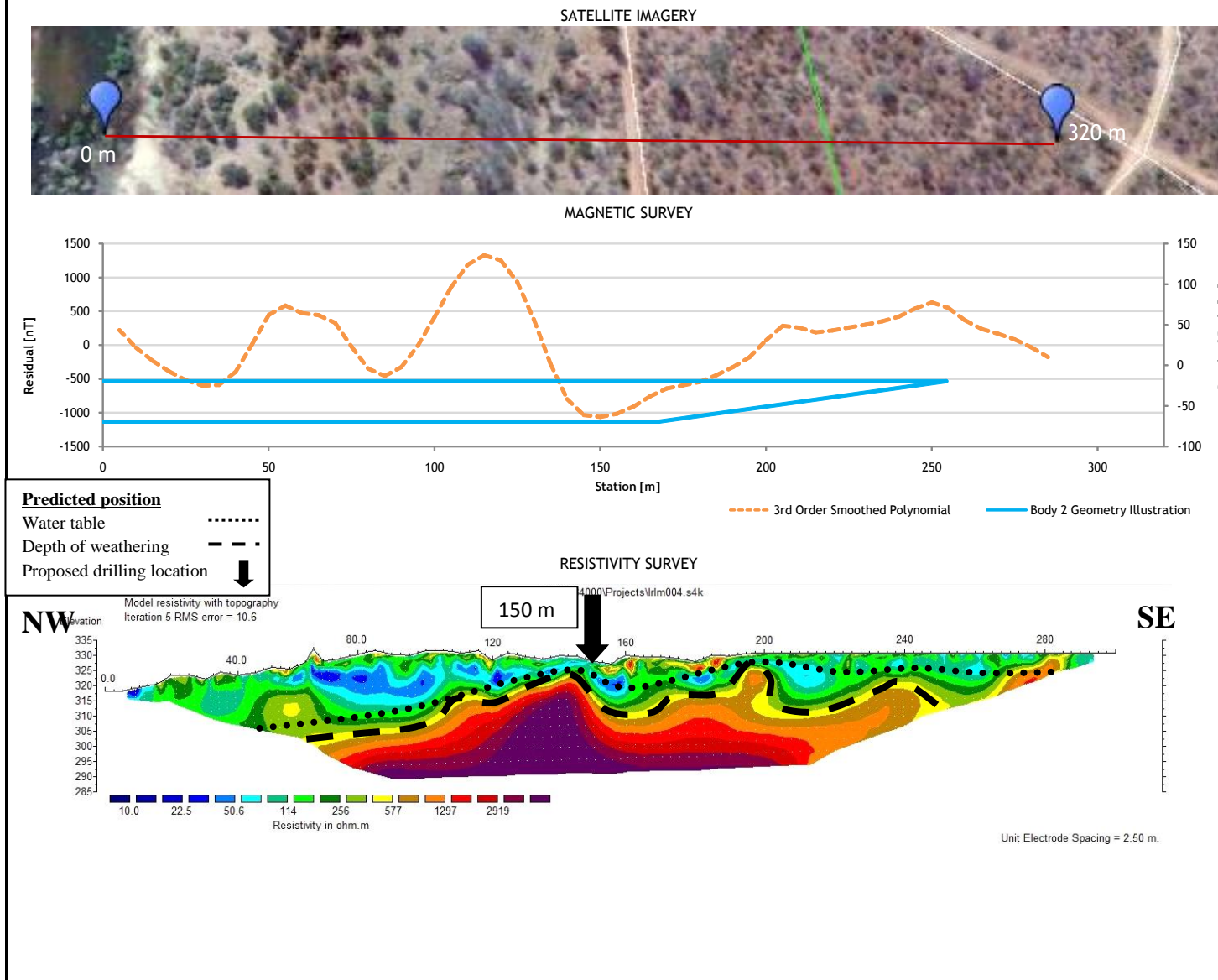
LETABA TRAVERSE LR003 - COMBINED GEOPHYSICAL INTERPRETATION



INTERPRETATION SUMMARY	
TRAVERSE INFORMATION	
INTERPRETED BODY GEOMETRY	
CENTER: 23 m/station (E-Line (Werner, 1956))	DIP: 45/75 degrees (Roux, 1980)
WIDTH: 85/200 meter	DEPTH: 20 meter
FIGURE DETAILS	
Data	Google Eart TM mapping service: 2015
Sources:	Imagery Date: 07/03/2014
FIGURE NO	MAP NUMBER GCS010
PREPARED BY: R Minnaar Hydrogeologist	REVIEWED BY: J Nel Hydrogeologist
DATUM: Cape	DATE: 25/07/2015
PROJECTION: Transverse Mercator lo31	
PROJECT: Letaba River K5-2338	

Figure 5 14 Geophysical traverse LM003 with incorporated magnetic and resistivity profiles (modified after Gokool et al., 2015).

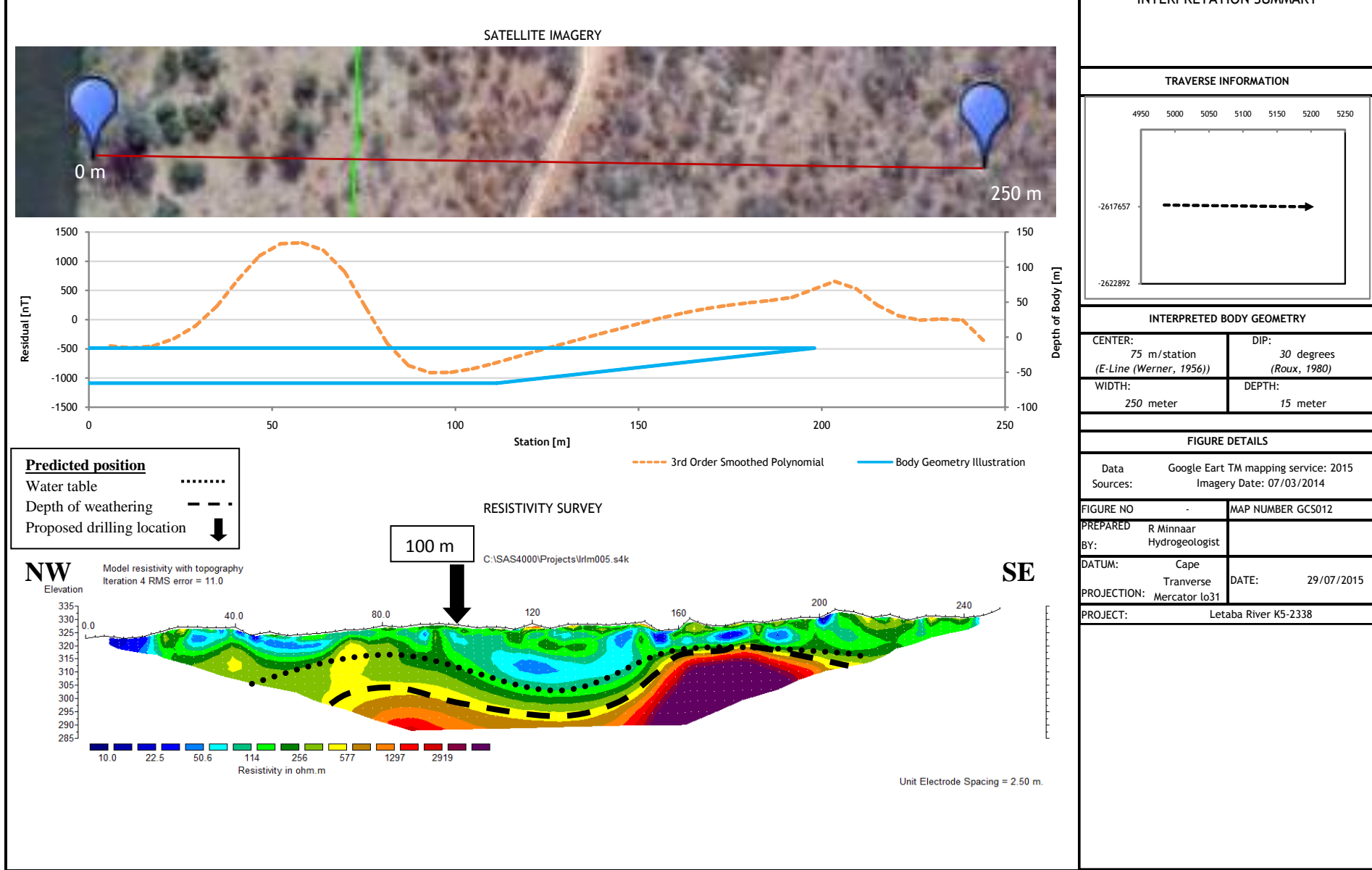
LETABA TRAVERSE LR004 - COMBINED GEOPHYSICAL INTERPRETATION



INTERPRETATION SUMMARY																					
<p>TRAVERSE INFORMATION</p>																					
<p>INTERPRETED BODY GEOMETRY</p> <table border="1"> <tr> <td>CENTER: 103 m/station (E-Line (Werner, 1956))</td> <td>DIP: 30 degrees (Roux, 1980)</td> </tr> <tr> <td>WIDTH: 300 meter</td> <td>DEPTH: 20 meter</td> </tr> </table>		CENTER: 103 m/station (E-Line (Werner, 1956))	DIP: 30 degrees (Roux, 1980)	WIDTH: 300 meter	DEPTH: 20 meter																
CENTER: 103 m/station (E-Line (Werner, 1956))	DIP: 30 degrees (Roux, 1980)																				
WIDTH: 300 meter	DEPTH: 20 meter																				
<p>FIGURE DETAILS</p> <table border="1"> <tr> <td>Data</td> <td>Google Eart TM mapping service: 2015</td> </tr> <tr> <td>Sources:</td> <td>Imagery Date: 07/03/2014</td> </tr> <tr> <td>FIGURE NO</td> <td>-</td> </tr> <tr> <td>MAP NUMBER</td> <td>GCS010</td> </tr> <tr> <td>PREPARED BY:</td> <td>R Minnaar Hydrogeologist</td> </tr> <tr> <td>REVIEWED BY:</td> <td></td> </tr> <tr> <td>DATUM:</td> <td>Cape</td> </tr> <tr> <td>PROJECTION:</td> <td>Transverse Mercator lo31</td> </tr> <tr> <td>DATE:</td> <td>29/07/2015</td> </tr> <tr> <td>PROJECT:</td> <td>Letaba River K5-2338</td> </tr> </table>		Data	Google Eart TM mapping service: 2015	Sources:	Imagery Date: 07/03/2014	FIGURE NO	-	MAP NUMBER	GCS010	PREPARED BY:	R Minnaar Hydrogeologist	REVIEWED BY:		DATUM:	Cape	PROJECTION:	Transverse Mercator lo31	DATE:	29/07/2015	PROJECT:	Letaba River K5-2338
Data	Google Eart TM mapping service: 2015																				
Sources:	Imagery Date: 07/03/2014																				
FIGURE NO	-																				
MAP NUMBER	GCS010																				
PREPARED BY:	R Minnaar Hydrogeologist																				
REVIEWED BY:																					
DATUM:	Cape																				
PROJECTION:	Transverse Mercator lo31																				
DATE:	29/07/2015																				
PROJECT:	Letaba River K5-2338																				

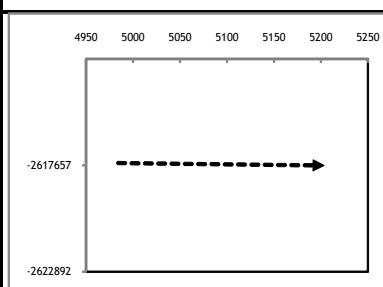
Figure 5.15 Geophysical traverse LM004 with incorporated magnetic and resistivity profiles (modified after Gokool et al., 2015).

LETABA TRAVERSE LR005 - COMBINED GEOPHYSICAL INTERPRETATION



INTERPRETATION SUMMARY

TRAVERSE INFORMATION



INTERPRETED BODY GEOMETRY

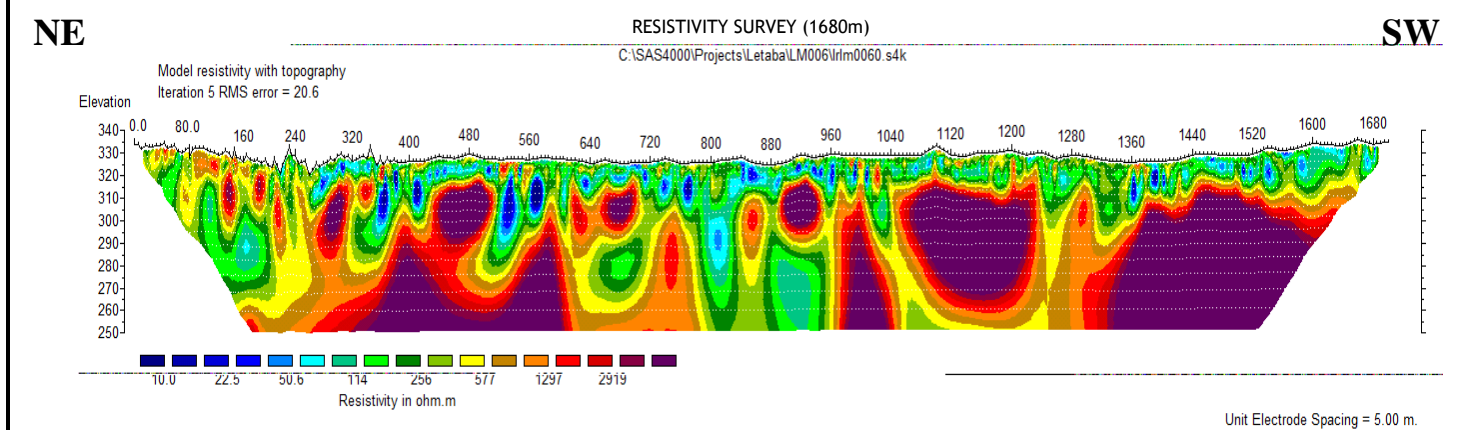
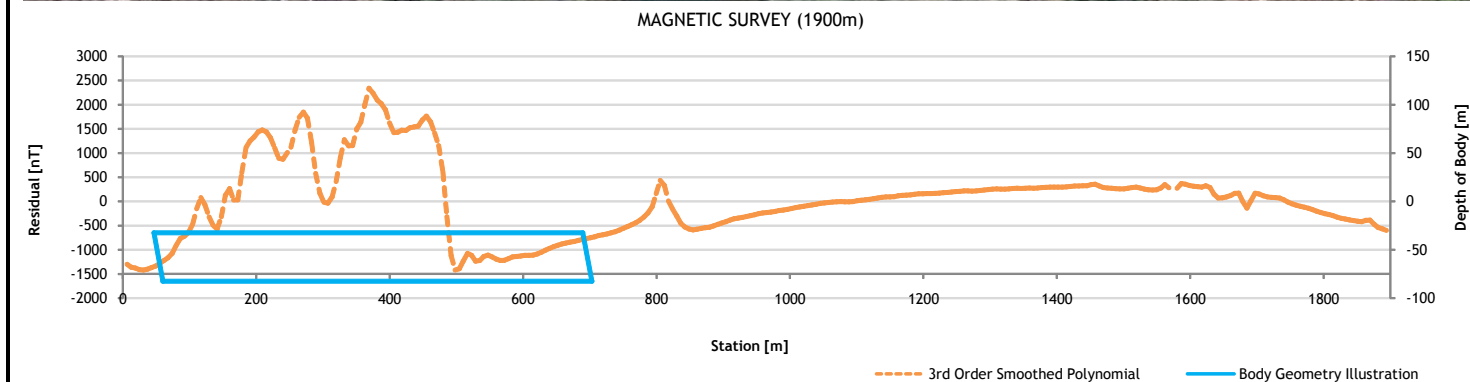
CENTER: 75 m/station (E-Line (Werner, 1956))	DIP: 30 degrees (Roux, 1980)
WIDTH: 250 meter	DEPTH: 15 meter

FIGURE DETAILS

Data	Google Eart TM mapping service: 2015	
Sources:	Imagery Date: 07/03/2014	
FIGURE NO	-	MAP NUMBER GCS012
PREPARED BY:	R Minnaar Hydrogeologist	
DATUM:	Cape	DATE: 29/07/2015
PROJECTION:	Tranverse Mercator lo31	
PROJECT:	Letaba River K5-2338	

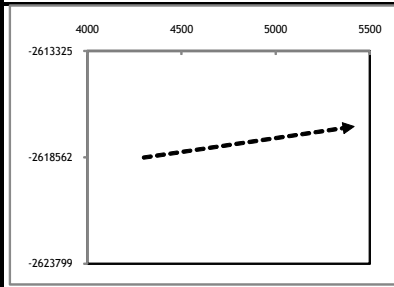
Figure 5.16 Geophysical traverse LM005 with incorporated magnetic and resistivity profiles (modified after Gokool et al., 2015).

LETABA TRAVERSE LR006 - COMBINED GEOPHYSICAL INTERPRETATION



INTERPRETATION SUMMARY

TRAVERSE INFORMATION



INTERPRETED BODY GEOMETRY

CENTER: 368 m/station (E-Line (Werner, 1956))	DIP: 30 degrees (Roux, 1980)
WIDTH: 643 meter	DEPTH: 32 meter

FIGURE DETAILS

Data	Google Eart TM mapping service: 2015	
Sources:	Imagery Date: 07/03/2014	
FIGURE NO	-	MAP NUMBER GCS013
PREPARED BY:	R Minnaar Hydrogeologist	
DATUM:	Cape	DATE: 29/07/2015
PROJECTION:	Tranverse Mercator lo31	
PROJECT:	Letaba River K5-2338	

Figure 5.17 Geophysical traverse LM006 with incorporated magnetic and resistivity profiles (modified after Gokool et al., 2015).

In summary, the geophysics provided the necessary data to identify suitable positions for the drilling of the boreholes and obtaining groundwater. It also provided information on the geological characteristic of the study site.

Numerous dykes were indicated on many of the transects, this will ultimately pose some difficulties with the interpretation of the groundwater movement and the conceptual model. The weathering and water table were interpreted in close proximity averaging around 12 m and 10 m respectively.

5.4 AQUIFER CHARACTERISATION

To characterise the aquifer of the study area (Figure 5.18) and provide information of groundwater flow, aquifer tests were conducted to obtain transmissivity (T) and hydraulic conductivity (K) values. To obtain the information three tests were conducted namely slug tests, step tests and constant rate tests (see section 4.6 AQUIFER TESTING). It must be taken into account that during these tests and analyses that many assumptions are made (refer to 2.5.7 Analysis of aquifer test).

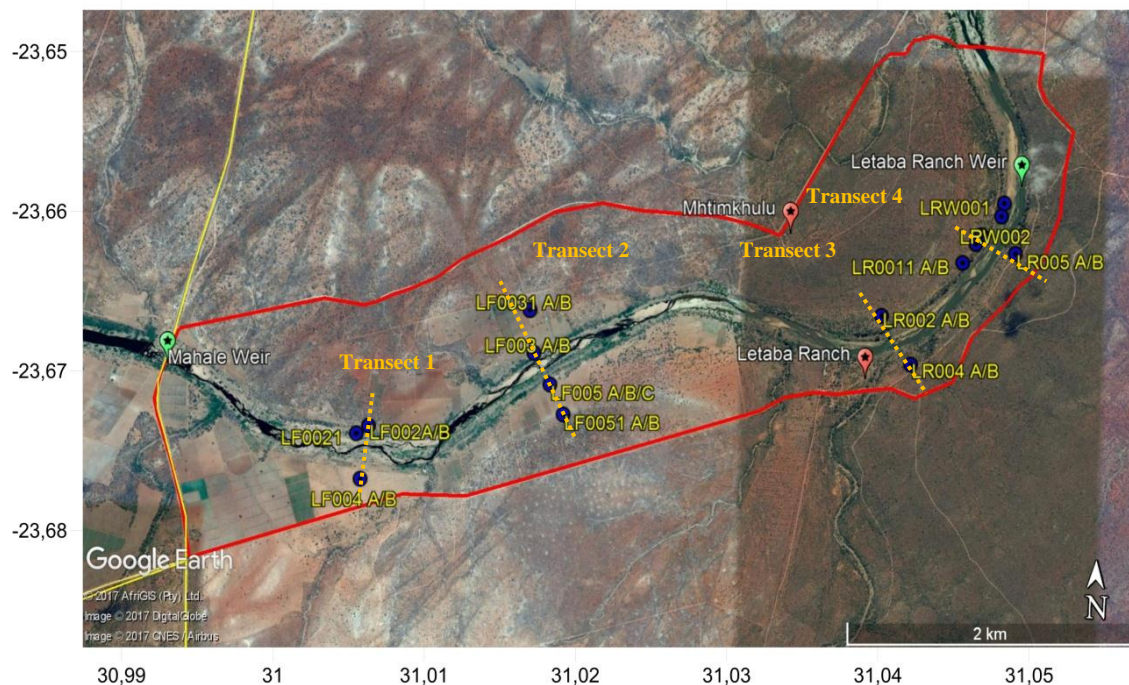


Figure 5.18 Overview of study site with borehole locations

5.4.1 Slug tests

The data obtained from the slug tests were entered into the software AQTESOLV for analysis. The parameters that were provided to the software are as follow:

- Observed displacement
- Static water column height
- Saturated thickness of the aquifer
- Depth to top of well screen.
- Length of well screen.
- Transducer depth.
- Inside radius of well casing.

The Time (sec) it took to recover 95% of the displacement and the amount of displacement that took place in 5 second intervals, were also recorded. This data was then used by the software to calculate the hydraulic conductivity and transmissivity through using the Bouwer and Rice (1976) solution. The data was also plotted into the FC-EXCEL macro (through using the Bouwer and Rice equation), to obtain the estimated yield of each borehole and to compare the software's results for the best possible representation of the K and T values. The results are displayed in **Table 5.3**.

When the values produced by the two data sets are compared, it is clear that very large differences are observed even to a few orders of magnitude. Of the 21 slug tests completed only 7 boreholes depicted a K and T value with similar values produced by both software's.

It was decided that the K and T values obtained from AQTSOLV would be used as, a data logger was utilised during these slug tests. Thus, excluding human error and producing the most accurate K and T values. It must be stated again that the slug test is a preliminary test and is mostly used in practice to get a first estimate of the borehole yield.

Boreholes LF002A, LF0031B, LF0021 and LF003A displayed the four lowest K and T values. LF0031B and LF0021 were expected as they displayed very low yields during drilling. LF003A did not have any water strikes during drilling and obtained its water

from seepage afterwards, thus we expected very low K and T values. LF002A stood out because it had a relatively high blow out yield of 1 L/s.

The highest K and T value were observed in boreholes LF002B, LR005A, LF0031A and LF003B. LF002B were the anomaly as, it indicated very high K and T values, although it produced a relatively low blow out yield of 0.4 L/s. The anomaly most probably comes from the faulty borehole construction, as a cavity formed just above the groundwater level from soil falling into the borehole.

The casing was also placed skew over the rimmed section of the borehole, thus not preventing soil from entering the borehole. The result is that water pushed into this cavity as the water rose from the slug test. LR005A and LF0031A were expected to have high K and T values, as they produced a blowout yield of between 3 and 5.7 L/s, with LF003B also displaying a high yield. This incurs that the tests were completed correctly and that the data was accurate.

5.4.2 Step tests

For this study step tests were only implemented to obtain a preliminary yield that would be optimum for the constant rate test (refer to 2.5.6 Pumping tests). An example of a step test on LR005B can be seen in Figure 5.19.

In the first step the borehole was pumped at a rate of 0.2 L/sec for 1 hour. Then the tap was opened to increase the yield to approximately 0.4 L/sec maintained for an hour. In the third step the tap was opened to obtain a yield of 0.7L/sec. The water level then dropped to the level of the pump within 20 minutes, because the abstraction rate exceeded the yield of the aquifer.

From this data alone, it can be observed that the optimum yield to pump the borehole would be between 0.4 and 0.7 L/sec. This is because only 3.4 m of drawdown were obtained when pumping at 0.4 L/s while the borehole was quickly dewatered at 0.7 L/s. Thus, to obtain the maximum drawdown to the fracture without dewatering the borehole, the constant rate yield would have to be between 0.4 and 0.7 L/sec. Although, this is only an indication and a more accurate yield was obtained through plotting the data in the FC-EXCEL sheet that uses the FC – Non Linear method to obtain the optimum yield for the constant test.

The results from the FC – Non Linear method is displayed in figure 5.20 and determines that if the borehole is pumped for eight hours the optimum yield will be 0.55 L/s while obtaining a drawdown of 13.31 m. This would then be ideal as there were 13.4 m of drawdown available. If the borehole were to be pumped for 24 hours the yield decreased to 0.47 L/s while obtaining a drawdown of 13 m.

The FC Excel software uses the equation (equation 2.) of Jacob (1947), who performed the first step test to determine what the drawdown would be within a borehole if it were to be pumped at different rates (Kruseman et. al, 1994).

$$s_w = B(r_{ew}, t)Q + CQ^2 \quad (5.1)$$

where:

$$B(r_{ew}, t) = B_{1(rw,t)} + B_2$$

$B_{1(rw,t)}$ = Linear aquifer – loss coefficient.

B_2 = linear well-loss coefficient.

C = non-linear well-loss coefficient.

r_{ew} = effective radius of the borehole.

r_w = actual radius of the borehole.

t = pumping time.

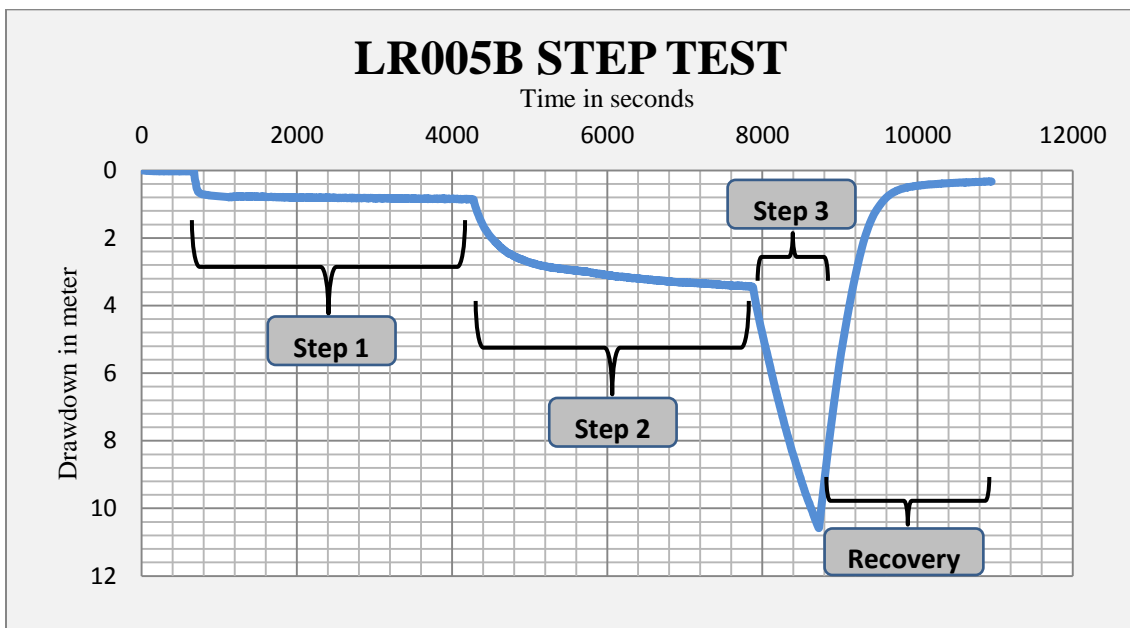


Figure 5.19 Step test performed on LR005B.

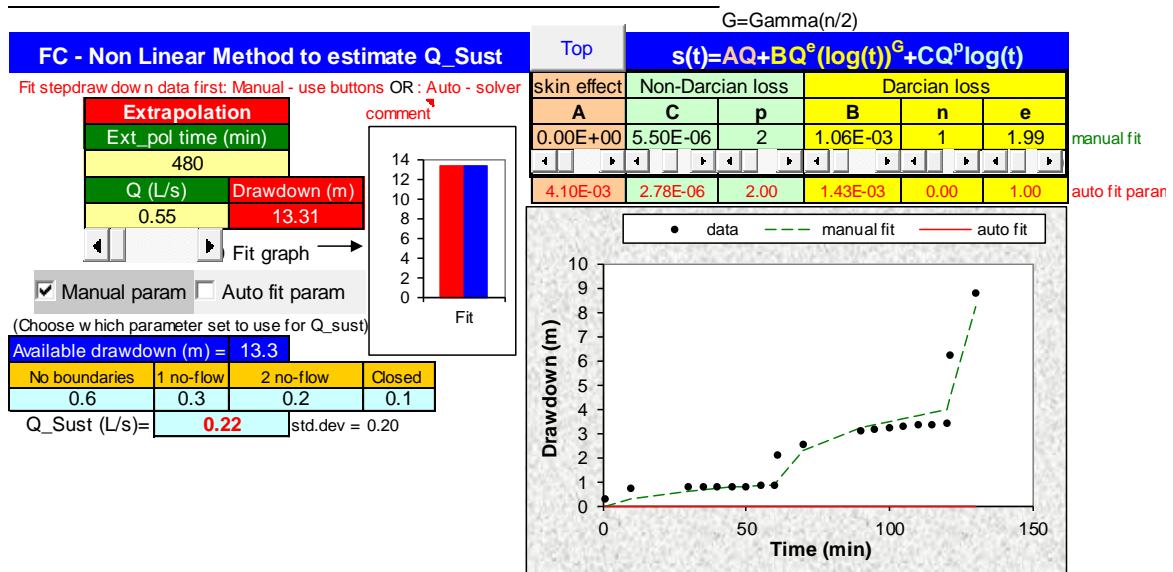


Figure 5.20 Results through using the FC – Non Linear Method.

Table 5.3 Initial K and T values from slug tests.

		FC-EXCEL			AQTSOLV	
BOREHOLE	Static water level (m)	Estimated Yield L/s	K (m/day)	T (m ² /day)	K (m/day)	T (m ² /day)
LF002A	11.700	0.110	0.081	0.996	0.033	1.598
LF002B	Could not do a proper slug test. Problems with BH construction.				45.090	139.800
LF003A	11.780	1.600	0.097	3.492	0.125	7.535
LF003B	11.790	5.000	0.289	2.373	1.518	12.600
LF004A	13.460	0.260	0.085	4.080	0.019	1.137
LF004B	13.360	2.650	0.878	1.440	0.411	0.670
LF005A	12.880	0.200	0.068	2.856	0.038	2.272
LF005B	12.660	0.040	0.012	0.352	0.012	0.339
LF0021	8.400	0.150	0.101	1.576	0.002	0.037
LF0031A	13.620	12.510	0.265	3.180	2.686	124.500
LF0031B	13.330	0.100	0.121	0.808	0.002	0.013
LF0051A	14.850	0.660	0.064	2.506	0.358	14.020
LF0051B	14.830	0.240	0.227	3.444	0.020	0.301
LR001A	10.400	0.220	0.120	3.600	0.024	1.191
LR002A	10.720	0.040	0.020	0.360	0.006	0.179
LR003A	11.420	0.000	0.000	0.000	0.005	0.017
LR004A	11.120	0.090	0.026	1.115	0.802	0.013
LR004B	11.070	0.370	0.605	7.823	0.177	2.268
LR005A	9.430	11.000	0.399	20.177	5.016	253.700
LR005B	9.750	1.000	1.092	15.561	0.291	4.134
LR0011A	10.220	0.000	0.060	2.880	0.009	0.583
LF005C	Could not do a proper slug test. Problems with BH construction.				0.111	0.166
LRW002	1.010	0.410	0.419	2.091	0.433	1.963
LRW001	1.400	0.160	0.177	1.876	0.214	1.868
LR001B	Water column too shallow for slug test.					
LR0011B	Water column too shallow for slug test.					

5.4.3 Constant rate tests

The optimum yield obtained from the step tests was then used and the boreholes were pumped until they were dewatered or as long as possible to obtain a test of 8 hours or no less than 2 hours. The data obtained from the slug tests were then entered into the software AQTESOLV for analysis (Figure 5.21). The parameters that were provided to the software are as follow:

- Aquifer Saturated thickness
- Full or partial penetration
- Observed displacement over time
- Yield (L/sec) over time
- Inside radius of well casing.

This data was then used by the software to calculate the K and T values using the Cooper – Jacob solution for unconfined aquifers (1946) (Appendix C). This solution was used by AQTSOLV for the interpretation of constant rate pumping tests within unconfined aquifers through the application of a simple correction to the drawdown data (Kruseman et. al, 1994).

Jacob (1946) correction:

$$s' = s - s^2/2b \quad (5.1)$$

where,

b = saturated thickness (L)

s = obsesrved drawdown (L)

s' = corrected drawdown (L)

It was decided on this method as there was no evidence that it was a confined aquifer, while the similar hydraulic gradients between the boreholes indicated that there was only one unconfined aquifer present.

Table 5.4 displays the results obtained.

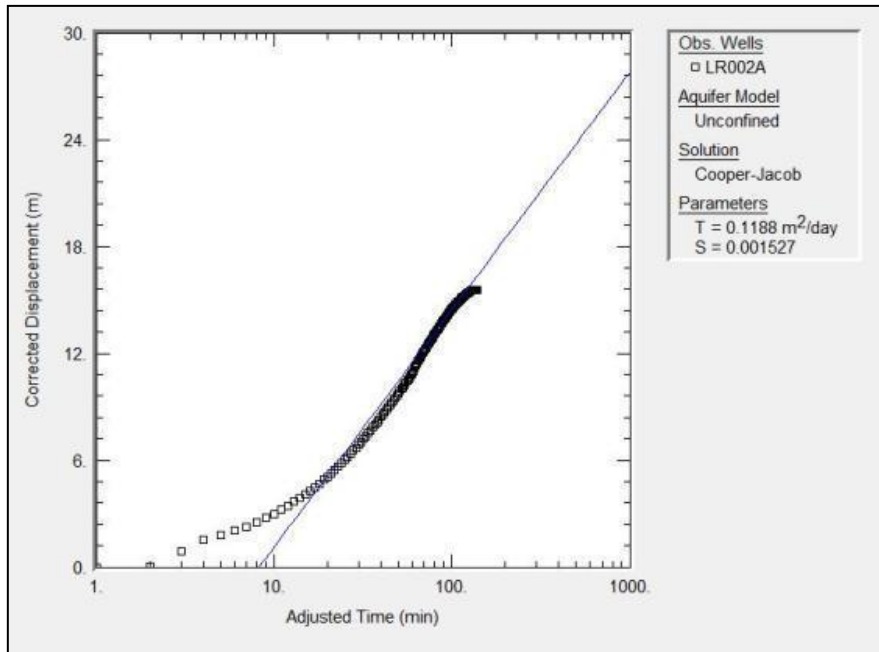


Figure 5.21 An example of the constant rate test data entered into AQT SOLV.

Table 5.4 Final K and T values obtained from the constant rate tests.

BOREHOLE	Constant rate tests				Slug tests	
	K (m ² /day)	T (m ² /day)	Storativity	Q L/s	K (m/day)	T (m ² /day)
LF0031A	3.544	164.200	0.000	STEP	2.686	124.500
LF002B	2.270	7.037	0.616	0.700	45.090	139.800
LR005A	0.533	26.970	0.047	1.600	5.016	253.700
LRW002	0.433	1.963		SLUG	0.433	1.963
LF004B	0.411	0.670		SLUG	0.411	0.670
LR004B	0.368	4.724	0.001	0.330	0.177	2.268
LR005B	0.255	3.626	0.144	0.710	0.291	4.134
LRW001	0.214	1.868		SLUG	0.214	1.868
LF003B	0.118	0.976	0.040	0.400	1.518	12.600
LF005C	0.111	0.166		SLUG	0.111	0.166
LF0051A	0.052	7.188	0.0003	1.000	0.358	14.020
LF005A	0.029	1.734	0.000002	0.150	0.038	2.272
LF0051B	0.028	0.419	0.002	0.150	0.020	0.301
LF0021	0.018	0.280	0.041	0.170	0.002	0.037
LR003A	0.009	0.099	0.005	0.100	0.005	0.017
LF005B	0.005	0.149	0.001	0.100	0.012	0.339
LR001A	0.004	0.223	0.018	0.410	0.024	1.191
LR002A	0.004	0.119	0.002	0.100	0.006	0.179
LR004A	0.003	0.138	0.002	0.160	0.802	0.013
LF0031B	0.002	0.013		SLUG	0.002	0.013
LF002A	0.002	0.079	0.003	0.150	0.033	1.598
LF003A	0.001	0.062	0.007	0.220	0.125	7.535
LF004A	0.001	0.045	0.004	0.150	0.019	1.137
LR0011A	0.001	0.043	0.004	0.110	0.009	0.583

5.4.4 Transmissivity

Of the 19 boreholes tested only 5 transmissivity values increased where the remaining 14 all decreased, when the transmissivities of the constant rate tests and slug tests are compared (Table 5.4

Table 5.4). This was expected as, the slug test only tests a small portion of the aquifer normally within the more weathered or unconsolidated zone and will thus, result in a higher transmissivity. Ultimately the transmissivity of the unconsolidated/weathered zone is tested and not as much the transmissivity of (for instance), the main fracture at 60 m in the hard rock/consolidated zone. Additionally the difference is not only dependent on the method that was used obtain the data, but also the method that was used to calculate the different parameters.

The transmissivity is directly proportional to the hydraulic conductivity and are related by the thickness of the aquifer. Fifteen of the boreholes displayed a low transmissivity of between 0.01 and 0.9 m²/day. This indicates that the transmissivity is corresponding with the local geology, as these are the typical K and T values found within crystalline rocks such as granites and gneisses.

The remaining boreholes corresponds to their yield with LF0031A, LR005A, LF002B and LF0051A displaying the highest transmissivities and yields. This infers that the transmissivities were tested and analysed correctly. From the low transmissivity values, it can be inferred that the aquifer is not a large inter-connected groundwater flow system, but rather associated with small low yielding fractures within granites and larger yielding fractures created by intrusive rocks.

When the transmissivities of the shallow boreholes (that were drilled with the intention of obtaining information on the shallow aquifer), are compared with the transmissivity of the deep boreholes (or deep aquifer) it is clear that there are no significant differences between the average transmissivities (Figure 5.22). The transmissivities indicate that two aquifers are not present, but rather one aquifer. It seems that the high transmissivities are more related to the specific location and whether a large fracture, induced by intrusive rocks, were intersected.

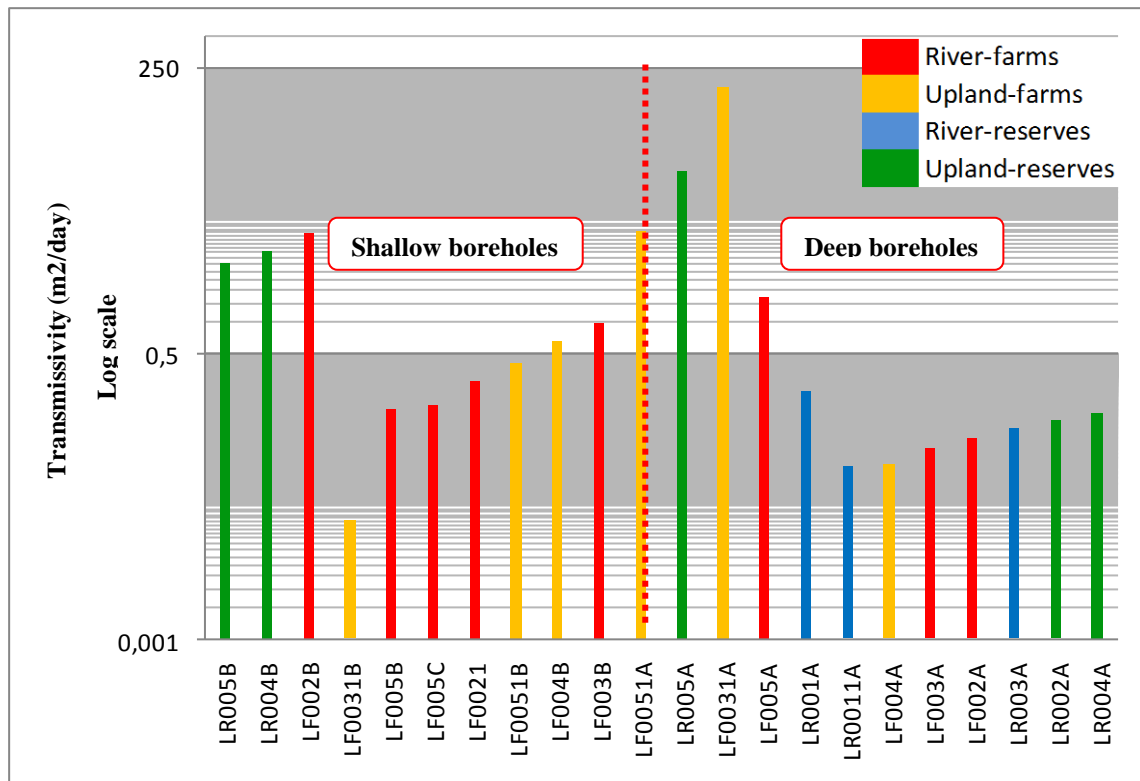


Figure 5.22 Comparison of all boreholes Transmissivity.

5.4.5 Hydraulic gradient distribution

Water levels taken on 15 February 2016 were plotted in cross-section relative to the position of the river along each transect. K and T values were included to provide an interpretation of the potential gains and losses of the Letaba River to the surrounding aquifer.

Each cross-section contained at least four (transect 3) or at most nine (transect 2) hydraulic heads to interpret the hydraulic gradients towards the river. There are many assumptions in using this method and the hydraulic gradient will differ slightly if boreholes from the different transects are used, although for this study the aim was to determine the movement towards or away from the river with the potential gains and losses.

The hydraulic gradients of transect 1: that consists of LF004, LF0021 and LF002 are plotted in Figure 5.23. The general flow direction is indicated from LF004 in the south to LF002 in the north. Thus, the river will be gaining water from the southern bank and losing water to the northern bank.

The transmissivity values indicate that there is a potentially high flow within the shallow fractured aquifer on the northern and southern bank, especially when compared to the deep (hard rock) aquifer. After the intersection with the river the shallow aquifer T values indicate a loss to the river, although a greater loss to the riparian zone (LF0021) and northern bank. The T values from the deeper boreholes (deep aquifer), infer that this aquifer is potentially detached from the shallow aquifer and river. Because, of their very low and similar T values.

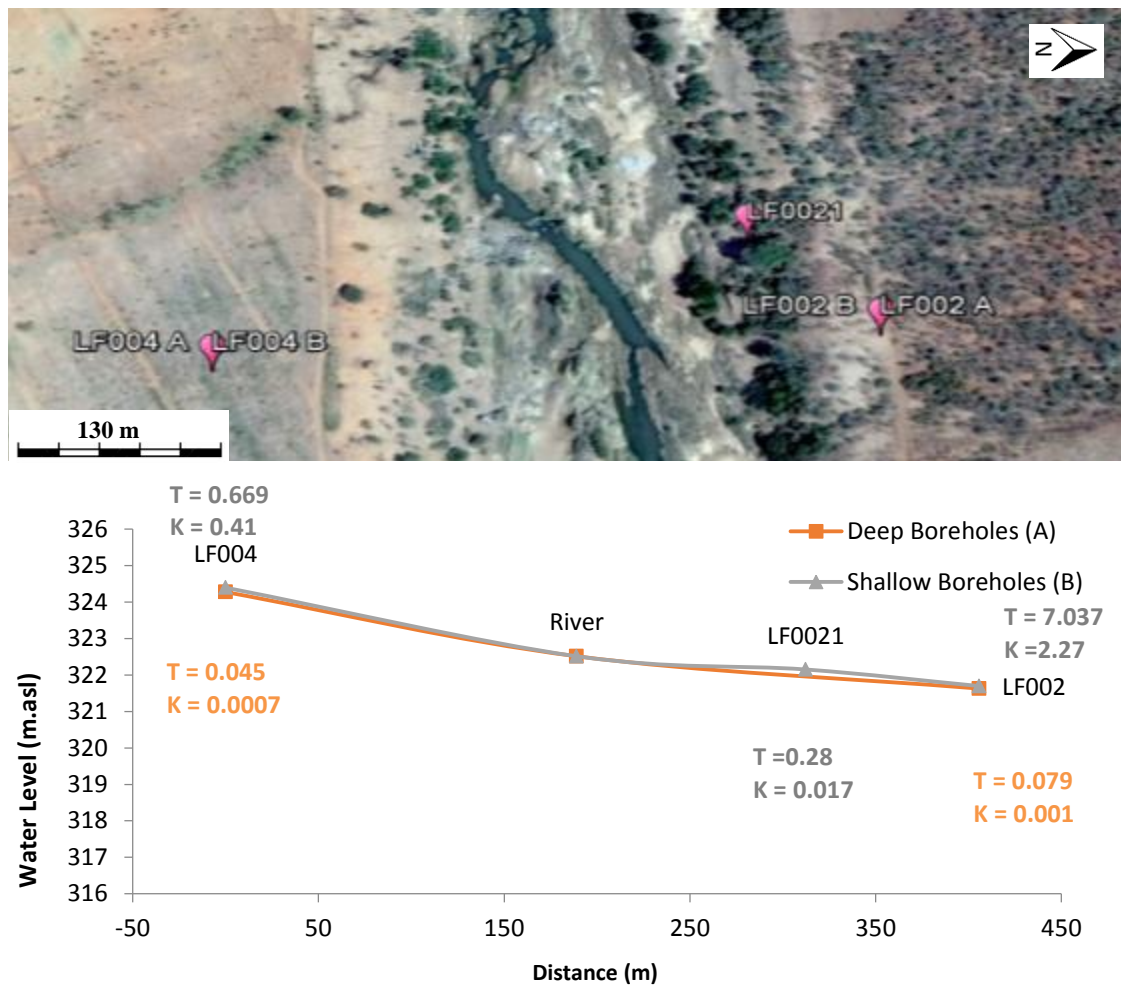


Figure 5.23 Hydraulic gradient cross-section plot of transect 1.

The hydraulic gradients of transect 2: that consists of LF0051, LF005, LF003 and LF0031 are plotted in Figure 5.24. The general flow direction is indicated from LF0031 in the north to LF0051 in the south, in contrast to transect 1. The hydraulic gradients within transect 2 indicate that both the fractured shallow and deep aquifer is disconnected from the river.

Thus, a through flow of the groundwater beneath the river is occurring with the river losing water to the aquifer. The T values of the deep aquifer indicate that the river is potentially losing water to the southern bank, although the shallow aquifer T values indicate a greater loss to the riparian zone.

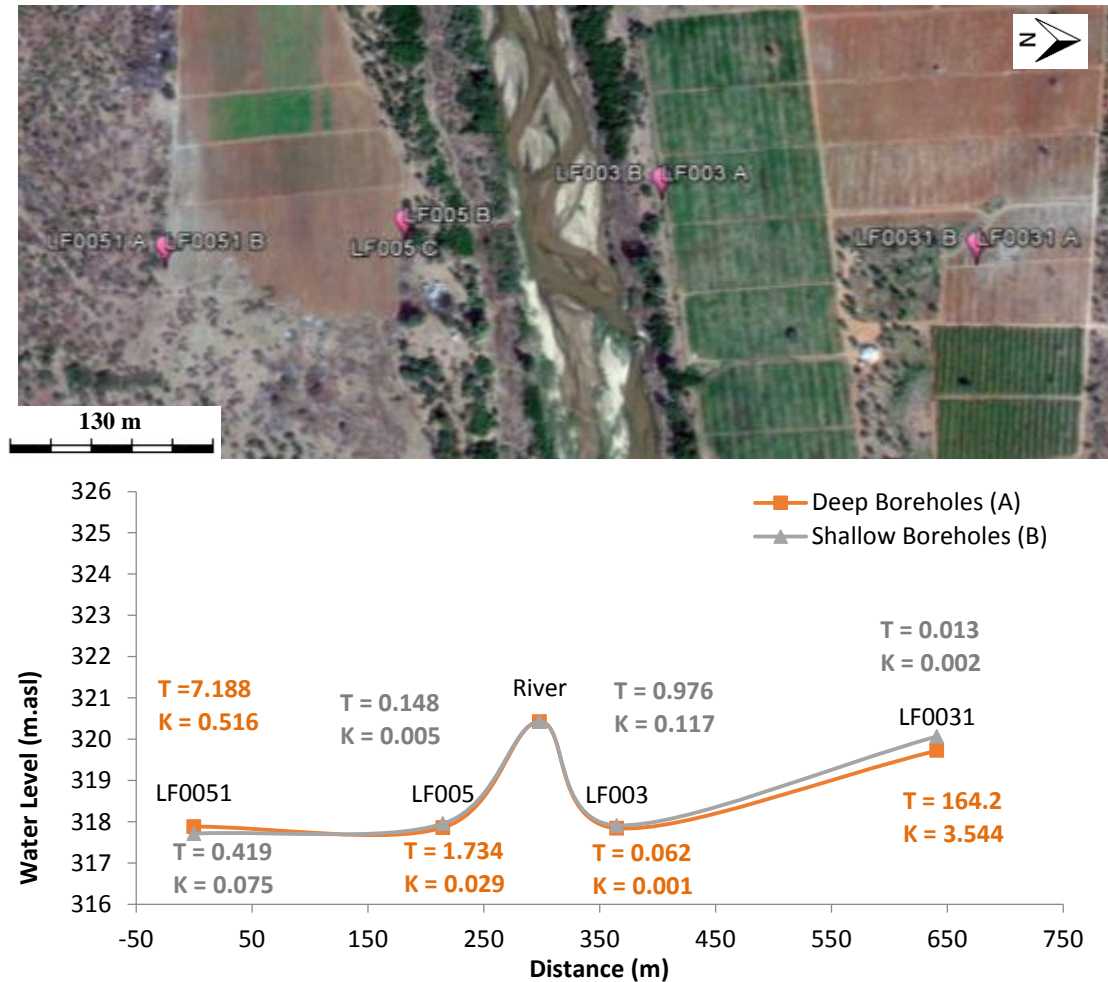


Figure 5.24 Hydraulic gradient cross-section plot of transect 2.

The hydraulic gradients of transect 3: that consists of LR002 and LR004 are plotted in Figure 5.25. The general flow direction is indicated from LR002 in the north to LR004 in the south after intersecting the river. This is similar to transect 2 and opposite to transect 1. The hydraulic gradient on this transect was not compared, as the shallow borehole (LR002B) were drilled dry. Furthermore, it never obtained water from the unconsolidated zone (such as LR003) and remained dry throughout the study period.

The T values display a relative small contribution from the northern bank to the river, with a slightly bigger loss of the river to the southern bank.

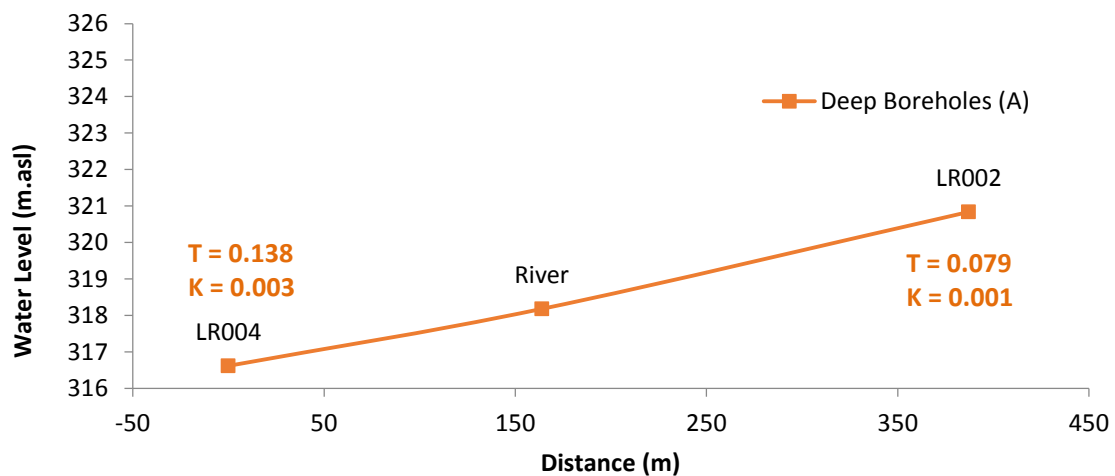


Figure 5.25 Hydraulic gradient cross-section plot of transect 3.

The hydraulic gradients of transect 4: that consists of LR005 and LR001 are plotted in Figure 5.26. The general flow direction indicated from the deep and shallow aquifers are towards the river, in both the northern and southern bank.

In disparity to transect 1, 2 and 3, the river would appear to be a gaining stream from both the northern and southern bank. The T values of the deep aquifer indicate a greater gain from the southern bank, while the shallow aquifer indicates a relatively small contribution.

A definitive difference was observed between the hydraulic heads of the deep the shallow aquifer, with the deeper aquifers indicating a slightly higher head. The possible reason for this is due to higher yielding deep fractures that were intersecting, thus increasing the pressure within the borehole resulting in a higher hydraulic head.

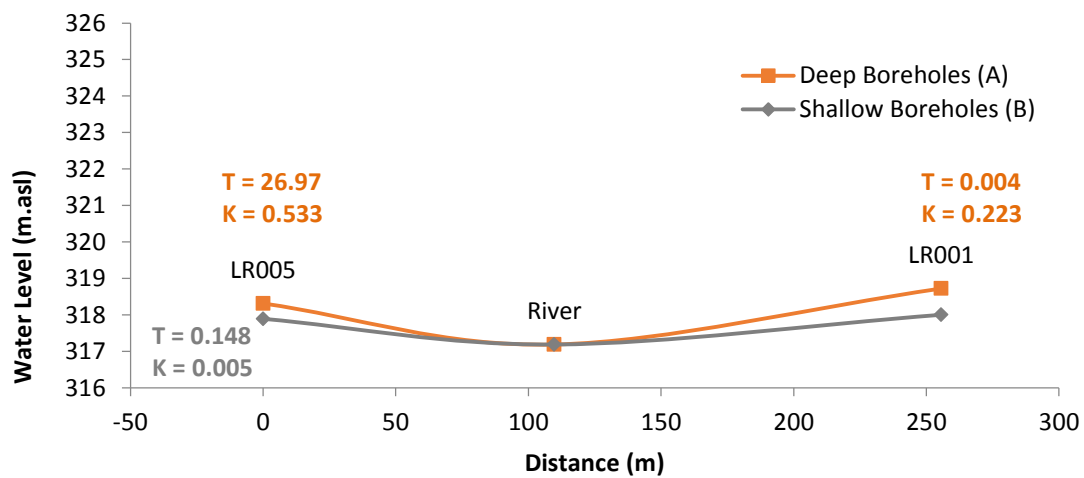


Figure 5.26 Hydraulic gradient cross-section plot of transect 4.

A second hydraulic gradient transect were drawn (transect 4-B): that consists of LR005, as well as LR0011 and is plotted in Figure 5.27. The reason for this was to display the influence that the dolerite dyke has on the hydraulic gradients, as LR0011 is located upstream of the dyke where LR001 is located downstream of the dyke.

The general flow direction is similar between the two transects, with a considerably lower contribution from LR0011, indicated by the T values. The higher hydraulic head observed within LR0011 indicates the effect of the dolerite dyke, blocking the water and creating a damming effect.

Again, the difference in hydraulic heads between the deep and shallow aquifer is indicated with the deeper aquifer displaying a slightly elevated hydraulic head. A greater contribution from the southern bank is also indicated again by the T values.

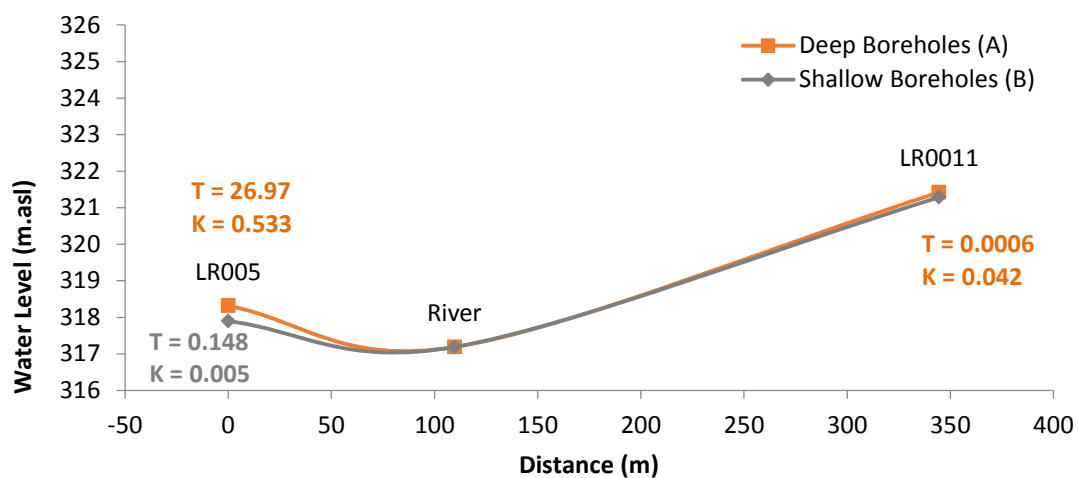


Figure 5.27 Hydraulic gradient cross-section plot of transect 4-B.

In summary, the hydraulic gradient showed a complicated losing and gaining stream configuration between groundwater and the river. The hydraulic gradients indicated a different scenario within each transect, transect 2 and 3 indicated a gain from the northern bank and a loss to the southern bank.

Conversely, transect 1 indicated a gain from the southern bank and a loss to the northern bank. Transect 4 and 4-B surprisingly displayed a different scenario again, indicating a gaining stream from both the northern and southern banks. However, there are some limitations to the transects in determining the direction of groundwater flow. Even though the transects provide a good indication of the groundwater flow direction, the most accurate indication will be to make use three borehole's groundwater levels in order to determine the precise groundwater flow direction.

A small difference was found between the hydraulic heads of the shallow boreholes (aquifer) and deep boreholes (aquifer), thus indicating that there is not a shallow or deep

aquifer but rather one aquifer with groundwater flowing through the unconsolidated zone, ultimately moving to deeper fractures in the consolidated zone. Although this is still an uncertainty as, it is assumed that the boreholes were properly sealed. The effect of the dolerite dyke was clearly observed between the hydraulic gradients within LR0011 and LR001. This will be further discussed in the section below (5.5.6 Fluid logging).

5.4.6 Fluid logging

To compare the wet and dry season two rounds of fluid logging were conducted throughout the piezometric network. The first round was taken in the wet season of 2015 (November), preceding the arrival of an extreme drought's peak in 2016. The second round was in August 2016, through which only one significant rainfall event in March 2016 occurred. The fluid logs will be discussed on a transect basis (refer to Figure 5.18).

Transect 1

LF002A (Farms, Regional, Deep)

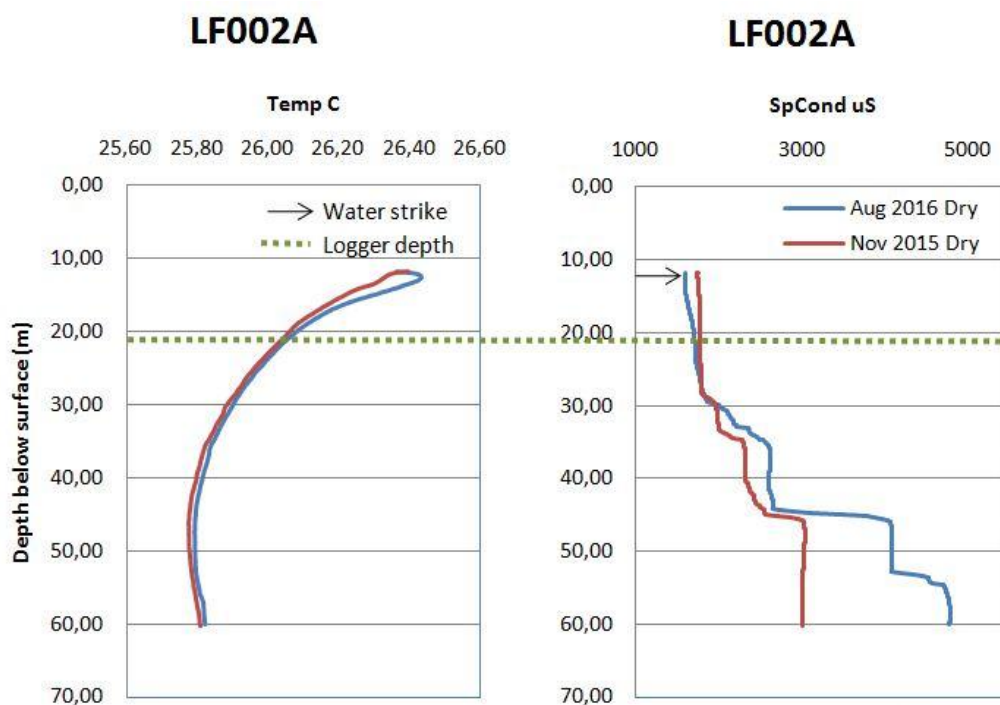
No significant differences were observed between the temperature profiles within LF002A (Figure 5.28), however a steady decrease in both profiles were observed with depth. This occurs because of the inflow of fresh water at the top of the borehole to the bottom. This inflow occurs from the preferential pathway that boreholes create, thus allowing water percolating through and to the groundwater system. The end result is warm water cooling down as it proceeds to the bottom of the borehole. Even though, solid casing were installed to 30 m the same temperature profile will be depicted. This is because the warm groundwater entering the gravel pack of the borehole will also increase the temperature of the water within the casing. The groundwater will then move down the gravel pack (artificial preferential flow path), until it reaches the bottom of the casing where it interacts with the rest of the groundwater. This can clearly be seen with the increase of (EC) at the end of the 30 m solid casing. This also infers that the borehole was not properly sealed off at the end of the solid casing.

An increase in EC was observed between the periods, this was expected due to the extremely low rainfall within this period and high evaporation rates. The outcome is

that very little water reaches the saturated zone of the aquifer. Furthermore, the EC displayed an increase to the bottom of the borehole. This is a result of the heavier salt water (high conductivity water) and debris, settling and moving down to the bottom of the borehole. In both surveys the fractures were indicated at the same location of 30 m, 35 m and 45 m by the sharp and sudden increase in conductivity. During drilling these fractures were not observed, while the water strike was at 11.6 m within a diabase dyke. The water strike was not indicated, due to the solid casing installed to seal of the possible shallow aquifer.

LF002B (Farms, Regional, Shallow)

A small increase in temperature is seen in the dry season of August 2016 (Figure 5.28). Similar to LF002A an inflow of fresh water at the top of the borehole is indicated again with the decrease of temperature to the bottom. In both surveys a small fracture is indicated through the sudden increase in EC, with a slight change in temperature at 12.8 m where warm water enters the borehole. The water strike was at 11.2 m (dolerite dyke), while the groundwater level was measured at 11.82 m, although with the casing taken into consideration this will be at the same position. LF002A/B is located within the riparian zone on the northern bank of the farms area. On this transect (Transect 1) the hydraulic gradient displays a loss to the northern bank from LF004A/B to LF0021 to LF002A/B, thus we expect to observe flow within these boreholes.



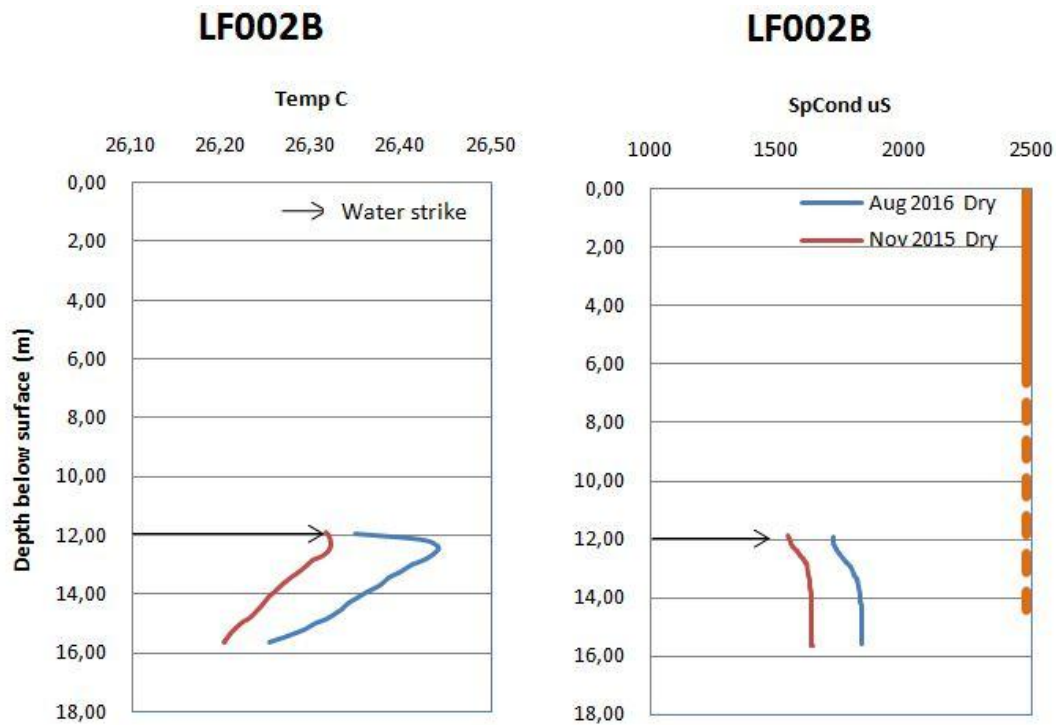


Figure 5.28 Fluid log of LF002 (A – above, B – below).

LF0021 (Farms, Riparian, Shallow)

A warmer temperature is observed within the dry season of August 2016 (Figure 5.29). The decrease in temperature with depth is only observed within the August survey, indicating on increased flow within the aquifer.

A temperature decrease with depth is observed in the August data set, thus indicating groundwater flowing into the borehole from the unconsolidated zone. This possibly occurred because of the single rainfall event in March 2016. The EC indicates an expected increase in August from the low rainfall received from the drought. This is also supported by the overall increase in temperature of the August profile. A high inflow of groundwater through the unconsolidated zone was expected for LF0021, as this is one of the boreholes located closest to the river within the riparian zone. Furthermore, it also had a hydraulic head lower than that of the river, thus any small rainfall event or increase in the river would possibly be indicated.

Several small fractures were indicated by the EC at 13 m, 15 m, 18 m and at 21 m. The EC anomalies are also supported by the temperature profile. The water strike was at 9.10 m (granite), although no fracture was indicated by the fluid logs at this depth.

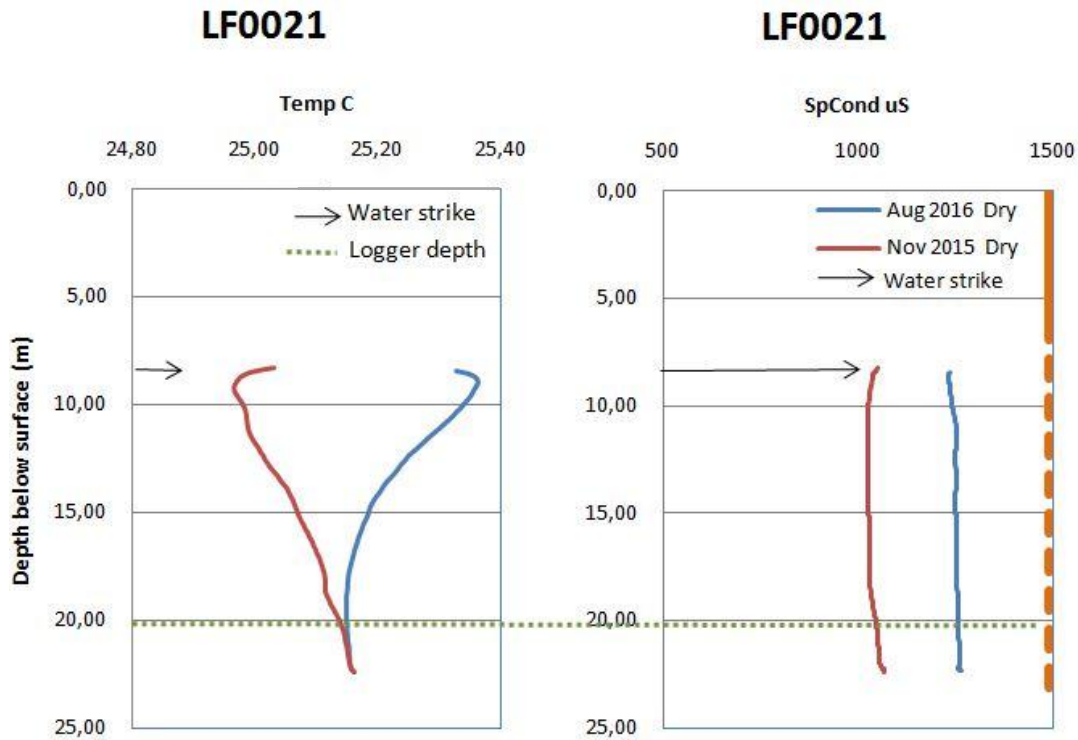


Figure 5.29 Fluid log of LF0021.

LF004A (Farms, Regional, Deep)

A steady temperature increase is displayed in both periods (Figure 5.30). This infers that no groundwater was received from the unconsolidated zone. Numerous small fractures are observed from the small, but sharp increases in temperature and EC. Thus, indicating that groundwater is being received mostly from fractures within the consolidated zone. This is supported by the temperature that increases to the bottom of the borehole as, warmer high EC groundwater enters the borehole through small fractures. A sharp increase is observed at 24 m where the solid casing ends.

At 35 m, 53 m, 64 m and 67 m the various small fractures are indicated by an increase in temperature and EC. The water strike was at 25 m (granite), although no fracture was indicated by the fluid logs at this depth.

LF004B (Farms, Regional, Shallow)

In August 2016 the typical increase in temperature is displayed where warmer groundwater is entering the borehole through the unconsolidated zone, possibly from the high rainfall event in March 2016 (Figure 5.30). A similar inflow is observed in LF004A, although with a smaller effect. A very high EC is observed in both LF004A/B,

possibly from contamination during the drilling process or from agricultural activities. This also explains the decrease in conductivity at the fracture indicated at 15 m. The water strike was at 12 m (dolerite), with the initial water level at 13.38 m. This level as increase to 11.13 m as the borehole developed through pumping.

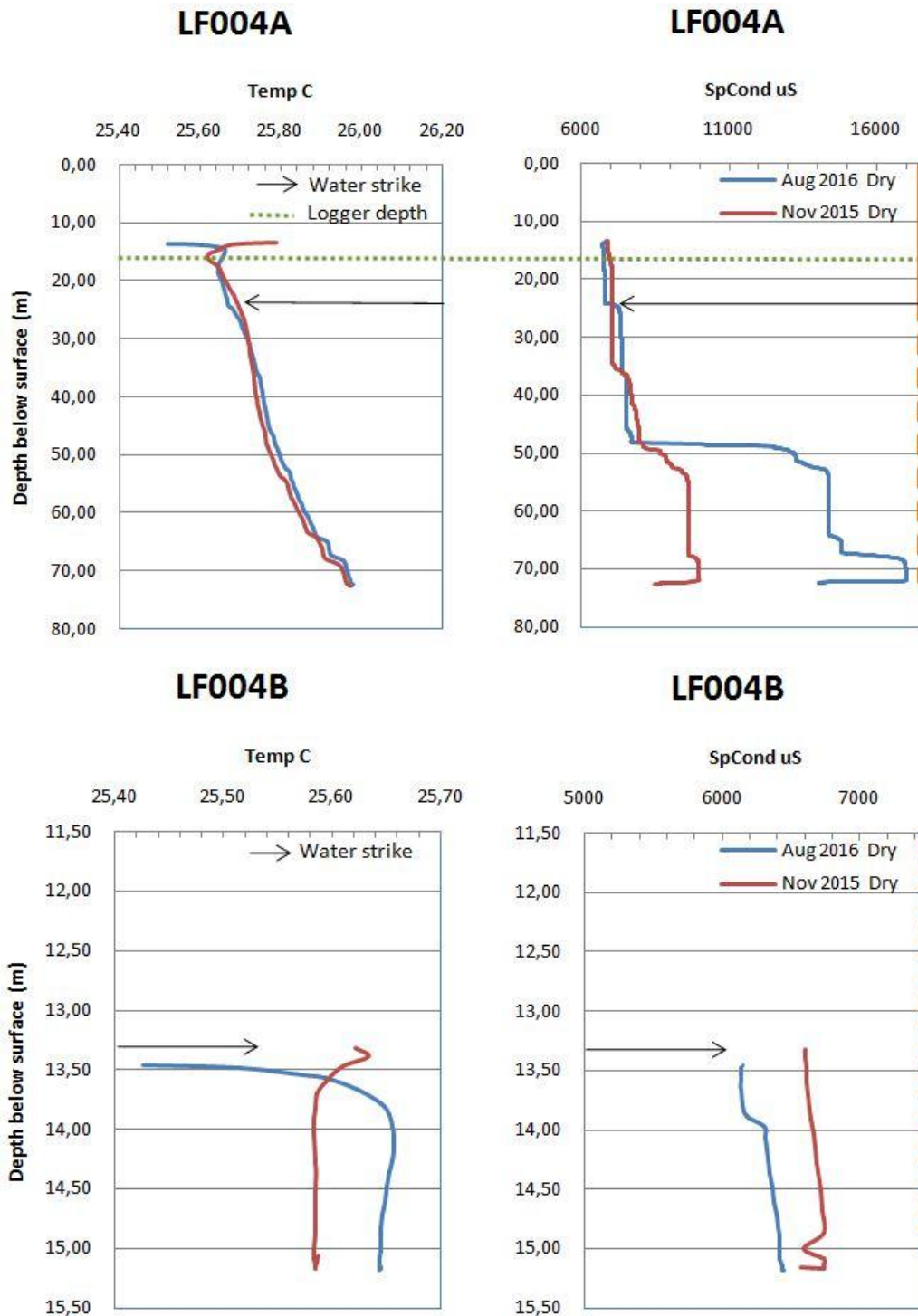


Figure 5.30 Fluid log of LF004 (A – above, B – below).

Transect 2

LF0031A (Farms, Regional, Deep)

A similar temperature and EC profile is observed between the two periods (Figure 5.31). Although, an increase in EC below the casing and decrease in EC within the casing is observed when the November 2015 and August 2016 profiles is compared.

This supports the phenomenon where salts within the boreholes start to settle to the bottom of the borehole, ultimately increasing the EC to the bottom of the borehole. In combination with the latter phenomenon the high EC groundwater could also be contributing to the increase in EC over time.

There is only a small gradual increase in temperature within the first meter, after which a fracture is indicated by a sudden increase in temperature and supported by the increase in conductivity at 25 m. Thus, most flow is coming from the fractures within the consolidated zone.

A sudden increase in conductivity is displayed at 20 m, however this is still located within the solid casing indicating a possible leak in the casing. The water strike was at 21 m (dolerite), and might be contributing to the increase in EC where the possible casing break is indicating.

LF0031B (Farms, Regional, Shallow)

Within LF0031B an increase in the EC and temperature is displayed, as expected from the consistently dry and warm conditions from the drought (Figure 5.31). A small amount of inflow is indicated from the increase in temperature with depth, similar to LF0031A. A small fracture was also observed at 17 m by a small, but sudden increase in temperature. This was also supported by the sudden increase in EC.

Both the deep and shallow borehole displayed a similar profile with small amounts of inflow from the unconsolidated zone, with most of the inflow originating from fractures within the consolidated zone. The water strike was at 19 m (dolerite), this fracture is indicated with a small but sudden increase in temperature and EC.

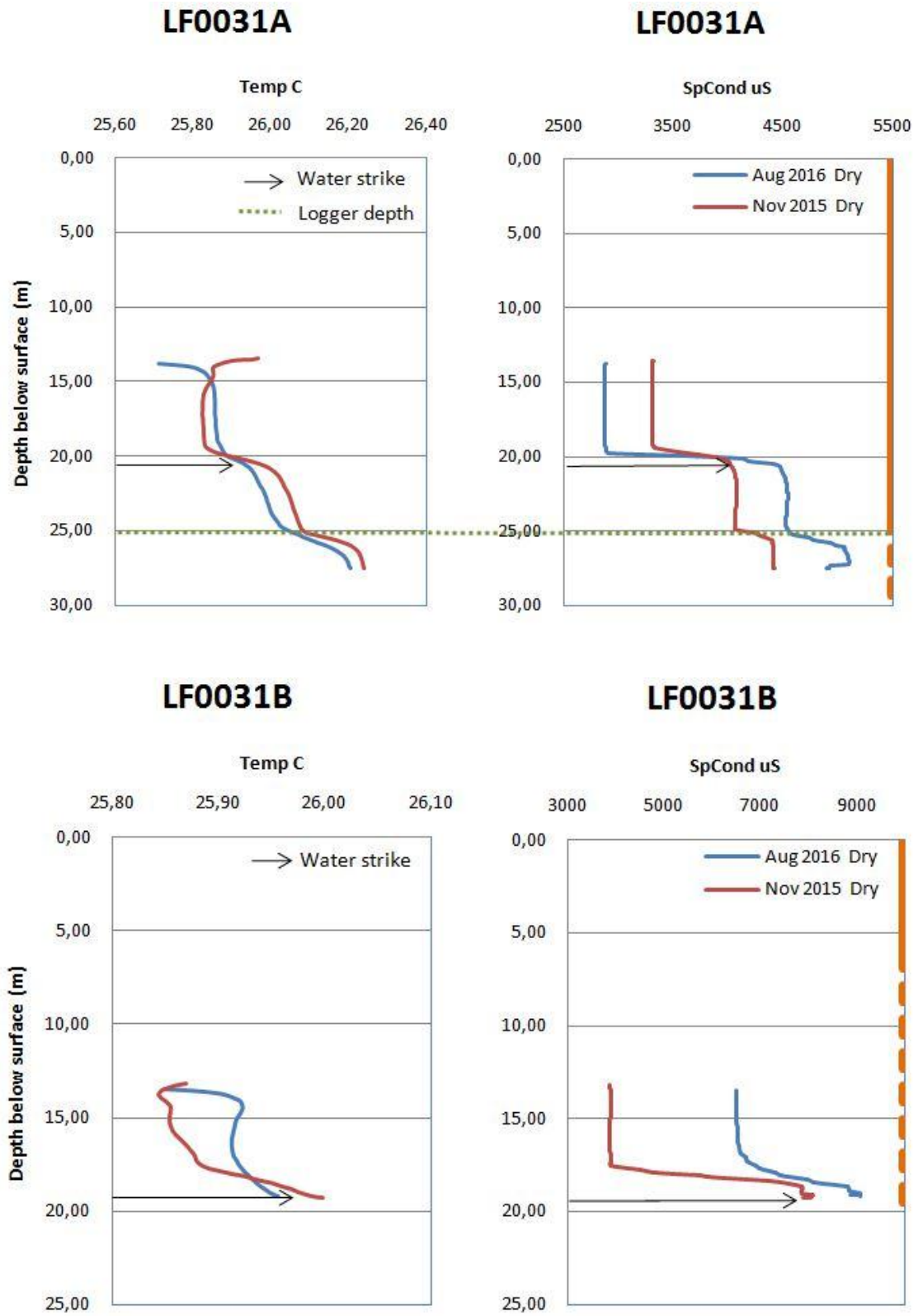


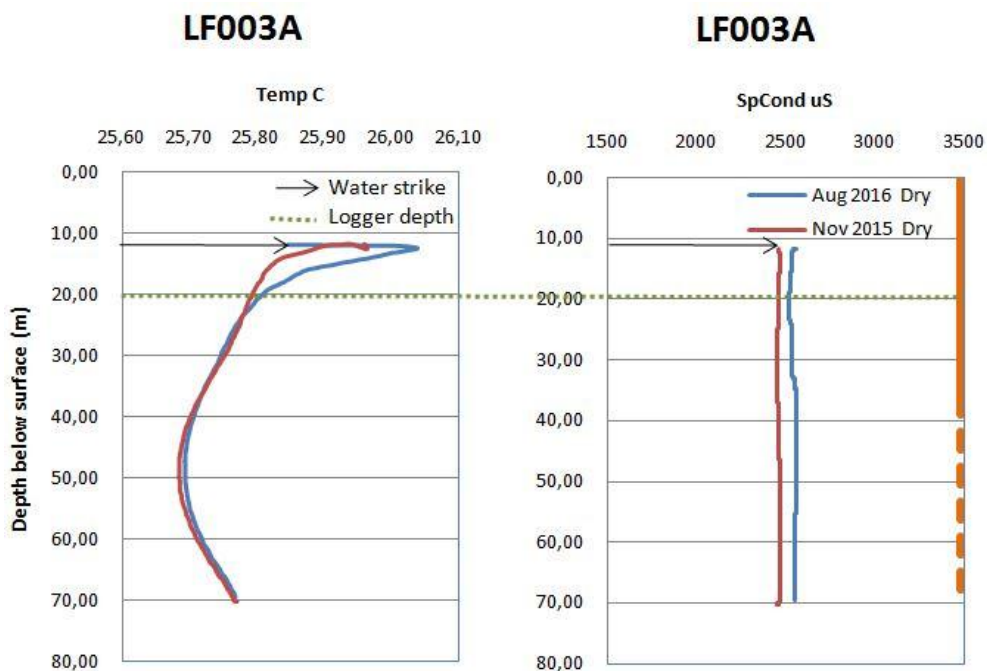
Figure 5.31 Fluid log of LF0031.

LF003A (Farms, Riparian, Deep)

No large temperature differences are observed between the two periods, although groundwater inflow is again observed in both surveys from the unconsolidated zone (Figure 5.32). This inflow is similar to some of the previous boreholes and is indicated by the decrease in temperature with depth. The EC is once more slightly higher in the dryer winter period, as expected. Numerous small fractures are indicated throughout the borehole, although the EC variations at 23 m and 33 m infer possible leakages within the solid casing. The temperature profile supports this, because the typical temperature profile is not displayed but rather a straighter profile as it decreases to the bottom. After the solid casing is passed the profile returns to normal. The water strike was at 15 m (dolerite dyke), however it was not displayed due to the installation of solid casing to seal off the top aquifer (if present).

LF003B (Farms, Riparian, Shallow)

The typical groundwater inflow from the unconsolidated zone is depicted in LF003B, with the decrease in temperature with depth (Figure 5.32). The EC displays a similar profile between the two seasons. The solid casing is also displayed at 15 m by the EC. At 19 m a possible fracture is indicated with the increase in temperature and EC. The water strike was at 12 m (dolerite), although it was only minor. The main fracture is indicated by the fluid logs at 19 m with the sudden increase in EC and temperature.



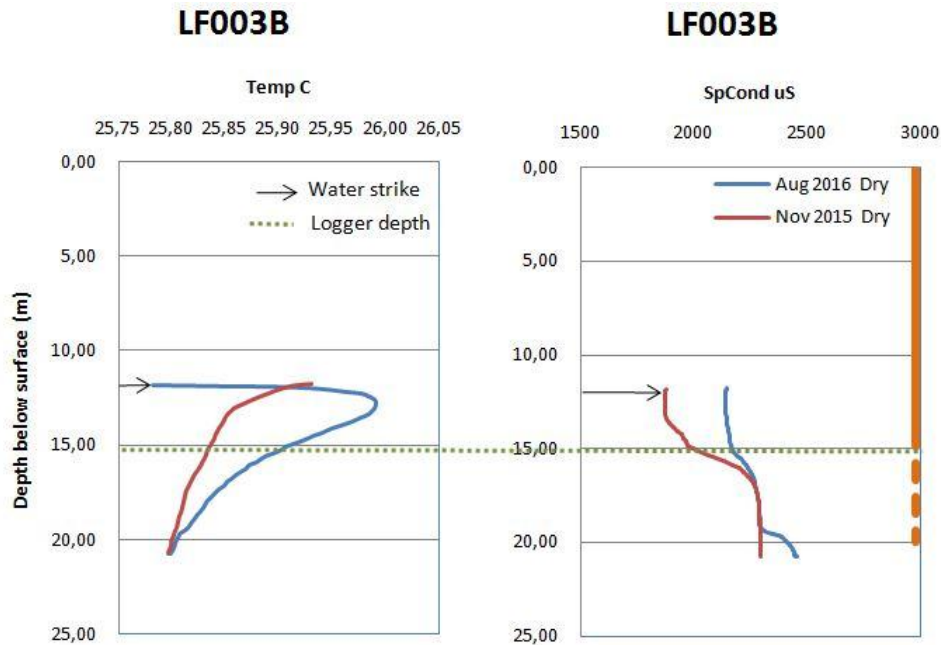


Figure 5.32 Fluid log of LF003.

LF005A (Farms, Riparian, Deep)

No significant temperature variations were observed between the two periods (Figure 5.33). The normal inflow through the unconsolidated zone is displayed by the temperature profile with water moving down the gravel pack and entering the borehole at the bottom of the solid casing. The solid casing is indicated at a depth of 30 m by the EC profile. Large fractures at 44 m and 62 m are indicated with the increase in EC and temperature. The water strike was at 32 m (granite), although no big fractures are indicated at this depth. A lower EC is displayed in August 2016 in contrast to most boreholes thus far. This is due to the location of the borehole, as the hydraulic gradients indicate that groundwater is moving from the northern bank (LF0031, LF003) on transect 2, through the river to the southern bank where LF005 (riparian zone) and LF0051 is located. Thus, after the March rain this borehole was possibly replenished by the river, ultimately lowering its EC through mixing.

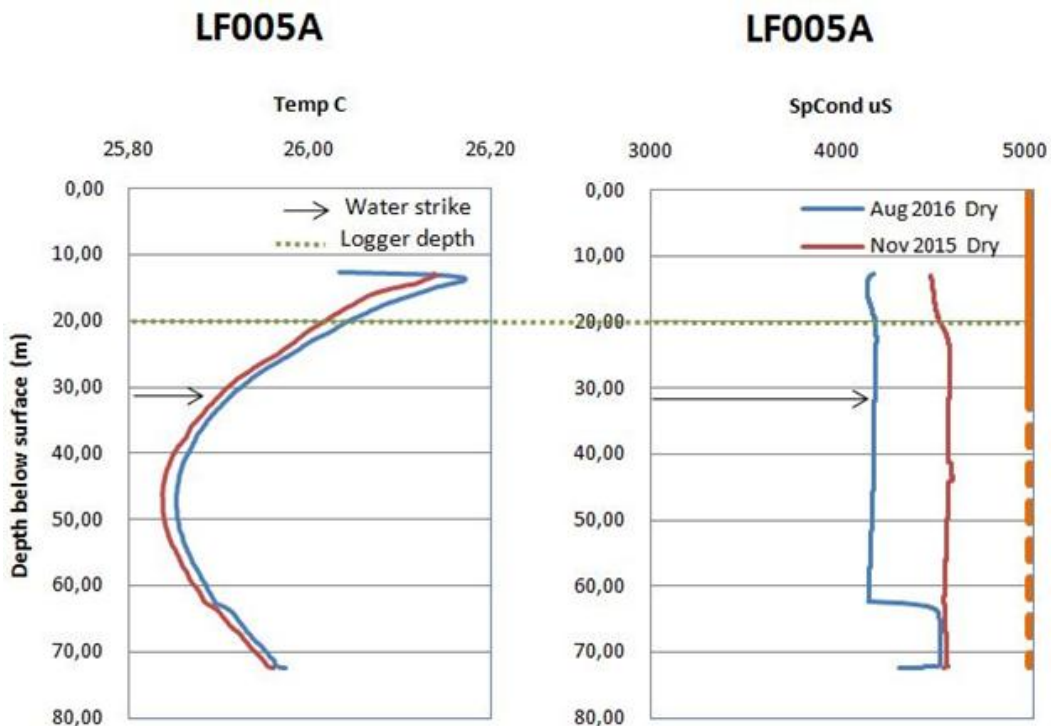
LF005B (Farms, Riparian, Shallow)

Similar to LF005A, the typical inflow from the unconsolidated zone is indicated (Figure 5.32). The temperature and EC indicate a relative similar profile between the two periods. Two main fractures are indicated at 30 m and 41 m by an increase in temperature and EC. The fracture at 41 m is also intersected at around 41 m within LF005A, they both also contain the exact EC and temperature values indicating that

they are interlinked by this and possibly more fractures. Both boreholes temperatures drop to around 41 m, providing some evidence that groundwater is moving through the unconsolidated zone, down the borehole (or preferential flow path) and into the fractures. The water strike was at 13 m (granite), although no fractures were indicated at this depth.

LF005C (Farms, Riparian, Shallow)

Only a small amount of water was available with the initial November 2015 fluid logs, thus only one survey was conducted in August 2016 (Figure 5.33). As seen in LF005A/B the typical inflow of groundwater from the unconsolidated zone is observed. A fracture is displayed at 13.5 m with (in contrast to most other boreholes), decrease in temperature. This phenomenon is also seen in LF004B, although it must be remembered that both these boreholes are very shallow with less than 1.7 m head of water. Thus, evaporation within the borehole will have a much bigger increase on its EC. The result is a borehole with very high EC (6000 $\mu\text{S}/\text{cm}$), ultimately displaying a decrease in EC at the fracture. The water strike was at 13 m (granite), although when the collar height is brought into consideration, the fracture identified above and water strike is at the same depth.



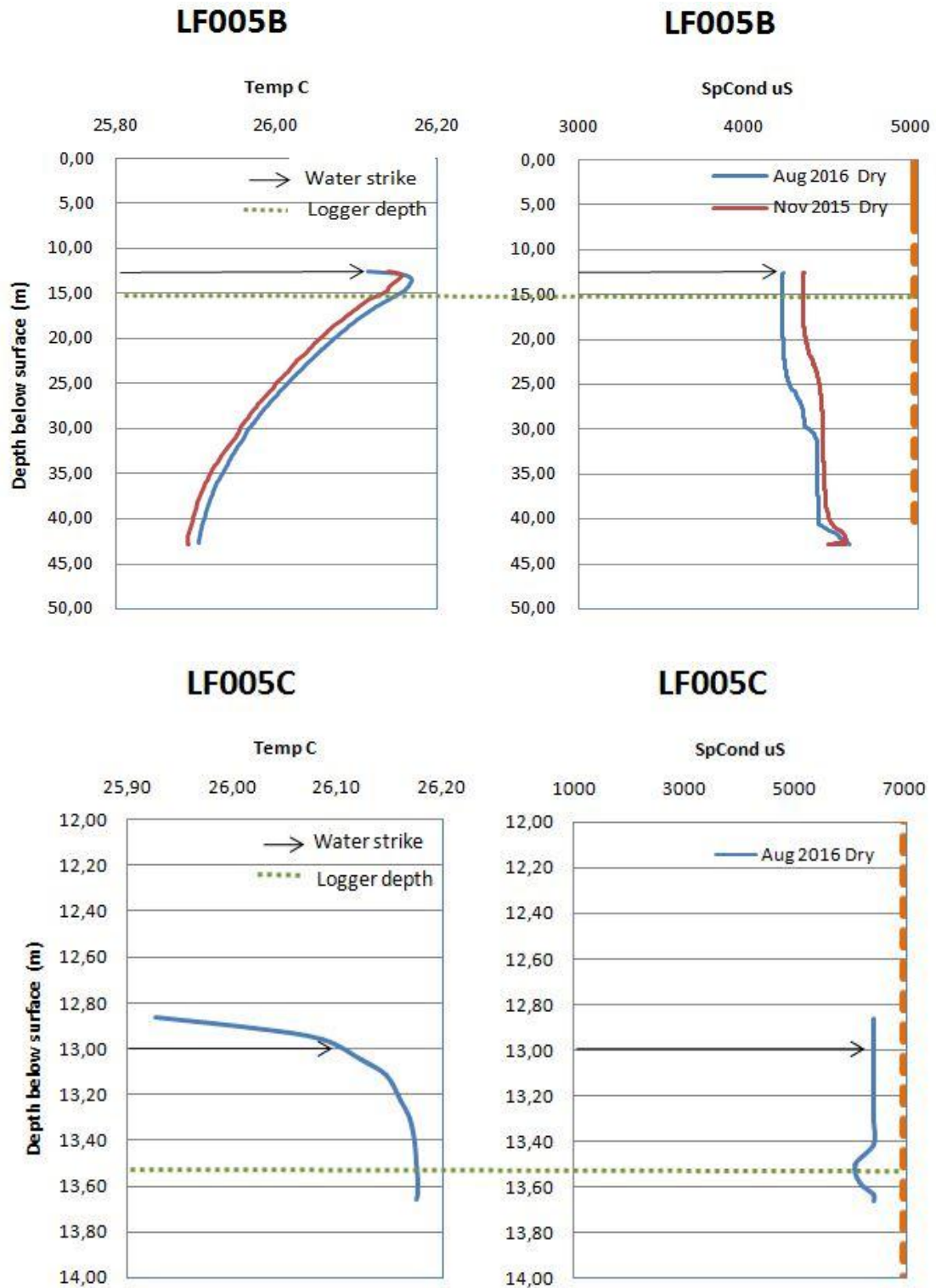


Figure 5.33 Fluid log of LF005 (A – above, B – mid, C – below).

LF0051A (Farms, Regional, Deep)

LF0051A display a temperature profile that is similar between the two periods, with the normal decrease with depth indicated by the temperature profile (Figure 5.34). Although, the exact temperature decrease profile is not observed and rather simulates the profile of LF003A. This infers that the solid casing might have some leakages.

The EC profile supports this as it indicates a definite break in the casing at 25 m, with a sudden increase. This sudden increase can also be the contribution of the water strike at 25 m. Again a slight increase in EC is observed below the casing, as a result of the phenomena where salts start settling down to the bottom of the borehole, ultimately increasing the EC at the bottom of the borehole.

No obvious large fractures were indicated by the EC profile after 25 m (granite). The end of the solid casing can be seen at 36 m with a small increase in both EC and temperature. As expected a higher EC and temperature is displayed in August 2016, from the higher temperatures and evaporation during the drought.

LF0051B (Farms, Regional, Shallow)

The decreasing temperature with depth from the inflow of groundwater into the borehole can be seen in the August profile (Figure 5.34). During the drought more evaporation took place increasing the EC, as well as the temperature from the warmer climates. Thus, warmer and higher EC groundwater will flow into the borehole. This can clearly be seen in the August 2016 profile with higher EC and temperatures displayed.

The November 2015 EC profile indicated a sudden increase at 26 m with a slight increase in temperature. This indicated a fracture through which warmer and higher EC groundwater enter the borehole. The EC from the groundwater entering the borehole from the unconsolidated material was still low, thus the fracture could be identified.

During the August profile the EC of the unconsolidated zone's groundwater have increased, as well as the fractures EC at 26 m, caused by the prolonged drought. Thus, the fracture was found to be less prominent in the profile. The water strike was at 16 m (granite), although no prominent fractures were indicated at this depth by the fluid logs.

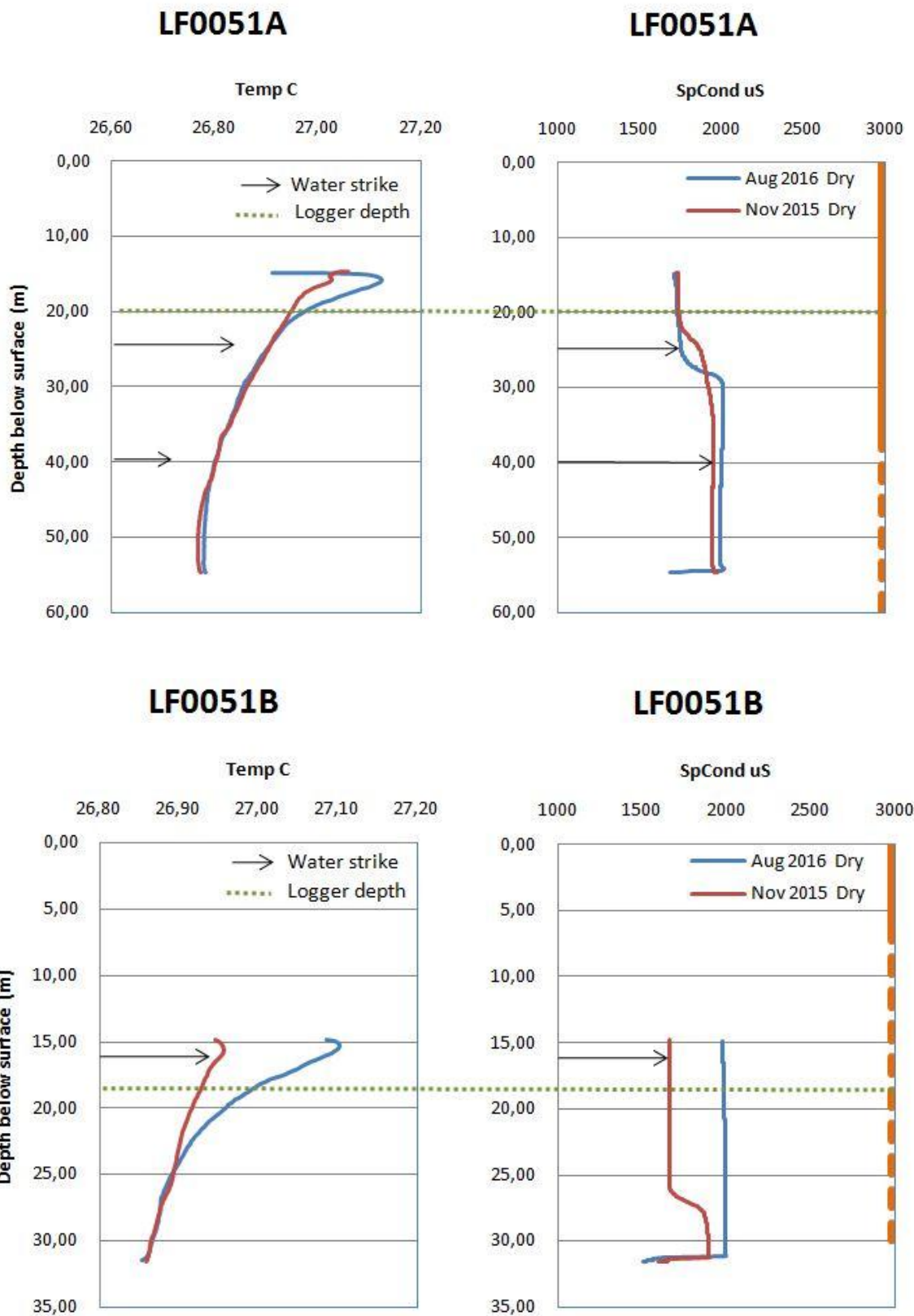


Figure 5.34 Fluid log of LF0051 (A- above, B – below).

Transect 3

LR002A (Protected area, Regional, Deep)

The temperature decrease from the inflow of fresh water through the unconsolidated zone into the gravel pack is displayed in both periods, although it seems to be better defined in the August fluid log (Figure 5.35). The end of the solid casing is only slightly indicated by the EC profile, inferring that only a small amount of leakage is occurring pass the solid casing seal. Two large fractures are indicated by increase of EC and temperature. The first fracture sits at 28 m where both Augusts and Novembers EC's indicated the fracture which is confirmed by the temperature decrease that stabilises beyond this depth. The water strike was at 25 m (granite), however no large fractures are indicated at this depth. The second fracture is located at 32 m and indicated by the August profile. The November profile does not indicate this fracture, although this fracture was possibly opened from various pumping tests done on the borehole between November 2015 and August 2016.

LR002A is a deep borehole located on the northern bank of the protected area. It possesses the highest hydraulic head of transect 3, thus it can be inferred that water is moving from the Northern bank to the Southern bank. LR002A displayed the recharge from the unconsolidated zone, thus indicating that water is moving towards the river.

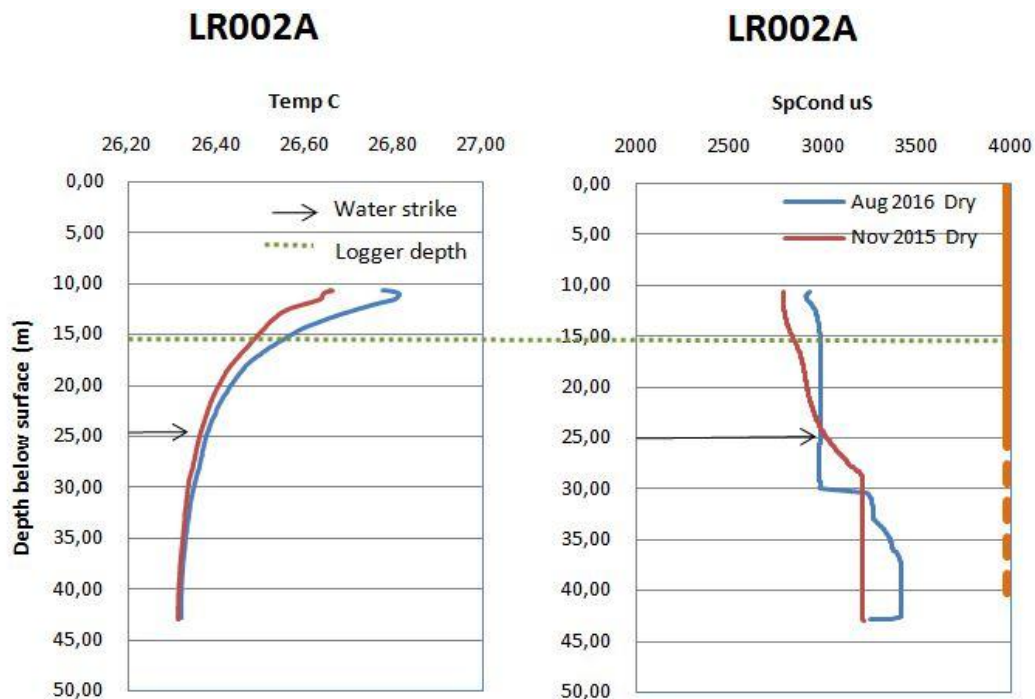


Figure 5.35 Fluid log of LR002A.

LR004A (Protected area, Regional, Deep)

LR004A was not yet drilled in November 2015, thus only one fluid log is available (Figure 5.36). This profile supports the interpretations that warm high EC water is moving from the unconsolidated zone into the gravel pack, moving downwards along the casing and gravel pack (preferential flow path).

The water then enters the borehole at the end of the solid casing as, it was not sealed properly. This occurrence is displayed by the high temperature indicated at around 12 m, decreasing to the bottom.

The water strike was at 13 m (granite), although no large fractures are displayed by the fluid logs at this depth. The solid casing is correctly indicated at 30 m with a sudden increase in EC. A very small fracture is indicated by the temperature at 43 m. Normal temperature decrease with depth from the inflow of fresh water is depicted.

LR004B (Protected area, Regional, Shallow)

LR004B displays a similar temperature profile than LR004A, with the decrease in temperature with depth from the inflow of fresh groundwater (Figure 5.36). The water strike was at the same position as LR004A on 13 m (granite).

However, only one fracture is indicated at 24 m, with a small and sudden decrease in EC. LR004A/B is located on the southern bank of the protected area and possesses the lowest hydraulic heads of transect 3. The slight increase in EC at the bottom of the borehole is most likely due to salts and material settling down to the bottom of the borehole.

This indicates that water is being lost from the river in the direction of the boreholes. The EC supports this theory through displaying a relatively low EC when compared to the opposite river bank at LR002A. The inflow of groundwater throughout the unconsolidated zone is observed in both boreholes, inferring that the water from the river is being lost to the aquifer through the unconsolidated zone.

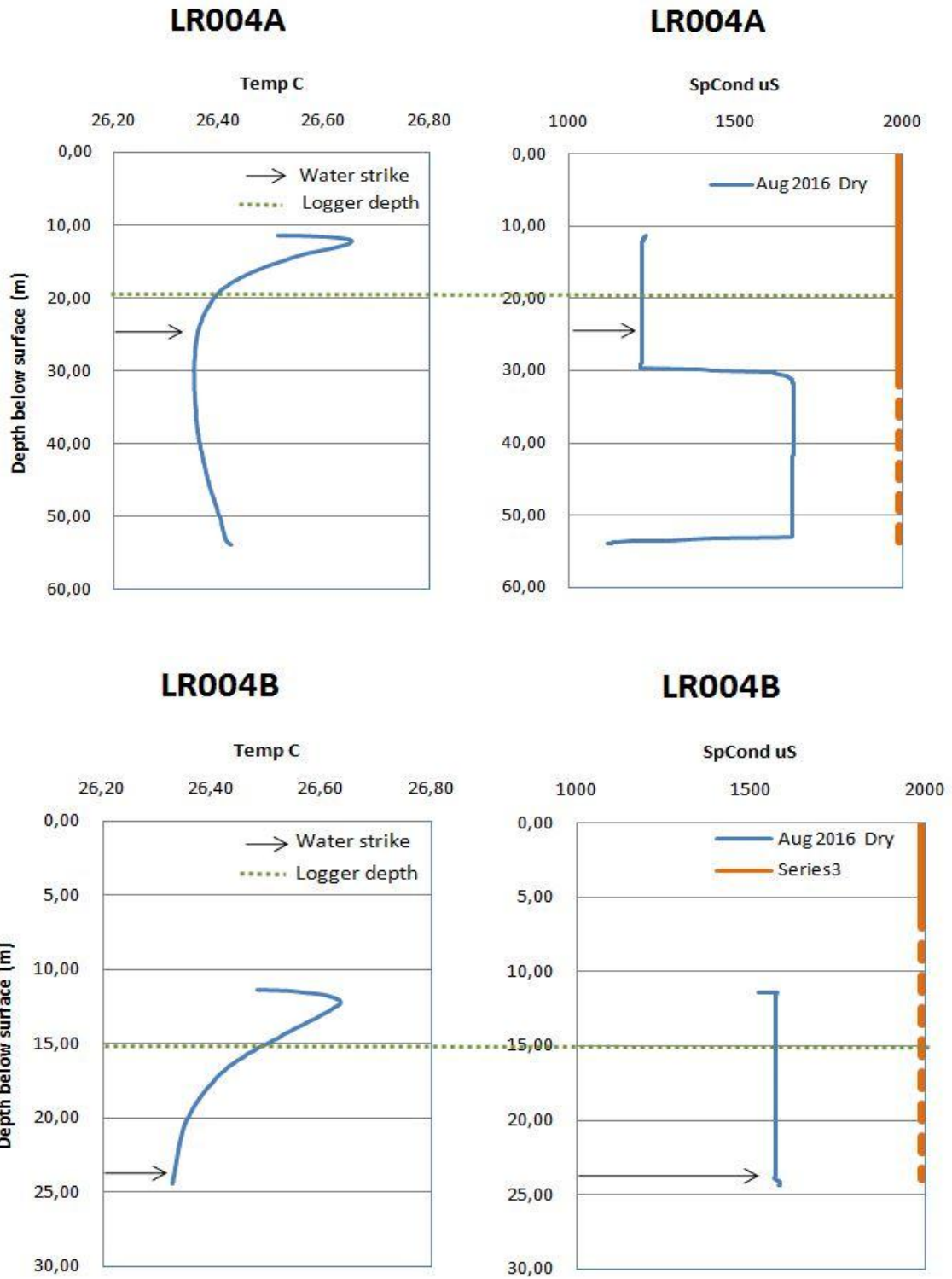


Figure 5.36 Fluid log of LR004 (A – above, B – below).

Transect 4

LR0011A (Protected area, Riparian, Deep)

Within both periods the temperature displays very little difference in temperature (Figure 5.37). In the August 2016 profile the first 20 m displays a slightly increased temperature when compared to the November 2015 profile. This indicates that warm fresh water is entering the gravel pack from the unconsolidated zone, flowing down to the bottom of the borehole.

The end of the solid casing is indicated by both the August and November profiles with a sudden increase in EC at approximately 30 m. The EC was much lower in the August profile, inferring that water might be moving from the river into the northern bank during high flows periods.

The water strike was at 10 m (at the granite/dolerite dyke contact), although this section was sealed off to differentiate between the shallow and deep aquifer. Fractures are displayed at 32 m and 47 m by the increase in EC and temperature.

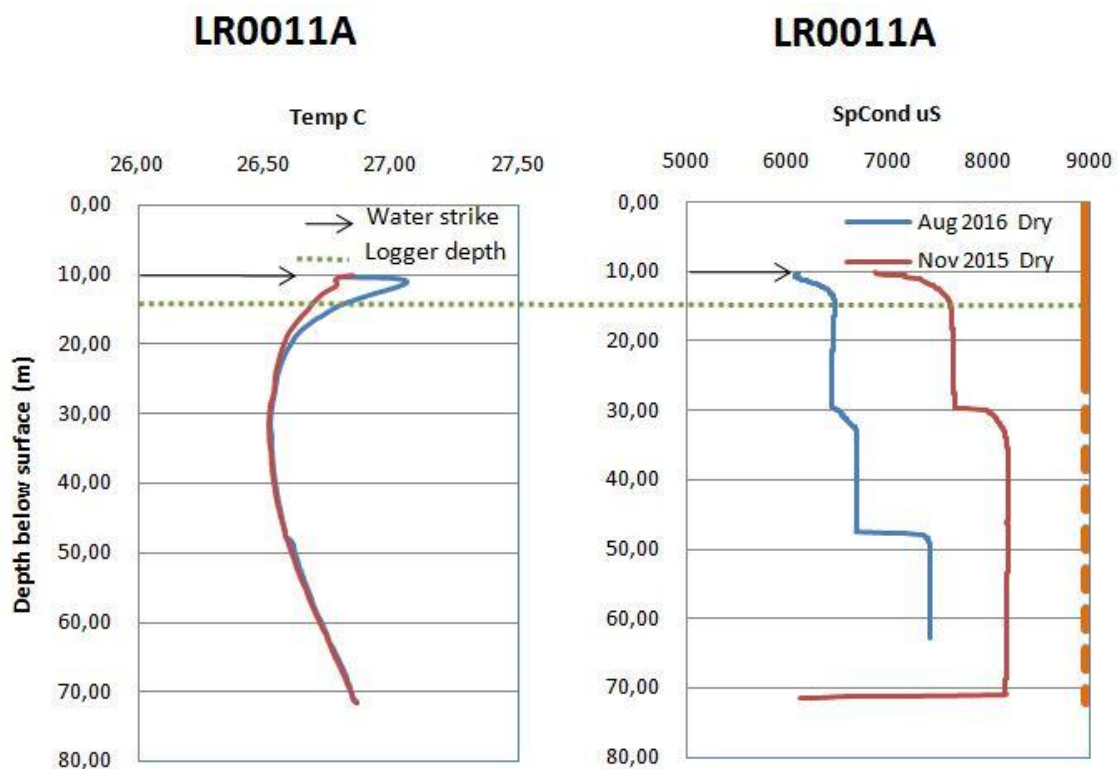


Figure 5.37 Fluid log of LR0011A.

LR001A (Protected area, Riparian, Deep)

The temperature profiles display no significant differences between the two periods (Figure 5.38). The decrease in temperature with depth found in many of the boreholes can also be observed in LR001A thus, indicating inflow of groundwater from the unconsolidated zone. The solid casing is indicated at around 28 m with a slight decrease in EC. This infers that the casing was not installed to the correct depth of 30 m or a leakage occurred within the casing.

The water strike was at 10 m (granite/dolerite contact), this section was sealed off to differentiate between the possible two aquifers. Various small fractures were observed at 35 m, 42 m, 47 m and 50 m by the increases in temperature and EC. A lower EC is observed in August when compared to the November profile, possibly from the high flow event during the March rainfall.

Unfortunately LR001B could not be analysed for fluid logging as there were too little water within the borehole to carry out the test.

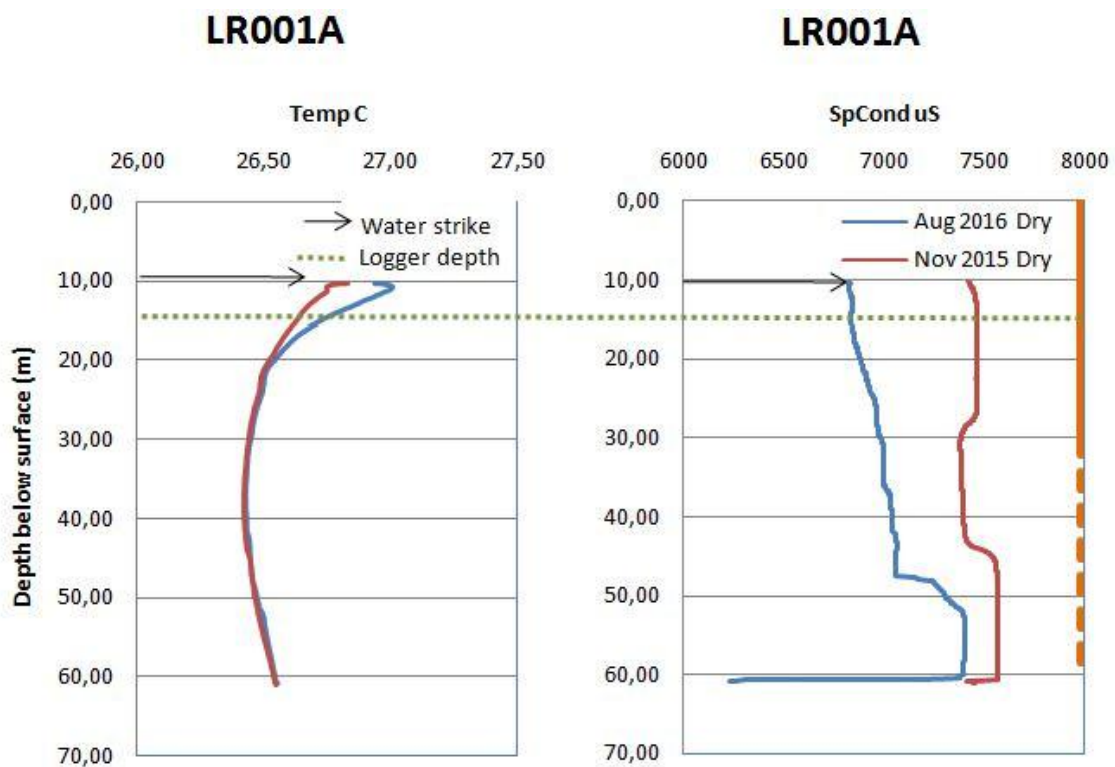


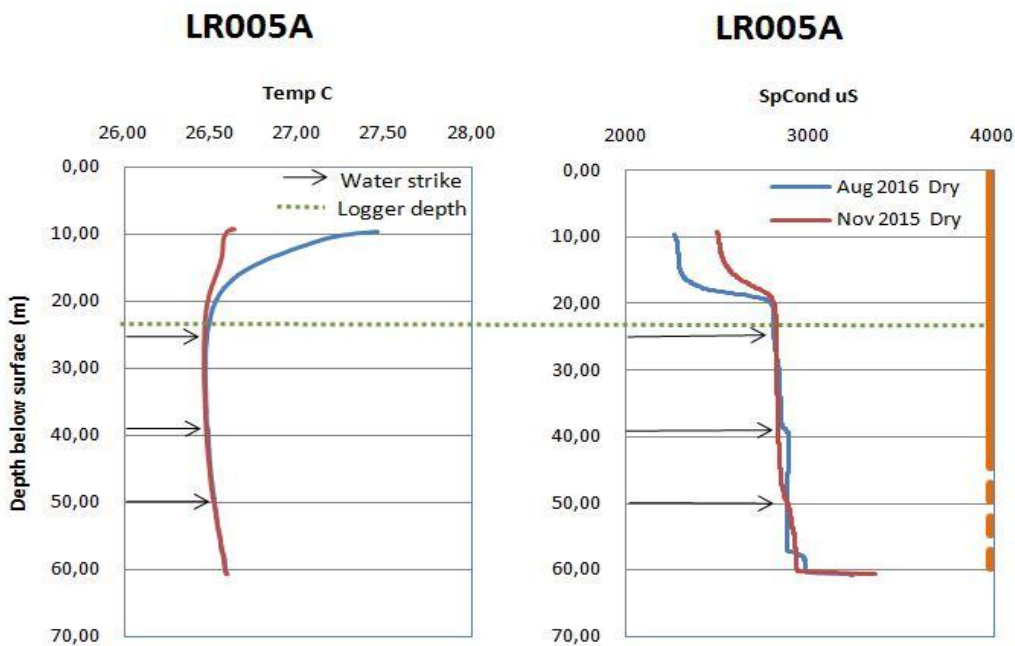
Figure 5.38 Fluid log of LR001A.

LR005A (Protected area, Regional, Deep)

The temperature demonstrates the anticipated decrease with depth due to inflow of fresh water from the unconsolidated zone (Figure 5.39). No large differences are observed between the two period's temperature and EC. The EC increases drastically to around 20 m, thus indicating a leak within the solid casing. The water strike is at 10 m (granite), this section was sealed off to differentiate between the possible deep and shallow aquifer. The solid casing end is indicated at around 40 m with only one prominent fracture at 57 m as indicated by the increase in EC.

LR005B (Protected area, Riparian, Shallow)

The temperature in the August 2016 profile indicates an anticipated increase in temperature, although the EC displays a decrease from the possible influence of the high flow event in March 2016 (Figure 5.39). The temperature displays the typical decrease with depth indicating that groundwater is flowing from the unconsolidated zone. The water strike was at 19 m (granite), although no large fractures are indicated at this depth. Two fractures are displayed at 16 m and 20 m by the slight increase in EC. The temperature decrease in both boreholes infers that that groundwater is moving through the unconsolidated zone towards the river. The low EC within the August 2016 profile indicate that it also has been replenished during the high flow event of March 2016.



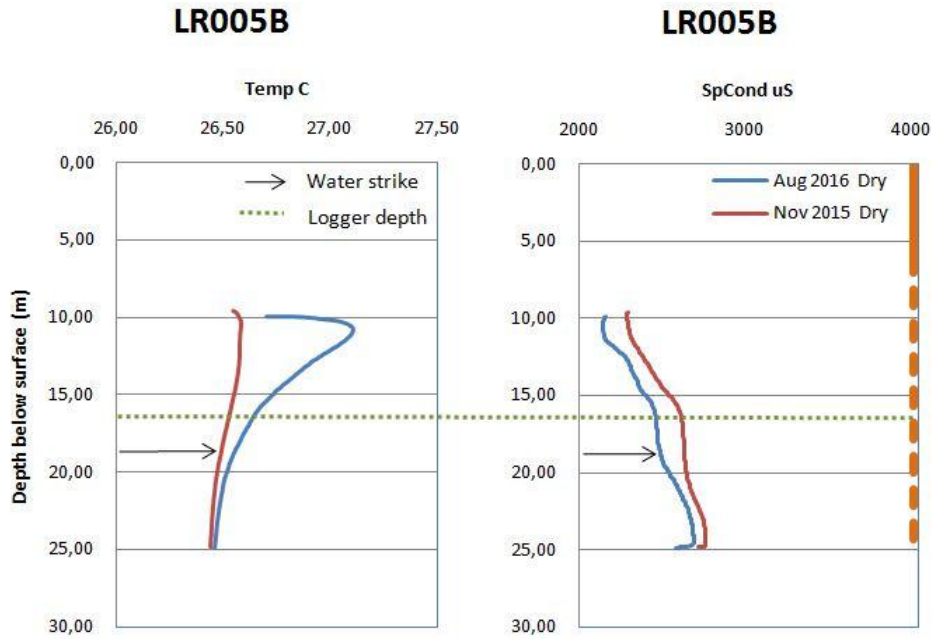


Figure 5.39 Fluid log of LR005 (A – above, B – below).

LR003 (Protected area, Riparian, Shallow)

Because LR003 did not contain any water in November 2015, only one fluid log is available (Figure 5.40). As expected no fractures are displayed by the EC or temperature, as this borehole was drilled dry. The typical inflow of groundwater from the unconsolidated zone is displayed with the decrease in temperature with depth. Explaining where this borehole obtained its water. A very high EC is depicted, as no water is moving through this borehole within fractures.

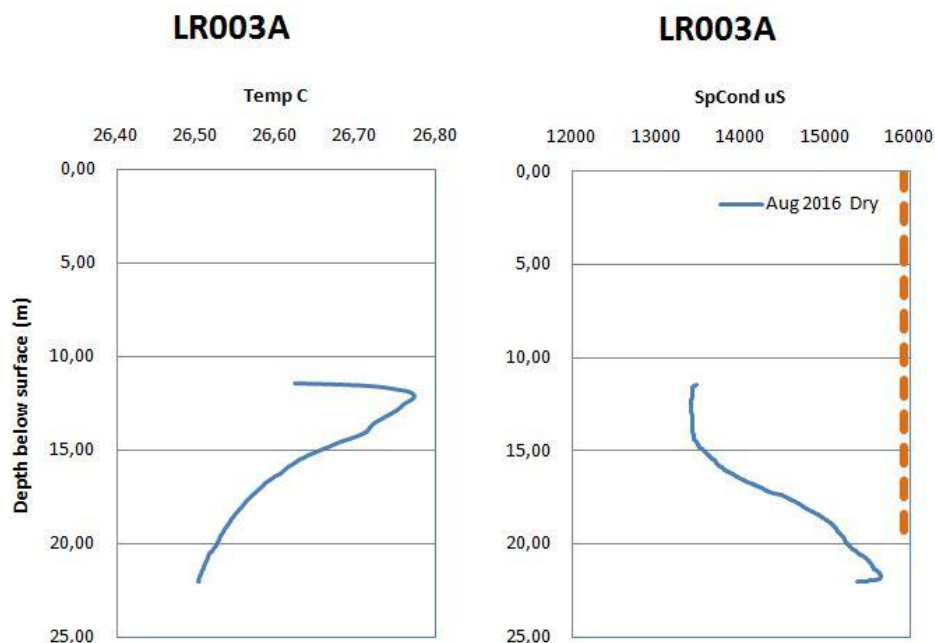


Figure 5.40 Fluid log of LR003.

Dolerite Dyke transect

LRW001 (Protected area, River bed, Shallow)

Both LRW001 and LRW002 were drilled after November 2015, thus only one fluid log is available (Figure 5.41). The temperature steadily increases to the bottom of the borehole, indicating that no groundwater is moving through the unconsolidated zone into the borehole, but rather through a fracture. The water strike was at 8 m (gneiss), this fracture is clearly indicated by an increase in temperature and EC at 8 m.

LRW002 (Protected area, River bed, Shallow)

The curved temperature profile from cold 21 °C to 23 °C at the bottom of the borehole indicate that cold fresh river water is percolating into the borehole. The water strike was at approximately 5 m (granite), this is the same fracture that is indicated by an increase in temperature at 4.6 m. The difference in depth is due to the collar height that was not taken into consideration.

LRW001 is situated downstream (northern side) of a large dolerite dyke that intersects the Letaba River at the Letaba Ranch weir (Figure 5.42). A small wall was built on top of the dolerite dyke as a continuation for the flow rating of the Letaba Ranch weir. This small wall creates a damming effect during high flow periods, while the dolerite cuts off groundwater movement. LRW002 is drilled upstream of the dolerite dyke (southern side), in order to determine the processes and movement of water across this impediment.

LRW001 indicates a very high EC of 7000 µS/cm, this was anticipated as all the surface water is being funnelled by the small cement wall to the weir. Alluvial groundwater is similarly being blocked off by the dolerite dyke. The fluid log indicated an increase in temperature from 24°C to 26°C, forming a relatively straight line to 8.5 m. This indicates that no inflow of groundwater from the unconsolidated zone is present, but that LRW001 rather receives its water from the fracture indicated by the sudden increase in EC at 8 m, also supported by the temperature increase.

LRW002 displayed much lower EC and temperature values. This is caused by the small cement wall and dolerite dyke that blocks off and funnels the river water alongside the dyke towards the Letaba Ranch gauging weir, clearly seen in the aerial image (Figure

5.42). This then ultimately forces the colder river water to flow into LRW002, providing it with its lower EC and temperature through mixing. This interaction can clearly be seen in the fluid logs with cold river water flowing in at 21°C, gradually increasing to the warmer groundwater flowing within the fracture at 4.6 m. The EC also supports this theory as, LRW002 displays a low EC of 1500 $\mu\text{S}/\text{cm}$. The only anomaly is the fact that the expected EC increase at the 4.6 m fracture was not observed, although this could be from the rapid mixing with the river inflow not allowing the low yielding fracture to display its true EC.

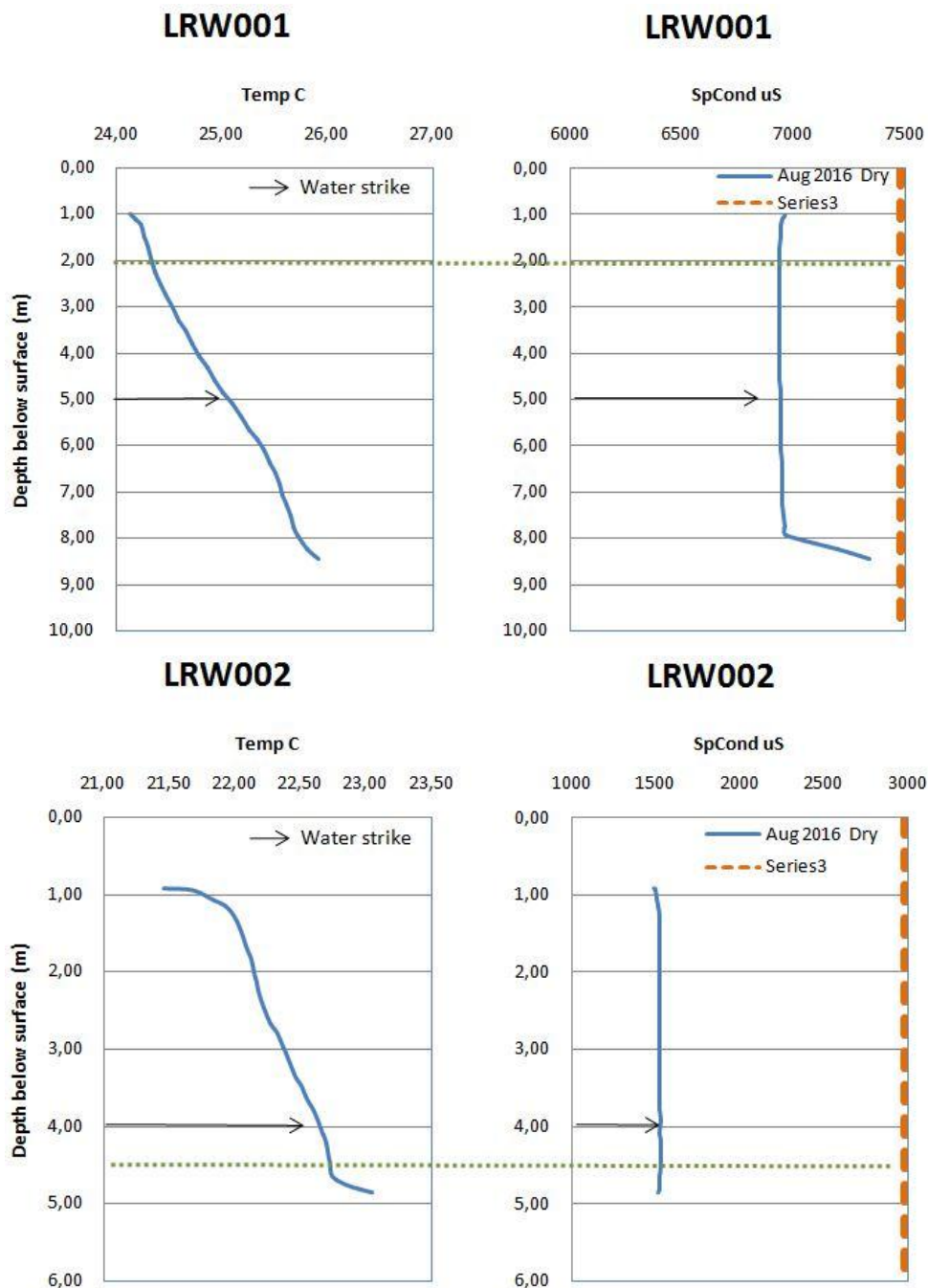


Figure 5.41 Fluid log of LRW001 (above) and LRW002 (below).

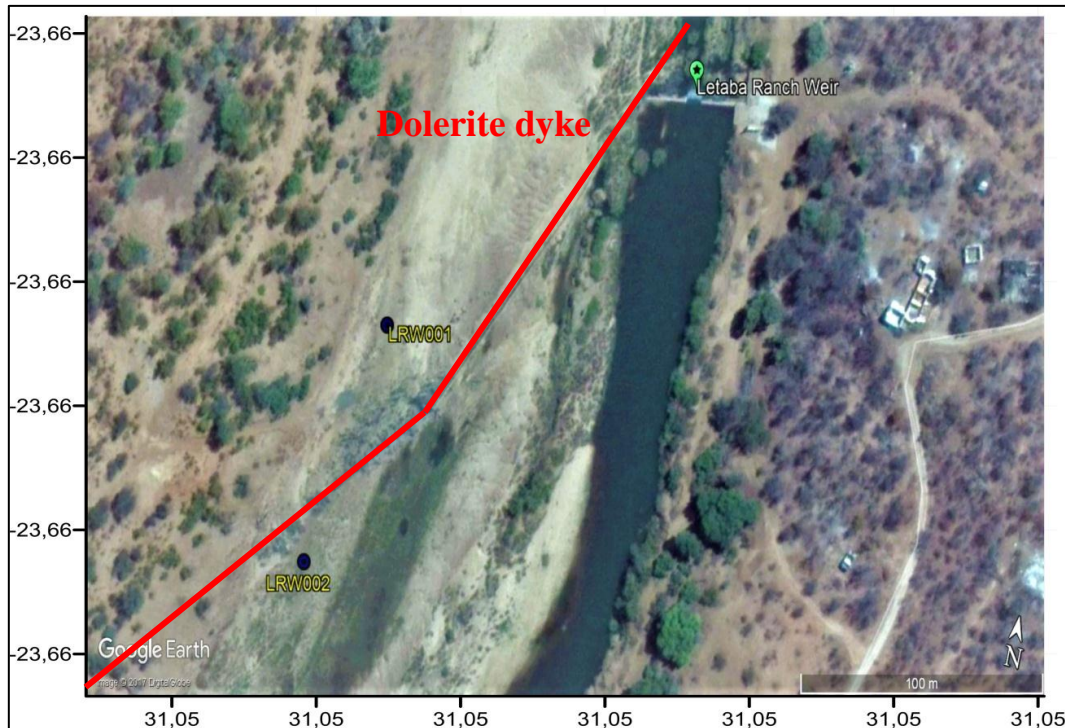


Figure 5.42 Dolerite dyke intersecting the Letaba River at LRW001/2.

In summary, it must be remembered that when the flood event took place, very little rainfall were received by the study site. While, some boreholes did not even display a reaction to the small rainfall events. Thus, the reaction of boreholes during the flood event can be inferred as reactions to the river and not to recharge or at least a combination of the two. When the EC is compared between the two periods of November 2015 and August 2016, it is clear there is generally a large difference between them, with the August profiles indicating lower EC's. This was due to the March 2016 rainfall event providing relatively lower EC rainwater and flood water to the freshly drilled high EC groundwater within the boreholes. This infers that the aquifer is strongly dependent on rainfall events, particularly regional boreholes that are located outside the riparian zone (e.g. LF0031, LF0051).

The large influence that the March 2016 high flow event had on the boreholes in close proximity to the river is evidence of the interconnectedness between the river and groundwater system. Most of the fluid logs also displayed the inflow of groundwater at the top of the borehole with the high temperature at the top decreasing to the bottom of the borehole or via a large fracture. This infers that most water percolates through the unconsolidated zone until it reaches the bedrock or consolidated zone. Although some of the groundwater finds its way to deeper fractures, it seems that most of the

groundwater moves along the boundary between the consolidated and unconsolidated zone. The fluid logs indicate that some of the solid casings contain leakages, thus indicating faulty borehole construction. This will ultimately influence data interpretation and must be seen as an assumption. The increase in EC to the bottom of the boreholes, due to salts and minerals are seen in almost all of the boreholes. This increased the difficulty to distinguish between fractures contributing higher EC groundwater and above mentioned phenomenon. Although, this and the general EC of the borehole and groundwater, was taken into consideration during the interpretation phase. While the increase in temperature also aided in the interpretation and differentiation between the phenomenon (normal increase) and fractures. However, this increase in EC to the bottom of the borehole due to salts/minerals are not always case. As, drillers normally stop drilling as soon as they get a water strike. Thus the fracture will be at the very bottom of the borehole. The flow of lower EC groundwater within a fracture will, ultimately decrease the EC at the bottom of the borehole. An example of this is borehole LF004B.

5.4.7 Down hole Camera

LR004A

The initial interpretation from the fluid logs indicated that groundwater from the unconsolidated zone was flowing down the gravel pack, entering the borehole at the end of the casing. This was confirmed with the down hole camera at 30 m (Figure 5.43), where water could be seen entering the borehole. A small very low yielding fracture was found at 34 m (Figure 5.44). The orientation of the fracture was vertical with a length of approximately 1 m. Water only seeped through slightly, while iron staining (caused by the oxidation of iron), could be seen on the fracture. Further down at 43 m a small fracture with a low yield was discovered (Figure 5.45), this was the same fracture that was indicated by the EC on the fluid log.

LF0051B

At 25.5 m a break in the perforated casing were observed (Figure 5.46). This indicates that the leakages indicated by the fluid logs within some of the other boreholes solid casings are plausible. At 26 m the fracture indicated by the fluid log were observed. This supports the theory that the groundwater entering the fracture consists of a higher EC and temperature.

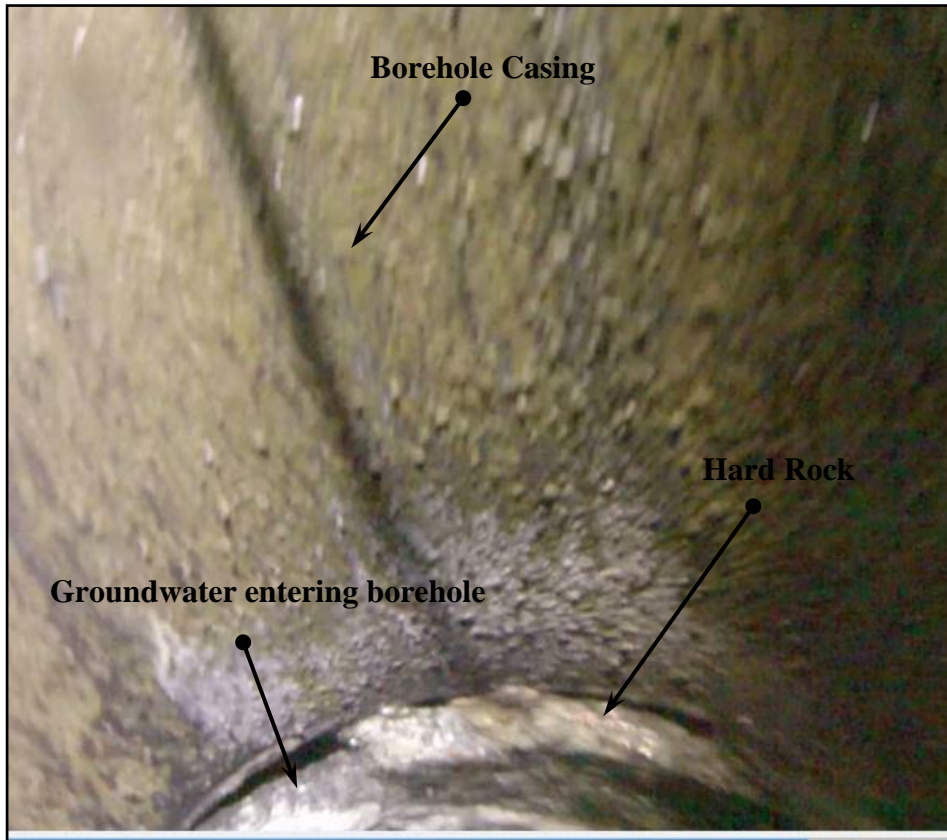


Figure 5.43 Groundwater enter the borehole at the bottom of the casing (LR004A).

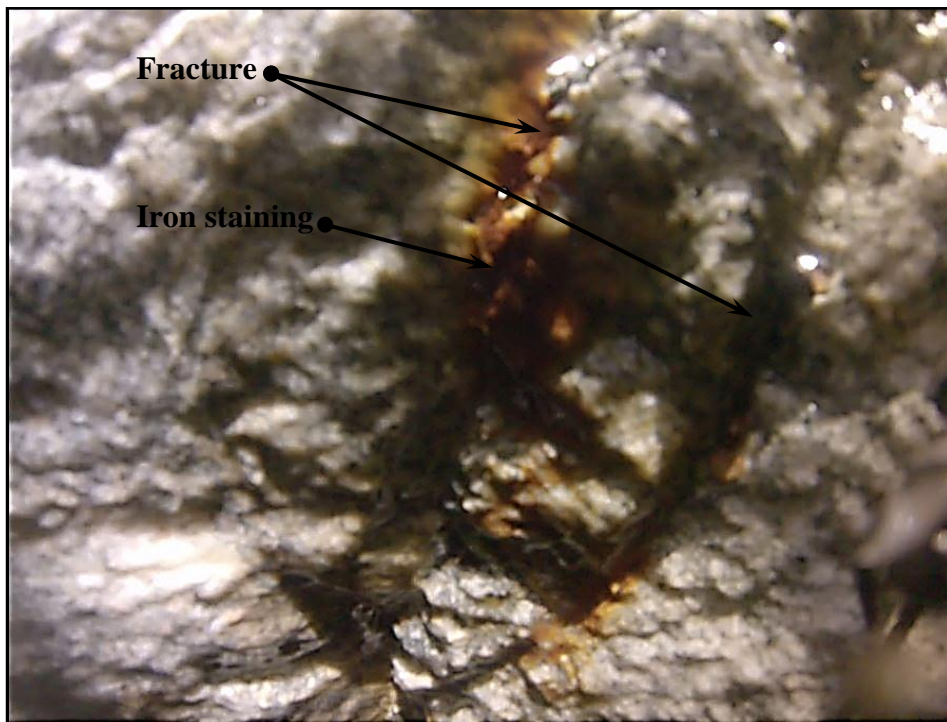


Figure 5.44 Fracture with iron staining at 34 m (LR004A).



Figure 5.45 Fracture at 43 m (LR004A).

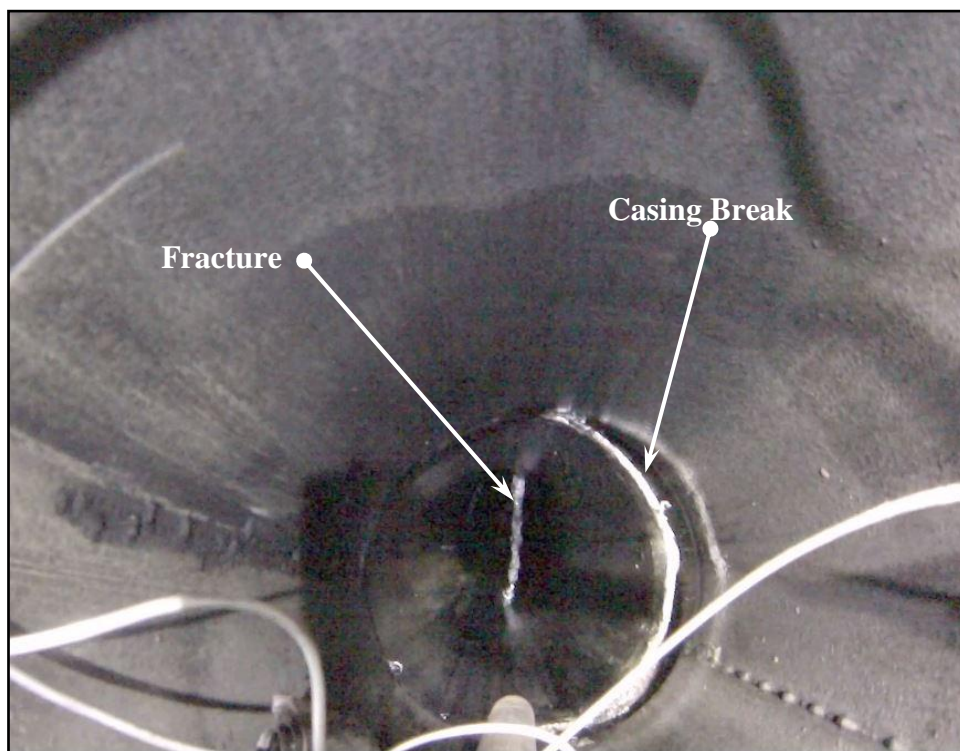


Figure 5.46 Casing break and fracture of borehole LF0051B.

5.4.8 Assessing peak flow transmission losses

During March 2016 a flood event occurred due to a high rainfall event higher up in the catchment, although the study site received extremely low rainfall. This flood event provided a great opportunity to observe the interaction between the river and the surrounding aquifer. Level loggers installed at Mahale weir and Letaba Ranch weir provided the data for the river increase, while data loggers installed within the boreholes provided each boreholes reaction (Figure 5.18). The amount of rainfall on the study site was recorded by the weather stations (Figure 5.2). A total of only 55 mm of rain fell through the month of March 2016 with the rainfall events occurring as follows;

- 12/03/2016 – 14 mm
- 18/03/2016 – 24 mm
- 19/03/2016 – 17 mm

The actual flood event occurred on 19/03/2016, raising the water level within the Letaba River up to 2.42 m higher than the baseflow elevation. With this sudden increase in river water level, connected aquifers were bound to react immediately or display a delayed reaction. The reaction of the boreholes in accordance to their transect are interpreted below.

Transect 1

Transect one included boreholes LF002A/B, LF0021 and LF004A/B. The hydraulic gradient of this transect indicated that the groundwater within this section is moving from the southern bank (LF004A/B) to the river and is then lost to the northern bank (LF0021, LF002A/B) (refer to Figure 5.18). This interpretation was supported by the March 2016 flood event, where LF0021 and LF002 display a definitive, but delayed reaction (Figure 5.47). LF004 (not plotted) however, did not display any reaction to the flood event. Thus, inferring that water was lost to the northern bank in transect 1. This was also supported by the fluid logs, where boreholes on the northern bank contained a lower conductivity than boreholes on the southern bank. Because, of the loss of river water to the groundwater (refer to section 5.4.6 Fluid logging).

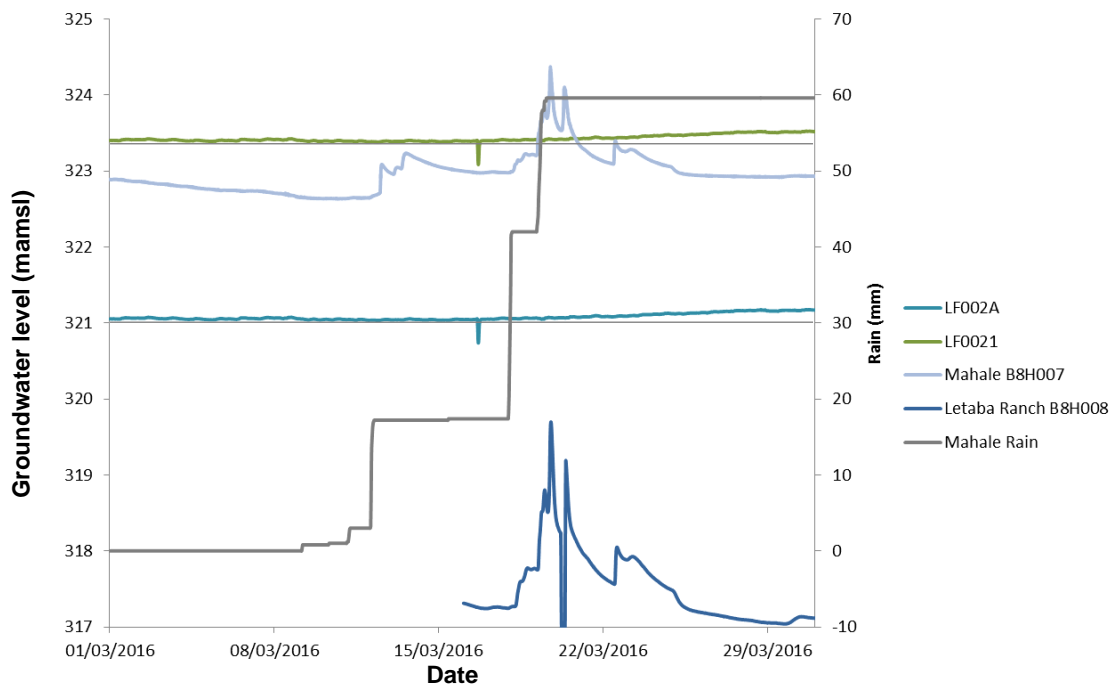


Figure 5.47 Reaction of boreholes to the flood event of March 2016 on transect 1 (Ridell, 2016).

Transect 2

Transect 2 include boreholes LF0031A/B and LF003A/B on the northern bank and boreholes LF005A/B/C and LF0051A/B on the southern bank. The hydraulic gradient of this transect indicated that the groundwater was moving from the northern bank to the southern bank, being detached from the Letaba River.

LF005A/C displayed a definitive immediate reaction to the change in water level of the river, from the first increase in river water level on the 13/03/2016 (Figure 5.48). LF0051A displayed a delayed reaction first to the rainfall on the 19/03/2016 and secondly to the flood event on the 23/03/2016, as expected and in co-ordinance to the hydraulic gradients.

Boreholes on the northern bank also supported this interpretations with neither LF0031 nor LF003 displaying any reactions to the flood event or rainfall events. The fluid logs also provides evidence for this interpretation, as LF005A/B indicated the largest decrease in conductivity after the flood event, as well as LF0051A displaying a small decrease. Where, LF003 and LF0031 both indicated an increase in conductivity (refer to section 5.4.6 Fluid logging).

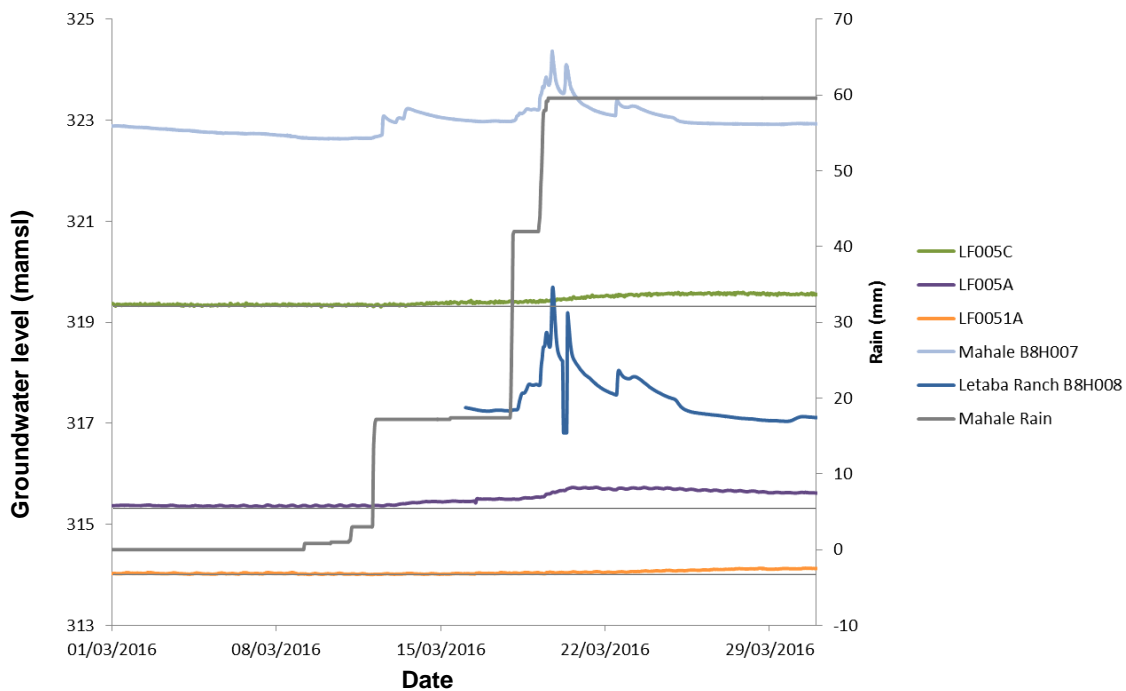


Figure 5.48 Reaction of boreholes to the flood event of March 2016 on transect 2 (Ridell, 2016).

Transect 3

Transect 3 include borehole LR002A on the northern bank and boreholes LR004A/B on the southern bank. The hydraulic gradient of this transect indicated that the groundwater was moving from the northern bank to the river, water from the river was then being lost to the southern bank.

Both LR002A and LR004A/B displayed a reaction to first rainfall and the increase in river water level on the 13/03/2016, only partially verifying the interpretations (Figure 5.49). Although, it must be remembered that LR004A/B is situated almost twice the distance from the river, inferring that LR002A only reacts to peak flow events when the elevation of the river water level exceeds that of its own groundwater level.

During low flow periods water will thus; continue to flow from the northern bank to the southern bank. The fluid logs support this theory with a higher conductivity in LR002A (3000 $\mu\text{S}/\text{cm}$) than observed within LR004A/B (1500 $\mu\text{S}/\text{cm}$), suggesting that river water is being lost to the southern bank (refer to section 5.4.6 Fluid logging).

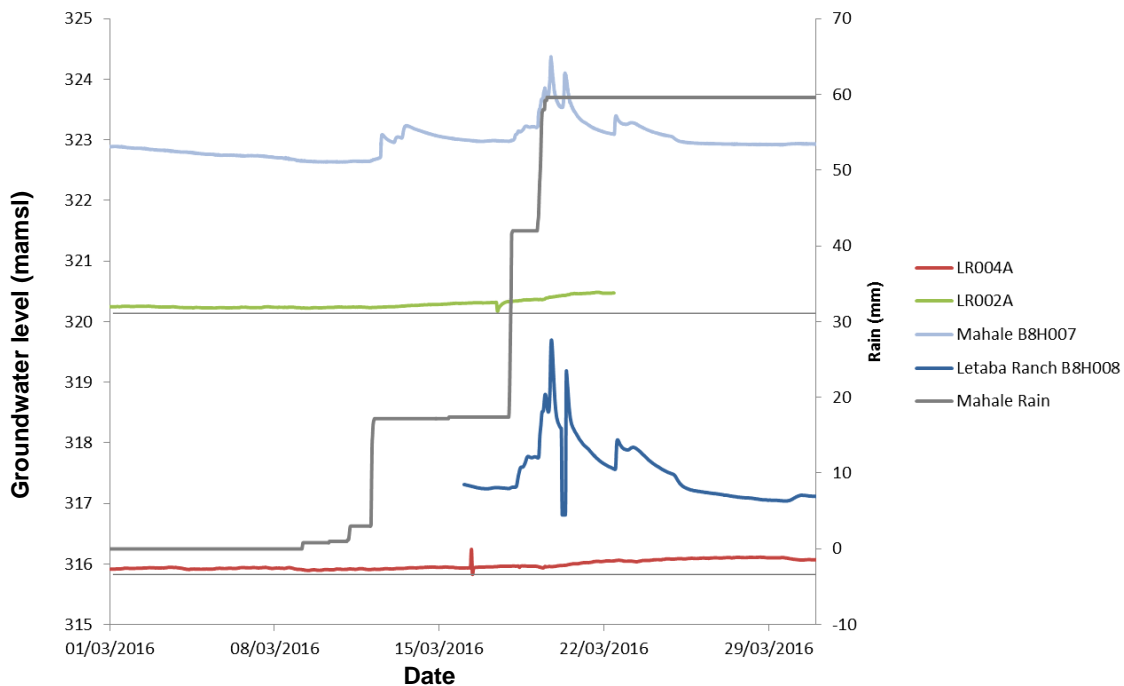


Figure 5.49 Reaction of boreholes to the flood event of March 2016 on transect 3.

Transect 4

Transect 4 include borehole LR001A/B on the northern bank and boreholes LR005A/B on the southern bank. The hydraulic gradient of this transect indicated that the groundwater was moving from both the northern bank and southern bank towards the river. Both LR001A/B and LR005A/B immediately reacted to the flood event, inferring that this process is reversed during peak flow events (Figure 5.50).

Thus during base flow both banks contribute to the river meanwhile, during peak flows the river recharges the aquifer and provides bank storage that will also recharge the aquifer. The fluid logs provide evidence for this interpretation, as boreholes LR0011A, LR001A and LR005A/B displayed a lower conductivity after the March 2016 flood event (refer to section 5.4.6 Fluid logging).

An example (LR005A) of this decrease in conductivity due to the reaction with the March 2016 flood is seen in Figure 5.51. The first decrease in conductivity already started on the 13th of March 2016, while the largest response was on the 15th of March 2016. This indicated when the largest amount of water from the river reached the borehole (LR005A).

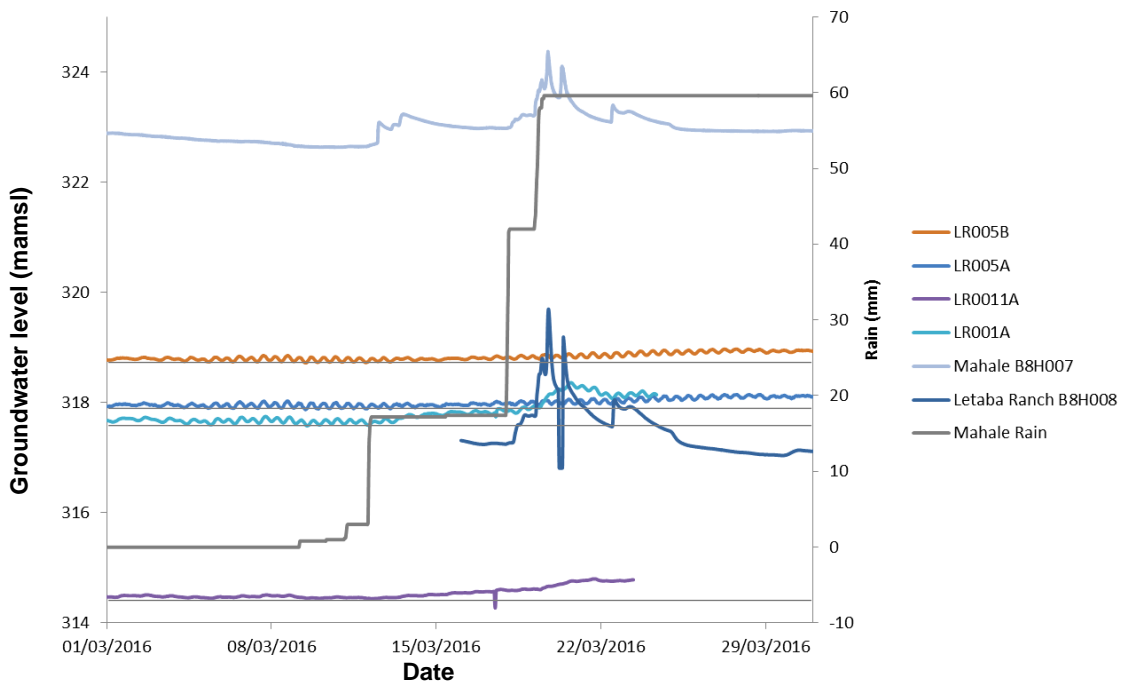


Figure 5.50 Reaction of boreholes to the flood event of March 2016 on transect 4.

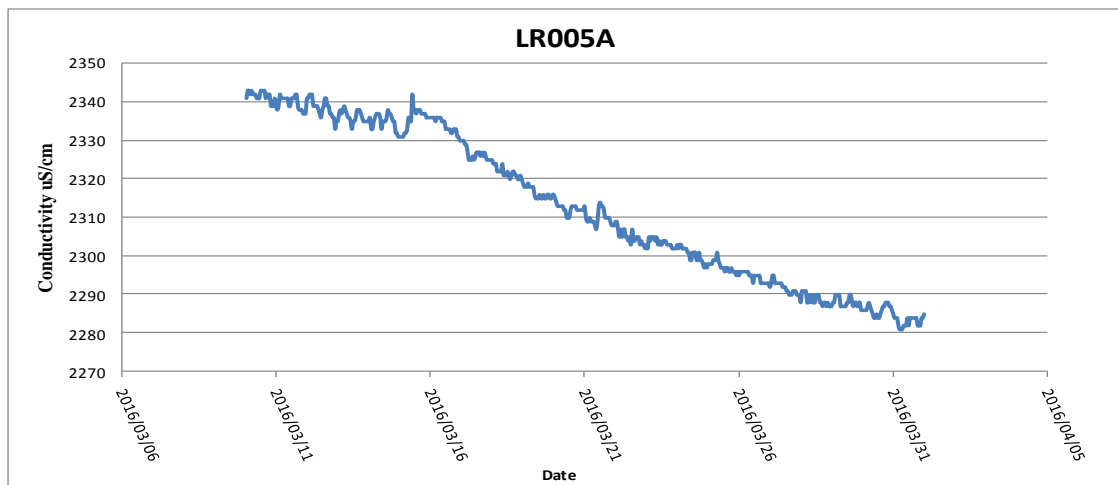


Figure 5.51 Borehole LR005A's conductivity reaction to rainfall and the March 2016 flood. Even though, the reaction was immediate and on the same day as the flood event, the decrease was still gradual.

5.4.9 Groundwater flow direction from hydraulic heads

The hydraulic heads of all the boreholes, as well as the water level taken within the river was plotted as contours in Surfer™ in order to incorporate groundwater movement in relative to the Letaba River (Figure 5.52). The key focus was on the difference in hydraulic heads before and after the March 2016 flood event, as well as wet and dry season comparison.

Transects 1: The hydraulic heads, peak flow transmission losses and fluid logs indicated, that groundwater is moving from the southern bank to the northern bank. Only a small variation was observed between the hydraulic heads before and after the flood event. Greater hydraulic heads were clearly displayed on the northern bank and not on the southern bank, supporting the interpretations.

Almost no variations were observed among the hydraulic heads of the wet and dry season, however this could be from the extremely low rainfall that occurred within this period.

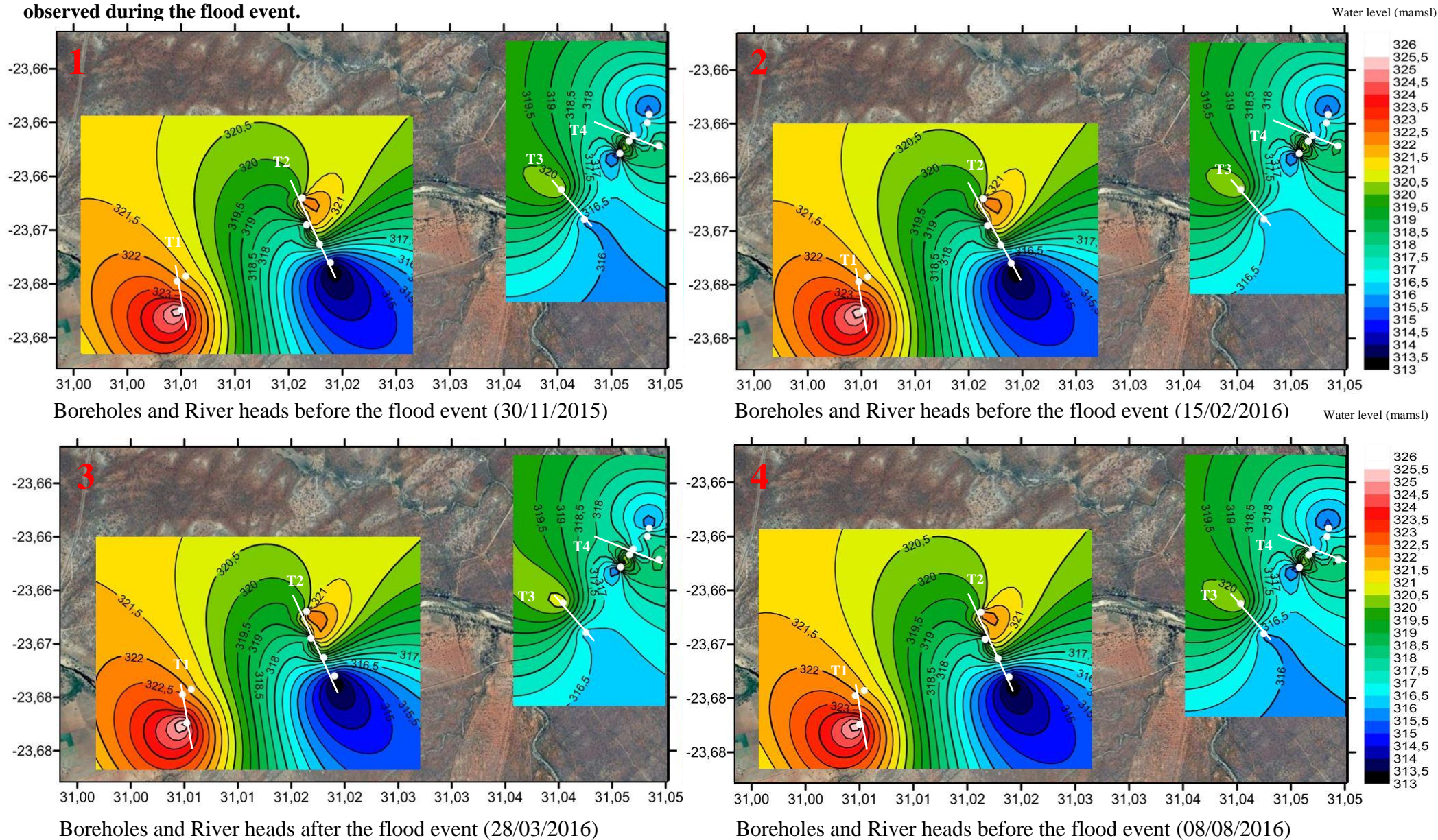
Transect 2: Similar to transect 1, the previous discussions and data were supported, with only a small variation in hydraulic heads observed on the southern bank. This infers that water was moving from the northern bank towards the southern bank, although the small reaction might indicate that the aquifer is detached within this transect, as predicted by the hydraulic gradients. Again, no great differences were indicated between the wet and dry season from the small amount of rainfall that occurred.

Transect 3: Similar to transect 2, the previous discussions and data were supported, with the hydraulic gradient distribution displaying that groundwater was moving from the northern bank to the southern bank. The increase in hydraulic heads on both banks indicates that during low flow events water is gained by the river, while during peak flow events water is lost to the surrounding aquifer. A definite decrease in hydraulic heads was displayed between the wet and dry season, this was predicted from the prolonged drought conditions.

Transect 4: Similar to transect 3, the previous discussions and data were supported, with the hydraulic gradient distribution displaying that groundwater was moving towards the river from both the northern bank and southern bank. The hydraulic heads displayed an increase after the March 2016 flood, thus supporting the interpretations that the river contributes to the surrounding aquifer during peak flows and receives water from the surrounding aquifer during low flows.

A definite decrease in hydraulic heads was displayed between the wet and dry season, this was predicted from the prolonged drought conditions.

Figure 5.52 Groundwater flow direction before (Top) and after (Bottom) the flood event. These figures were created to indicate the rise and fall of the study sites groundwater level before and after the flood event. The first figure and last figure were expected to be similar, as the groundwater levels were taken long before and long after the flood event. The second figure starts to show a small reaction, most probably from the small rainfall events. In figure three a definite difference can be observed during the flood event.



5.4.10 Groundwater stream flow process across dolerite dyke

The dolerite dyke transect (as explained in section 5.4.6 Fluid logging), were also monitored during the flood event of March 2016 in order to obtain a better understanding of the movement of groundwater among the many dolerite dykes located within the study site (see Figure 5.53 below).

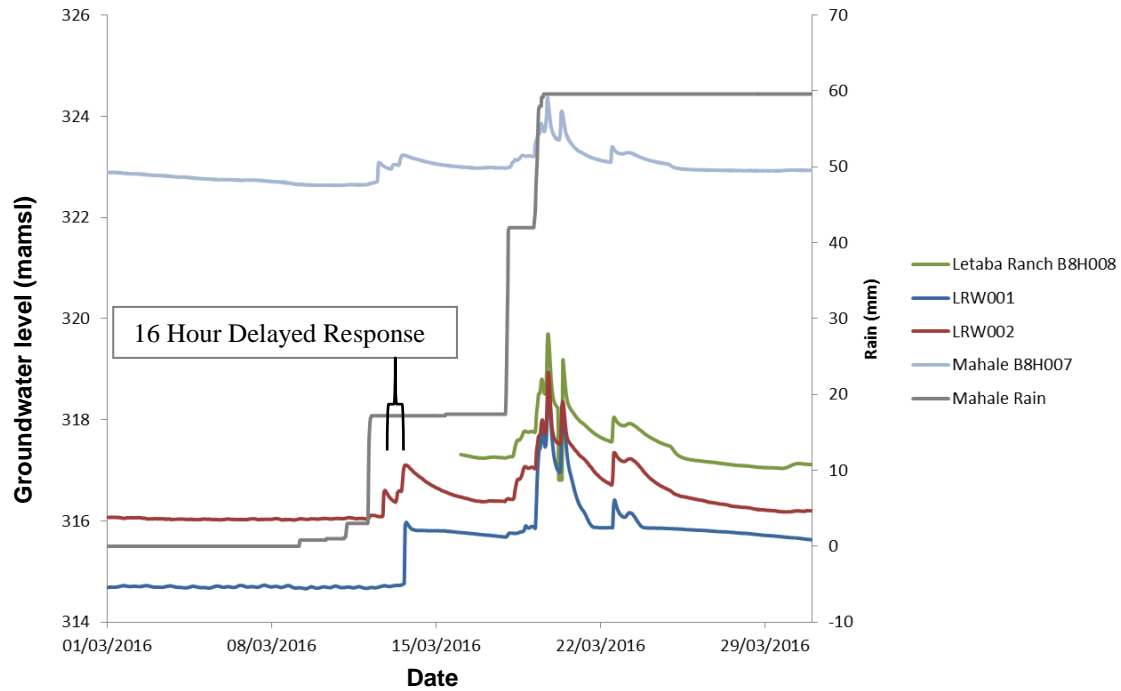


Figure 5.53 Groundwater-Streamflow processes across dolerite dyke

The first response to the flood event that started on 13/03/2016 was observed at the Mahale weir (upstream). This response was also seen in LRW002, while an expected delayed response within LRW001 (downstream) was observed 16 hours later. The reason being, that the dolerite dyke intercepts the movement of groundwater within the consolidated and unconsolidated zone. This is similar to the way that the cement wall on top of the dyke intercepts the river flow.

The fluid logs support this theory as LRW002 displays a lower temperature of around 22°C from the interaction with the river water, whereas LRW001 displays a temperature of between 24 and 26°C. The conductivity also provided evidence, with LRW002 displaying a low conductivity of 1500 $\mu\text{S}/\text{cm}$ and LRW001, displaying a high conductivity of 7000 $\mu\text{S}/\text{cm}$ (refer to section 5.4.6 Fluid logging). After the second peak flow of the flood event (19/03/2016), both boreholes reacted in a similar way. This is due to the river rising high enough to create a connection over the dyke between the two

boreholes. After the flood waters have subsided, LRW002 indicated a faster decrease in water level due to the channelling of water by the dyke towards the weir. For LRW001 a steadier decrease in water level was observed, because of the limited movement of groundwater blocked off by the dolerite dyke.

In summary, the March flood event was a great opportunity to monitor the surrounding groundwater's reaction to the high flow period. It provided data that assisted in the interpretation of the groundwater's flow direction. It also shed some light on the amount of interaction taking place between the surface water and groundwater. Over all the reactions mostly correlated with the hydraulic gradients and fluid logs interpretations, although there were some more complicated reaction observed that will be clarified through the stable isotope analysis.

5.4.11 Isotope analysis

Stable isotopes of oxygen and hydrogen found within water are excellent tracers of the origin of water and can give a good indication of its movement. Water molecules possess a fingerprint that is based on the differing proportions of oxygen and hydrogen isotopes. During precipitation the rain is enriched in ^{18}O and ^2H , thus rain that falls at the end of the precipitation event will be more enriched in ^{18}O and ^2H .

Isotopes samples were collected at 19 boreholes (Figure 5.54), while stream samples were taken at the Mahale weir, Letaba Ranch weir (representing transects 3 and 4), transect 2 and transect 1. These samples were then plotted against the Global Meteoric Water Line (GMWL) (Figure 5.55 and Figure 5.56). Rain samples were also collected at Mahale and Letaba Ranch game reserves ($\delta^{18}\text{O} = -1.9$ to -2.2‰ , $\delta^2\text{H} = -1.6$ to -1.8‰), that indicated enriched isotopic signatures. This was expected for a semi-arid region, as the high atmospheric and land surface temperatures will cause more evaporation, resulting in an enriched isotopic signature.

Transect 1

On transect 1 isotope samples were collected at borehole's LF004A/B, LF0021 and LF002A, together with a stream sample. LF004A and B displayed a similar isotopic signature, although both contained a less enriched $\delta^2\text{H}$ (-10.2‰) and $\delta^{18}\text{O}$ (-1.8‰) value than the rest of the samples taken on transect 1.

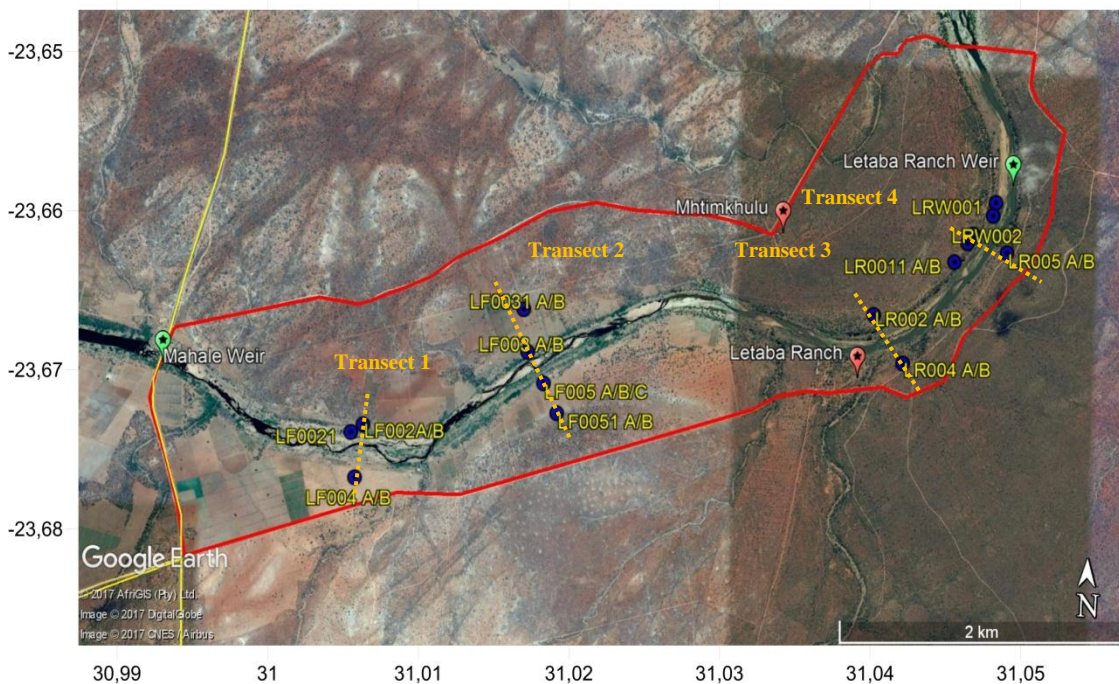


Figure 5.54 Overview of borehole locations and transects.

The river sample is slightly more enriched ($\delta^{18}\text{O} = -1.8\text{‰}$, $\delta^2\text{H} = -8\text{‰}$) than LF004A/B, this indicates that groundwater is contributing to the stream and gets enriched from evaporation after entering the stream. LF002A and LF0021 displayed the most enriched isotopic signatures on transect 1 ($\delta^{18}\text{O} = -1.4$ to -1.5‰ , $\delta^2\text{H} = -6$ to -7‰), indicating mixing of groundwater, river water and rain water that has undergone evaporation.

The isotopic signatures of transect 1 supports the interpretation from the other data collected, that groundwater is moving from the southern bank to the northern bank, while intersecting the river along the way. However all the samples on transect 1 indicated a relatively enriched isotopic signature, especially when compared to the other transects. This is possibly from additional mixing with enriched rainwater.

Transect 2

On transect 2 isotope samples were collected at borehole's LF0031A/B, LF003A, LF005A/B and LF0051A/B, together with a stream sample. LF0031A and LF0031B indicated a relatively similar isotopic signature (ranging from: $\delta^{18}\text{O} = -3.2$ to -3.6‰ and $\delta^2\text{H} = -20.9$ to -21.1‰), while both were the most enriched on transect 2. LF003B displayed a similar isotopic signature ($\delta^{18}\text{O} = -3.5\text{‰}$, $\delta^2\text{H} = -20.2\text{‰}$), than LF0031A/B.

The stream sample on transect 2 displayed an isotopic signature more comparable to the stream sample at transect 1 ($\delta^{18}\text{O} = -1.8\text{‰}$, $\delta^2\text{H} = -9.16\text{‰}$), while indicating a much more enriched isotopic signature than the boreholes on transect 2. This infers that there is little to no interaction between the river and the groundwater. LF005A/B and LF0051A/B displayed similar isotopic signatures (ranging from: $\delta^{18}\text{O} = -3.7$ to -4.2‰ and $\delta^2\text{H} = -22$ to -24.4‰), although less enriched than LF003B and LF0031A/B.

The isotope data from transect 2 corresponds with the rest of the findings at this location, that water is moving from the northern bank to the southern bank and does not intersect the river. Thus, the groundwater is detached from the river on transect 2, as all the boreholes display a more depleted isotopic signature than the river sample.

The most enriched sample from the boreholes are LF0031A/B located on the northern bank and decreases to the southern bank. This indicates some slight mixing with rainwater, this mixing decreases towards the southern bank and supports the initial interpretation of groundwater movement from north to south.

Transect 3

On transect 3 isotope samples were collected at borehole's LR002A and LR004A/B, together with a stream sample. LR002A displayed an isotopic signature more enriched than all the boreholes on transect 2 and 3 ($\delta^{18}\text{O} = -3.1\text{‰}$, $\delta^2\text{H} = -19.2\text{‰}$). This enrichment could be due to additional mixing with rainwater.

LR004A and LR004B display a relatively depleted isotopic signature (ranging from: $\delta^{18}\text{O} = -3.8$ to -4.7‰ and $\delta^2\text{H} = -22.3$ to -28.2‰), when compared to the river sample ($\delta^{18}\text{O} = -1.3\text{‰}$, $\delta^2\text{H} = -9\text{‰}$), even though LR004B indicated slight enrichment. This infers that groundwater is not being lost from the river towards LR004A/B.

The hydraulic gradient, fluid logs and March flood reactions suggests otherwise, although both situations can be explained by a dolerite dyke discovered running between LR004A/B and the river. During low flow periods water is being lost to the southern bank and gets blocked by the impermeable dolerite dyke, although during high flow periods this dyke is over flown causing a reaction with LR004A/B.

In conclusion the isotopes mostly concurred with the rest of the data obtained, with groundwater moving from the northern bank to the southern bank. Although it also indicated the large effect dykes can have on the flow direction of groundwater.

Transect 4 A

On transect 4 A isotope samples were collected at borehole's LR005A/B and LR001A, together with a stream sample. LR005A/B and LR001A display some of the most depleted isotopic signatures of all the boreholes (ranging from: $\delta^{18}\text{O} = -4$ to -4.6‰ and $\delta^2\text{H} = -24.4$ to -28.5‰), and is much more depleted than the isotopic signature of the river sample ($\delta^{18}\text{O} = -1.2\text{‰}$, $\delta^2\text{H} = -7.5\text{‰}$).

This indicates little to no interaction between the groundwater and river. It is also in correlation with the rest of the data, which suggests groundwater contributing to the river from the northern and southern bank.

Transect 4 B

On transect 4 B isotope samples were collected at borehole's LR005A/B and LR0011A, together with a stream sample. LR0011A displayed a relatively similar isotopic signature as LR001A ($\delta^{18}\text{O} = -4.2\text{‰}$, $\delta^2\text{H} = -23.8\text{‰}$), compared against a similar river sample ($\delta^{18}\text{O} = -1.2\text{‰}$, $\delta^2\text{H} = -7.5\text{‰}$). This again indicated groundwater contribution to the river from both banks.

Borehole within river bed:

LRW001 located on the downstream side of the Letaba weir and dolerite dyke situated underneath the weir, displayed a relatively depleted sample ($\delta^{18}\text{O} = -3.3\text{‰}$, $\delta^2\text{H} = -20\text{‰}$), when compared to the river sample ($\delta^{18}\text{O} = -1.2\text{‰}$, $\delta^2\text{H} = -7.5\text{‰}$). Thus, indicating relatively little interaction between the river and the groundwater on the downstream side of the dyke.

Similar to transect 3, it indicates the significant effect that dolerite dykes have on the groundwater system within this area and how it blocks and channels the groundwater flow.

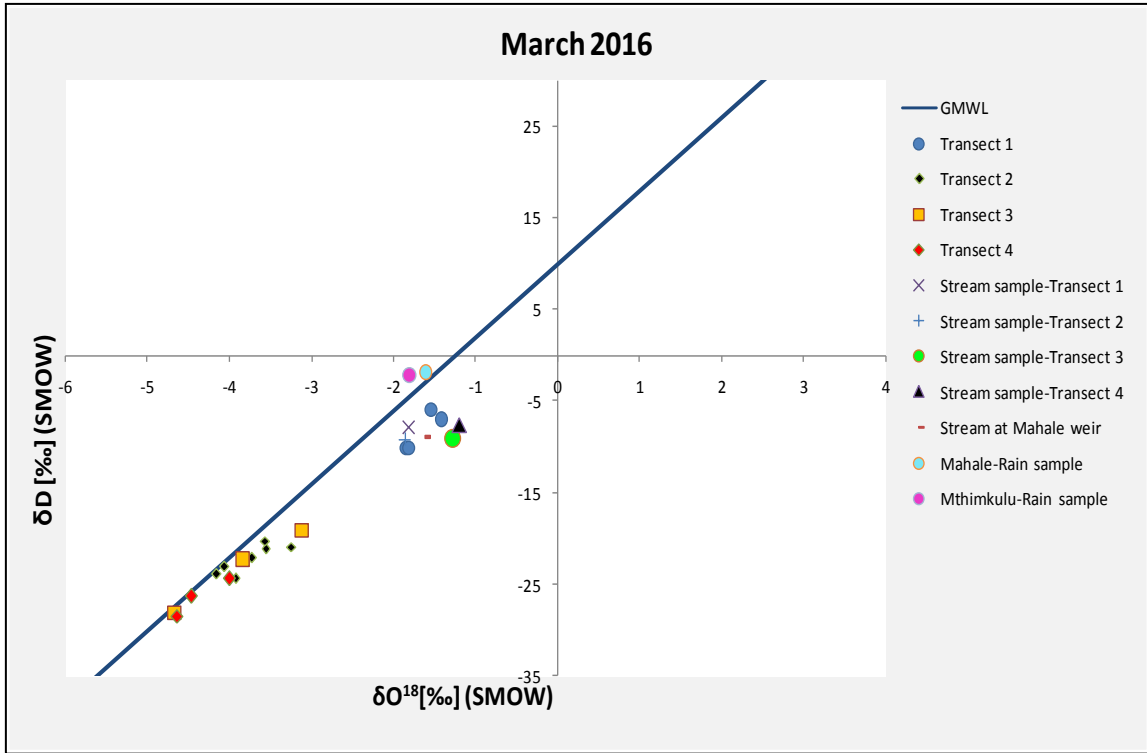


Figure 5.55 A graph indicating the relationship between $\delta^2\text{H}$ and $\delta^{18}\text{O}$ values of samples taken on the study site in terms of each transect.

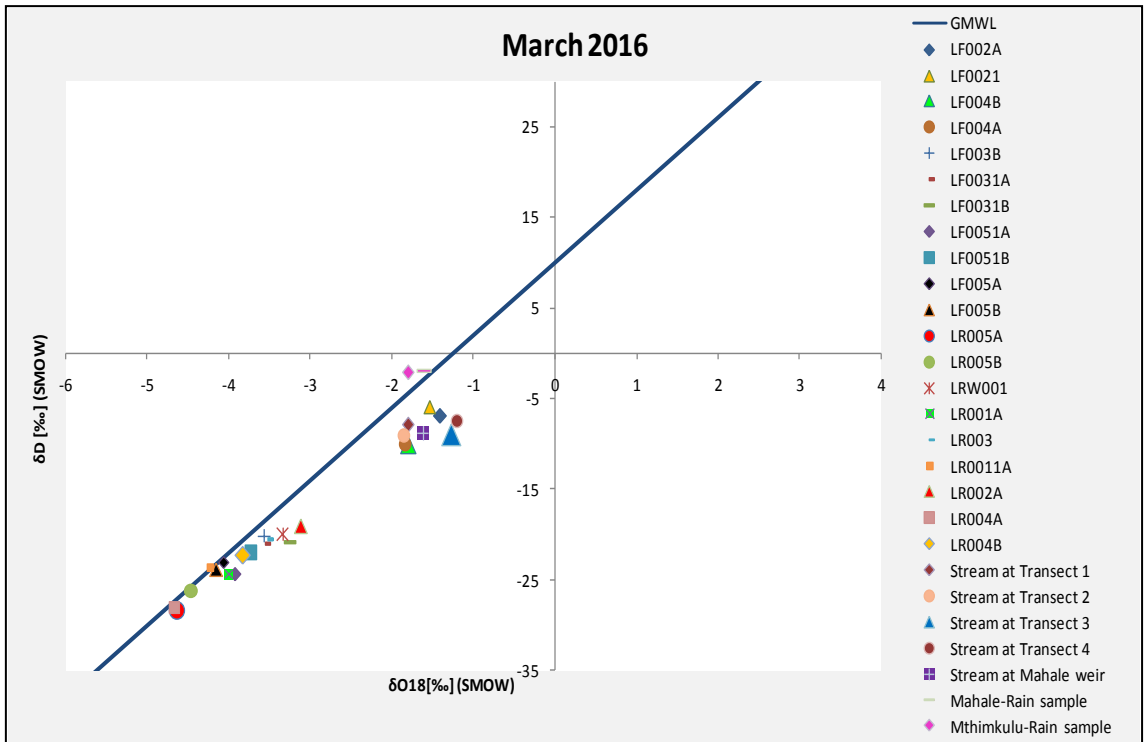


Figure 5.56 A graph indicating the relationship between $\delta^2\text{H}$ and $\delta^{18}\text{O}$ values of samples taken on the study site in terms of each borehole.

5.4.12 Groundwater – surface water mass balance

The chemical base flow separation technique was implemented for the mass balance, as the data required for this technique were obtained during the March rainfall event. This technique estimates the groundwater contribution and surface runoff (quickflow), through the chemical contribution of stream water and two end-members.

However, the assumption that it is based on, states that the groundwater end-member can be accurately defined and remains constant. The required data for this method is the stream discharge and trace element concentration through a single storm event, as well as the trace element concentration amount in the precipitation and groundwater.

The data were obtained from the Letaba Ranch weir and borehole LRW002, as this borehole is located within the river channel and directly connected to the stream flow during this period.

The formulas that are used in this formula are as follows:

$$Q_q = Q_s - Q_b \quad (5.2)$$

And

$$Q_s c_s = Q_b c_b + Q_q c_q \quad (5.3)$$

That is then simplified to:

$$Q_b = Q_s \left(\frac{c_s - c_q}{c_b - c_q} \right) \quad (5.4)$$

where:

Q_s = Streamflow in m³/sec.

Q_b = Baseflow in m³/sec.

Q_q = Quickflow in m³/sec.

Q (discharge) in m³/sec.

C (concentration) in µg/L.

T (time) in hours

The baseflow, quickflow and streamflow were then calculated and plot against time for further analyses (Figure 5.57).

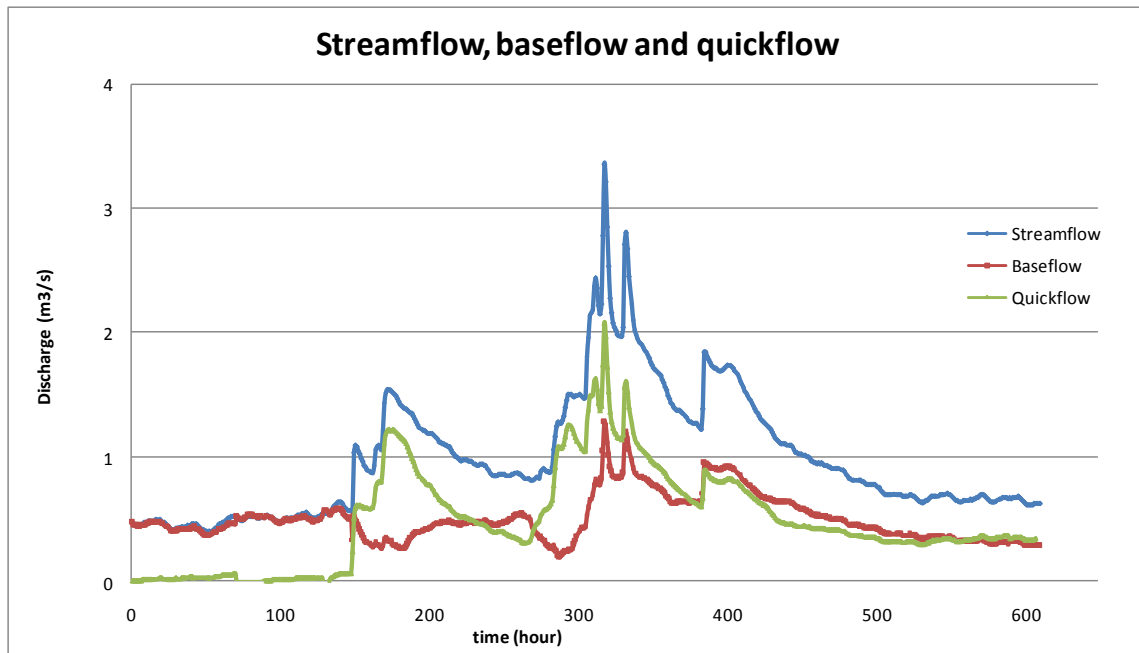


Figure 5.57 Graph comparing streamflow, baseflow and quickflow.

The first reaction to the rain event already started at hour 60, this was caused by the rain and runoff from the immediate surroundings. During this period soils absorb most of the rain falling within the catchment and needs to become saturated before the runoff starts. The first big reaction to the rainfall event occurred at hour 150, with a sudden and steep reaction (rising limb). This reaction is from the entire catchments response to the rainfall event. It indicates that soils are saturated throughout the catchment and the runoff has reached the river.

However, the steepness of the graph suggests that very little infiltration occurred and that most of the rain were transferred into surface runoff. The rain intensity increased three times throughout the storm, with the three peaks clearly visible on the graph.

As the streamflow and quickflow increased a decrease is observed within the baseflow. This is called negative baseflow and occurs when the rivers water level is lower than the surrounding groundwater level before the heavy rain, thus groundwater is flowing towards the river. Although when the rivers water level rises from the heavy rain it starts to flow towards the groundwater, thus resulting in negative baseflow (Basak, 2007).

The second peak at hour 280 displays the same negative base flow seen in the first peak at hour 150. This infers that the rivers water level is still higher than the surrounding groundwater's level and the river water is still flowing towards the groundwater.

The third peak at hour 380 does not indicate the negative baseflow seen in peak 1 and 2, with a decrease in quickflow. This is because at this stage the surrounding groundwater's level have increased to the same/higher as the rivers water level. The rain has stopped as well as the quickflow, resulting in the decrease seen in (Figure 5.56).

The decrease in quickflow also indicates that the aquifers and soils are now fully saturated and contributing to the river. The recession limbs of all three peaks decreases slowly over time, while the streamflow remains high. This infers that it is a large catchment and the rainfall was widely distributed. After the rain event the baseflow returns back to normal while the streamflow and quickflow remains high. This suggests again that little infiltration occurred. The geology supports this interpretation with most of the site being dominated by granites that restricts infiltration due to its resistance to weathering and hardness.

In summary, the rainfall event the baseflow ultimately increases after every streamflow peak. From 17% to 37% to 50% of the discharge volume, while the quickflow decreases with every streamflow peak, from 76% to 61% to 47%. This indicates the lag time for the aquifers to start contributing to the river. When this and the two decreases in baseflow at peak 1 and 2 is taken into consideration, it infers that initially there is a large loss to the groundwater. After which the groundwater starts contributing back to the river.

This concurs with the peak flow transmission losses and fluid logs that indicated a reverse in the river from a gaining to a losing system during this high flow period.

All the information that was analysed in the previous sections will be summarised in the conceptual model chapter to follow.

Chapter 6 - CONCEPTUAL MODEL: DISCUSSION AND ASSUMPTIONS

A conceptual model normally comprises of a set of postulations that visually or verbally portrays the aquifer systems, based on observations in the field and the interpretation of data (Adams et al., 2004).

When developing a conceptual model, it is important to have a good understanding of the interaction processes and how it relates to the actual hydrological processes. Groundwater surface water interactions will vary considerably depending on the scale and locality. Deep confined aquifers will normally not have a major impact on groundwater discharge to rivers, where as a local groundwater flow system will display a larger contribution. Thus, it is important to have an understanding of the interactions on a both temporal and spatial scale when describing the processes (Tanner, 2013).

The data and interpretations from Chapter 5 are consolidated into a site specific conceptual model of the groundwater and the surface water interaction of the Letaba River and the surrounding aquifer (Figure 6.1). The conceptual model will be discussed in terms of transects 1 to 4, as previously interpreted in the previous sections.

6.1. TRAVERSE 1

On traverse 1 the hydraulic gradient indicated that groundwater was moving from the southern bank (LF004A/B), to the northern bank (LF0021/, LF00A/B), while the aquifer tests displayed higher transmissivity and storativity values for the shallow boreholes. The higher T and S values were expected for the shallow boreholes, as water would move and be stored more easily within the unconsolidated zone. The higher K and T values on the northern bank also indicated a loss from the river to the northern bank.

The fluid logs supported the hydraulic gradient and K/T values interpretation with boreholes on the southern bank displaying a far lower EC than boreholes on the southern bank. All of the shallow boreholes also indicated lower EC values than the deeper boreholes, suggesting that groundwater was mostly moving within the unconsolidated zone.

The March flood in 2016 displayed a delayed, but definite reaction to the northern bank. While boreholes on the southern bank did not display any reaction to the flood event, however a more prominent reaction was observed to the small rainfall event. These reactions infer that groundwater is moving from the southern to the northern bank.

Lastly the isotopic signatures supported the rest of the data, indicating that water was moving from the southern bank, intersecting the river and contributing to the northern bank. Where, groundwater, river water and some rain water mixing is taking place (Figure 6.2).

6.2 TRAVERSE 2

On traverse 2 the hydraulic gradients indicated that groundwater was moving from the northern bank (LF0031A/B, LF003A/B), to the southern bank (LF005A/B, LF0051A/B), in contrast to transect 1. The interesting aspect was that the groundwater system was also depicted as a detached system with a large difference between the river level and the deep/shallow riparian boreholes hydraulic heads. Thus, a through flow is occurring from the northern bank to the southern bank. The T values of the deep aquifer indicate that the river is losing water to the southern bank, although the shallow aquifer T values indicate a greater loss to the riparian zone. Boreholes on the southern bank indicated high T values, suggesting a larger loss of the river to the southern bank. While a relatively high T value in the shallow borehole LF003B, suggested a small loss of the river to the northern banks riparian zone.

The fluid logs displayed a generally decreasing EC profile from north to south, supporting the hydraulic gradient interpretations. Riparian boreholes indicated a low EC, supporting the T values with a small loss to the northern bank riparian zone.

LF005A/B displayed an immediate reaction, with LF0051A/B displaying a delayed reaction to the March 2016 flood event. LF003A/B and LF0031A/B displayed almost no reaction, thus supporting the hydraulic gradients and T value interpretations. With groundwater moving from north to south on transect 2, while a large loss of the river to the southern bank occurs and a small loss to the northern bank riparian zone.

Lastly the isotopic analyses supported the data, indicating a through flow from the northern bank to the southern bank, thus the groundwater system is detached from the

river. However, mixing of the river water with the groundwater system was not indicated, as the T values suggested. Thus, the river only interacts with the groundwater during high flow events, where some water is lost to the southern bank and small amounts to the northern banks riparian zone (Figure 6.2).

6.3 TRAVERSE 3

The hydraulic gradient on traverse 3 indicated that groundwater is moving from the northern bank (LF002) towards the river, while a loss is occurring from the river to the southern bank (LR004A/B). The low T values of borehole LR002 indicate that the contribution is relatively small, while the high T values of borehole LR004 indicated a large loss to the southern bank.

The fluid logs supported the hydraulic gradients interpretation with LR002 displaying an EC (3000 $\mu\text{S}/\text{cm}$) twice as high as LR004A/B (1500 $\mu\text{S}/\text{cm}$). The March 2016 flood event provided some interesting data with both boreholes having a reaction to this event. Although, it must be remembered that LR004A/B is situated almost twice the distance from the river, inferring that LR002A only reacts to peak flow events when the elevation of the river water level exceeds that of its own. During low flow periods water will thus; continue to flow from the northern bank to the southern bank (Figure 6.2). This was also supported by the mass balance.

The isotope analyses supported the initial theory and indicated that groundwater was moving from the northern bank to the river, although it did not support the March flood reaction and EC profiles suggested that groundwater was being lost to the southern bank. The reason for this was a dolerite dyke (discovered in the field), running between LR004A/B and the river. This dyke can also be seen in the geophysical traverse of LM004 (Figure 5.15).

During low flow periods this impermeable dyke blocks the groundwater, lost from the river to the southern bank, from interacting with the groundwater on the other side (LR004A/B), of the dyke. However during high flow periods the groundwater level on the river side of the dolerite dyke is higher than the dyke's elevation underground, thus it is over flown allowing the reaction with the groundwater on the other side of the dyke.

6.4 TRAVERSE 4

On traverse 4 the hydraulic gradient indicated that groundwater was moving from the both the north-western bank (LR001A/B) and south-eastern bank (LR005A/B) towards the river. This is in contrast to all other transects that indicated a loss to either the northern or southern bank. The T values also indicated that the south-eastern bank is making a much larger contribution to the river.

Similar to transect 3, both LR001A/B and LR005A/B immediately reacted to the flood event, inferring that this process is reversed during peak flow events. Thus, during base flow both banks contribute to the river while, during peak flows the river recharges the aquifer. The fluid logs provide evidence for this interpretation, as boreholes LR001A and LR005A/B displayed a lower conductivity after the March 2016 flood event. This was also supported by the mass balance.

The isotope analyses supported this interpretation, indicating that groundwater was moving from LR001A (northern bank) and LR005A/B (southern bank) towards the river on traverse 4A (Figure 6.2). A similar groundwater movement was indicated on traverse 4B that includes LR0011A and LR005A/B.

6.5 DOLERITE DYKE INFLUENCE

It was expected that the dolerite dyke and small cement wall (on top of the dyke), would form an impermeable layer and prohibit surface and groundwater from moving through. This was confirmed by the data of the fluid logs, hydraulic heads and reaction to the March flood.

LRW001 indicated a low head of 1.41 mbgl, while LRW002 indicated a higher head of 1.02 mbgl. This occurs because, the dolerite dyke blocks groundwater moving along the river, thus creating a damming effect ultimately raising the groundwater level. The cement wall in return helps to block surface water from moving through this section of the wall.

The fluid logs supported this interpretation, as LRW001 displayed a high EC of around 7000 $\mu\text{S}/\text{cm}$ and high water temperatures decreasing from 24 °C to 26 °C at the bottom of the borehole. Thus, indicating that no cold fresh water from the river or

unconsolidated zone is flowing into the borehole. The only water entering the borehole is from the fracture at 8 m. LRW002 in contrast indicated a low EC of 1500 $\mu\text{S}/\text{cm}$ and a low curved temperature profile that also increased to the bottom. This low EC and temperature infers that water is flowing in at the top of the borehole through the unconsolidated zone. While the cold temperature suggests that the water originates from the river.

During the March 2016 flood event LRW002 was the first to react on the 12/03/2016 at 18:43, while LRW001 first started reacting on 13/03/2016 (26 hours later). Thus, again signifying the large effect the dyke has on the movement of the groundwater.

The isotope analyses supported these findings and indicated that there was little to no reaction between LRW001 (downstream of dyke) and the river, even though the borehole is located within the river bed.

In summary, the conceptual model indicates that in the farms area the groundwater is moving independently of the river. It flows from the southern bank to the northern bank on transect 1 and back to the southern bank on transect 2, becoming detached from the river. During high flow periods the river only contributes more to the northern bank on transect 1, while transect 2 receives a small amount of contribution through the riparian zone.

At the protected area the groundwater mostly flows towards the river. Except during high flow periods when the stream changes from a gaining stream to a losing stream, contributing to the surrounding aquifer.

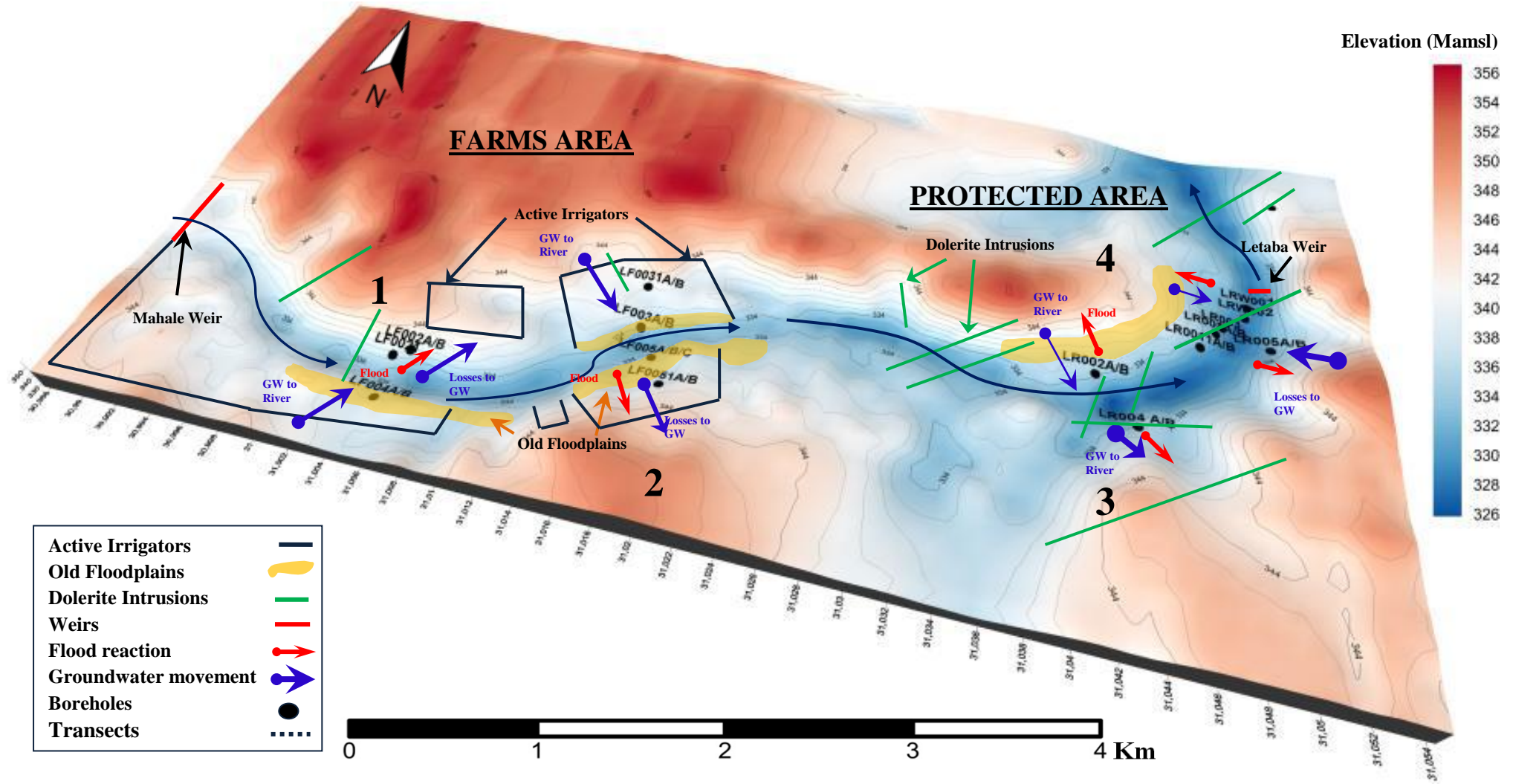


Figure 6.1 Conceptual model of study site.

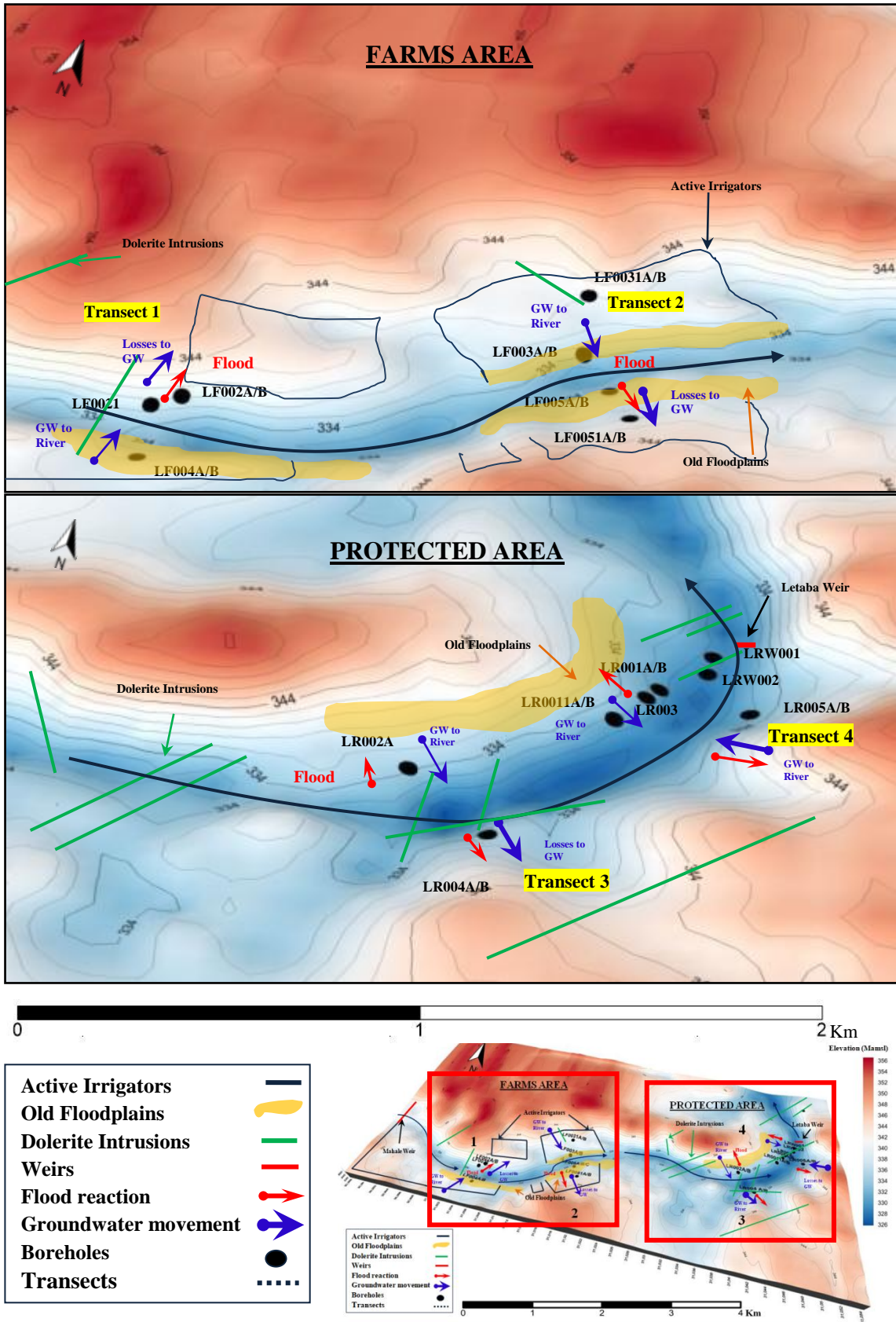


Figure 6.2 Conceptual model of the protected area and farms area.

Chapter 7 - CONCLUSIONS AND RECOMMENDATIONS

7.1 CONCLUSION AND DISCUSSION

To determine the connectivity of geohydrological processes and the interaction with the surface hydrology of the Letaba River, numerous techniques were used to obtain the necessary data.

Techniques applied at the study site include:

- Geophysics for:
 - Siting of boreholes
 - Geological characterisation
- Drilling of 28 boreholes
- Aquifer characterisation
 - Slug tests
 - Step tests
 - Constant rate tests
- Data loggers for hydraulic gradient monitoring
- Fluid logging for borehole profiling
- Sampling for isotopic analyses
- Weather stations for climatic monitoring

The analysed data provided the basis for the final conceptual model of geohydrological processes interacting with a perennial river at the Letaba study site, which ultimately presented an overview of the complex interaction between the groundwater and surface water of the Letaba River. The study site had to be divided into four transects, because of the scale. Each traverse indicated a different system of groundwater movement and interaction with the surface hydrology.

The final system of groundwater movement is explained below in terms of each transect:

Traverse 1: groundwater is moving from the southern bank to the northern bank intersecting the river. The river gains water from the southern bank, but loses more

water to the northern bank. During high flows water is then lost to the southern bank, while some mixing with rainwater is also indicated by the isotopes.

Traverse 2: groundwater is moving from the northern bank to the southern bank, while the hydraulic gradients and isotopes indicated a detached system. During high flow periods some of the water will be lost to the southern bank, although some water will percolate through the riparian zone on the northern bank.

Traverse 3: groundwater is moving from the northern bank to the southern bank intersecting the river. The northern bank makes a small contribution to the river, while the river loses a large amount of water to the southern bank, as indicated by the K and T values. Even though, to the southern bank it does not reach the boreholes LR004A/B, because of a dolerite dyke that separates the river. During high flow the system changes into a losing stream to both banks, although a larger amount is still contributed to the southern bank overflowing the dyke and ultimately recharges the groundwater on the other side (LR004A/B).

Traverse 4: groundwater is moving from both banks to the river, with the southern bank making the largest contribution to the river. Relatively similar to traverse 3 the system changes from a gaining stream to a losing stream during high flow periods.

The hydraulic gradients between the shallow boreholes (aquifer) and deep boreholes (aquifer) did not show a large variation. Furthermore the aquifer tests did show a reaction when the shallow/deep boreholes were tested. Therefore, indicating that there is only one aquifer present. This was also supported by the isotopes, with little difference between the isotopic signatures of the deep and shallow boreholes. The fluid logs indicate that groundwater is moving from the top of the borehole down the gravel pack and into the borehole. Thus, rain will percolate through the unconsolidated zone until it hits the hard rock (consolidated zone). From there it will move along the contact and percolate further down when any fractures are intersected. Although, because the fluid logs indicated this, it means that the construction of the boreholes were not completed properly or leakages have occurred. This increased the difficulty in accurate interpretations. Old alluvial deposits found on the southern bank of traverse 1 and 2, creates good conditions in terms of geology for groundwater movement. This was indicated by the high transmissivity values obtained by the aquifer tests within these

alluvial deposits. On the other hand, as Becker et al. (2004), and Kalbus et al. (2008), states: the accurate quantification of groundwater – surface water interaction remains a difficult task, because of heterogeneity and scale. It is important to remember that all the methods that were implemented within this study have assumptions (see section 2.6 GENERAL ASSUMPTIONS).

Ultimately the main aims and objectives were achieved. The conceptual model provided an excellent demonstration and explanation of the connectivity of the groundwater – surface water interaction within the Letaba River.

Key objectives achieved:

- The extent of the study site, time line, borehole placement and geological/aquifer characterisation provided the necessary data for a good characterisation for the spatial and temporal interaction between the aquifers of the Letaba River.
- The groundwater hydraulics gradients and March flood event provided the ideal data to determine the groundwater flow paths and their interaction with the Letaba River.
- The monitoring of the boreholes through the four weather seasons and March flood event provided ideal data to determine changes in groundwater flow paths and their interaction with seasonal variability.
- Again, the March flood and weather stations provided the necessary data to determine the aquifers reaction during rainfall events, as well as during high flow events.
- Ultimately the function and behaviour of the groundwater – surface water interaction was depicted in the conceptual model.
- The study provided valuable information and a better understanding on the complex nature of groundwater - surface water interaction within catchments of the Kruger National Park, thus it can be used for better water resource management within the KNP. In addition the findings can ultimately be implemented throughout South Africa, providing better management of this sparse resource.
- The results and deficiencies of this study will also provide ideal information when commencing new groundwater – surface water interaction projects. Generally groundwater – surface water interaction is depicted as a simple process, although this study has indicated that this is not the case. The interactions differ greatly over

short distances, placing emphases on the importance of understanding these processes. This is especially important when management of water resources is exercised. This in return places emphases on the importance of groundwater – surface water interaction studies and maintaining these study sites for future and long term research.

7.2 RECOMMENDATIONS FOR FUTURE RESEARCH

It has become clear through this research that the connectivity between the surface water and groundwater is extremely complex. Further research and monitoring is essential to fully understand this complex interaction.

Although, extensive infrastructure was installed to capture the hydro-geological processes on site certain gaps are still found. If an incremental stream and rainfall sampler is installed samples can be taken during and following each rainfall event, as it is during these events when the interaction between the surface water and groundwater are at their highest. These samples can then be tested for isotopes (for example: oxygen 18 and deuterium) with major/minor constituents (for example: chloride, magnesium, silicon, sodium etc.). This will aid in the interpretation of the groundwater movement, as well as enabling the use of more methods.

Boreholes that indicated leakage or faulty construction should be fixed, as proper interpretation of the data cannot be obtained when inaccurate data is measured. If this is not properly fixed one would be unable to tell whether two aquifers are present within the study site.

More boreholes should be drilled further away from the river, so as to obtain the movement of groundwater on a more regional scale. A better hydraulic gradient interpretation can therefore be achieved and data can be obtained of the water level fluctuations during rainfall events without any interference from the river.

The top of the Mahale weir should be smoothed out with cement to provide an even surface for the water to flow over. The overflow of the weir can then be measured during high flow events. A V-notch should also be installed that can be used for the accurate measurement of flow during low flow periods. This will aid in the calculations of a mass balance between the weirs. Accurate measurements of the farmers abstracting

from the river should also be confirmed ultimately aiding in the mass balance construction.

Future research should include a numerical model (Modflow, Feflow etc.), of the study site. This will enable the prediction of future scenarios of various input and output factors for example: over abstraction, transmission losses, high flow event, extreme droughts etc. This will provide important information for management of catchments in semi-arid regions and can thus be applied to similar environmental settings.

Because of the location of the study site that stretches over a farm area and two reserves, it provides the ideal setting for further research in the comparison between these two settings. For instance: the influence of agricultural activities on the groundwater, surface water and ultimately the ecological reserve flows.

Further research can also be done in terms of geology, as two types of dykes were intersected (dolerite, basalt) during the drilling program. Dykes play a large role in groundwater movement especially on this specific study site where multiple dykes are observed. The basalt dykes indicated more fracturing during drilling, thus indicating that groundwater movement might be more associated with basalt dykes than dolerite dyke. This will ultimately result in better interpretation of the groundwater movement.

7.3 RECOMMENDATIONS FOR MANAGEMENT

This study has indicated that it is irrational to study and manage groundwater and surface water resources separately. It also indicated the complexity of the interaction between these two resources. A lack in understanding the connection will most certainly lead to ineffective and unsustainable management of these resources. When over abstraction of the aquifer, damming/rerouting or contamination occurs the impact on this complex system can be devastating. Therefore, it is recommended that more strict regulations are implemented on surface water and groundwater management to ultimately protect and provide sustainable development for both resources, as well as still providing downstream water users with adequate amount of water supply and sustaining the environmental flow requirements of the Groot Letaba River. Further research on this subject is highly recommended, as this study has indicated the complexity of this interaction and the assumptions associated with the current research techniques, thus further research is crucial to fully understand these processes.

REFERENCES

- Adams, S., Titus, R. and Xu, Y. (2004). Groundwater recharge assessment of the Basement aquifers of the central Namaqualand. WRC Report. No.1093/1/041.
- AGWF (Australian Government Water for the Future). (2012). Methods for estimating groundwater discharge to streams – summary of field trials. The Australian Government - Water for the Future - Water Smart Australia program.
- Basak, N. N. (2007). Irrigation Engineering. © 1999 Tata McGraw-Hill Publishing Company Limited. ISBN 0-07-463538.
- Becker, M.W., Georgian, T., Ambrose, H., Siniscalchi, J., and Fredrick, K. (2004). Estimating flow and flux of groundwater discharge using water temperature and velocity. *Journal of Hydrology* 296 (1–4), 221–233. doi:10.1016/j.jhydrol.2004.03.025.
- Bencala, K. E. And Walters, R. A. (1983). Simulation of Solute Transport in a Mountain Pool-and-Riffle Stream: A Transient Storage Model, *Water Resour. Res.*, 19(3), 718–724.
- Bouwer, H. and Rice, R. C. (1976). A Slug Test for Determining Hydraulic Conductivity of Unconfined Aquifers with Completely or Partially Penetrating Wells. *Water Resources Research*, vol 12 no.3, pp. 423-428.
- Freeze, R. A. and Cherry, J. A. (1979). *Groundwater*, Prentice Hall Inc., Upper Saddle River. Eaglewood Cliffs, NJ.
- Carter, R. W. and Davidian, J. (1968). General procedures for gaging streams, U.S. Geol. Surv. *Techniques of Water Resources Investigations*, Book 3, Chapter A-6.
- Conant, B. (2004). Delineating and quantifying ground water discharge zones using streambed temperatures, *Ground Water*, 42(2), 243– 257.
- Cook, P. G. and Herczeg, A. L. (Eds) (2000). *Environmental tracers in subsurface hydrology*, Kluwer, Boston.

- Cullum, C. and Rogers, K. H. (2011). A framework for the classification of drainage networks in savanna landscapes. Water Research Commission Report No K5/1790.
- Darcy, H. (1856). The Public Fountains of the City of Dijon, Dalmont, Paris.
- Davie, T. (2002). Fundamentals of Hydrology, Routledge, New York.
- Department of Water Affairs. (2006a). Groundwater reserve determination studies in the Letaba catchment, project 2005/018. Report 102197/G2.
- Department of Water Affairs. (2006b). The Groundwater Dictionary. A Comprehensive Reference of Groundwater Related Terminology. Second Edition.
- Department of Water Affairs and Forestry (1999). Water resources protection policy implementation. Integrated manual. Report N/28/99.
- Department of Water Affairs and Forestry (2004). Groundwater Protection - Involving Community Members in a Hydrocensus. Toolkit for water services: Number 3.1.
- Du Toit, W. H. (1998). 2330 Phalaborwa 1:500 000 Hydrogeological map series of the Republic of South Africa.
- Dyson, M., Bergkamp, G. and Scanlon, J. (eds). (2003). The Essentials of Environmental Flows. IUCN, Gland, Switzerland and Cambridge, UK. xiv + 118 pp.
- EPA. (2000). Proceedings of the Ground-Water/Surface-Water Interactions Workshop. United States Environmental Protection Agency. EPA/542/R-00/007.
- Freeze, R. A. and Cherry, J. A. (1979). Groundwater, Prentice Hall Inc., Upper Saddle River.
- Gokool, S., Riddell, E. S., Strydom, T., Jarman, C., Nel, J. M. and Swemmer, A. (2015). Quantification of transmission processes along the Letaba River for improved delivery of environmental water requirements (Ecological Reserve). Deliverable No. 3: Project K5/2338/1
- Gordon, R. P. (2013). Quantifying groundwater-surface water interactions to improve the outcomes of human activities. Dissertations - ALL. Paper 38.

- Groundwater Resource Directed Measures (GRDM) (2013). v4.0.0.0 software developed by Department of Water Affairs (DWA).
- Halford, K. J. and Mayer, G. C. Problems associated with estimating ground water discharge and recharge from stream-discharge records, *Ground Water*, 38(3), 331–342, 2000.
- Handcock, R. N., Torgersen, C. E., Cherkaurer, K. A., Gillespie, A. R., Tockner, K., Faux, R. N. and Tan, J. (2012). *Thermal Infrared RemoteSensing of Water Temperaturein Riverine Landscapes. Fluvial Remote Sensing for Science and Management, First Edition.* Edited by Patrice E. Carbonneau and HervéPiégay.© 2012 John Wiley and Sons, Ltd. Published 2012 by John Wiley and Sons, Ltd.
- Hawkins, J. W. and Evans, R. S. (2004). Uses of the borehole camera in hydrologic investigations related to coal mining. *Proceedings America Society of Mining and Reclamation*, 2004.
- Hawkins, J. W., Brady, K. B. C., Barnes, S. and Rose, A. W. (1996). Shallow Ground Water Flow in Unmined Regions of the Northern Appalachian Plateau: Part 1. Physical Characteristics, Annual Meeting of the American Society for Surface Mining and Reclamation, Knoxville, TN, May 1996, pp. 42-51.
- Heath, R. C. (1983). *Basic groundwater hydrology: U.S. Geological Survey Water Supply paper 2220.*
- Hinkle, S. R., Duff, J. H., Triska, F. J., Laenen, A., Gates, E. B., Bencala, K. E.,Wentz, D. A. and Silva, S. R. (2001). Linking hyporheic flow and nitrogen cycling near the Willamette River – a large river in Oregon, USA, *J. Hydrol.*, 244(3–4), 157–180.
- Isiorho, S. A. and Meyer, J. H. (1999). The effects of bag type and meter size on seepage meter measurements, *Ground Water*, 37(3), 411– 413.
- Jensen, A. M., Neilson, B. T., Mckee, M. and Chen, Y. Q., (2012). Thermal remote sensing with an autonomous unmanned aerial remotesensing platform for surface stream temperatures. Utah Water Research Laboratory. 8200 Old Main

Hill Logan, UT, USA. Published in: Geoscience and Remote Sensing Symposium (IGARSS), 2012 IEEE International.

Johnson, M. R., Anhaeusser, C. R., and Thomas, R. J. (2006). The Geology of South Africa. Johannesburg: Geological Society of South Africa and Council for Geoscience. Page: 57 - 89.

Kalbus, E. Reinstorf, F. and Schirmer, M. (2006). Measuring methods for groundwater – surface water interactions: a review. *Hydrol. Earth Syst. Sci.*, 10, 873–887.

Kalbus, E., Schmidt, C., Reinstorf, F., Krieg, R. and Schirmer, M. (2008). How streambed temperatures can contribute to the determination of aquifer heterogeneity. *Grundwasser* 13 (2), 91–100.

Kawecki, M. W. (1995). Meaningful interpretation of step-drawdown tests. Hydrology division, Saudi Arabian oil company. Vol 33, No.1-Ground water-January – February 1995.

Kearey, P. Brooks, M. and Hill, I. (2002). An introduction to geophysical exploration. Third edition. Blackwell Science Pty Ltd. p262.

Kendall, C. and Caldwell, E. A. (1998). Fundamentals of Isotope Geochemistry, Isotope Tracers in Catchment Hydrology, edited by: Kendall, C. and McDonnell, J. J., Elsevier Science, Amsterdam.

Kilpatrick, F. A. and Cobb, E. D. (1985). Measurement of discharge using tracers, U.S. Geol. Surv., Techniques of Water-Resources Investigations, Book 3, Chapter A-16.

Kilpatrick, F. A. and Schneider, V. R. (1983). Use of flumes in measuring discharge, U.S. Geol. Surv., Techniques of Water-Resources Investigations, Book 3, Chapter A-14.

Kruseman, G. P. and de Ridder, N. A., (1994). Analysis and evaluation of pumping test data. Second edition. International institute for land reclamation and improvement, Wageningen. ILRI Publication 47.

Kresic, N. (2007). Hydrogeology and groundwater modelling. 2nd edition. CRC press. Taylor and Francis group, LLC.

- Landon, M. K., Rus, D. L. and Harvey, F. E. (2001). Comparison of instream methods for measuring hydraulic conductivity in sandy streambeds, *Ground Water*, 39(6), 870–885.
- Levy, J. (2011). Review: groundwater management and groundwater/surface-water interaction in the context of South African water policy. *Hydrogeology journal*, 20: 205–226.
- Mace, R. E., Austin, B., Edward, A. S. and Batchelder, R. (2007). Surface water and groundwater—together again? State Bar of Texas 8th annual changing face of water rights in Texas.
- Mack, T. J., Johnson C. D. and J. W. Lane. (1998). Geophysical Characterization of a High-Yield, Fractured-Bedrock Well. Seabrook, New Hampshire, U.S. Geological Survey, Open-File Report 98-176, 22 p.
- Madlala, T. E. (2015). Determination of groundwater-surface water interaction, upper Berg River catchment, South Africa (Masters Thesis). Department of Earth Sciences, Faculty of Sciences, University of the Western Cape.
- Mchalski, A. (1989). Application of Temperature and Electrical Conductivity Logging in Ground Water Monitoring. Whitman Companies Inc.
- Molle, F., Wester., P. and Hirsch, P. (2010). River basin closure: Processes, implications and responses. *Agricultural Water Management* 97. 569-577.
- Moss, R. Jr. and Moss, G. E. (1989). Handbook of Ground Water Development. Roscoe moss company, Los Angeles.
- Murdoch, L. C. and Kelly, S. E. (2003). Factors affecting the performance of conventional seepage meters, *Water Resour. Res.*, 39(6), 1163, doi:10.1029/2002WR001347, 2003.
- National Geo-Spatial Information. 2331CA Mbaula Topographic map series of the Republic of South Africa.
- Nonner, J. C. (2003). Introduction to Hydrogeology. Swets and Zeitlinger B.V., Lisse. ISBN 90 265 1869 2, ISBN 90 265 1930 3.

- Ochoa, C. G., Fernald, A. G., Guldán, S. J., Tidwell, V. C., and Shukla, M. K. (2013). Shallow aquifer recharge from irrigation in a semi-arid agricultural valley in New Mexico, *J. Hydrologic Engineering*, 18, 1219–1230, 2013a.
- Pollard, S. and du Toit, D. (2011). Towards Adaptive Integrated Water Resources Management in Southern Africa: The Role of Self-organisation and Multi-scale Feedbacks for Learning and Responsiveness in the Letaba and Crocodile Catchments *Water resources management*, Volume 25, Issue 15, pp 4019-4035.
- Ransley, T., Tottenham, R., Baskaran, S. and Brodie, R. (2007). Development of method to map potential stream-aquifer connectivity: a case study in the Border Rivers Catchment. Bureau of Rural Sciences, Canberra.
- Riddell, E. S. Nel, J. Fundisi, D. Jumbi, F. van Niekerk, A. and Lorentz, S.A. (2014). Ephemeral Hydrological Processes in Savannas. Water Research Commission Report No. TT 619/14.
- Riddell, E. S., Gokool, S., Raubenheimer, R., Strydom, T., Nel, J. M., Jarman, C. and Swemmer, A. (2016). Quantification of transmission loss processes along the Letaba River. WRC Report No. K5/2338/1. Deliverable 6.
- Riddell, E. S., Peterson, R., van Niekerk, A., Fundisi, D., Nel, J., Thibela, D. L. (2012). S.A: Surface Water, Groundwater and Vadose Zone Interactions in Selected Pristine Catchments on the Kruger National Park. WRC Progress Report 3 - Report on conceptual model development for southern and northern Supersites in KNP, K5/2051.
- Roux, A. T. Biesheuvel, K., Corner, B., Goddard, P. (1980). Geophysical field manual for technicians. No.1 The magnetic method. South African Geophysical Association (SAGA).
- Runkel, R. L., McKnight, D. M., and Rajaram, H. (2003). Modeling hyporheic zone processes, *Adv. Water Resour.*, 26(9), 901–905.
- Saayman, I., Colvin, C., Weaver, J., Fraser, L., Zhang, J., Hughes, S., Tredoux, G., Höhn, A., Le Maitre, D., Rusinga, F., and Israel, S. (2004). Interactions between groundwater and surface water: assessment of the Langebaan lagoon as a study area. Division of Water, Environment and Forestry Technology, CSIR.

- Seago, C. Hattingh, L. C. Mwaka, B. Cai, R. and Botha, F. (2007). Surface/groundwater interaction: Using water balancing, hydraulic modeling and real-time monitoring to develop a truly Integrated Decision Support System (IDSS). Department of Water Affairs and Forestry, Directorate: Water Resource Planning Systems, Pretoria, South Africa.
- Sholkovitz, E., Herbold, C. and Charette, M. (2003). An automated dye-dilution based seepage meter for the timeseries measurement of submarine groundwater discharge. *Limnology Oceanography Methods*, 1, 14-28.
- Schmidt, C., Bayer-Raich, M., and Schirmer, M. (2006). Characterization of spatial heterogeneity of groundwater-stream water interactions using multiple depth streambed temperature measurements at the reach scale. *Hydrol. Earth Syst. Sci.*, 10, 849–859, 2006, <http://www.hydrol-earth-syst-sci.net/10/849/2006/>.
- Shepherd, R. G. (1989). Correlations of Permeability and Grain-Size, *Ground Water*, 27(5), 633–638.
- Sophocleous, M. (2002). Interactions between groundwater and surface water: the state of the science. *Hydrogeology Journal* (2002) 10:52-67.
- Spane, Jr. F. A. and Vermeul, V. R. (1994). Summary and evaluation of hydraulic property data available for the Hanford site upper basalt confined aquifer system. U.S. Department of Energy under contract DE-AC06-76RLO 1830.
- Strydom, T., Riddell, E. S., Swemmer, A., Nel, J. M. and Jarman, C. (2014). Quantification of transmission processes along the Letaba River for improved delivery of environmental water requirements (Ecological Reserve). Deliverable No. 1: Project K5/2338/1.
- Swarzenski, P. W., Reich, C. D., Spechler, R. M., Kindinger, J. L. and Moore, W. S. (2001). Using multiple geochemical tracers to characterise the hydrogeology of the submarine spring of Crescent Beach, Florida. *Journal of Chemical Geology*, 179, 187-202.
- Tanner, J. L. (2013). Understanding and modelling of surface and groundwater interactions. (PhD dissertation) Rhodes University.

- Todd, D. K., Mays, L. W. (2005). *Groundwater Hydrology*, Wiley, Hoboken.
- Tetzlaff, D., Carey, S. K., Laudon, H. and McGuire, K. (2010). Catchment processes and heterogeneity at multiple scales benchmarking observations, conceptualisation and prediction. *Hydrol. Process.* 24, 2203–2208.
- Van Niekerk, A. (2014). A spatial-temporal conceptualization of groundwater flow distribution in a granite fractured rock aquifer within the southern supersite research catchment of the Kruger National Park. Dissertation submitted to the University of the Western Cape (South Africa), in the fulfilment of the degree of Master of Science.
- Van Tonder, G. J. and Vermeulen, D. (2005). The applicability of slug tests in fractured-rock formations. *Water SA* vol. 31 no. 2 pp. 157-160.
- Van Zijl J. S. V. (1985). *A Practical Manual on the Resistivity Method*. CSIR report K79.
- Wenninger, J., Uhlenbrook, S., Lorentz, S. and Leibundgut, C. H. (2008). Identification of runoff generation processes using combined hydrometric, tracer and geophysical methods in a headwater catchment in South Africa. *Hydrological Sciences Journal*, 53 (1): 65-80.
- Winter, T. C., Harvey, J. W., Franke, O. L and Alley, W. M. (1998). *Groundwater and Surface water a single resource*. US Geological survey circulation 1139 ISBN 0–607–89339–7.
- www.idc-online.com, (2017). Hydrogen and its components. [Http://http://www.idc-online.com/technical_references/pdfs/chemical_engineering/Hydrogen_and_its_components.pdf](http://www.idc-online.com/technical_references/pdfs/chemical_engineering/Hydrogen_and_its_components.pdf). Date accessed: 02/12/2017.
- www.geotron.co.za, (2017). Geotron model g5 proton memory magnetometer. www.geotron.co.za/mmeter.htm. Date accessed: 31/12/2017.
- www.southafricatoursandtravel.com, (2017). Interactive map of South Africa, its provinces and its major cities <https://www.south-africa-tours-and-travel.com/map-of-south-africa.html>. Date accessed: 31/12/2017.

APPENDIX A



Appendix A-1: ABEM Terrameter that was used for the geophysical survey (Strydom, 2014).



Appendix A-2: The drilling rig is a modified old 10 ton 6x6 SAMIL truck with a super rock 5000 air percussion rig and a 900CFM compressor.



Appendix A-3: An example of a water strike at LF004A.



Appendix A-4: An example of the shallow and deep boreholes drilled at LF004A.



Appendix A-5: Analysis of core log samples.

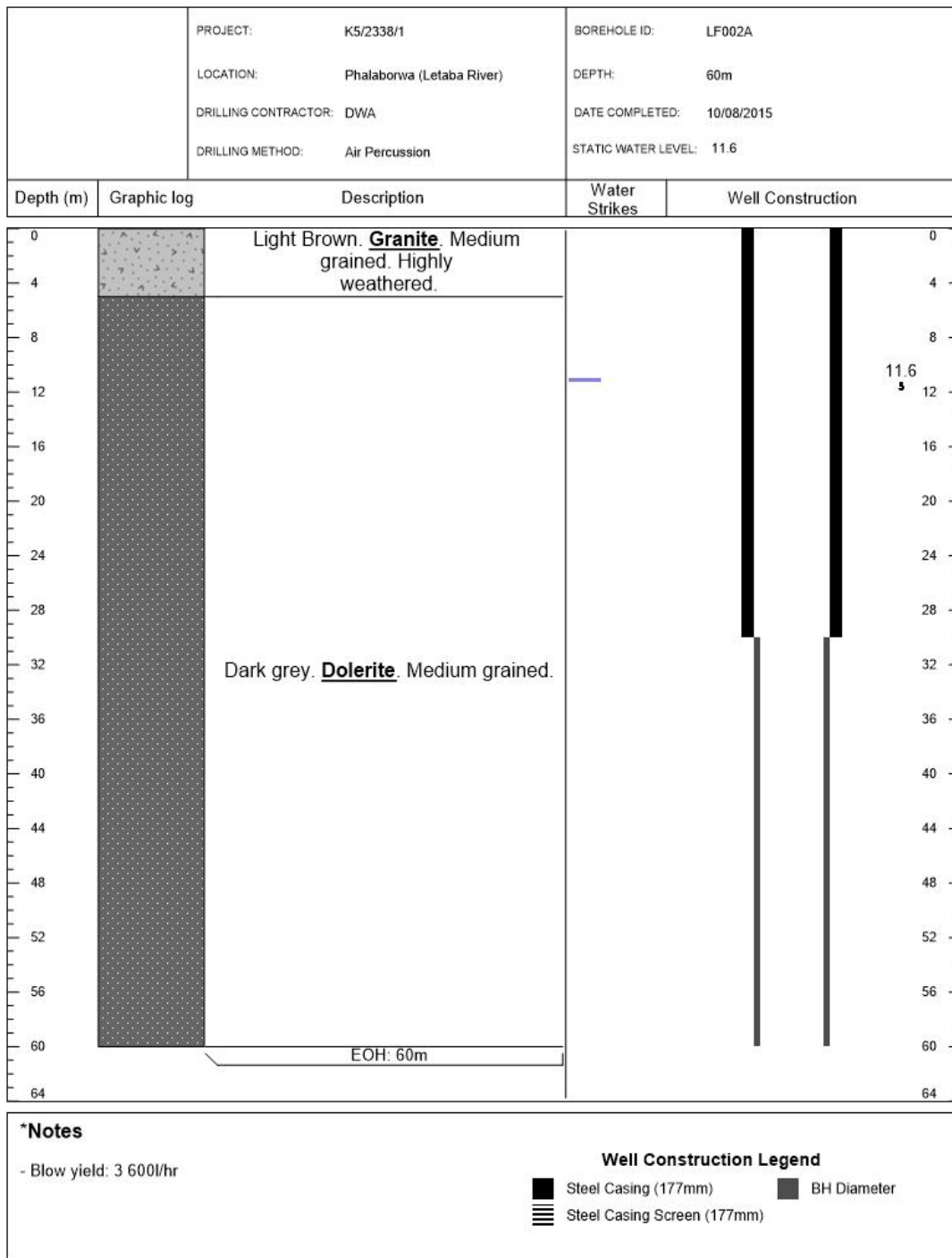


Appendix A-6: Solinst™ TLC dipmeter.



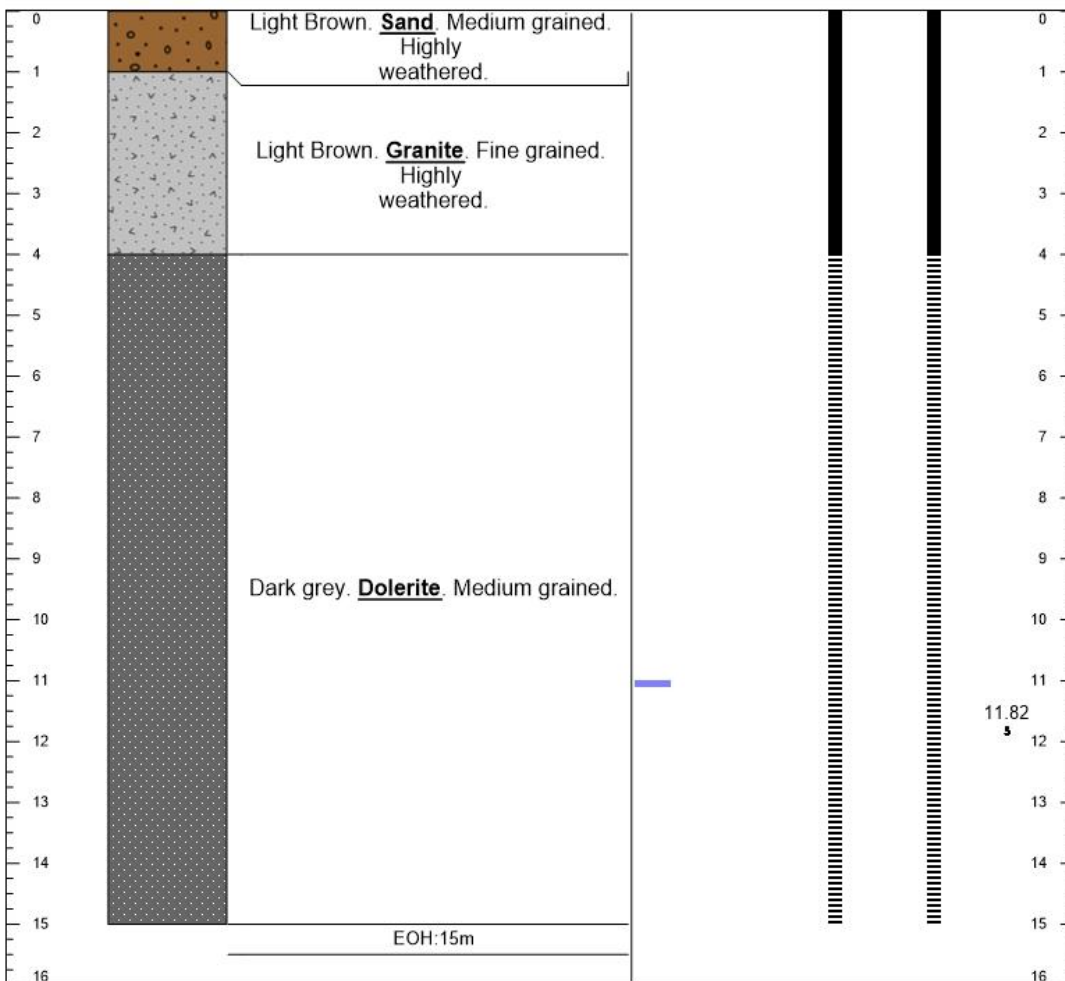
Appendix A-7: Slug used for slug tests.

APPENDIX B



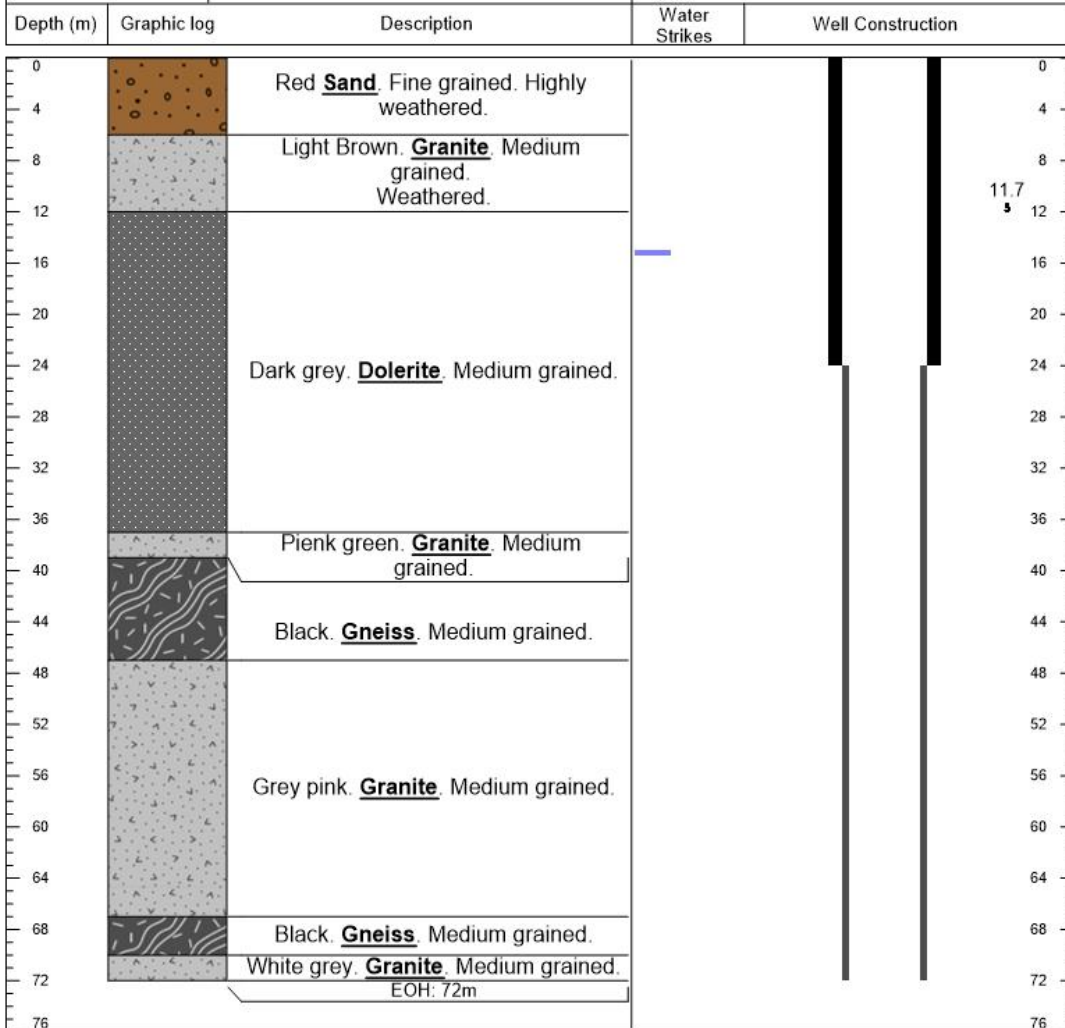
PROJECT:	K5/2338/1	BOREHOLE ID:	LF002B
LOCATION:	Phalaborwa (Letaba River)	DEPTH:	15m
DRILLING CONTRACTOR:	DWA	DATE COMPLETED:	10/09/2015
DRILLING METHOD:	Air Percussion	STATIC WATER LEVEL:	11.82

Depth (m)	Graphic log	Description	Water Strikes	Well Construction
-----------	-------------	-------------	---------------	-------------------



*Notes		Well Construction Legend	
- Blow yield: 1 440l/hr		■ Steel Casing (177mm)	■ BH Diameter
		▨ Steel Casing Screen (177mm)	

PROJECT:	K5/2338/1	BOREHOLE ID:	LF003A
LOCATION:	Phalaborwa (Letaba River)	DEPTH:	72m
DRILLING CONTRACTOR:	DWA	DATE COMPLETED:	09/06/2015
DRILLING METHOD:	Air Percussion	STATIC WATER LEVEL:	11.7



***Notes**

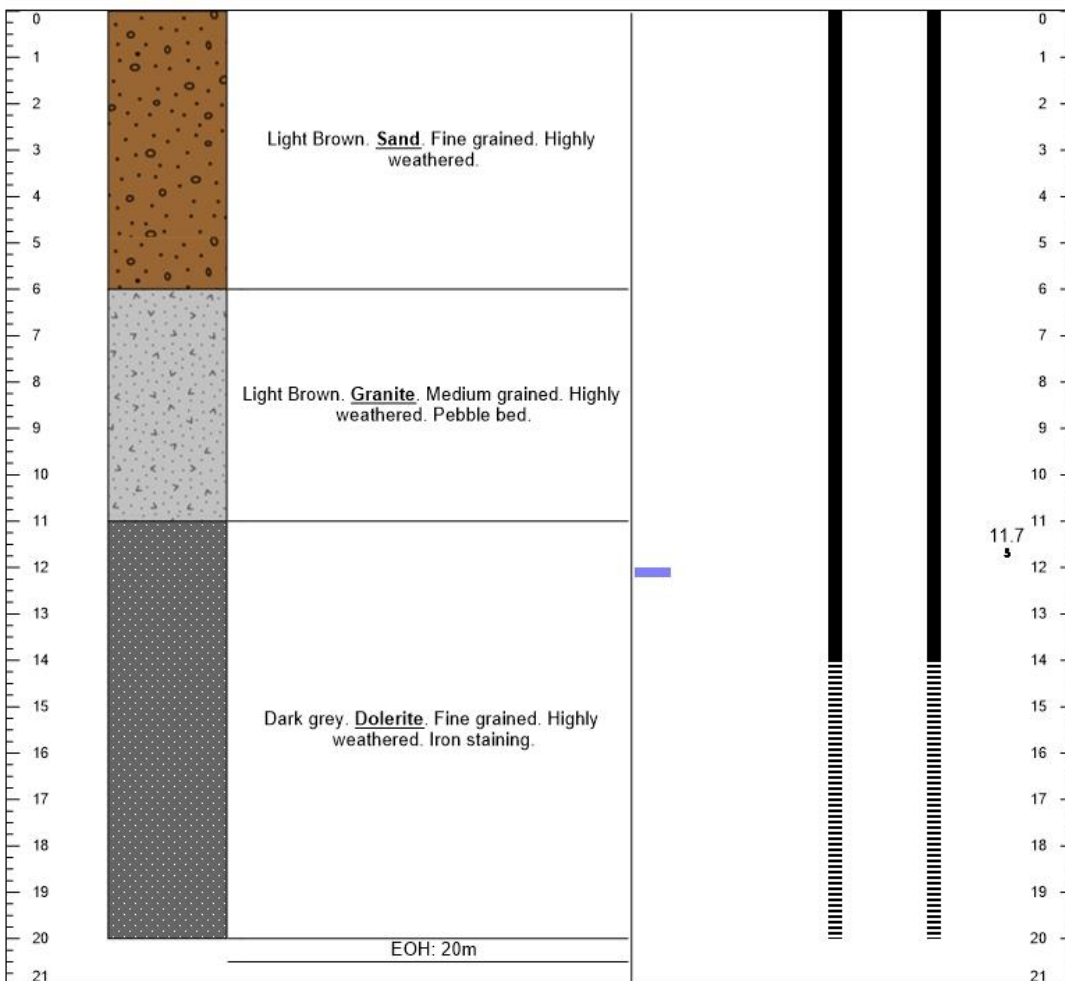
- Blow yield: 1 080l/hr

Well Construction Legend

- Steel Casing (177mm)
- Steel Casing Screen (177mm)
- BH Diameter

PROJECT:	K5/2338/1	BOREHOLE ID:	LF003B
LOCATION:	Phalaborwa (Letaba River)	DEPTH:	20m
DRILLING CONTRACTOR:	DWA	DATE COMPLETED:	01/06/2015
DRILLING METHOD:	Air Percussion	STATIC WATER LEVEL:	11.7

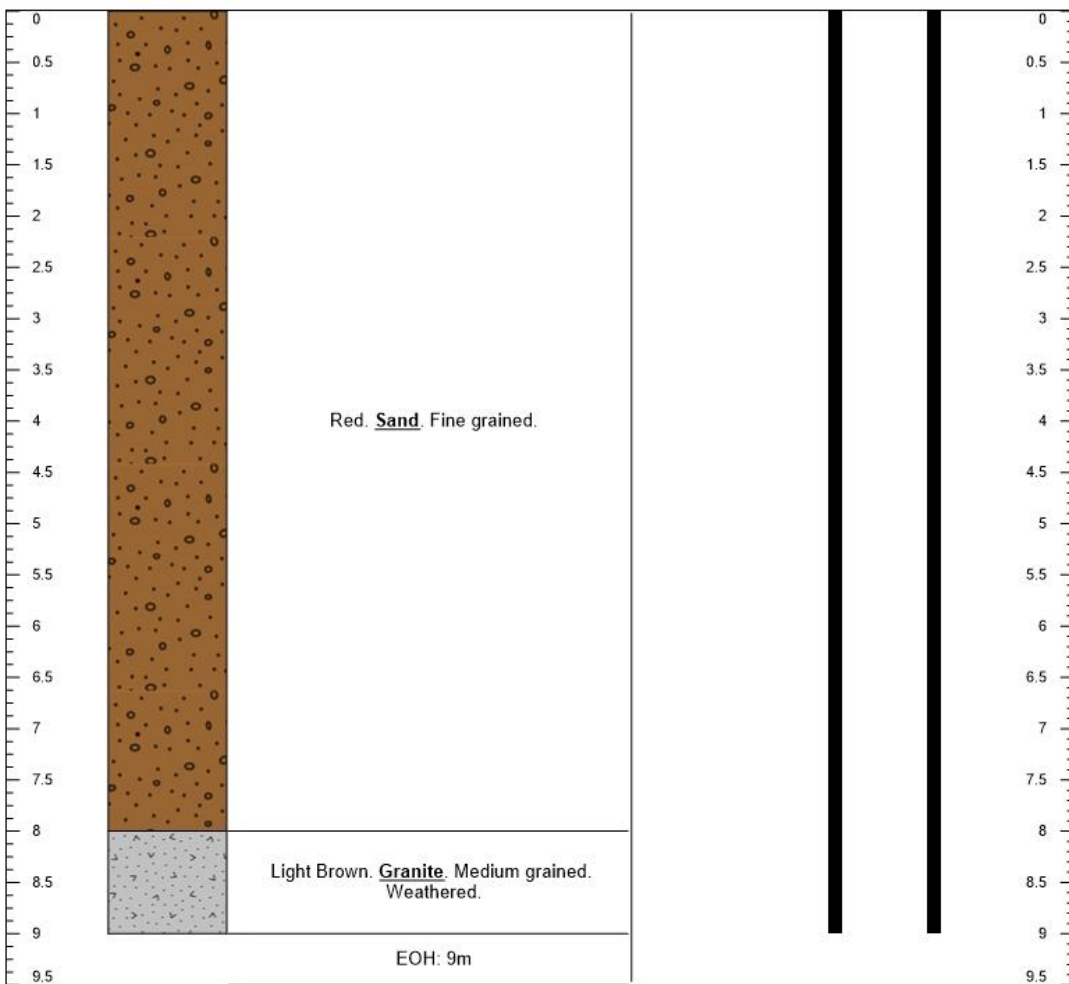
Depth (m)	Graphic log	Description	Water Strikes	Well Construction
-----------	-------------	-------------	---------------	-------------------



*Notes		Well Construction Legend	
- Blow yield: 1 800l/hr		■ Steel Casing (177mm)	■ BH Diameter
		▬ Steel Casing Screen (177mm)	

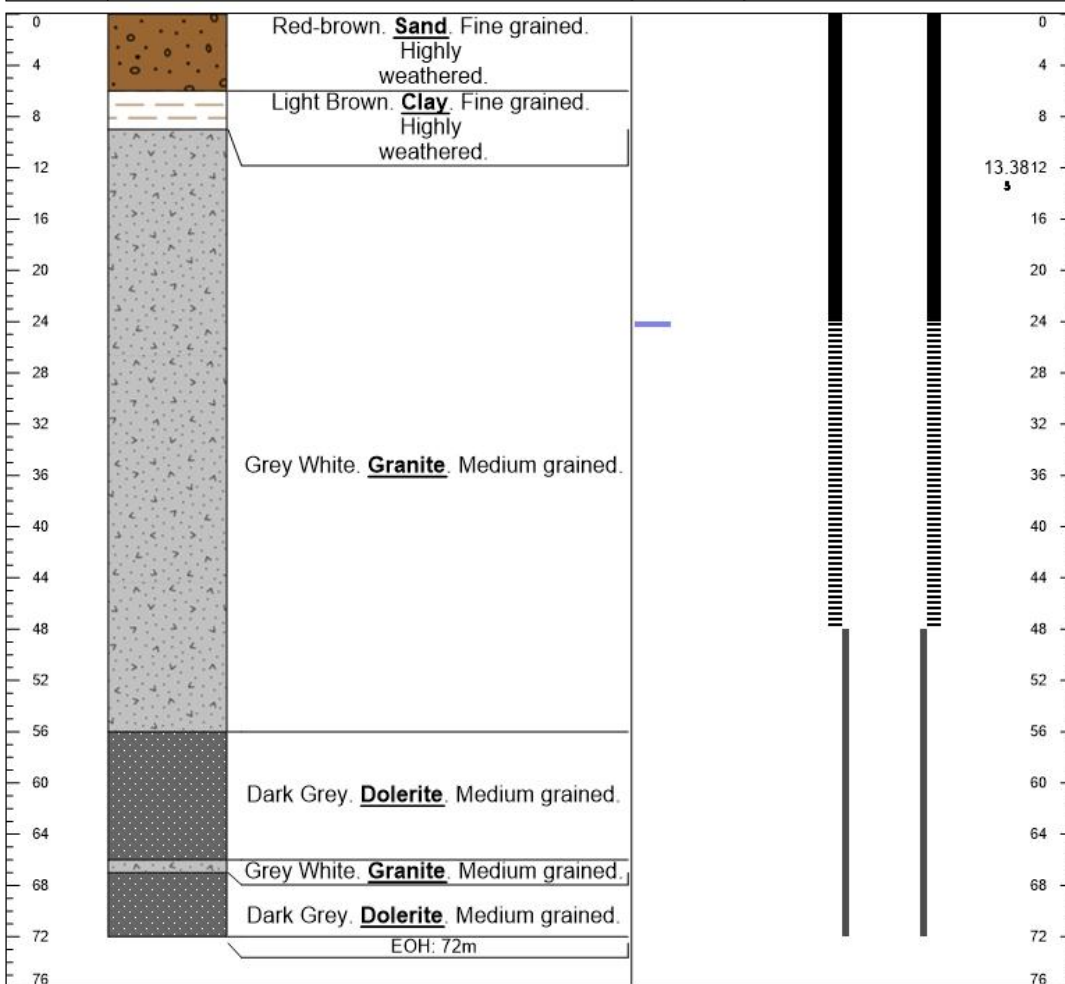
PROJECT:	K5/2338/1	BOREHOLE ID:	LF003C
LOCATION:	Phalaborwa (Letaba River)	DEPTH:	9m
DRILLING CONTRACTOR:	DWA	DATE COMPLETED:	11/06/2015
DRILLING METHOD:	Air Percussion	STATIC WATER LEVEL:	

Depth (m)	Graphic log	Description	Water Strikes	Well Construction
-----------	-------------	-------------	---------------	-------------------



*Notes	Well Construction Legend	
	■ Steel Casing (177mm)	■ BH Diameter
	▬ Steel Casing Screen (177mm)	

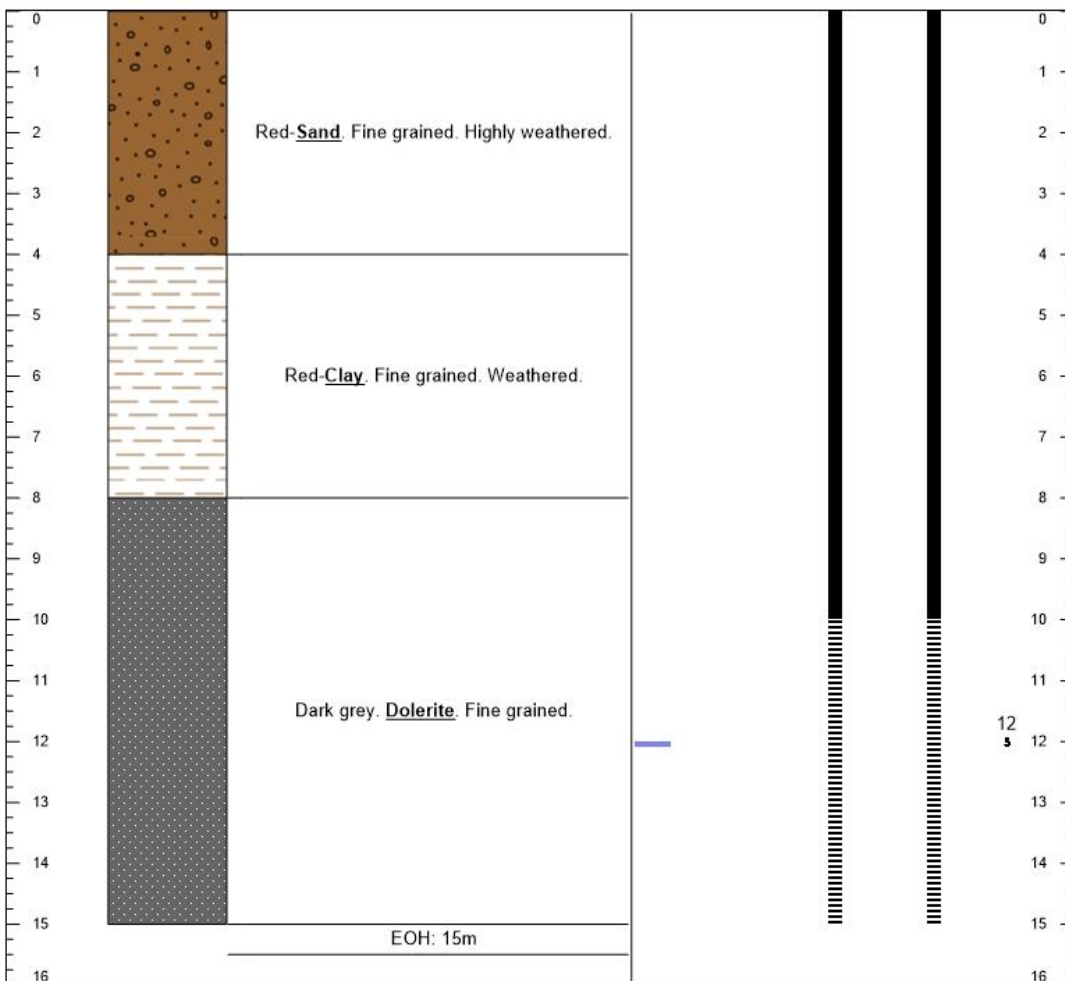
PROJECT: K5/2338/1		BOREHOLE ID: LF004A		
LOCATION: Phalaborwa (Letaba River)		DEPTH: 72m		
DRILLING CONTRACTOR: DWA		DATE COMPLETED: 10/22/2015		
DRILLING METHOD: Air Percussion		STATIC WATER LEVEL: 13.38		
Depth (m)	Graphic log	Description	Water Strikes	Well Construction



*Notes		Well Construction Legend	
- Blow yield: 1 800l/hr		■ Steel Casing (177mm)	■ BH Diameter
		▨ Steel Casing Screen (177mm)	

PROJECT:	K5/2338/1	BOREHOLE ID:	LF004B
LOCATION:	Phalaborwa (Letaba River)	DEPTH:	15m
DRILLING CONTRACTOR:	DWA	DATE COMPLETED:	23/10/2015
DRILLING METHOD:	Air Percussion	STATIC WATER LEVEL:	13.35

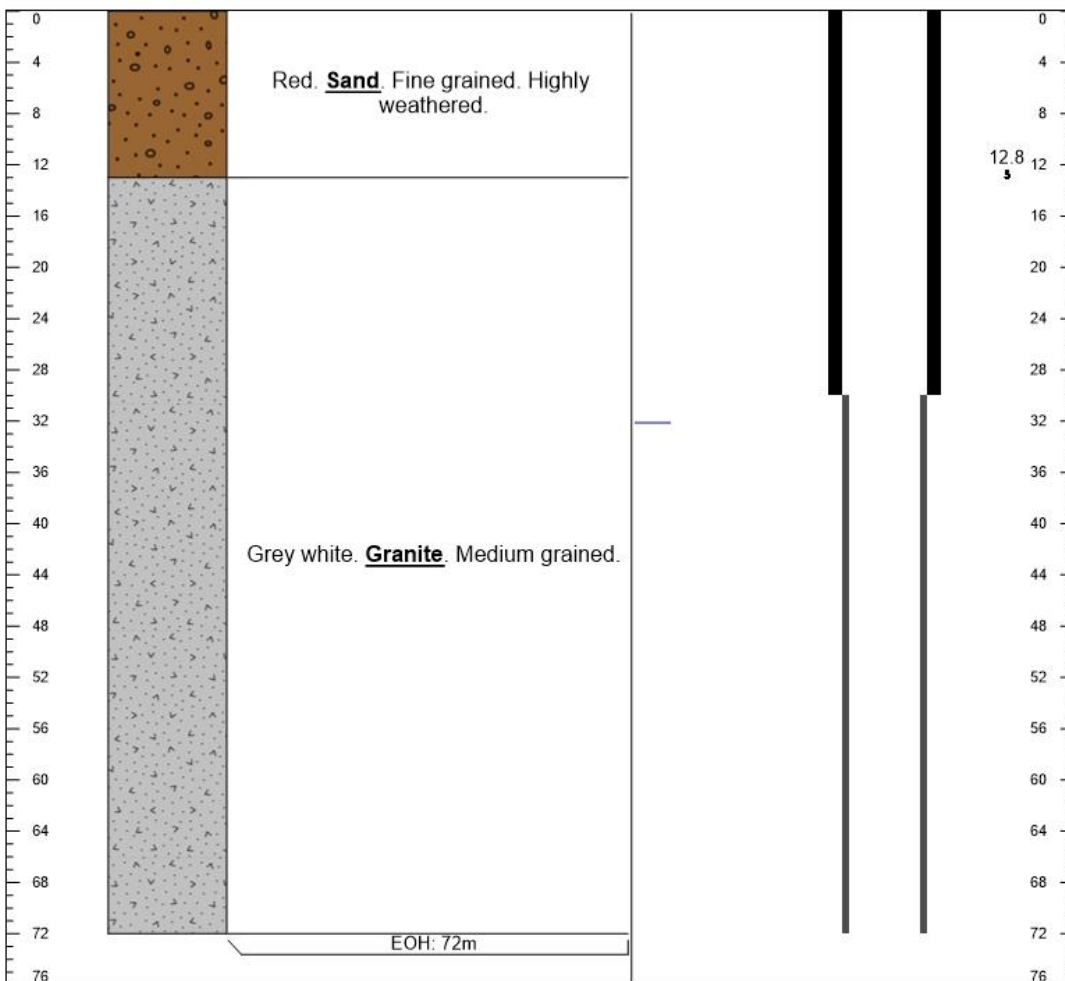
Depth (m)	Graphic log	Description	Water Strikes	Well Construction
-----------	-------------	-------------	---------------	-------------------



*Notes		Well Construction Legend	
- Blow yield: 1 800l/hr		■ Steel Casing (177mm)	■ BH Diameter
		▬ Steel Casing Screen (177mm)	

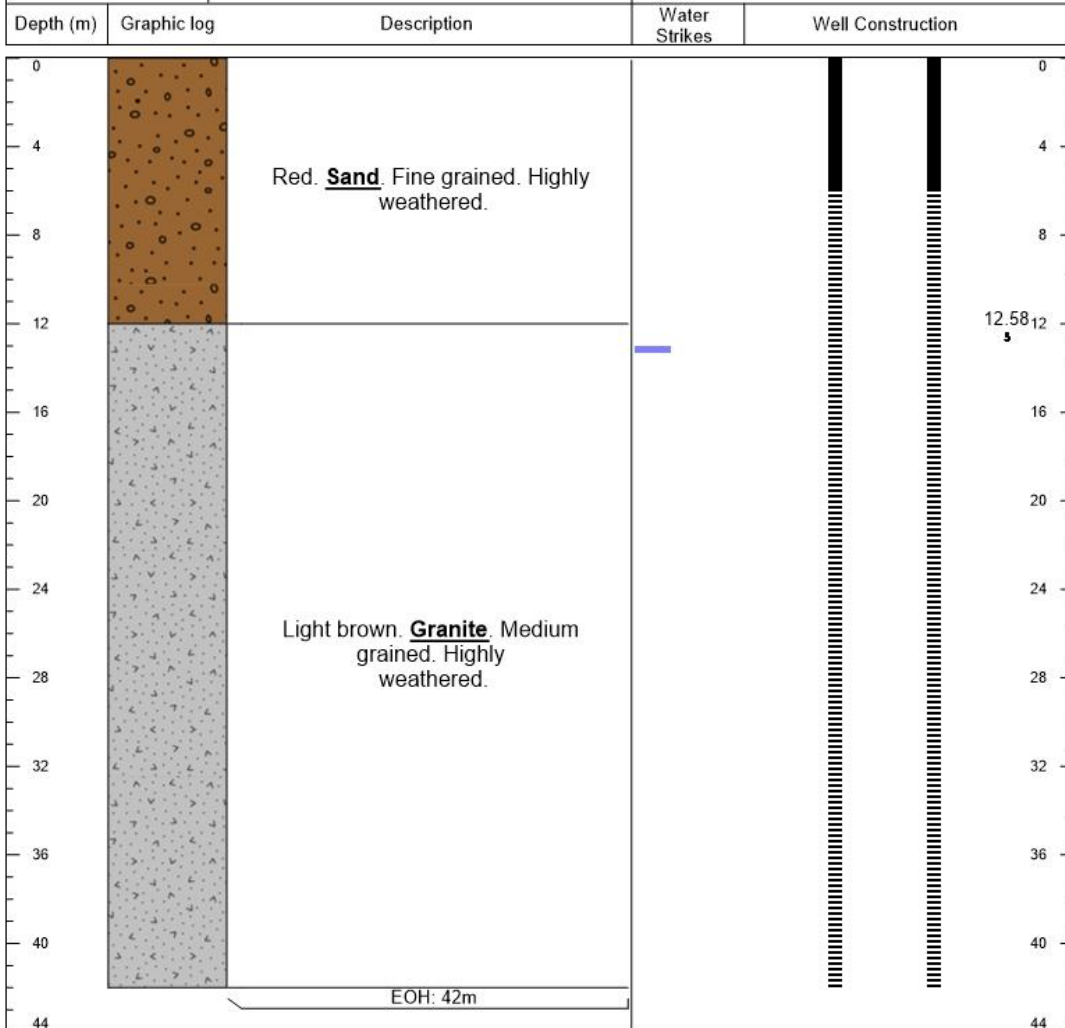
PROJECT:	K5/2338/1	BOREHOLE ID:	LF005A
LOCATION:	Phalaborwa (Letaba River)	DEPTH:	72m
DRILLING CONTRACTOR:	DWA	DATE COMPLETED:	04/06/2015
DRILLING METHOD:	Air Percussion	STATIC WATER LEVEL:	12.8

Depth (m)	Graphic log	Description	Water Strikes	Well Construction
-----------	-------------	-------------	---------------	-------------------



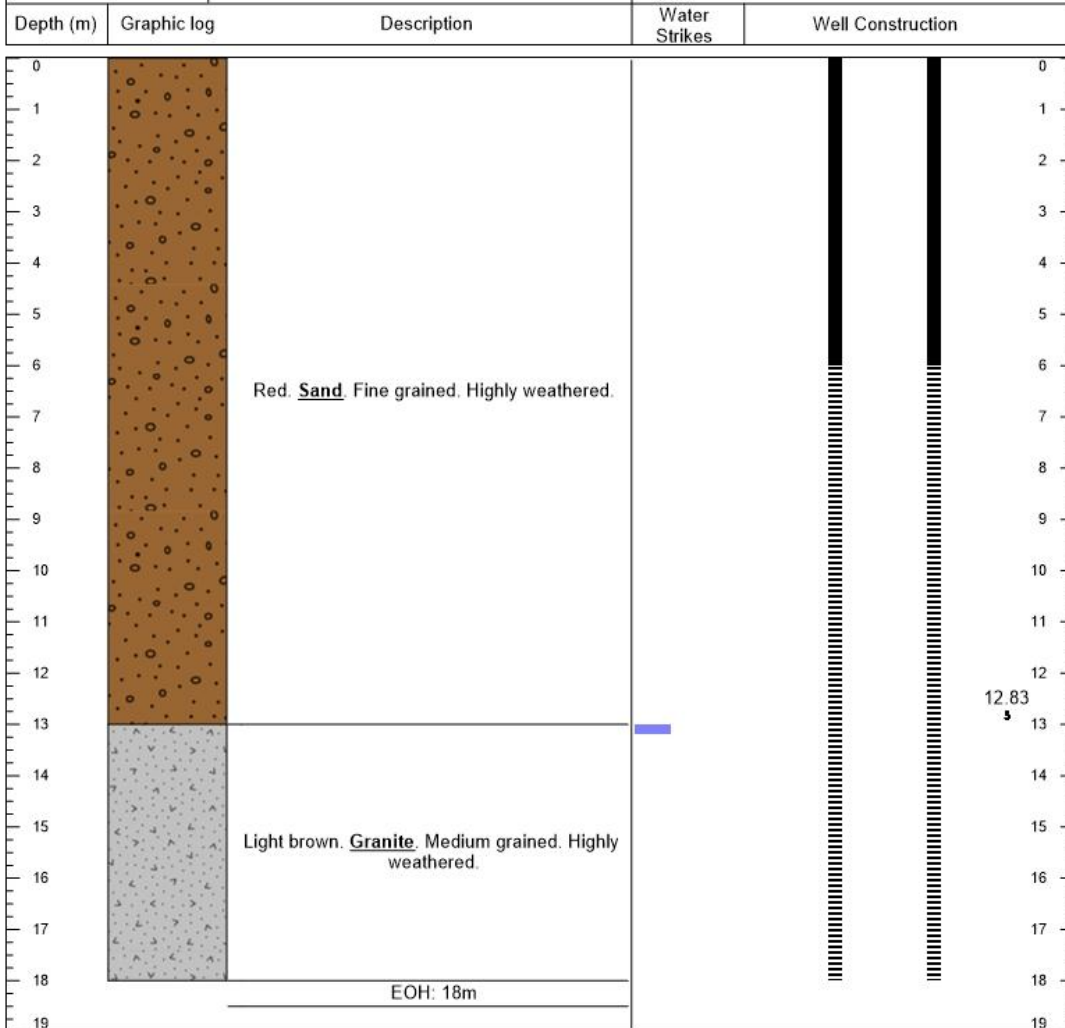
<p>*Notes</p> <p>- Blow yield: 1 800l/hr</p>	<p>Well Construction Legend</p> <p>■ Steel Casing (177mm) ■ BH Diameter</p> <p>▬ Steel Casing Screen (177mm)</p>
---	--

PROJECT:	K5/2338/1	BOREHOLE ID:	LF005B
LOCATION:	Phalaborwa (Letaba River)	DEPTH:	42m
DRILLING CONTRACTOR:	DWA	DATE COMPLETED:	09/06/2015
DRILLING METHOD:	Air Percussion	STATIC WATER LEVEL:	12.58



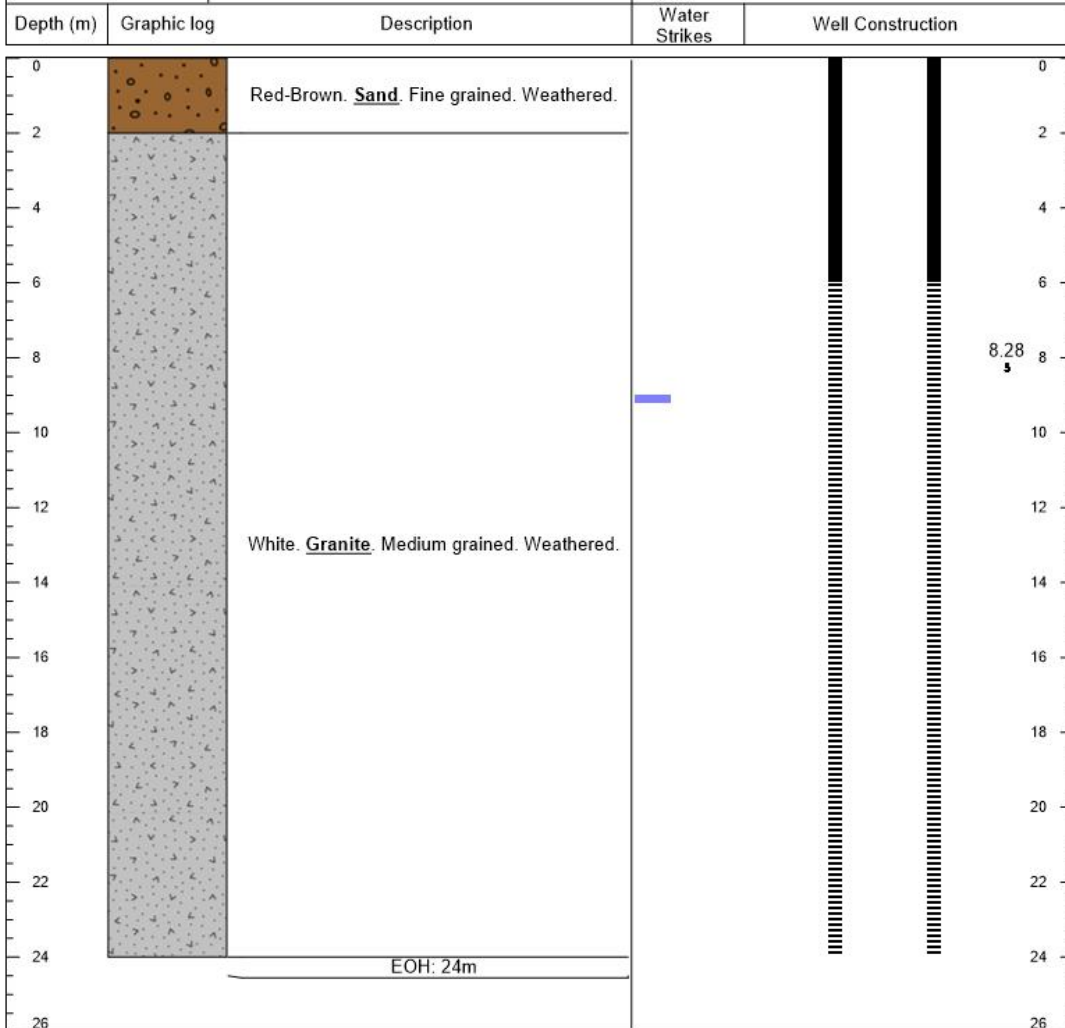
*Notes		Well Construction Legend	
- Blow yield: 1 800l/hr		Steel Casing (177mm)	BH Diameter
		Steel Casing Screen (177mm)	




PROJECT:	K5/2338/1	BOREHOLE ID:	LF005C
LOCATION:	Phalaborwa (Letaba River)	DEPTH:	18m
DRILLING CONTRACTOR:	DWA	DATE COMPLETED:	14/07/2015
DRILLING METHOD:	Air Percussion	STATIC WATER LEVEL:	12.83



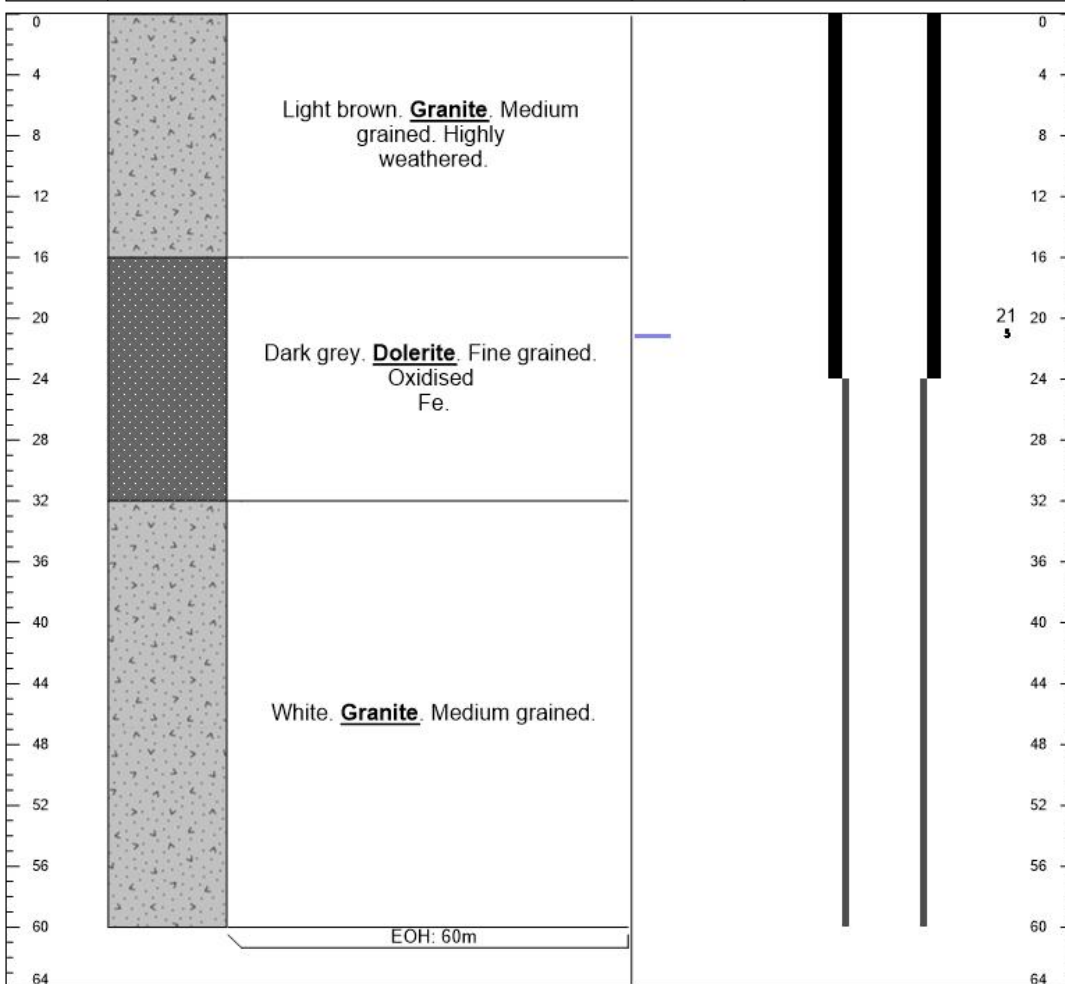
*Notes		Well Construction Legend	
- Blow yield: 1 800l/hr		Steel Casing (177mm)	BH Diameter
		Steel Casing Screen (177mm)	

PROJECT:	K5/2338/1	BOREHOLE ID:	LF0021
LOCATION:	Phalaborwa (Letaba River)	DEPTH:	24m
DRILLING CONTRACTOR:	DWA	DATE COMPLETED:	11/01/2015
DRILLING METHOD:	Air Percussion	STATIC WATER LEVEL:	8.28



*Notes		Well Construction Legend	
- Blow yield: 720l/hr		 Steel Casing (177mm)	 BH Diameter
		 Steel Casing Screen (177mm)	

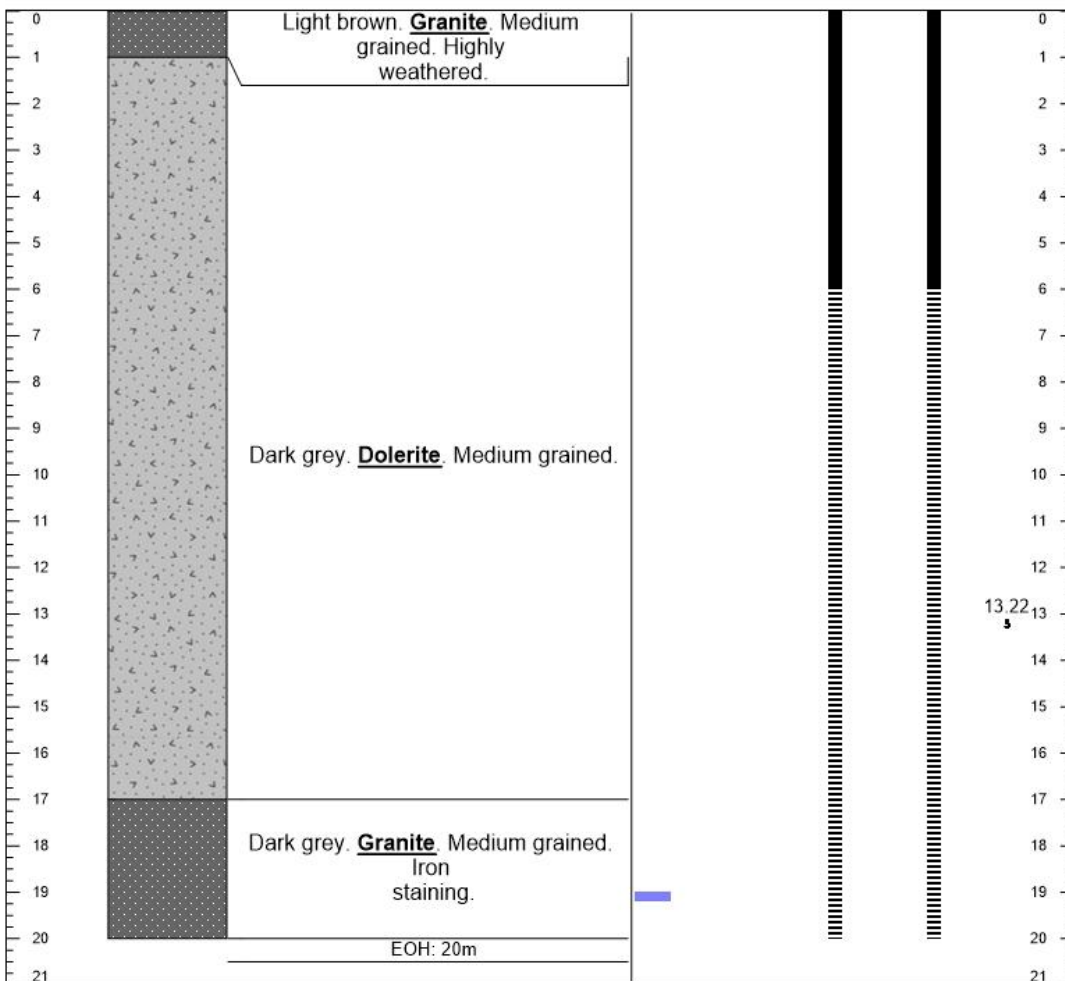
PROJECT: K5/2338/1		BOREHOLE ID: LF0031A	
LOCATION: Phalaborwa (Letaba River)		DEPTH: 60	
DRILLING CONTRACTOR: DWA		DATE COMPLETED: 25/05/2015	
DRILLING METHOD: Air Percussion		STATIC WATER LEVEL: 13.48	



*Notes		Well Construction Legend	
- Blow yield: 10 800l/hr		Steel Casing (177mm)	BH Diameter
		Steel Casing Screen (177mm)	

PROJECT:	K5/2338/1	BOREHOLE ID:	LF0031B
LOCATION:	Phalaborwa (Letaba River)	DEPTH:	20m
DRILLING CONTRACTOR:	DWA	DATE COMPLETED:	
DRILLING METHOD:	Air Percussion	STATIC WATER LEVEL:	12.68

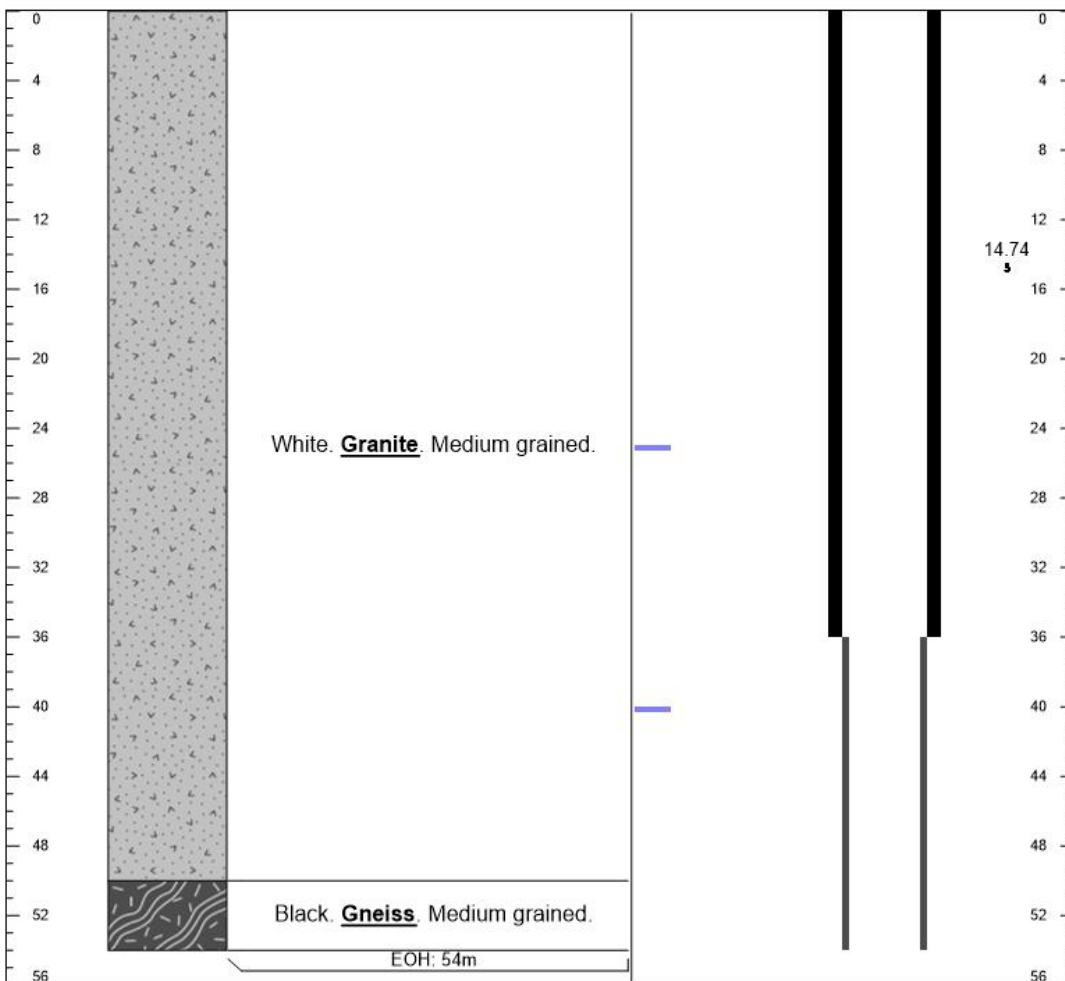
Depth (m)	Graphic log	Description	Water Strikes	Well Construction
-----------	-------------	-------------	---------------	-------------------



*Notes		Well Construction Legend	
- Blow yield: 3 600l/hr		■ Steel Casing (177mm)	■ BH Diameter
		▨ Steel Casing Screen (177mm)	

PROJECT:	K5/2338/1	BOREHOLE ID:	LF0051A
LOCATION:	Phalaborwa (Letaba River)	DEPTH:	54m
DRILLING CONTRACTOR:	DWA	DATE COMPLETED:	11/06/2015
DRILLING METHOD:	Air Percussion	STATIC WATER LEVEL:	14.74

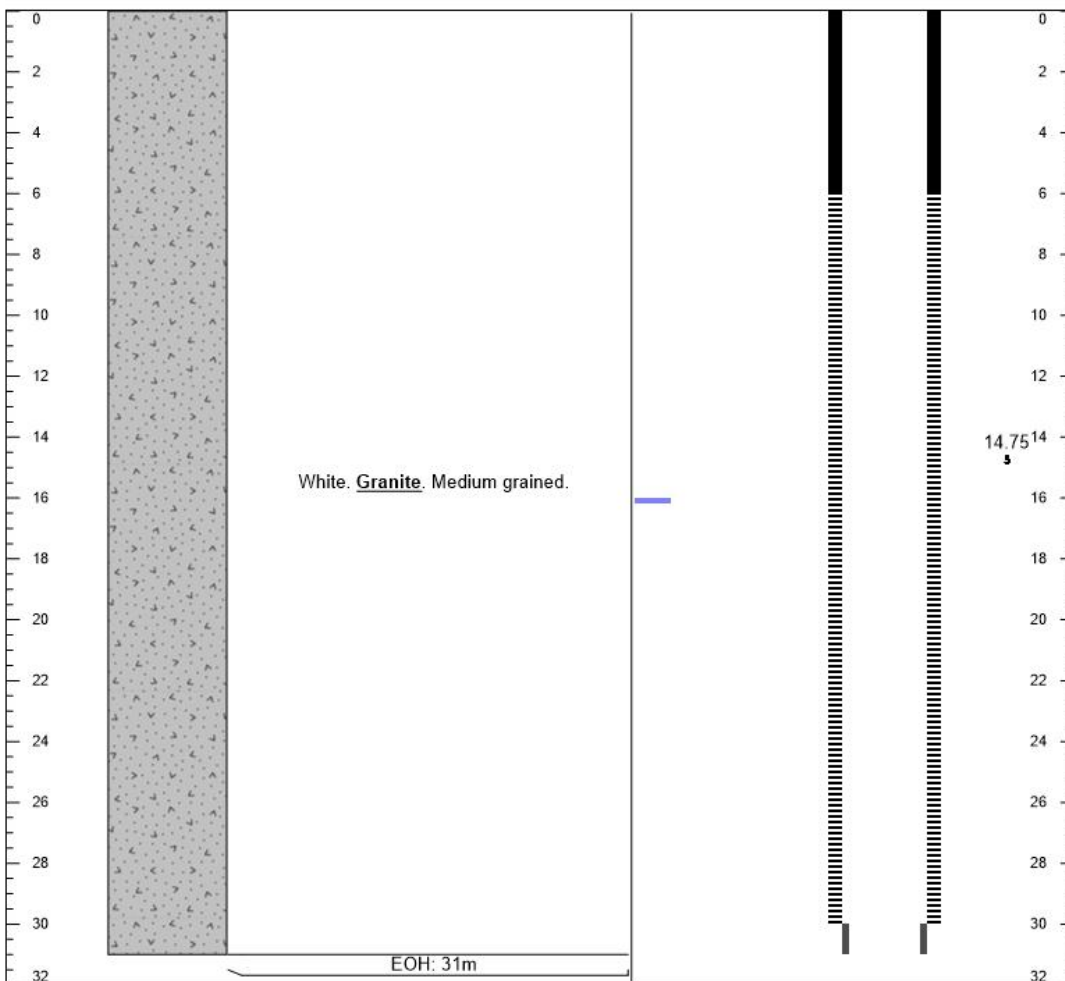
Depth (m)	Graphic log	Description	Water Strikes	Well Construction
-----------	-------------	-------------	---------------	-------------------



*Notes		Well Construction Legend	
- Blow yield: 5 400l/hr		■ Steel Casing (177mm)	■ BH Diameter
		≡ Steel Casing Screen (177mm)	

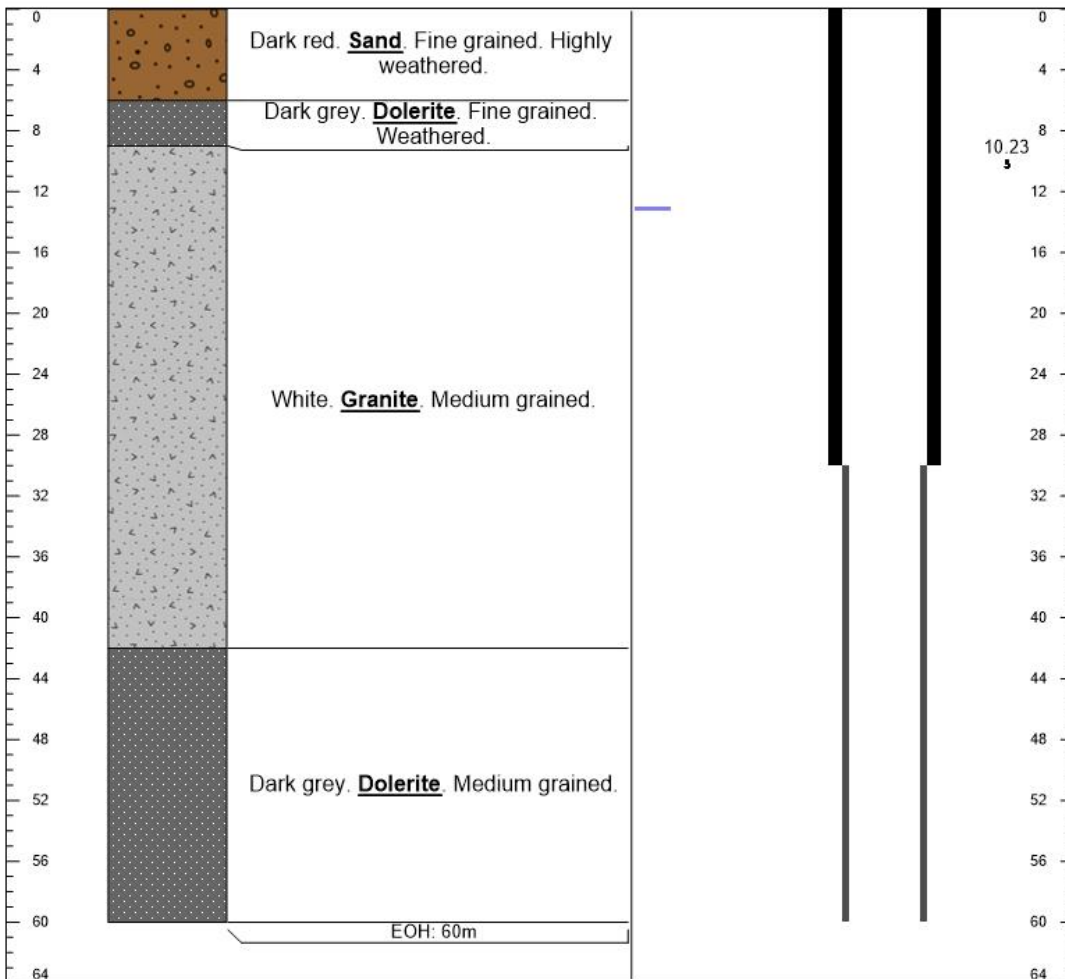
PROJECT:	K5/2338/1	BOREHOLE ID:	LF0051B
LOCATION:	Phalaborwa (Letaba River)	DEPTH:	30m
DRILLING CONTRACTOR:	DWA	DATE COMPLETED:	25/06/2015
DRILLING METHOD:	Air Percussion	STATIC WATER LEVEL:	14.75

Depth (m)	Graphic log	Description	Water Strikes	Well Construction
-----------	-------------	-------------	---------------	-------------------



*Notes		Well Construction Legend	
- Blow yield: 3 600l/hr		■ Steel Casing (177mm)	■ BH Diameter
		▬ Steel Casing Screen (177mm)	

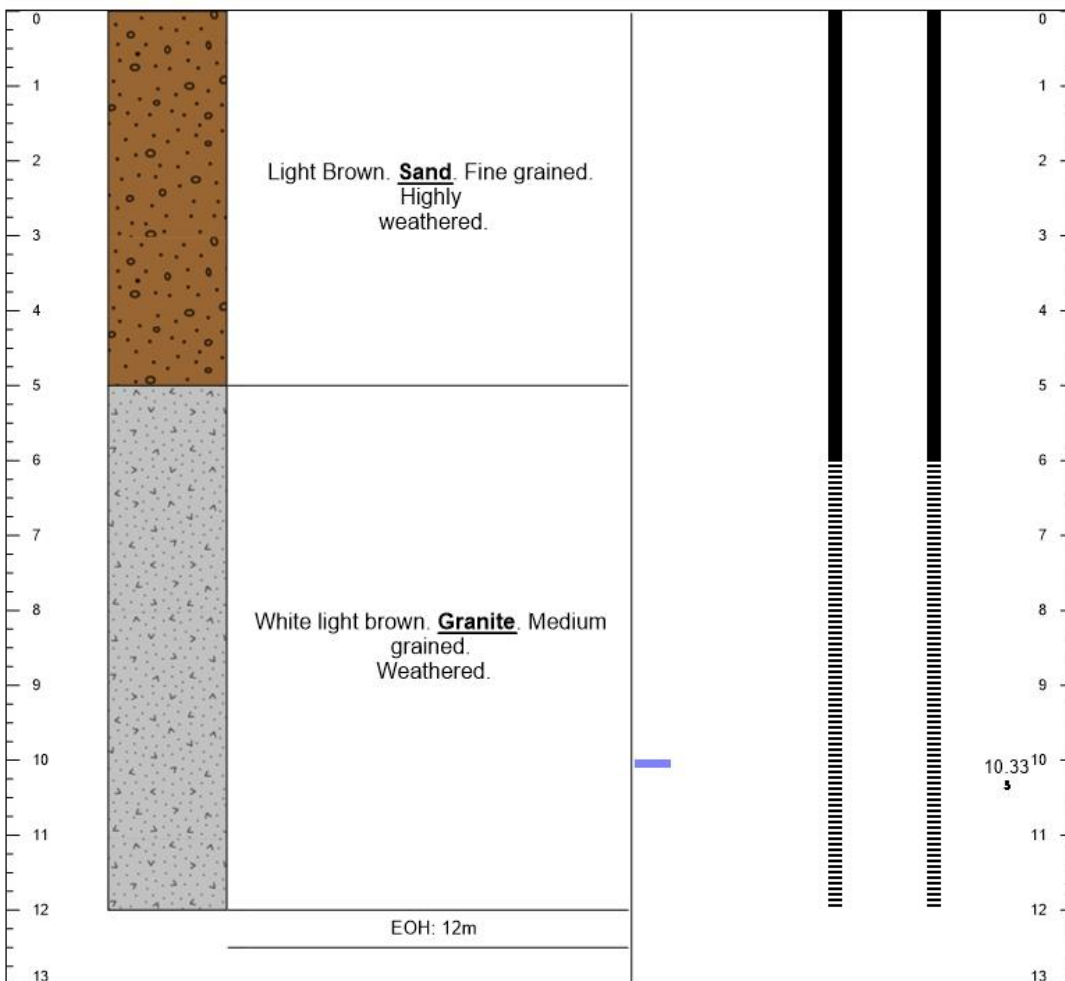
PROJECT: K5/2338/1		BOREHOLE ID: LR001A		
LOCATION: Phalaborwa (Letaba River)		DEPTH: 60m		
DRILLING CONTRACTOR: DWA		DATE COMPLETED: 03/09/2015		
DRILLING METHOD: Air Percussion		STATIC WATER LEVEL: 10.23		
Depth (m)	Graphic log	Description	Water Strikes	Well Construction



*Notes		Well Construction Legend	
- Blow yield: 1 800l/hr		■ Steel Casing (177mm)	■ BH Diameter
		▬ Steel Casing Screen (177mm)	

PROJECT:	K5/2338/1	BOREHOLE ID:	LR001B
LOCATION:	Phalaborwa (Letaba River)	DEPTH:	12m
DRILLING CONTRACTOR:	DWA	DATE COMPLETED:	08/09/2015
DRILLING METHOD:	Air Percussion	STATIC WATER LEVEL:	10.33

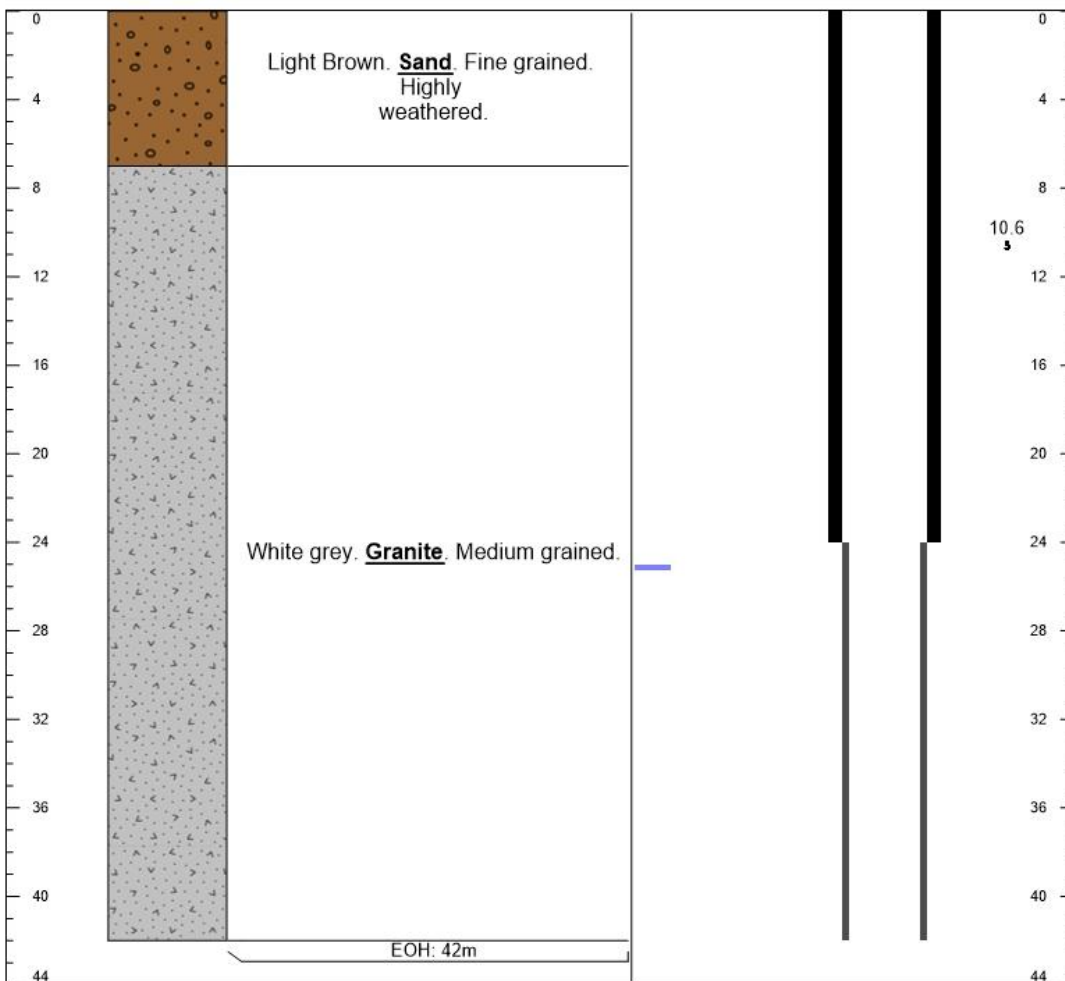
Depth (m)	Graphic log	Description	Water Strikes	Well Construction
-----------	-------------	-------------	---------------	-------------------



*Notes		Well Construction Legend	
- Blow yield: 1 800l/hr		■ Steel Casing (177mm)	■ BH Diameter
		▨ Steel Casing Screen (177mm)	

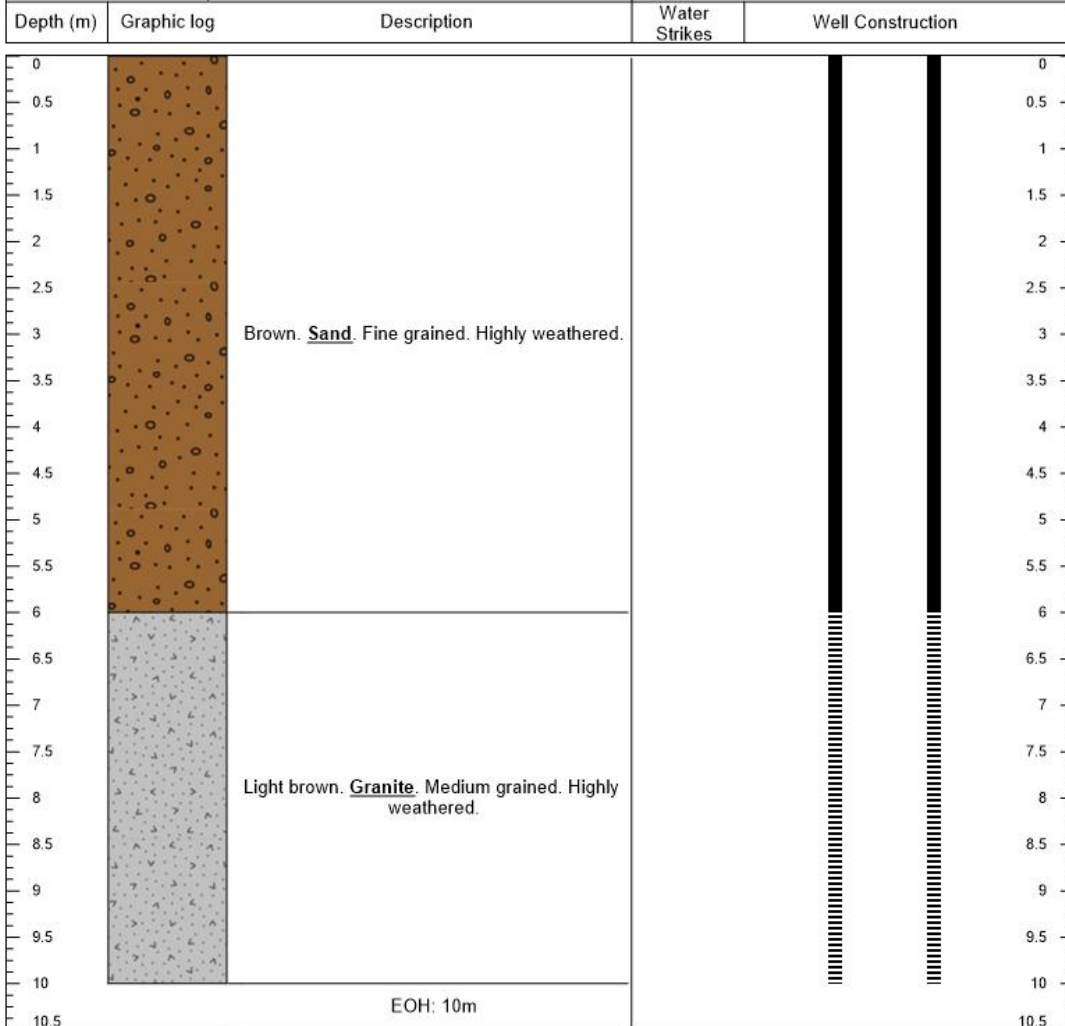
PROJECT:	K5/2338/1	BOREHOLE ID:	LR002A
LOCATION:	Phalaborwa (Letaba River)	DEPTH:	42m
DRILLING CONTRACTOR:	DWA	DATE COMPLETED:	28/09/2015
DRILLING METHOD:	Air Percussion	STATIC WATER LEVEL:	10.6

Depth (m)	Graphic log	Description	Water Strikes	Well Construction
-----------	-------------	-------------	---------------	-------------------



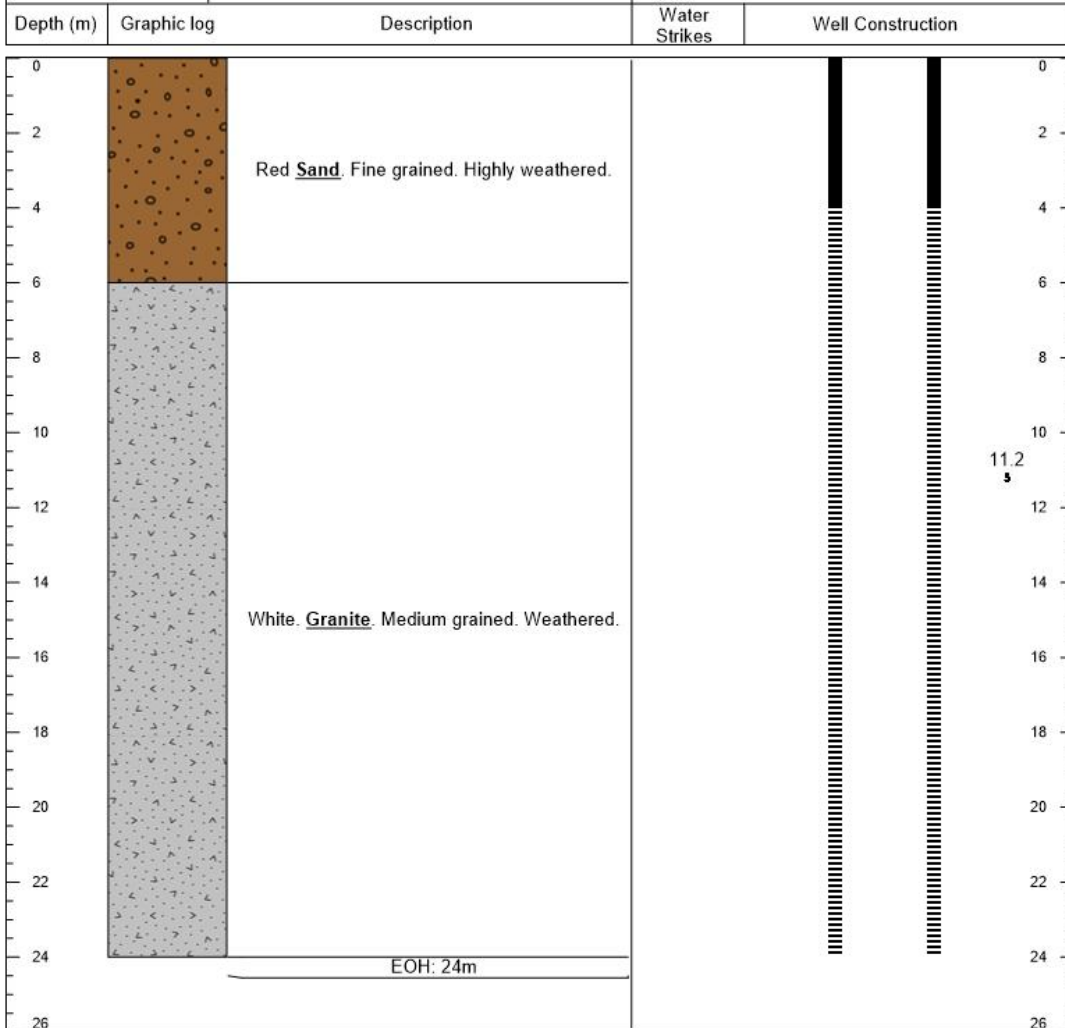
*Notes		Well Construction Legend	
- Blow yield: 1 800l/hr		■ Steel Casing (177mm)	■ BH Diameter
		≡ Steel Casing Screen (177mm)	



PROJECT:	K5/2338/1	BOREHOLE ID:	LR002B
LOCATION:	Phalaborwa (Letaba River)	DEPTH:	10m
DRILLING CONTRACTOR:	DWA	DATE COMPLETED:	01/10/2015
DRILLING METHOD:	Air Percussion	STATIC WATER LEVEL:	Dry



*Notes	Well Construction Legend	
	Steel Casing (177mm) Steel Casing Screen (177mm)	BH Diameter

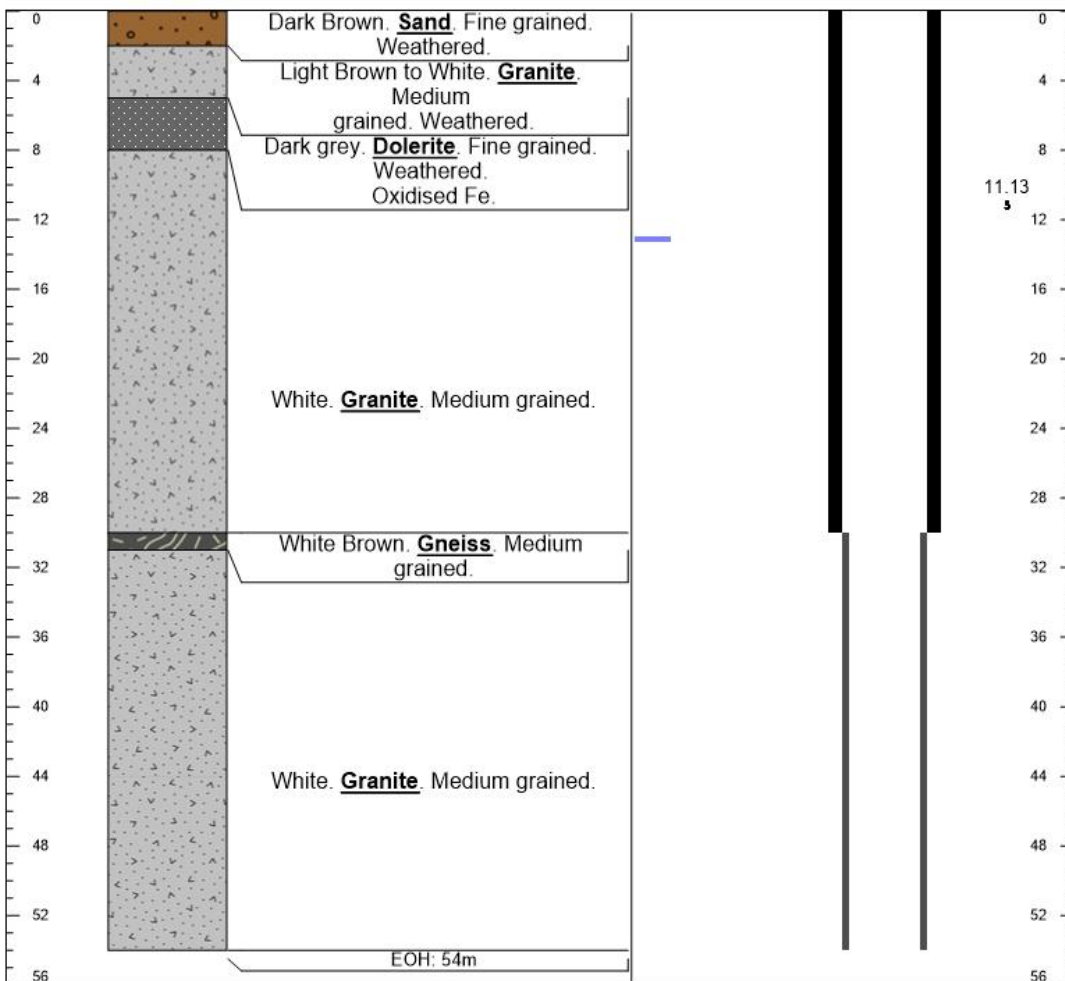
PROJECT:	K5/2338/1	BOREHOLE ID:	LR003
LOCATION:	Phalaborwa (Letaba River)	DEPTH:	24
DRILLING CONTRACTOR:	DWA	DATE COMPLETED:	26/09/2015
DRILLING METHOD:	Air Percussion	STATIC WATER LEVEL:	11.2



*Notes	Well Construction Legend	
	 Steel Casing (177mm)	 BH Diameter
	 Steel Casing Screen (177mm)	

PROJECT:	K5/2338/1	BOREHOLE ID:	LR004A
LOCATION:	Phalaborwa (Letaba River)	DEPTH:	54m
DRILLING CONTRACTOR:	DWA	DATE COMPLETED:	02/12/2015
DRILLING METHOD:	Air Percussion	STATIC WATER LEVEL:	11.13

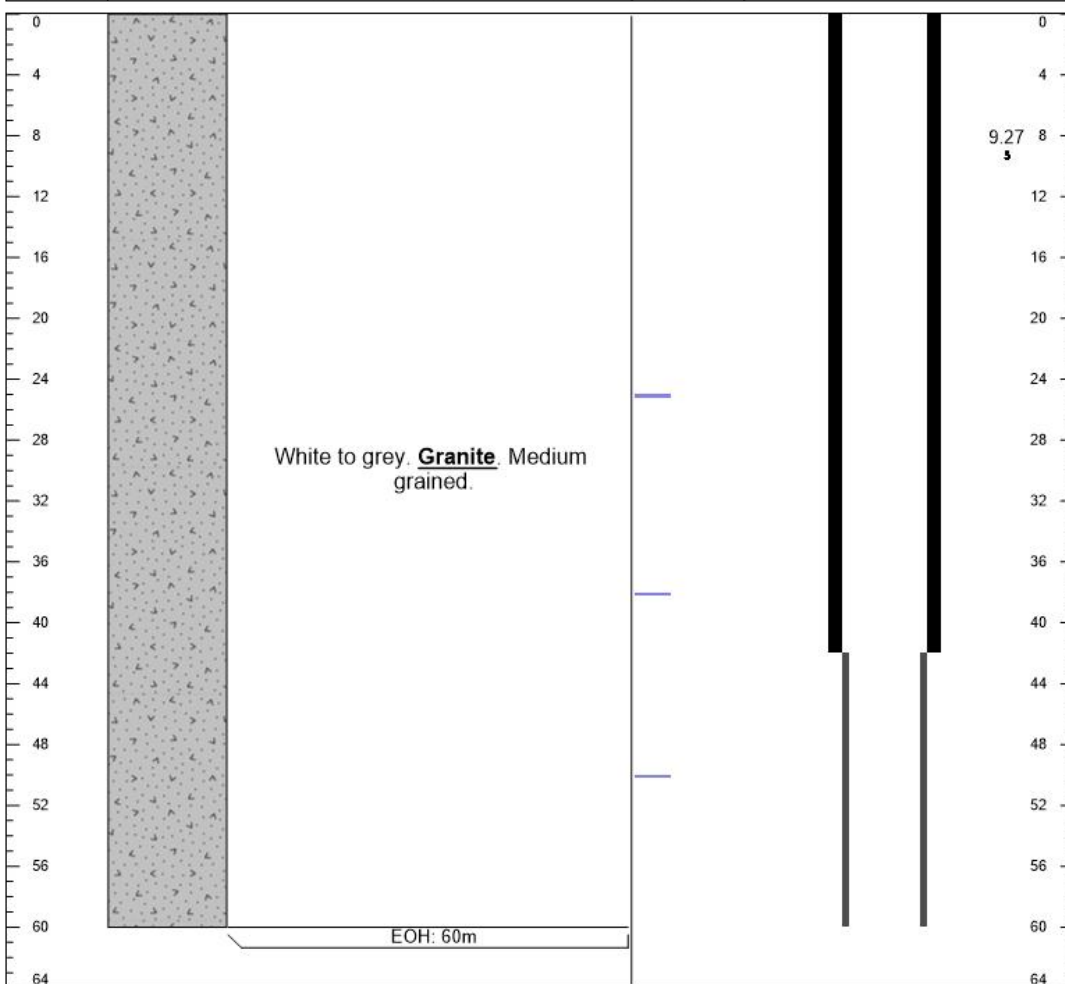
Depth (m)	Graphic log	Description	Water Strikes	Well Construction
-----------	-------------	-------------	---------------	-------------------



*Notes		Well Construction Legend	
- Blow yield: 1 800l/hr		■ Steel Casing (177mm)	■ BH Diameter
		▬ Steel Casing Screen (177mm)	

PROJECT:	K5/2338/1	BOREHOLE ID:	LR005A
LOCATION:	Phalaborwa (Letaba River)	DEPTH:	60
DRILLING CONTRACTOR:	DWA	DATE COMPLETED:	09/07/2015
DRILLING METHOD:	Air Percussion	STATIC WATER LEVEL:	9.27

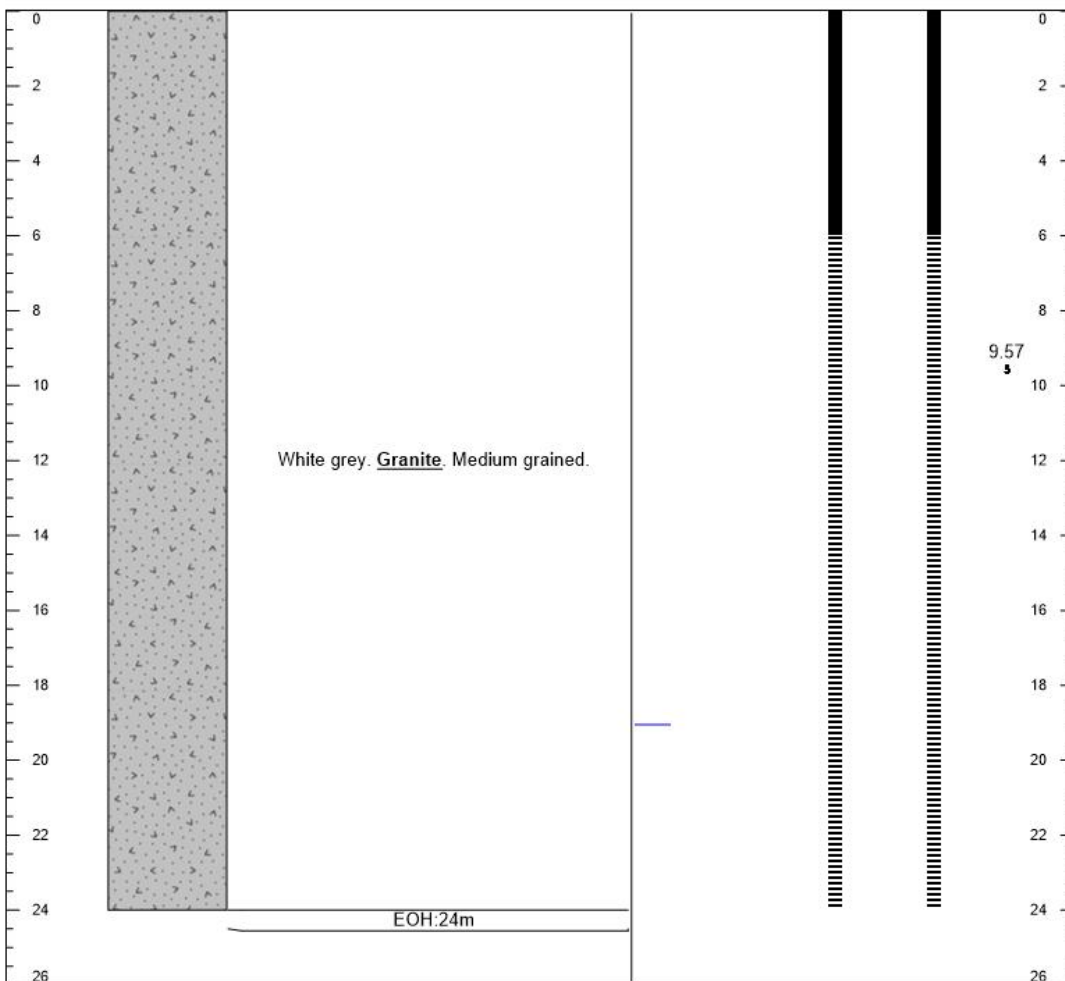
Depth (m)	Graphic log	Description	Water Strikes	Well Construction
-----------	-------------	-------------	---------------	-------------------



*Notes		Well Construction Legend	
- Blow yield: 104 652/hr		■ Steel Casing (177mm)	■ BH Diameter
		≡ Steel Casing Screen (177mm)	

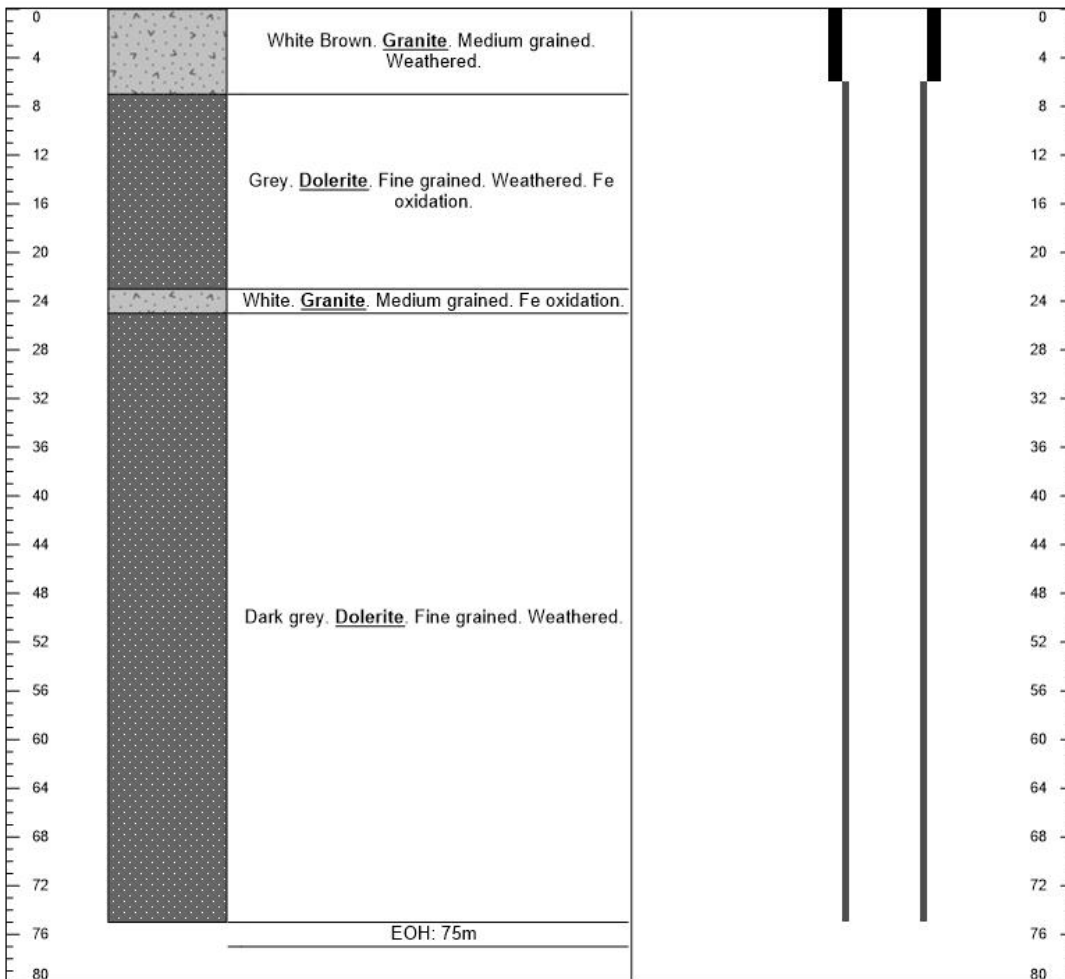
PROJECT:	K5/2338/1	BOREHOLE ID:	LR005B
LOCATION:	Phalaborwa (Letaba River)	DEPTH:	24
DRILLING CONTRACTOR:	DWA	DATE COMPLETED:	7/13/2015
DRILLING METHOD:	Air Percussion		9.57

Depth (m)	Graphic log	Description	Water Strikes	Well Construction
-----------	-------------	-------------	---------------	-------------------



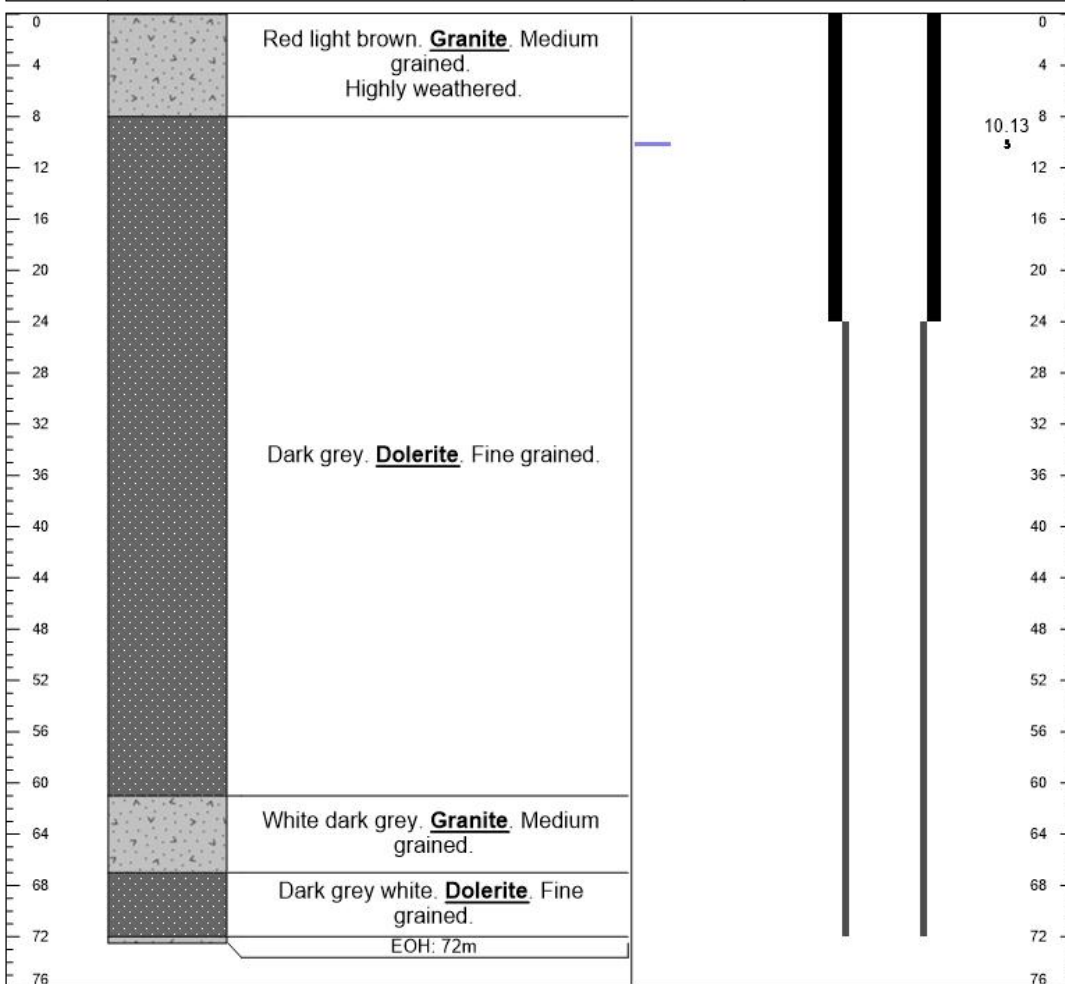
*Notes	Well Construction Legend
- Blow yield: 6 480l/hr	Steel Casing (177mm) Steel Casing Screen (177mm) BH Diameter




PROJECT: K5/2338/1		BOREHOLE ID: LR006		
LOCATION: Phalaborwa (Letaba River)		DEPTH: 75m		
DRILLING CONTRACTOR: DWA		DATE COMPLETED: 24/11/2015		
DRILLING METHOD: Air Percussion		STATIC WATER LEVEL: Dry		
Depth (m)	Graphic log	Description	Water Strikes	Well Construction



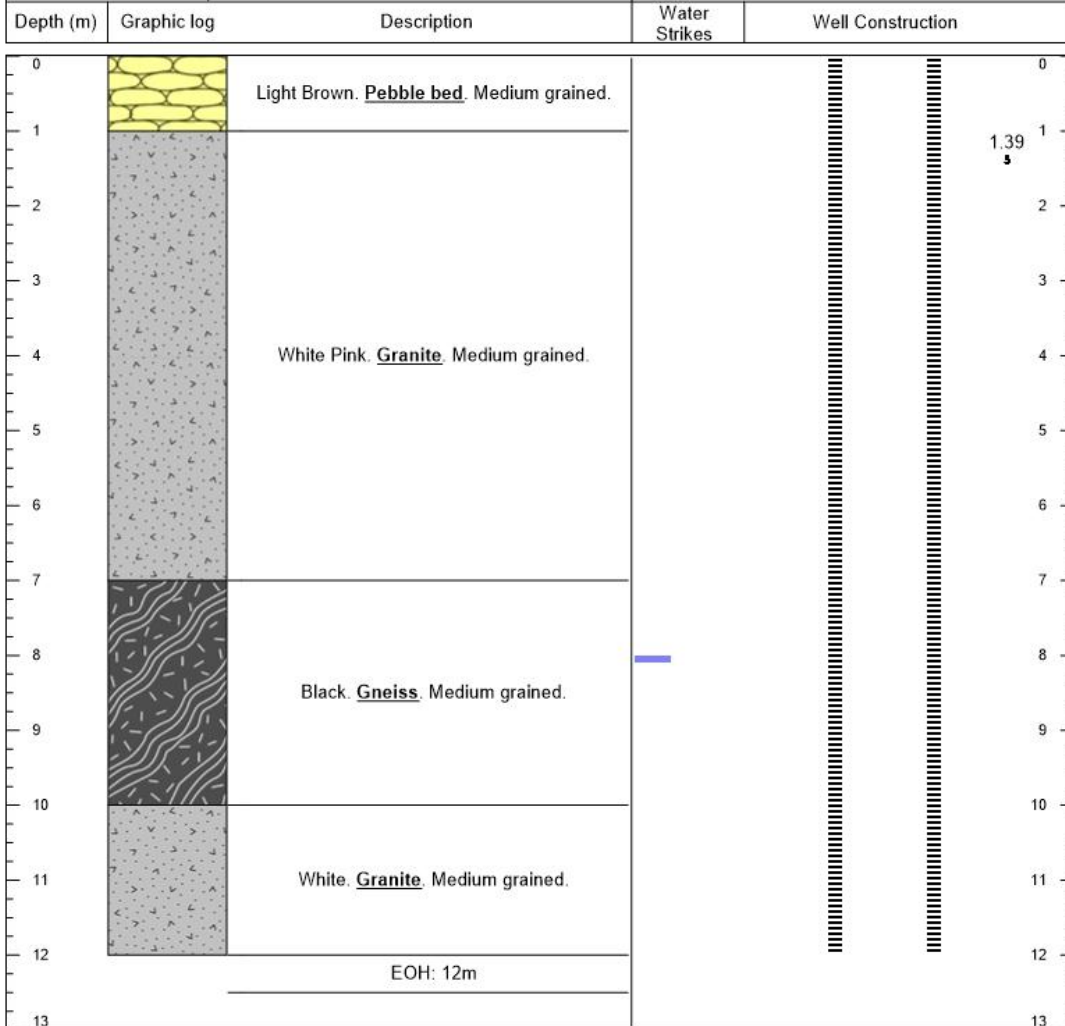
*Notes	Well Construction Legend	
	■ Steel Casing (177mm)	■ BH Diameter
	≡ Steel Casing Screen (177mm)	




PROJECT: K5/2338/1		BOREHOLE ID: LR0011A	
LOCATION: Phalaborwa (Letaba River)		DEPTH: 72m	
DRILLING CONTRACTOR: DWA		DATE COMPLETED: 14/09/2015	
DRILLING METHOD: Air Percussion		STATIC WATER LEVEL: 10.13	



*Notes		Well Construction Legend	
- Blow yield: 360l/hr		 Steel Casing (177mm)	 BH Diameter
		 Steel Casing Screen (177mm)	

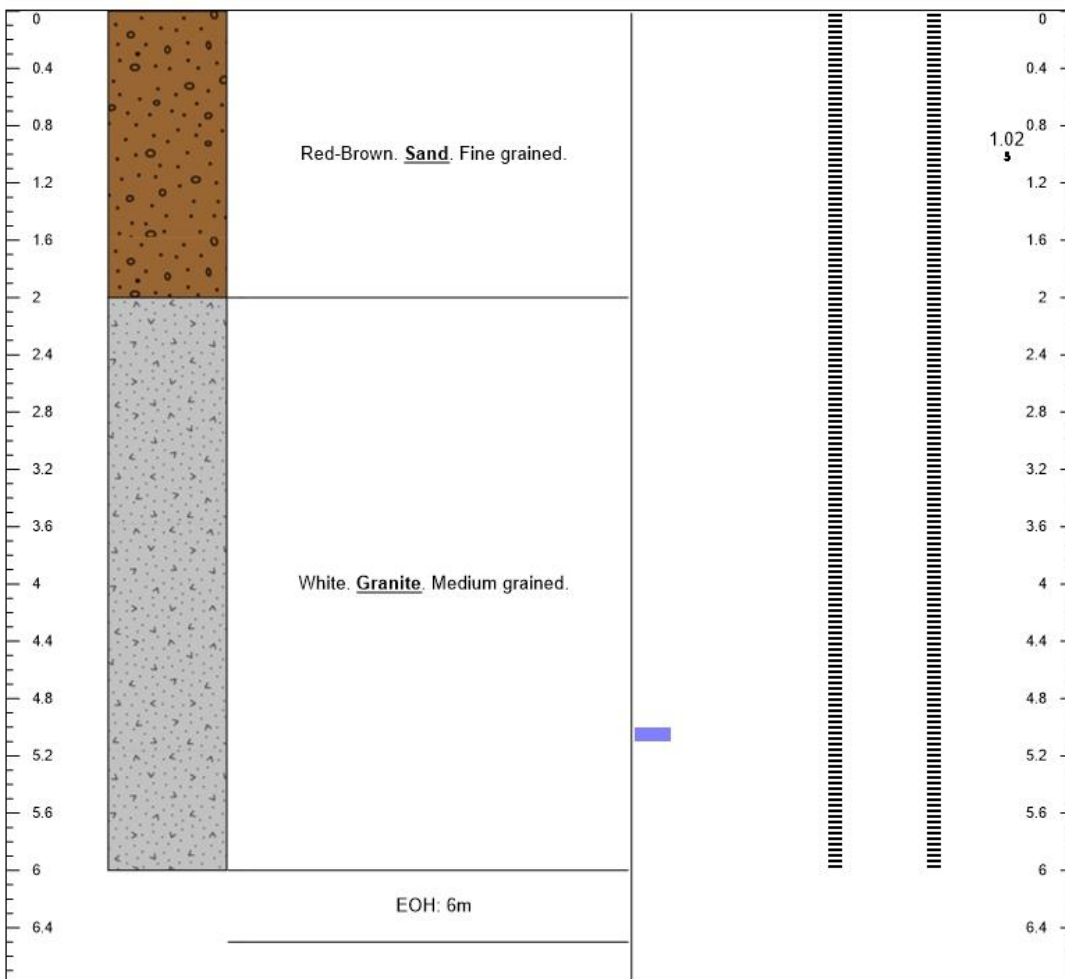
PROJECT:	K5/2338/1	BOREHOLE ID:	LRW001
LOCATION:	Phalaborwa (Letaba River)	DEPTH:	12m
DRILLING CONTRACTOR:	DWA	DATE COMPLETED:	26/11/2015
DRILLING METHOD:	Air Percussion	STATIC WATER LEVEL:	1.39



*Notes		Well Construction Legend	
- Blow yield: 720l/hr		 Steel Casing (177mm)	 BH Diameter
		 Steel Casing Screen (177mm)	

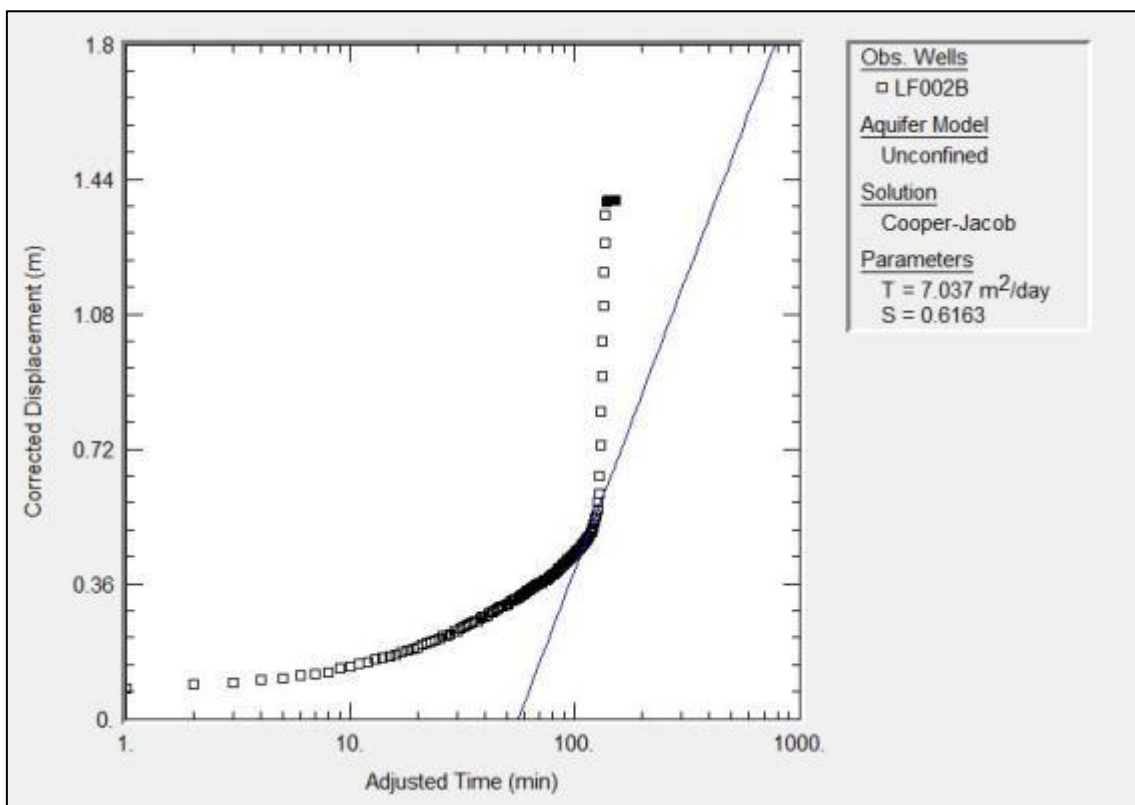
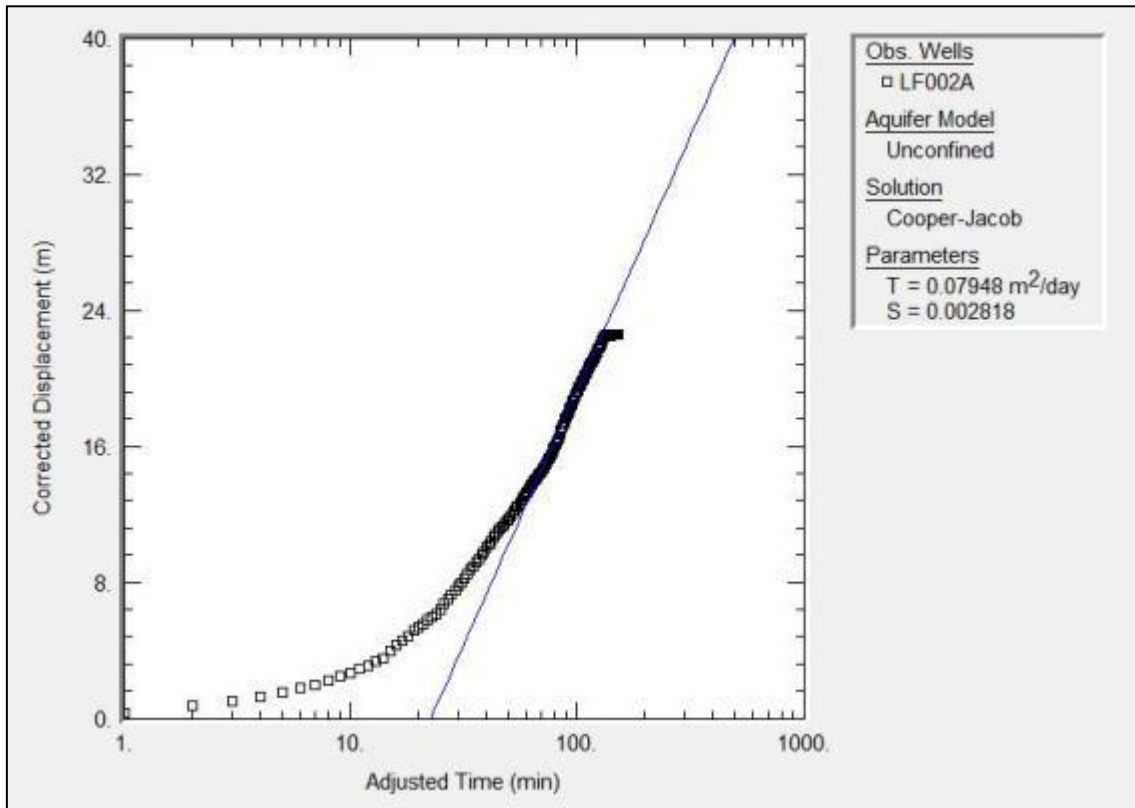
PROJECT:	K5/2338/1	BOREHOLE ID:	LRW002
LOCATION:	Phalaborwa (Letaba River)	DEPTH:	6m
DRILLING CONTRACTOR:	DWA	DATE COMPLETED:	30/11/2015
DRILLING METHOD:	Air Percussion	STATIC WATER LEVEL:	1.02

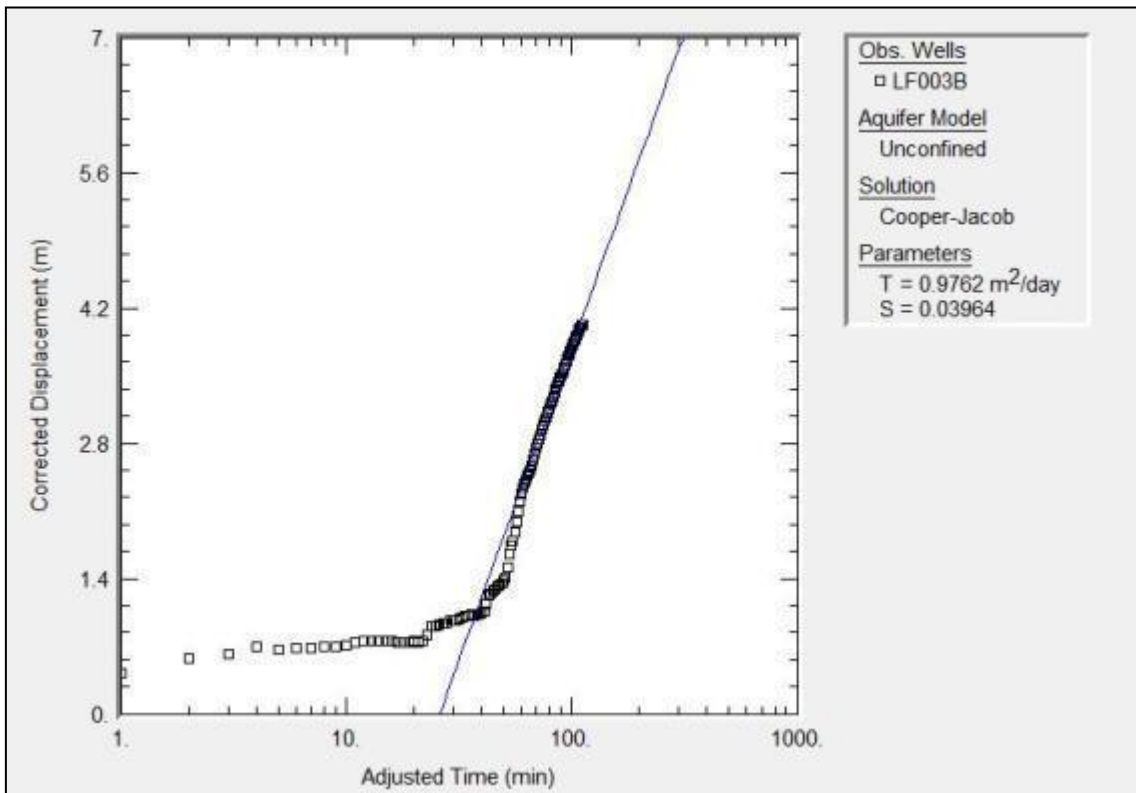
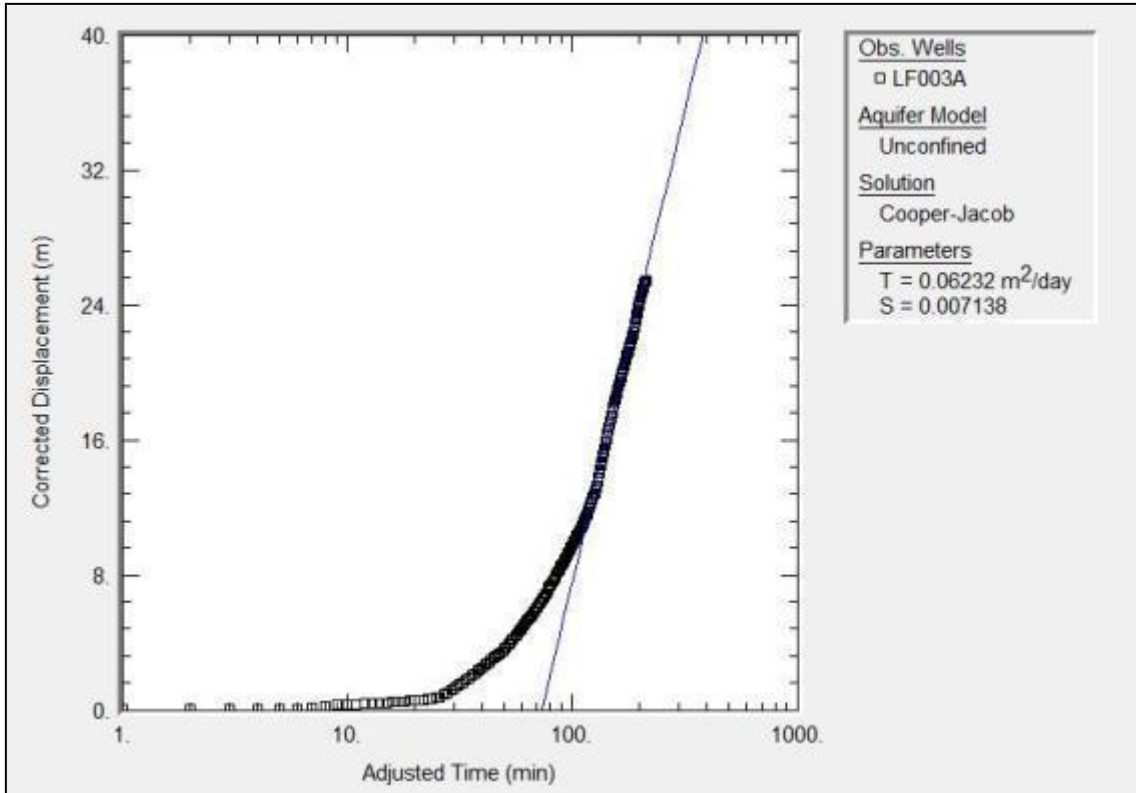
Depth (m)	Graphic log	Description	Water Strikes	Well Construction
-----------	-------------	-------------	---------------	-------------------

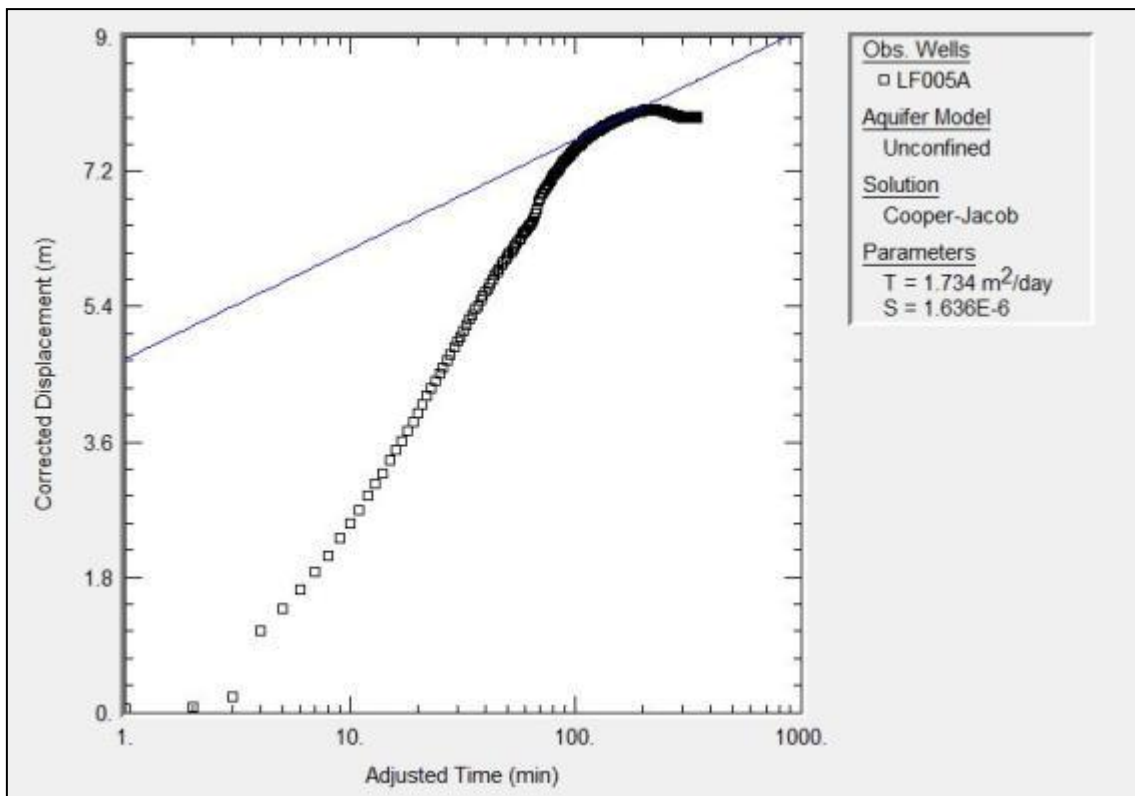
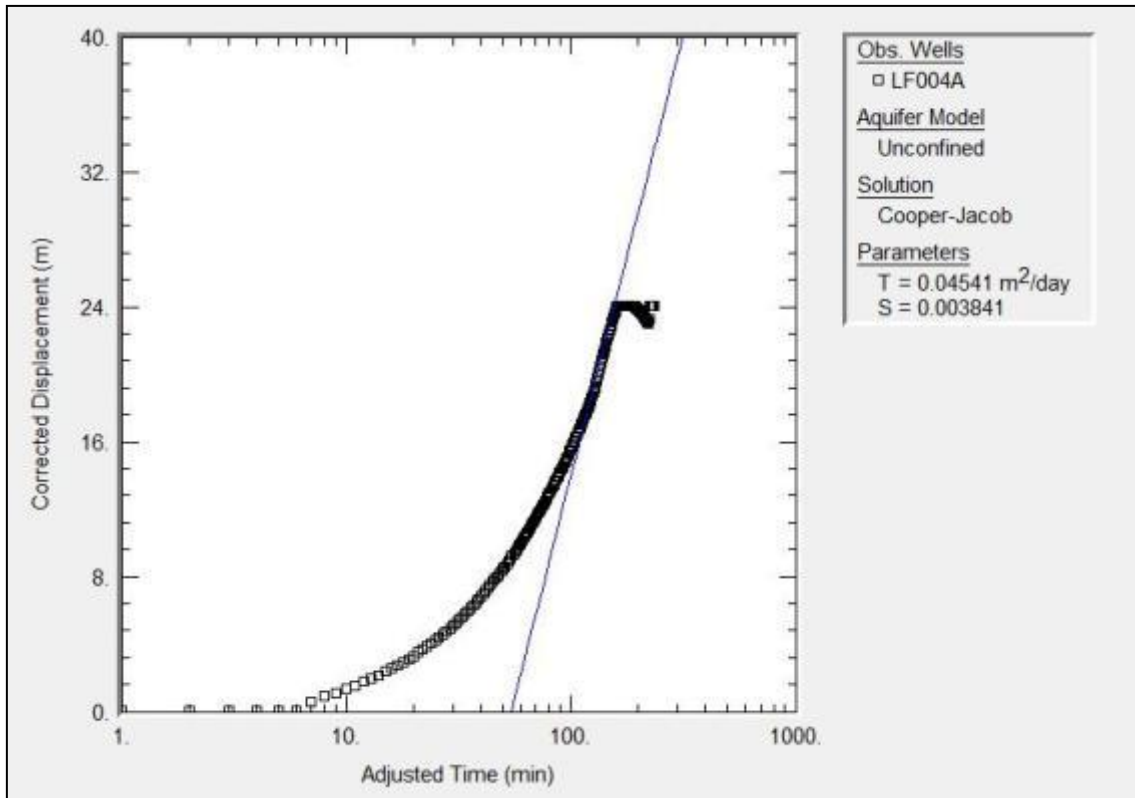


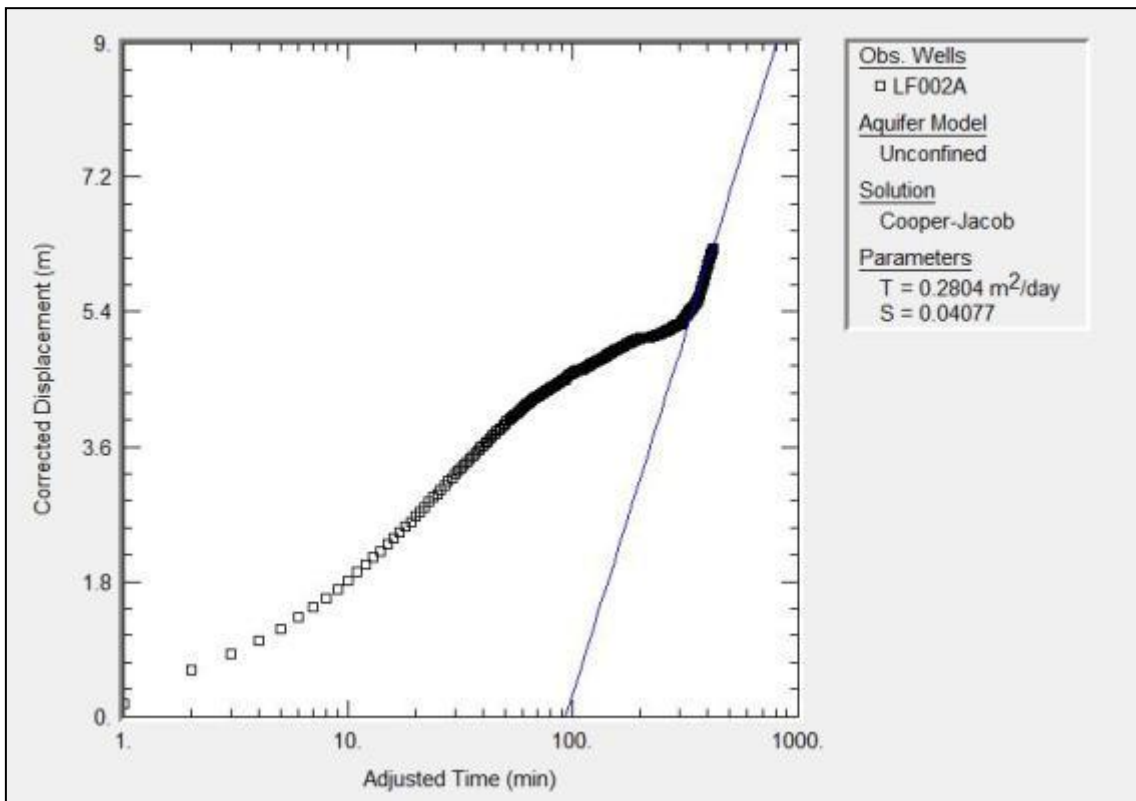
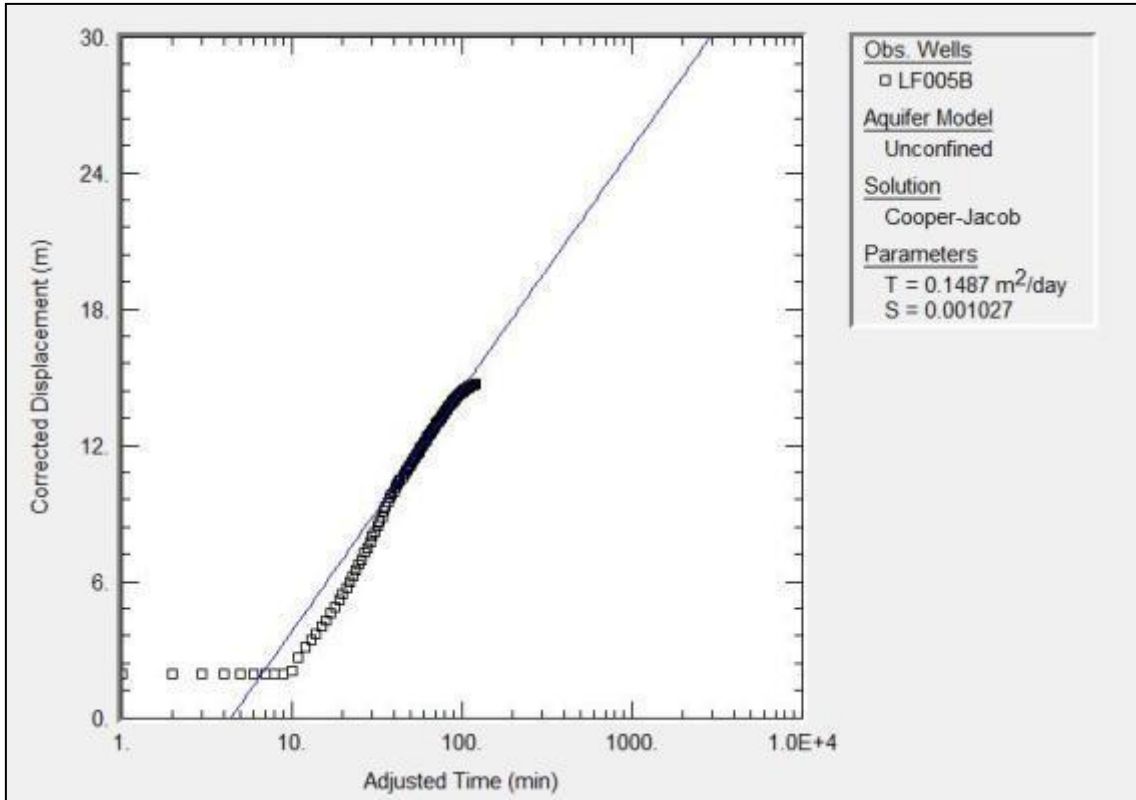
*Notes		Well Construction Legend	
- Blow yield: 720l/hr		■ Steel Casing (177mm)	■ BH Diameter
		▨ Steel Casing Screen (177mm)	

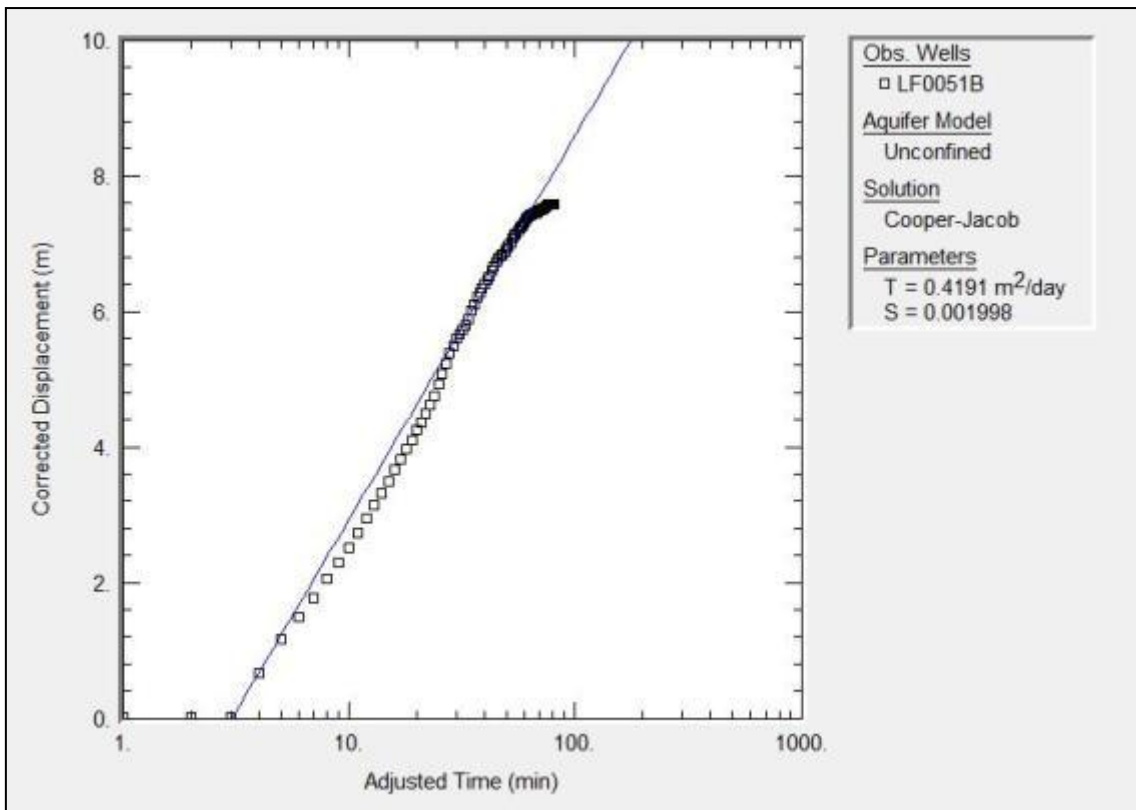
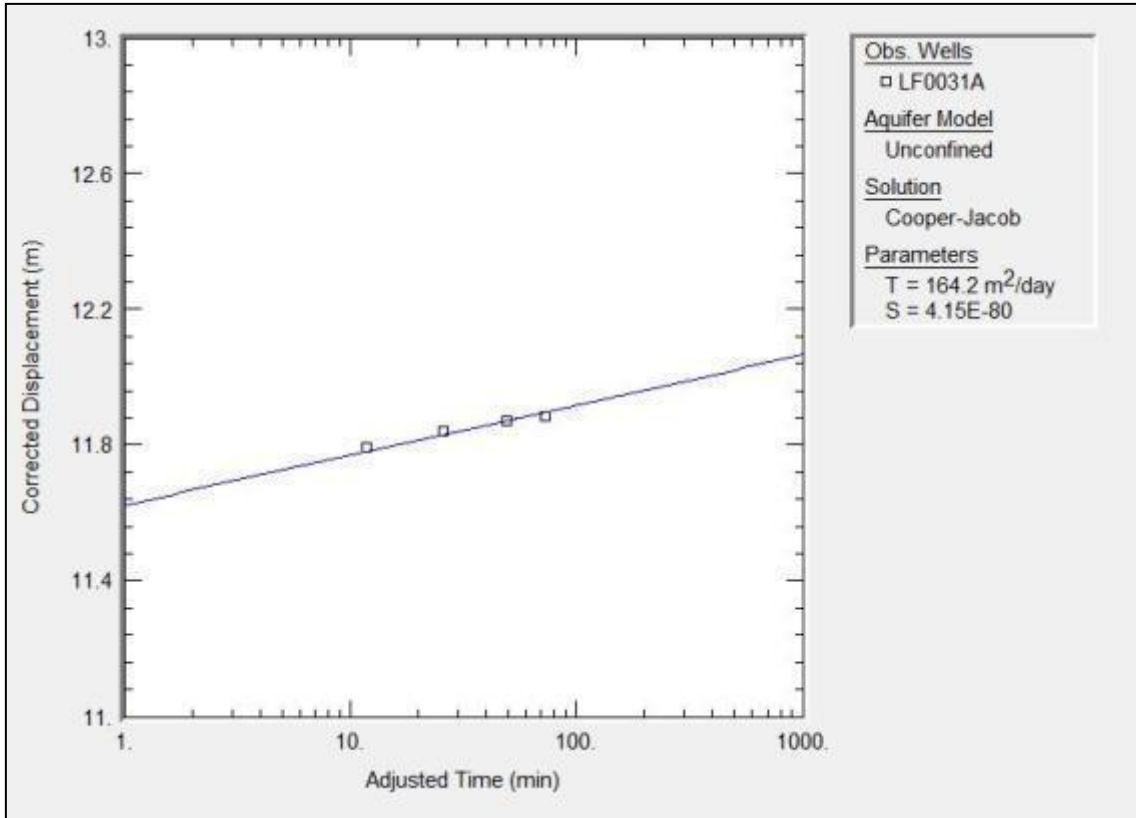
APPENDIX C

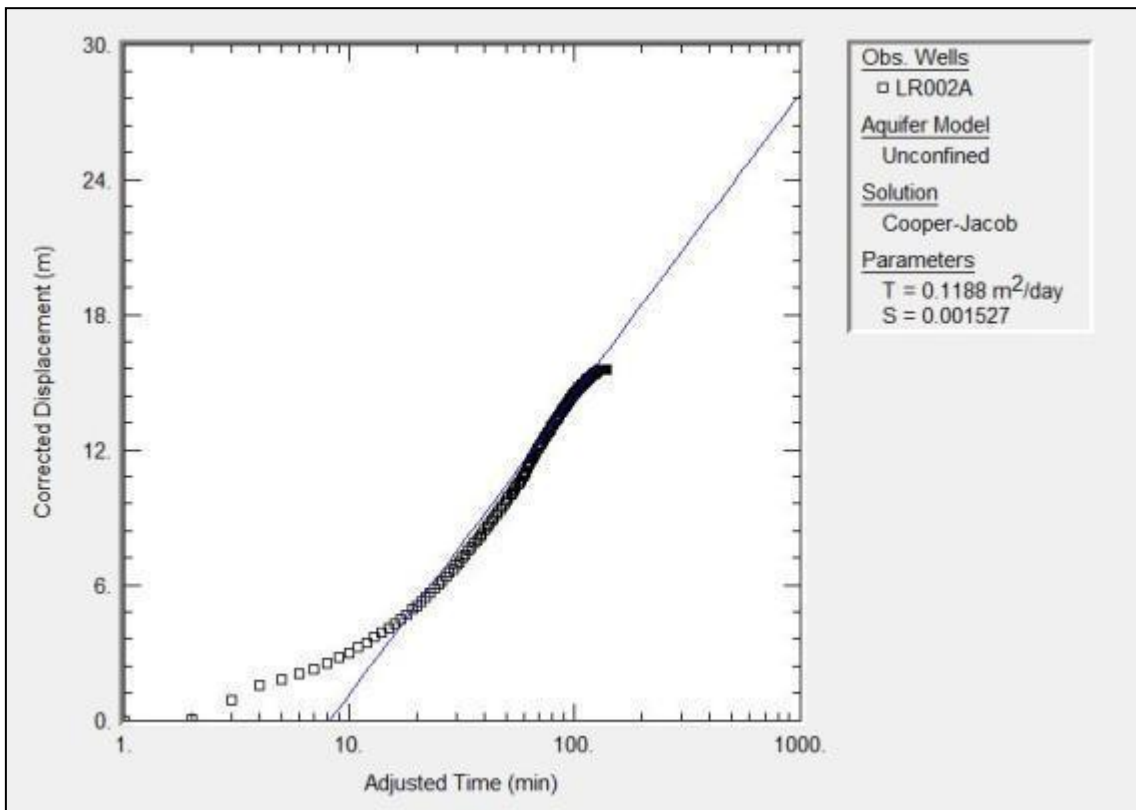
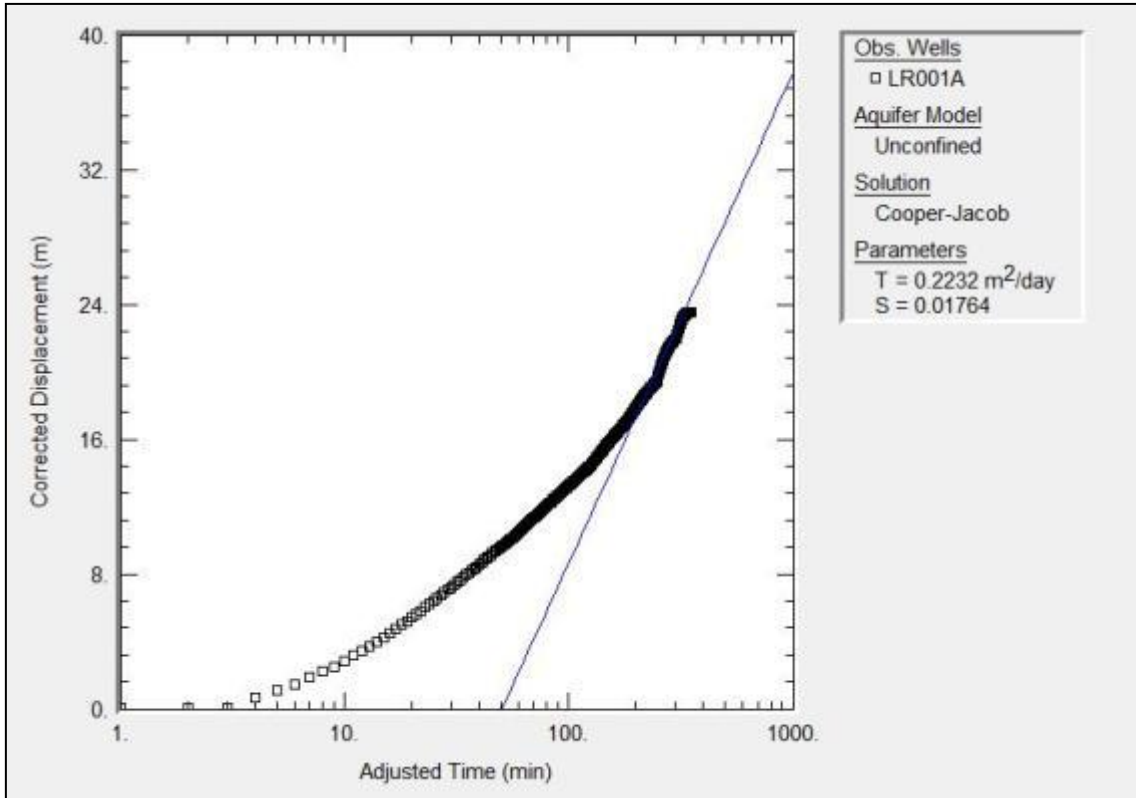


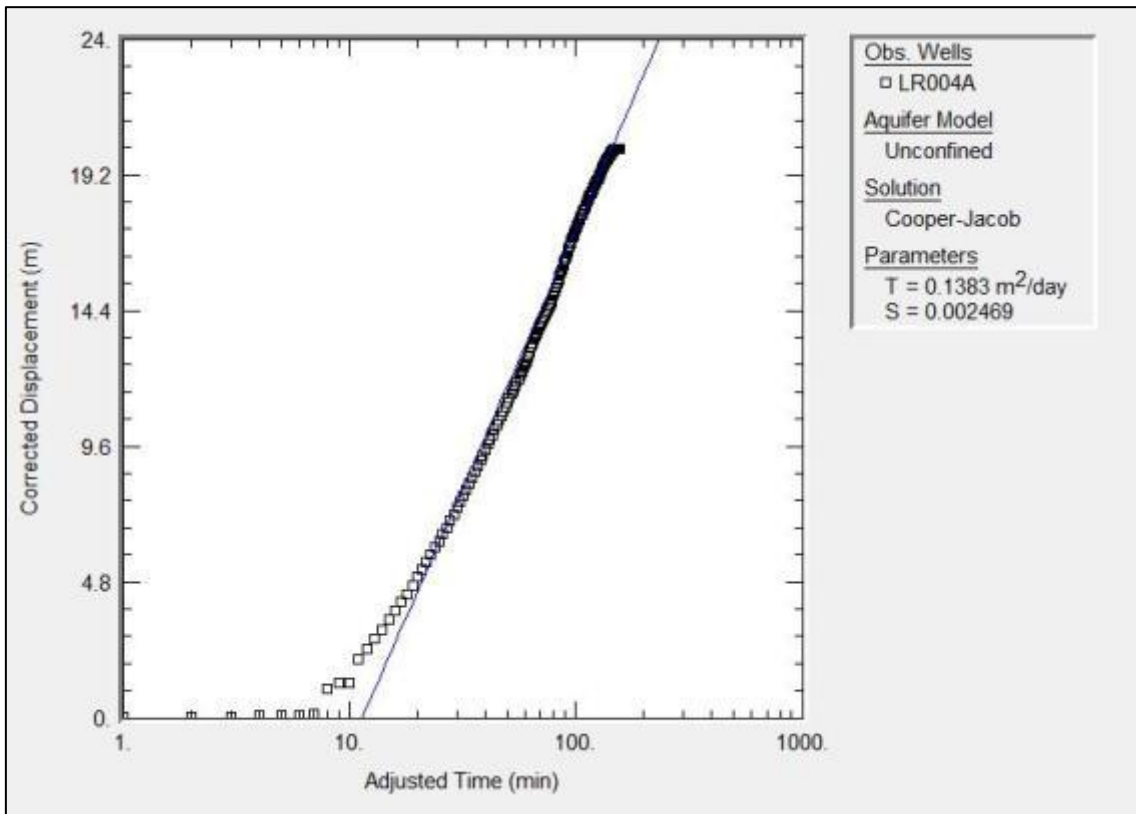
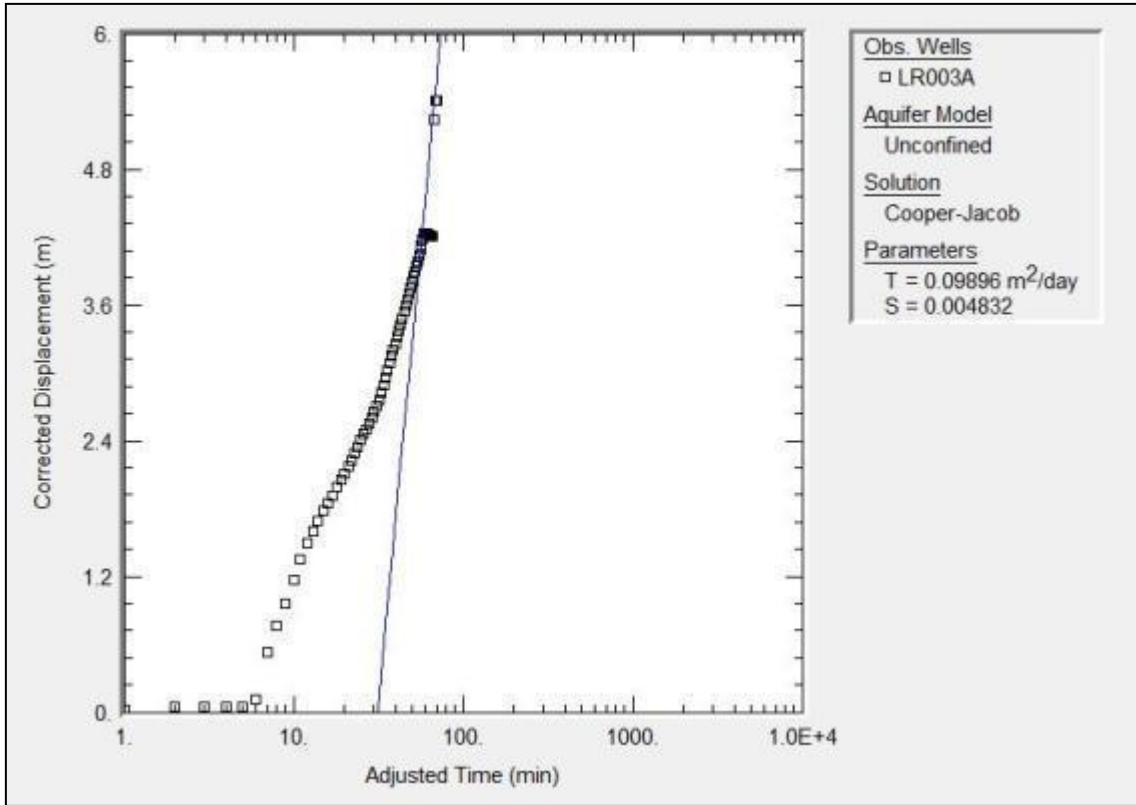


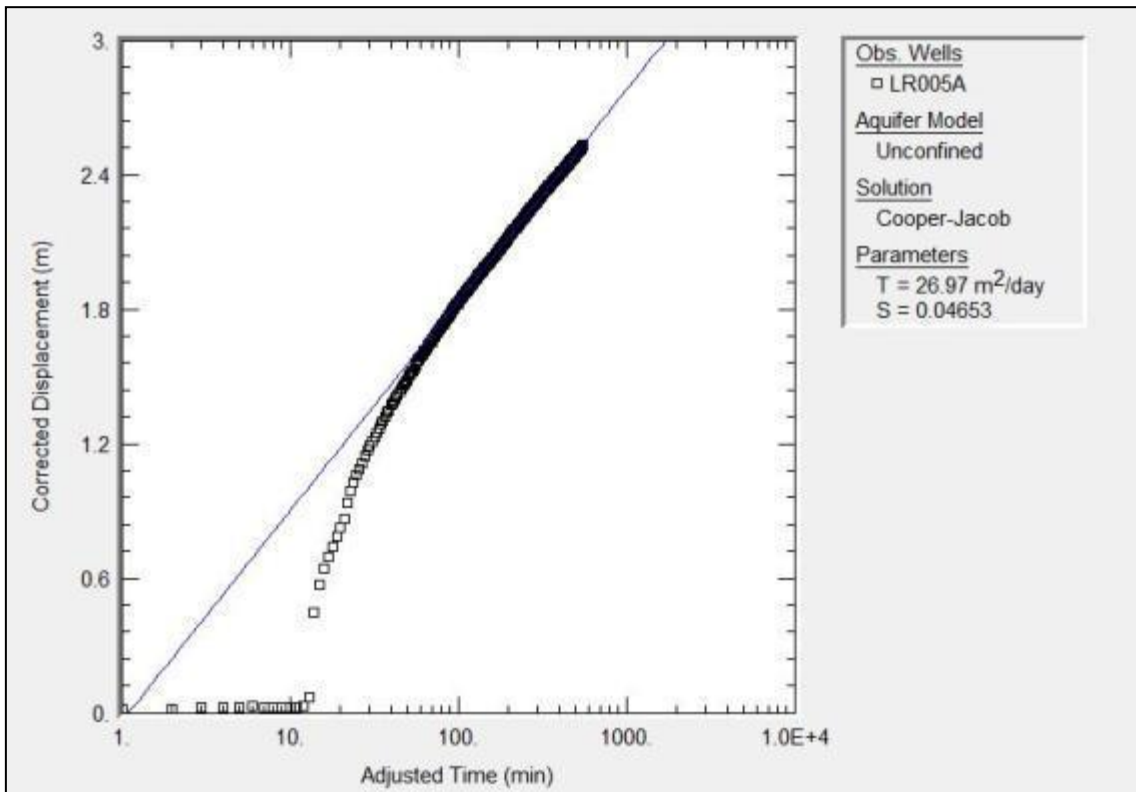
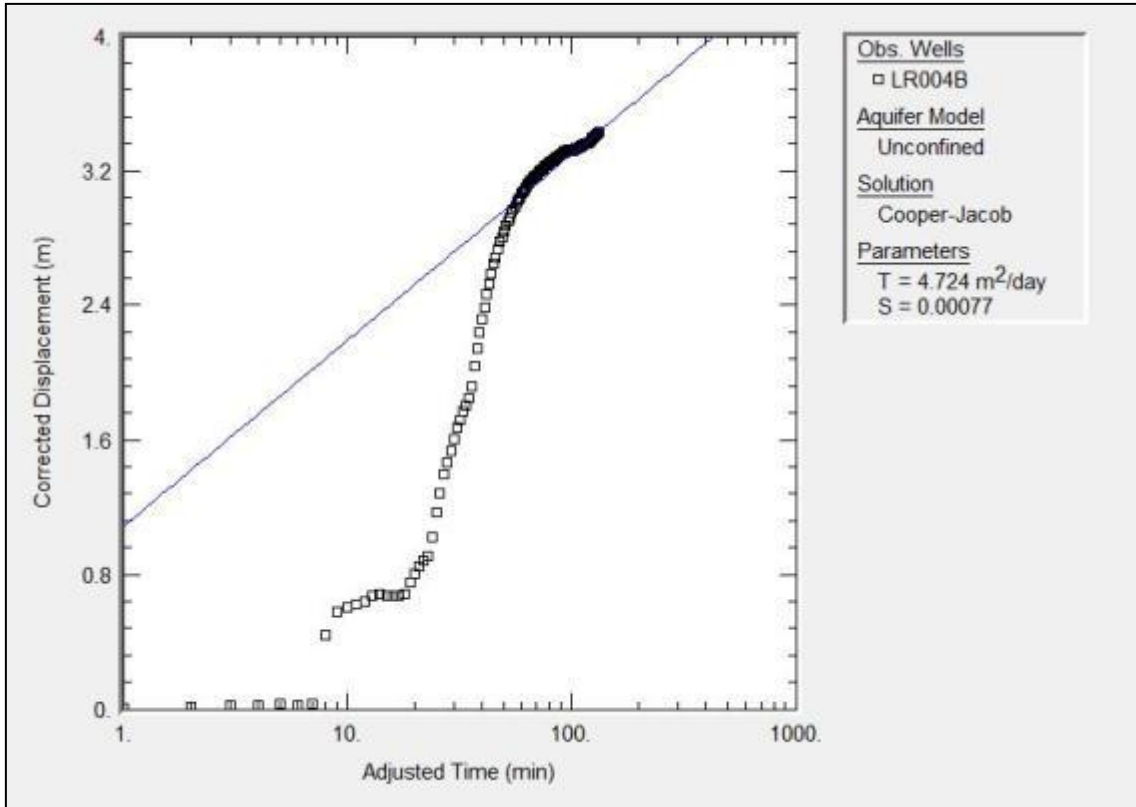


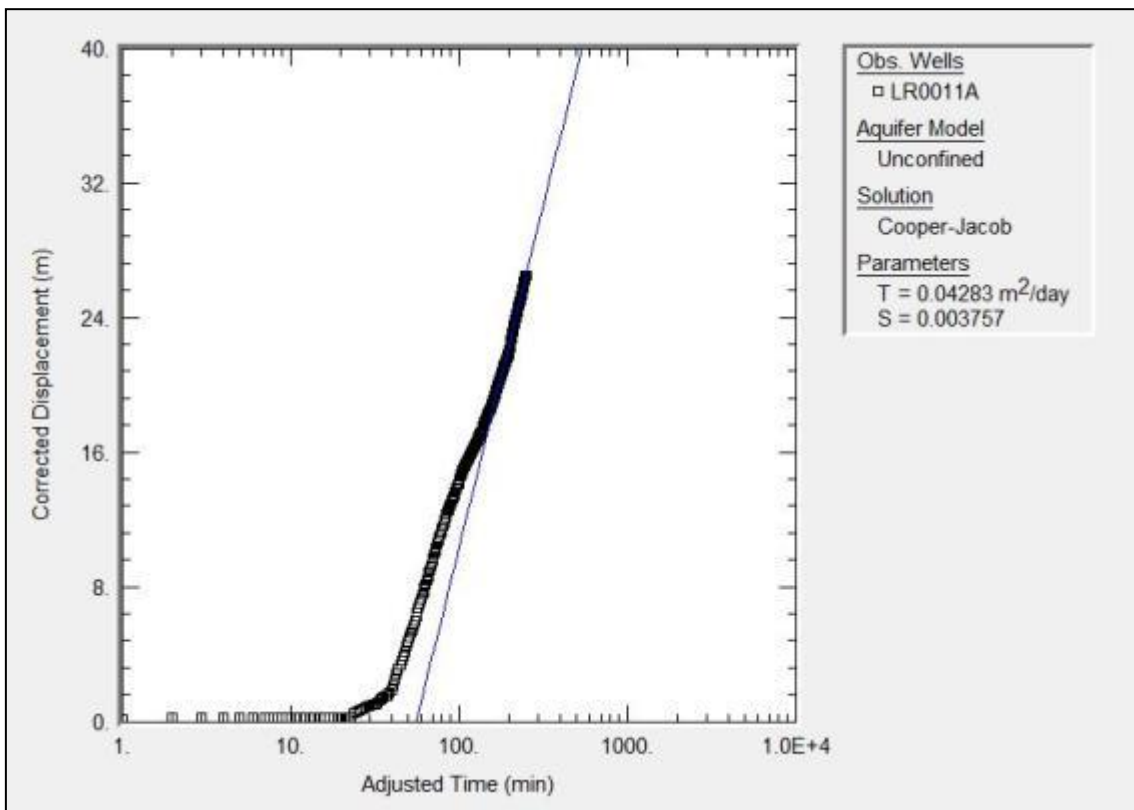
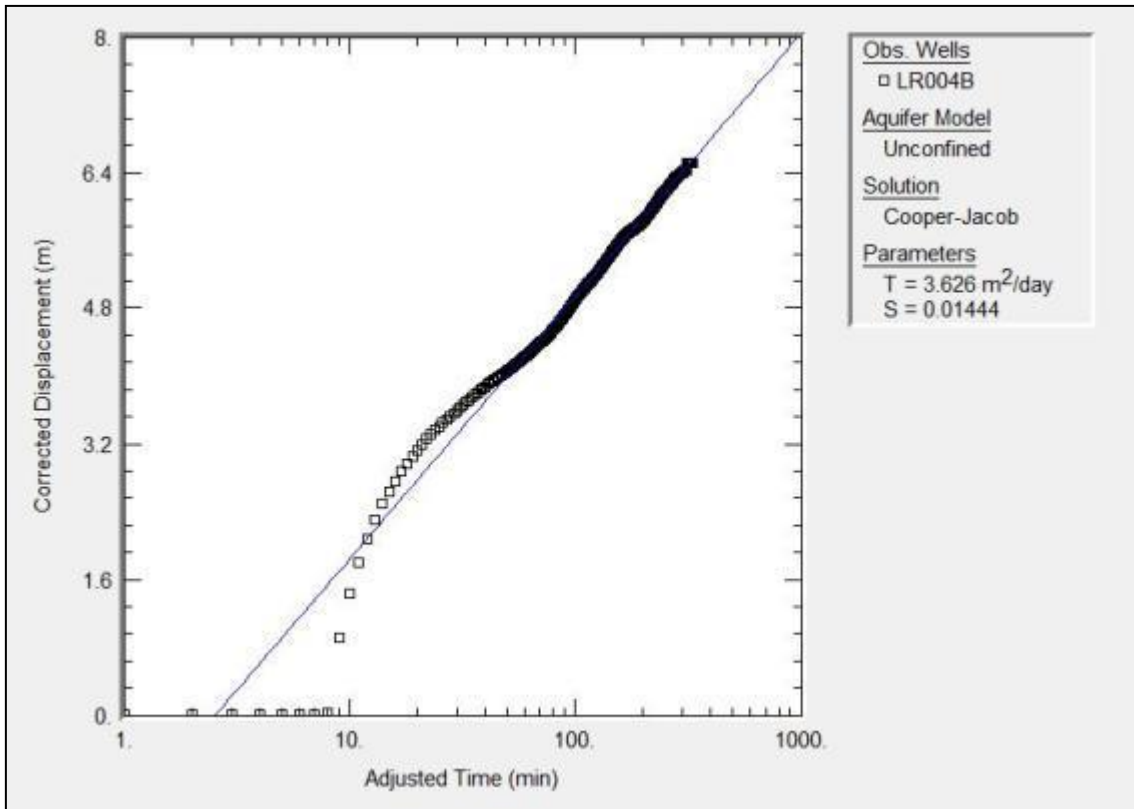












APPENDIX D



Appendix D-1



Appendix D-2

ABSTRACT

Continued population and economic growth within South Africa have led to increased water use by industry, agriculture, mining, domestic users and other uses over the past few decades. This increased usage has come close or even surpassed the threshold of renewable water resources within river basins. It was recognised that South Africa faces significant challenges in terms of water reform, involving major administrative and policy shifts, thus the attention has shifted to implementation. Water resource management has become of utmost importance to ensure that water users still receive an adequate supply, while at the same time the environmental flows are managed. Surface and groundwater processes have typically been studied as separate disciplines, regardless of their obvious association. They are both components of the hydrologic system however, they are not isolated components and interact in a range of climatic and physiographic landscapes. Thus, the contamination over usage or development of one affects the other. Consequently, a better understanding of the primary principles of the connectivity between the groundwater and surface water is essential for the successful management of water resources. This is particularly true upstream of the Kruger National Park, because of the limited understanding of groundwater – surface water interaction within catchments.

This resulted in the initiation of this dissertation to determine the connectivity of geohydrological processes and the interaction with the surface hydrology of the Letaba River, to ultimately provide guidance for successful management of water resources. There are many techniques to measure groundwater – surface water interaction, although for this dissertation the following methods were implemented: hydraulic gradients, geological characterisation, aquifer characterisation, fluid logging, environmental tracer method and the chemical base flow separation method. All of the results were then incorporated to provide a final conceptual model, indicating the interaction between the geohydrology and hydrology of the Letaba River.

The study site had to be divided into four transects, because of the scale. As anticipated, a simple losing or gaining stream was not indicated by the analyses. But, rather a complex system of groundwater movement and interaction with the surface hydrology for each transect, ultimately changing with seasonal variability and peak flow conditions. It has become clear through this research that the connectivity between the

surface water and groundwater is extremely complex. Thus, indicating the importance of groundwater management to protect and provide sustainable development for both resources. Even though a good infrastructure for data capturing have been implemented certain gaps are still found. Further research and monitoring is essential to ultimately fully understand this complex interaction.

OPSOMMING

Voortgesette bevolking en ekonomiese groei binne Suid-Afrika het die afgelope paar dekades tot gevolg gehad dat water, nywerhede, landbou, mynbou, huishoudelike verbruik en ander gebruike toegeneem het. Hierdie verhoogde verbruik het naby die drempel van hernubare waterbronne in die rivier komme voorgekom of selfs oortref. Daar is verneem dat Suid-Afrika beduidende uitdagings in terme van water hervorming ondervind, met groot administratiewe en beleids verskuiwings en daarom het die aandag verskuif na implementering. Waterhulpbron bestuur het uiters belangrik geword om te verseker dat water verbruikers steeds voldoende toevoer kry, terwyl die omgewings vloei terselfdertyd bestuur word. Oppervlak- en groundwater prosesse is tipies as afsonderlike disziplinêre bestudeer, ongeag hul ooglopende assosiasie. Hulle is albei komponente van die hidrologiese stelsel, maar hulle is nie geïsoleerde komponente nie en wissel in verskillende klimaat- en fisiografiese landskappe. Dus, sal die besmetting, oor gebruik of ontwikkeling van die een die ander een beïnvloed. Gevolglik is 'n beter begrip van die primêre beginsels van die verbindings tussen die groundwater en oppervlak water noodsaaklik vir die suksesvolle bestuur van waterhulpbronne. Dit geld veral vir die areas stroomop van die Nasionale Kruger wildtuin, weens die beperkte begrip van die groundwater – oppervlak water interaksie binne die opvangs gebiede.

Dit het gelei tot die inisiëring van hierdie proefskrif om die konnektiwiteit van geohidrologiese prosesse en die interaksie met die oppervlak hidrologie van die Letaba rivier te bepaal, ten einde leiding te gee vir die suksesvolle bestuur van waterhulpbronne. Daar is baie tegnieke om groundwater – oppervlak water interaksie te meet, maar vir hierdie proefskrif is die volgende metodes geïmplementeer: hidroliese gradiënte, geologiese karakterisering, akwifer karakterisering, boorgat waterprofile, “environmental tracer method” en die “chemical base flow separation” metode. Al die uitslae is dan opgeneem om 'n finale konseptuele model te verskaf, wat die wisselwerking tussen die geohidrologie en hidrologie van die Letaba - rivier aandui.

Die studie area was in vier deursnitte verdeel, weens die skaal en omvang. Soos verwag, is 'n eenvoudige stroom wat water verloor of by kry, vanaf die grondwater sisteem nie deur die ontledings aangedui nie. Maar eerder 'n komplekse stelsel van grondwater beweging en interaksie met die oppervlak hidrologie vir elke deursnit, wat uiteindelik verander met seisoenale veranderlikheid en hoë vloeitoeestande. Uit hierdie navorsing het dit duidelik geword dat die verbinding tussen die oppervlak water en grondwater uiters kompleks is. Dus, dui dit op die belangrikheid van grondwater bestuur om volhoubare ontwikkeling vir beide bronne te beskerm en te voorsien. Selfs al is 'n goeie infrastruktuur vir data vaslegging geïmplementeer, word daar steeds sekere leemtes ondervind. Verdere navorsing en monitering is noodsaaklik om hierdie komplekse interaksie ten volle te verstaan.